Deposit & Copying of Dissertation Declaration

UNIVERSITY OF CAMBRIDGE

Board of Graduate Studies

Please note that you will also need to bind a copy of this Declaration into your final, hardbound copy of thesis - this has to be the very first page of the hardbound thesis.

1 Surname (Family Name)	Forenames(s)	Title
SCOTT	KIRSTEN MAURINE	DR

2 Title of Dissertation as approved by the Degree Committee

Exploring neuro-immune interactions in neurodegeneration: the role of B lymphocytes in Parkinson's Disease

In accordance with the University Regulations in *Statutes and Ordinances* for the PhD, MSc and MLitt Degrees, I agree to deposit one print copy of my dissertation entitled above and one print copy of the summary with the Secretary of the Board of Graduate Studies who shall deposit the dissertation and summary in the University Library under the following terms and conditions:

1. Dissertation Author Declaration

I am the author of this dissertation and hereby give the University the right to make my dissertation available in print form as described in 2. below.

My dissertation is my original work and a product of my own research endeavours and includes nothing which is the outcome of work done in collaboration with others except as declared in the Preface and specified in the text. I hereby assert my moral right to be identified as the author of the dissertation.

The deposit and dissemination of my dissertation by the University does not constitute a breach of any other agreement, publishing or otherwise, including any confidentiality or publication restriction provisions in sponsorship or collaboration agreements governing my research or work at the University or elsewhere.

2. Access to Dissertation

I understand that one print copy of my dissertation will be deposited in the University Library for archival and preservation purposes, and that, unless upon my application restricted access to my dissertation for a specified period of time has been granted by the Board of Graduate Studies prior to this deposit, the dissertation will be made available by the University Library for consultation by readers in accordance with University Library Regulations and copies of my dissertation may be provided to readers in accordance with applicable legislation.

3 Signature	Date
KMScott	29/11/2019

Corresponding Regulation

Before being admitted to a degree, a student shall deposit with the Secretary of the Board one copy of his or her hard-bound dissertation and one copy of the summary (bearing student's name and thesis title), both the dissertation and the summary in a form approved by the Board. The Secretary shall deposit the copy of the dissertation together with the copy of the summary in the University Library where, subject to restricted access to the dissertation for a specified period of time having been granted by the Board of Graduate Studies, they shall be made available for consultation by readers in accordance with University Library Regulations and copies of the dissertation provided to readers in accordance with applicable legislation.

Exploring neuro-Immune interactions in neurodegeneration: The role of B lymphocytes in Parkinson's disease

Kirsten Maurine Scott

Lucy Cavendish College

Department of Clinical Neuroscience

University of Cambridge

This thesis is submitted for the degree of Doctor of Philosophy

June 2019

DECLARATION

This dissertation is the result of my own work and includes nothing which is the outcome of work done in collaboration except as declared in the acknowledgements and specified in the text.

It is not substantially the same as any that I have submitted, or, is being concurrently submitted for a degree or diploma or other qualification at the University of Cambridge or any other University or similar institution except as declared in the acknowledgements and specified in the text. I further state that no substantial part of my dissertation has already been submitted, or, is being concurrently submitted for any such degree, diploma or other qualification at the University of Cambridge or any other University or similar institution except as declared in the Preface and specified in the text.

In accordance with the Department of Clinical Neuroscience guidelines, this thesis does not exceed 65,000 words, and it contains less than 150 figures.

Kirsten Maurine Scott
MA (Edin), MBBS(London), MPhil (Cantab), MRCP (London)
Cambridge

THESIS ABSTRACT

Exploring neuro-immune interactions in neurodegeneration: the role of B lymphocytes in Parkinson's disease

Background:
Inflammation in the brain (as defined by microglial activation) and in the periphery (serum cytokines) is well described in Parkinson's disease (PD). I hypothesised that immune factors play a role in determining disease progression focusing on the contribution of B lymphocytes. These cells play a number of roles including antibody production, maintenance of subcapsular sinus macrophages, antigen presentation and regulation of T cell activity.

Methods:
I phenotyped peripheral blood B lymphocytes in 3 clinical cohorts and cerebrospinal fluid (CSF) B lymphocytes in a subgroup of patients using flow cytometry (79 PD patients, 65 controls in total). The patients were risk stratified by their risk of progression to dementia. Controls were age and gender matched. I also performed a systematic review and meta-analysis of the literature on alpha-synuclein antibodies and then designed an assay to measure antibodies to alpha synuclein species and peptides. I piloted the assay in 39 patients and controls. I also used the 6-OHDA lesioned mouse model of PD and examined disease course by testing motor capacity in mice lacking B lymphocytes (μMT), in mice depleted of B cells using an anti-CD20 monoclonal antibody and in wild type controls (C57bl/5). Dopaminergic cell counts and staining were compared. I examined the phenotype and distribution of B lymphocytes in alpha synuclein transgenic models of Parkinson's disease using flow cytometry.

Results:
B lymphocytes were decreased in PD patients at high risk of progressing to early dementia compared to matched controls. A higher proportion of IL10 producing regulatory B lymphocytes was associated with better outcomes. Alpha synuclein transgenic mice also had reduced circulating B lymphocytes. Mice with a genetically driven B lymphocyte deficiency developed a worse motor phenotype and showed more extensive loss of midbrain dopaminergic cells than wild type controls. Meningeal and skull B lymphocytes had a different phenotype to circulating B lymphocytes but were not different between controls and transgenic animals.

Conclusions:
My data suggest that B cells play a protective role in PD, potentially via regulation of immune responses to aberrant forms of alpha synuclein or cell death. Modulating this compartment by increasing IL10 producing B lymphocytes would be a reasonable therapeutic strategy. Exploring the function and behaviour of meningeal B lymphocytes in health and disease may reveal further therapeutic targets.

This PhD thesis is dedicated to my husband, John Somner and to my children, Torrin and Evan, for their unending patience with late night and weekend lab visits and absence from family adventures while writing up.

It is also dedicated to my good friend and brilliant colleague Nicholas Blair who died on the 30th of September 2018 from leukaemia. Even from his ITU bed, he joked that it had been a drastic measure to get out of writing up his PhD thesis. I promised him that I would make sure I would complete mine.

ACKNOWLEDGEMENTS

Thank you to my supervisors Menna Clatworthy and Roger Barker who have provided guidance, support and encouragement throughout my PhD and to Caroline Williams-Gray who supervised the clinical aspects relating to Parkinson's disease.

There are many people in both labs and in other departments who have also helped. Their contributions are described in detail below including contributions to the collection of data.

Thanks to the NIHR cell phenotyping hub where I did the flow cytometry for the patient study and to the staff at the UBS Phenomics animal facility where I did most of the animal experiments. .

Thanks to my funders, the Wellcome Trust PhD program for clinicians.

Clinical studies

Recruitment of patients and controls for the clinical studies described in this thesis was carried out by Caroline Williams-Gray, Ruwani Wijeyekoon, Antonina Kouli, Melanie Jensen and myself from our weekly PD research clinic and through contacting existing patients through the clinic database. None of this would have been possible without administrative support provided by the clinic staff (Molly O'Reilly, Lindsey Wilkin and Marta Camacho). Some of these participants were also used in studies looking at T cell senescence (Williams-Gray et al., 2018) and monocyte function (Wijeyekoon et al., 2018).

For cohort 1, clinical assessments were done by Caroline Williams-Gray, Ruwani Wijeyekoon or myself and PBMC separation was done by the remaining two clinicians with help from a research assistant, Shaista Hayat, for a 9 month

period while I was on maternity leave (SH did the PMBC separations and B cell staining during this period and I ran the flow cytometry in the evening). Otherwise all B cell staining and subsequent processing was performed by me. The processing of serum for alpha synuclein MSD assay was done together with Caroline Williams-Gray and Ruwani Wijeyekoon.

Data collection for cohort 2 was done in conjunction with an Mphil student Melanie Jensen (MJ) that I co-supervised with Caroline Williams-Gray. I designed the B cell aspects of her project, planning her B cell panel prior to her arrival. I supervised the initial optimisation and titration of antibodies, training her how to do PBMC extraction, immunocytochemistry and flow cytometry. I helped her to recruit patients and did some of the clinical assessments on the patients that we recruited (other clinicians in the lab also contributed to doing the clinical assessments including Julia Greenland, Caroline Williams-Gray, Tom Stoker and Ruwani Wijeyekoon). Apart from the initial few patients, MJ ran the flow cytometry. For this part of my thesis, I have analysed and gated the raw fcs files that MJ collected and combined the resulting data with the clinical data for subsequent analyses. All data analysis and manipulation in the results section was done by me.

For cohort 3,. the flow cytometry panel was designed and piloted by me (with input and advice from Menna Clatworthy and Caroline Williams-Gray) (CWG). I trained another PhD student, Antonina Kouli (AK) to do the PBMC extractions and staining as well as the flow cytometry. Flow cytometry for the first ten patients was done by me, subsequent participants were then run by AK. All data analysis on the raw fcs files and clinical data in this thesis was done by me.

A modified version of sections 3.3, 3.4 and 3.5 has been published in a special edition of the journal Frontiers in Neurology (Scott, Kouli, Yeoh, Clatworthy, &

Williams-Gray, 2018). I wrote the manuscript based on work done for this chapter, performed all of the data analysis and created the figures. I received critical feedback and review from my supervisor Menna Clatworthy and from Caroline Williams-Gray who directly supervises my work in the Barker lab. Two other students (Antonina Kouli and Su Ling Yeoh) repeated the literature review independently, searching for papers and hand reviewing the bibliographies so that we could be sure that we had found all of the relevant papers. All data analysis, study design and write up were performed by me.

Yvonne Clements, a representative from MSD gave me advice on setting up the antibody assays and supervised the first trial run that I performed using commercially available antibodies. When I ran the final assays using patient serum samples, I received help with some of the wash steps and preparation of the reagents from Amanda Warner, an undergraduate student and Imtiaz Solim, a research assistant. I trained both of them and supervised the performance of the assays.

Mouse studies

Thanks to Pam Tyers who trained me how to do surgery in the mice and in most of the animal husbandry and procedures that I used throughout my PhD. Along with Zachary Fitzpatrick she helped with performing some of the surgeries on the 6OHDA mice. Zachary Fitzpatrick and Gordon Frazer (from the Clatworthy lab) also help with processing meningeal tissue for flow cytometry and confocal microscopy. They performed the confocal microscopy and quantification of B cells on this tissue for me. Rebeccah Mathews tirelessly helped with many of the rotarod tests, mouse genotyping, animal husbandry and processing tissues for flow cytometry when I had large experiments involving multiple mouse organs and animals. Many of these experiments would have been difficult to perform without her help. Ondrej Suchanek helped with gating of B cell populations and

provided meningeal tissue from experiments that he was doing looking at tissue resident B cells. He performed the intra-vesical e.coli injections in the UTI model in μMT mice. Maria Grazia Spillantini and Michal Wegrzynowicz provided tissue from MI-2 transgenic alpha synuclein mice from animals they were using for experiments.

Thanks to Martin Rice, Emma Blanchard, Kate Tansley and for advice and training on the running of animal studies. I supervised two undergraduate summer students who helped with some of the animal work. Jenny Whitby did some of the initial behavioural experiments on the thy1 SNCA mice and Georgia Wright did some of the stereology for the 6OHDA studies.

Thanks to my mother Julia Hasler and my parents in law, Peter and Carola Somner who did a lot of extra child care to facilitate additional visits to the lab on weekends or during the holidays.

Thank you to Kayla Friedman and Malcolm Morgan of the Centre for Sustainable Development, University of Cambridge, UK for producing the Microsoft Word thesis template used to produce this document.

TABLE OF CONTENTS

1 INTRODUCTION

Parts of this introduction have been published as part of a systematic review and meta-analysis (Scott et al., 2018).

In this chapter I will give a brief introduction to the immune system to give some context to my PhD. I will then summarise previous trials of immunomodulating therapies in PD, briefly reviewing the literature on PD pathology, disease heterogeneity and the role of inflammation before giving some examples of how B lymphocytes could be involved in disease pathogenesis and progression. I will also mention the possible important role of meningeal immunity.

1.1 Brief introduction to the immune system

The immune system has evolved to protect organisms, including human beings, from microbes, damage, toxins and cancer. Inflammatory or auto-immune disorders occur when there is a loss of tolerance: the immune system becomes misdirected to a self-antigen (for example the neuro-muscular junction in Myasthenia Gravis). Mammalian immune systems can be simplistically divided into “innate” and “adaptive” immune systems. The innate immune system provides an immediate response to molecular structures expressed on microbes or viruses. This response is largely the same each time and is provided by phagocytes, dendritic cells, neutrophils, NK cells, innate lymphoid cells and the complement system (Chaplin, 2010). This is a cascade of proteins triggered by early infection that leads to increased phagocytic activity and activation of cell-killing ‘membrane attack complex’ (as well as playing a regulatory role)(Ricklin, Reis, & Lambris, 2016). The adaptive immune response (consisting of B lymphocytes and T lymphocytes) is specific to particular pathogens (and their antigens) and is increased by repeated exposure. The two systems are linked: immunoglobulins (antibodies) secreted by B lymphocytes can activate complement to increase phagocytosis and innate immune cells such as dendritic cells can present fragments of ingested antigen via receptors on their surface

(major histocompatibility complex MHC) receptors to T cells to activate them (Chaplin, 2010). B lymphocytes provide 'humoral' immunity by secreting antibodies specific to particular antigens. These can facilitate phagocytosis by opsonising the antigen (making it more attractive to a phagocyte) or by antibody mediated cytotoxicity (NK cells) (see later discussion on the roles of B lymphocyte). T lymphocytes (CD4 +or CD8+) provide cell mediated immunity whereby they are able to kill phagocytes that have ingested or become infected by intracellular pathogens (that can't be accessed by circulating antibodies)(Chaplin, 2010).

Many of the functions of the immune system are regulated by cytokines, a diverse range of proteins that are able to support immune cell survival, facilitate proliferation, activate effector lymphocytes, regulate the immune response by inhibiting activation and many others (Abbas et al., 2014). Chemokines are a subset of cytokines that regulate cell migration and movement (for example movement of immune cells into and out of secondary lymphoid tissue such as lymph nodes and the spleen). There are specific groups of cytokines associated with particular responses, for example a T helper 1 response (Th1) is associated with the cytokine interferon γ (activates macrophages to ingest pathogens), a T helper 2 response (Th2) is associated with the cytokines interleukin-4 (IL-4), IL-5 and IL6 (mainly in response to helminths) and T helper 17 response is associated IL-17 and IL-22 which recruit other immune cells and drive further inflammation (Abbas et al., 2014).

Circulating immune cells (in the blood) are a tiny fraction of the immune system: many immune cells are concentrated in lymph nodes or the spleen (where, for example a T lymphocyte with a specific antigen receptor is more likely to encounter a dendritic cell presenting its cognate antigen)(Ruddle & Akirav, 2009). There are also tissue resident immune cells. In the brain these

include microglia (long lived innate immune cells capable of adopting a phagocytic phenotype that are self-renewing and derived from the yolk sac) and macrophages (that are probably derived from the circulating pool)(Li & Barres, 2018). There are also tissue resident immune cells in the meninges that contribute to homeostasis (Derecki et al., 2010). Although the brain used to be regarded as 'immune privileged' we now also know that circulating lymphocytes 'patrol' the brain for pathogens (Engelhardt, 2010).

Over the last few decades the response of the immune system to the damaged central nervous system (CNS) has received increasing attention (Chitnis & Weiner, 2017). The focus of my PhD has been on B lymphocytes in Parkinson's disease because i) B lymphocytes are an important part of the immune response ii) the immune response is likely to be involved in PD iii) they offer an attractive therapeutic target with one of the many existing therapies that modulate the B lymphocyte response and iv) there were very few studies on B cells in PD or its models when I started.

1.2 Parkinson's disease

Parkinson's disease (PD) is a common neurodegenerative disorder, affecting 2-3% of people over the age of 65 (Pringsheim et al., 2014). Current therapies are symptomatic, mainly addressing the motor features of the disease (tremor, rigidity and bradykinesia) by replacing the dopamine that is lost as a result of cell death in the substantia nigra pars compacta. Dopamine replacement does not address the multitude of non-motor features of the disease such as hyposmia, postural instability, dementia, gut dysfunction, sleep disturbance or mood symptoms (Schapira, Chaudhuri, & Jenner, 2017). It also does not stop the disease from progressing. There are currently no disease modifying therapies available. There is therefore an urgent need to better understand disease

pathogenesis and to develop therapies that prevent these complications and stop disease progression.

In recent years, targeting the immune system has been suggested as a therapeutic strategy not only in PD (Gendelman et al., 2017) but also in other neurodegenerative diseases including Alzheimer's disease (AD) (Butchart et al., 2015; McGeer, Rogers, & McGeer, 2016) and Amyotrophic Lateral Sclerosis (ALS)(Khalid et al., 2017). A number of clinical trials of immune modulating therapies have been completed in PD.

Minocycline, a tetracycline analogue (usually used as an antibiotic) showed good results in pre-clinical models preventing loss of dopaminergic neurons and associated microglial activation (reviewed in (Cankaya et al., 2019). It is thought to reduce microglial activation and T cell transmigration with fewer effects on the peripheral immune system(Stirling et al., 2005). A phase II trial in early disease (less than five years from diagnosis in medication naïve patients) showed that although it was well tolerated there was no evidence of efficacy either at the 12 month or 18 month end points (NINDS NET-PD Investigators, 2006, 2008). The trial was originally designed as a futility trial with the conclusion being that the results did not reach the futility threshold and that therefore large phase III trials should build on these results but these trials have not been done. It is possible that the lack of efficacy was because the treatment was only targeting microglia whilst ignoring the peripheral immune response. It is also possible that the reason the trail failed was because the follow up time was inadequate and the primary end point (change in Unified Parkinson's Disease Rating Scale, UPDRS, a common measure of function in PD) was not sufficiently sensitive to detect changes over such a small period of time.

In a similar vein, pioglitazone, used for the treatment of type 2 diabetes, had also been shown to have good outcomes in pre-clinical animal models (mainly in rodents)(Bonato et al., 2018). It also reduces microglial and astrocytic activation and was therefore considered a good candidate (NINDS NET-PD Investigators, 2015). In a randomised, double blind placebo controlled trial, participants were either given 15mg or 45mg of pioglitazone or placebo (in addition to a baseline monoamine oxidase inhibitor which they were on prior to the trial). At 44 weeks there was no difference in UPDRS scores between the groups. Again, this may be because targeting microglia is not enough to slow disease progression. The follow up period may also not have been long enough to detect the relevant differences.

Only one trial in PD so far has targeted the peripheral immune response, aiming to increase regulatory T cells using sargramostim (also known as granulocyte macrophage colony stimulating factor (GM-CSF) building on evidence from cross-sectional studies that these played a protective role (Gendelman et al., 2017). This trial showed proof of mechanism in that all subjects showed an increase in the number and proportion of T regulatory cells and there were some positive trends in the clinical outcomes (magnetoencephalography recorded cortical motor activities). However the trial was very small (N=17 in the treatment group and N=20 in the placebo) and there were a number of concerning adverse events (including vasculitis, urticaria and a stroke in one patient)(Gendelman et al., 2017). GM-CSF has many other effects on immune cells apart from expanding regulatory T cells which may have been responsible for these adverse effects. Additional trials using large numbers are required, potentially using a safer drug to boost the regulatory T cells.

In Alzheimer's disease (AD), the field has spent the last two decades focused on therapies aiming to remove the amyloid pathology associated with disease

(Panza et al., 2019). There has been a recent high profile failure of monoclonal antibodies to amyloid and indeed all therapies attempting to clear it (Mullard, 2019) although there are still some trials in prodromal cohorts which have more promise (Panza et al., 2019). As a result, the field has started to look at downstream pathways for potential targets for disease modification, including the immune response. There has been one phase 1 trial of etanercept (targeting tumour necrosis factor alpha, TNFα) in AD, again based on data from clinical cohorts showing that higher levels of TNFα are associated with faster cognitive decline, particularly when combined with recurrent infection (Holmes et al., 2009b). The primary outcomes were safety and tolerability rather than clinical efficacy. We therefore await further trials.

Both the clinical presentation and disease progression is very heterogenous in PD and this may be an additional reason for a lack of positive trials of potential disease modifying therapies (Greenland, Williams-Gray, & Barker, 2019). Differences in the immune response to the primary pathology of PD may be one of the explanations for the clinical heterogeneity observed. It is important to understand the pathways involved (and whether these are protective or harmful) in order to identify appropriate drug candidates for repurposing in clinical trials.

1.2.1 Disease heterogeneity

There is substantial variability in disease course, with around half of patients developing dementia and two-thirds developing postural instability over the first 10 years from diagnosis. One quarter have a more benign course (Greenland et al., 2019; Williams-Gray et al., 2013). Both of these complications impair quality of life as well as resulting in increasing health care costs (Aarsland et al.,, 2000).

In our lab we have followed a large number of incident PD cases across several epidemiological studies. The CamPaIGN study (Cambridgeshire Parkinson's Incidence from GP to Neurologist) consisted of a population based cohort of PD patients diagnosed between 2000-2002 with long term (ongoing) follow up (Evans et al., 2011; Williams-Gray et al.,, 2007; Williams-Gray et al., 2009, 2013). Through this study, we have identified, clinical parameters available at the time of diagnosis which allow stratification of patients into 'high risk' and 'low risk' groups for an early dementia (independent of age) using simple bedside cognitive tests (semantic fluency and pentagon copying) and tau genotype (MAPT H1/H1) genotype. This common inversion polymorphism on chromosome 17 is associated with dementia risk in PD as well as susceptibility to a number of neurodegenerative tauopathies (Williams-Gray et al., 2009).The high dementia risk group has the H1/H1 MAPT genotype, semantic fluency <20 in 90s and pentagon copying score <2 (this has a positive predictive value for dementia of 58% at 5 years and 90% at 10 years)(Williams-Gray et al., 2013). The low risk group has the H2 genotype, semantic fluency >20 and pentagon copying score > 2 (positive predictive value for dementia 0% at 5 years, 29% at 10 years). It is also possible to calculate a patient's risk of a "poor outcome" five years after diagnosis (either postural instability, dementia or death) using age, motor UPDRS (axial score) and semantic fluency based on a predictive model developed by our group across two independent population based cohorts (Velseboer et al., 2016).

Although we have tools to predict prognosis in PD, our understanding of the underlying biological factors that determine disease progression and the development of dementia is limited. There is mounting evidence for the role of the immune system in disease susceptibility and it is also possible that immune factors may contribute to ongoing disease progression in susceptible individuals.

1.2.2 Neuropathology of PD

In common with many other neurodegenerative diseases, PD is characterised pathologically by aggregation of misfolded protein (alpha synuclein in the case of PD), inflammation (mainly in the form of microglial activation) and synapse loss.

Aggregated alpha synuclein is found in the form of Lewy bodies, primarily affecting the substantia nigra which is involved in the control of movement and some cognitive functions (Spillantini et al., 1997). Mutations in the SNCA gene that codes for alpha synuclein are associated with a range of clinical presentations of familial PD, confirming the pathological relevance of this protein (Goedert et al, 2013; Kara et al., 2014; Polymeropoulos et al., 1997; Singleton et al., 2003; Vekrellis et al., 2011). Other abnormal proteins including tau and neurofibrillary tangles are also found in the PD brain as well as amyloid pathology more typical of Alzheimer's disease (Irwin, Lee, & Trojanowski, 2013). The pathology and the clinical manifestations of PD, however, extend beyond the substantia nigra and include other brainstem sites, the cerebral cortex and also the autonomic and enteric nervous systems (e.g. the gut). There is evidence from post-mortem studies to suggest that the pathology may start in the gut or the olfactory epithelium and then spread to and through the brain via the vagal or olfactory nerves, initially into the brain stem and then beyond into the midbrain and out to the cortex (Braak et al., 2006). Inoculating mice with alpha synuclein pre-formed fibrils in the gastric wall results in aggregates in the brainstem (vagal nucleus) which supports this hypothesis (Uemura et al., 2018). Such findings have led to the prion hypothesis of neurodegenerative disease, with alpha synuclein acting in a prion like fashion, as it passes from one cell to another (Goedert, 2015) although this remains strongly disputed as PD is not 'contagious' in the same way as true prion disease. However, it is possible that

immune cells in the periphery and the CNS are involved with the transfer or clearance of alpha synuclein species.

The extent to which activated microglia or other immune cells contribute to cell death associated with this pathology and to the propagation and spread of alpha synuclein pathology is not known. It is also not clear how signals received from the peripheral immune system affect this relationship.

1.3 Parkinson's disease and inflammation

Over three decades ago, 'activated' microglia, the resident innate immune cells of the central nervous system (CNS), were described in post mortem PD brains (McGeer et al. 1988). They were defined as 'activated' based on their morphology (amoeboid, in preparation for adopting a more phagocytic phenotype) and expression of HLA-DR (from group II of the major histocompatibility complex (MHC)). MHC Class II molecules on the cell surface are involved in antigen presentation to CD4 T cells. The microglia were also noted to have melanin debris intracellularly suggesting that they had phagocytosed the pigmented neurons in the substantia nigra (McGeer et al., 1988). Imaging studies using the PET ligand PK11195 subsequently showed increased uptake in PD patients compared to controls, suggesting increased microglial activation (Gerhard et al., 2006). It has been difficult to disentangle whether this is just a secondary phenomenon or whether these activated microglia contribute to ongoing cell death, driving further disease progression.

With the advent of large scale genomics, genetic evidence suggests that the MHC locus is indeed involved in disease susceptibility and this is not just a bystander effect. There are now a number of genetic studies including large meta-analyses of genome wide association studies (GWAS) data from 13,708 cases and 95,282 controls demonstrating an association between SNPs in HLA-

DR and PD risk (Nalls et al., 2014). Data-driven pathway analyses of two independent GWAS showed an increase in pathways involved in 'leucocyte/lymphocyte activity' and also 'cytokine mediated signalling' conferring increased susceptibility to PD even after the known associations with the MHC Class II locus were removed (Holmans et al., 2013). Variants in the LRRK2 locus on chromosome 12 are also associated with PD: common variants modulating disease risk with a small effect size while dominant mutations are the commonest Mendelian genetic cause of PD. The same variants are also associated with inflammatory bowel disease (Hui et al., 2018). The physiological functions of this protein are unclear but it has been linked to the control of neurite morphology, vesicle trafficking, dopamine receptor homeostasis, regulation of immune pathways, autophagy and insulin signalling (Wallings, Manzoni, & Bandopadhyay, 2015).

There is also epidemiological evidence, including a meta-analysis of six large studies showing that non-aspirin NSAIDs have a protective effect on the incidence of PD with the effect particularly enhanced in regular users ((RR 0.71, 95% CI 0.58-0.89) (Gagne & Power, 2010) and one large prospective study in 136,137 people showing that ibuprofen (but not other NSAIDs) has a protective effect on susceptibility to PD (Gao et al. 2011). However, the most recent meta-analysis involving 17 studies and 2,498,258 participants (14,713 PD patients) showed no overall effect of NSAID use suggesting that the effect may only be true in certain sub-populations (depending on disease stage) or confounded by the indications for medication use (Poly et al., 2019). In an insurance-based US case-control study (48,295 incident PD cases and 52,324 controls), inosine monophosphate dehydrogenase inhibitors (including azathioprine) and corticosteroids were found to have a protective effect on PD incidence (Racette et al., 2018). The same authors found decreased incidence in a population who had received organ transplantation compared to controls (89,790 incident cases

of PD and 118,095 population based controls), speculating that this was due to the associated immunosuppression (Fan et al., 2019).

In PD, midbrain neurons are particularly vulnerable to pro-inflammatory cytokines (presumably mostly produced by neighbouring microglia) such as TNF-α and IFNγ (Kannarkat, Boss, & Tansey, 2013; Mount et al., 2007). Increased pro-inflammatory cytokines have been found in post mortem brain and CSF (including IL-6, IL1β, TGF-β and IFNγ) (reviewed in (Kannarkat et al., 2013)). In animals it is possible to model some aspects of PD (mainly midbrain dopaminergic cell loss) solely with the injection of LPS either into the brain or the periphery (Kannarkat et al., 2013). T cells from PD patients cause death of autologous induced pluripotent stem cell derived dopaminergic midbrain neurons in in-vitro cultures suggesting that this may be one relevant mechanism of neurodegeneration (Sommer et al., 2018).

An increase in central pro-inflammatory cytokines may be mirrored or driven by changes in the serum with evidence that there is elevation of peripheral cytokines in PD patients compared to controls. In a cross-sectional cohort, patients had significantly higher cytokine levels at baseline and in response to lipopolysaccharide (LPS) stimulation in vitro (MCP-1, RANTES, IL-8, IFNγ, IL1β,, TNFα)(Reale et al., 2009). We have now shown that this also has prognostic implications. In a cohort study based in Cambridge and Newcastle, our group found that a more pro-inflammatory serum cytokine profile was associated with more rapid motor and more impaired cognitive function over a three year period (Williams-Gray et al., 2016). We identified the 'pro-inflammatory' component from principal components analysis of the results from a ten cytokine panel.

A number of studies have looked at changes in the peripheral T cell compartment with some evidence to suggest chronic immune activation in the

periphery in PD patients compared with controls (e.g. (Baba et al., 2005)(Saunders et al., 2012)). More recently, alpha synuclein specific T cells have been described that are more frequent in PD patients compared to controls (Sulzer et al., 2017). Epitopes from one specific region of alpha synuclein (Y39) were displayed by HLA DRB5*01 and DRB1*15:01 (which are both associated with PD) suggesting an mechanistic link for the genetic association (Sulzer et al., 2017). During my PhD, our group described aberrant replicative senescence in T cells, in particular in CD8 cells which fail to develop the CD28loCD57hi phenotype, even in the context of prior CMV infection which typically drives this. Hence, altered T cell senescence in PD may affect the response to neurodegeneration (Williams-Gray et al., 2018). There is also a growing literature on monocytes in PD, with some evidence to suggest that there is ongoing peripheral activation (via a switch to 'classical' from 'non-classical' monocytes)(Grozdanov et al., 2014)(Kannarkat et al., 2013), again suggesting that activation of the immune response is associated with PD.

Modulating the immune response in animal models of PD improves disease outcomes. For example, in toxin induced animal models of PD, animals lacking mature lymphocytes (e.g. $RAG1^{-/-}$ mice), CD4 cells or T-Cell receptors show an attenuated disease course (Brochard et al., 2009) (Lira, Kulczycki, Slack, Anisman, & Park, 2011)). Targeting toll-like receptor4 (a receptor involved in recognising polysaccharide motifs, TLR4)(Noelker et al., 2013) and Fcγ receptors (He, Le, & Appel, 2002) also improves disease outcomes. Other therapies that have been successful in animal models (mainly rodent based models) include fingolimod, tanshinoine, dimethyl fumarate and thalidomide (reviewed in Martinez & Peplow, 2018).

Taken together, this suggests that the immune system may be playing a critical role in PD that is more than just a bystander effect or epiphenomenon. B

lymphocytes are an important part of the immune response. A decrease in circulating B lymphocytes or their transcripts in PD has been described (Gruden et al., 2012; Kedmi et al., 2011; Stevens et al., 2012). However, no studies to date have attempted to look at B lymphocyte subsets or function in PD or to interrogate the mechanism behind this observation. In addition, alpha synuclein-specific IgG antibodies have been described in PD, but their role is unclear with many conflicting studies (see later section on antibodies in PD and the systematic review and meta-analysis in chapter 3).

1.4 B lymphocytes

1.4.1 B lymphocyte development

B lymphocytes are part of the adaptive immune system although there are some B cells that have a more 'innate' role (B1 cells in the peritoneum and marginal zone B cells in the spleen) (reviewed in Abbas, AK, Lichtman, AH, Pillai, 2014), pg2).

At the simplest level, B lymphocytes are defined by their expression of clonally diverse cell surface immunoglobulin receptors that can recognise particular antigens. They begin their development in the fetal liver and then bone marrow with further development in secondary lymphoid tissue (lymph nodes and the spleen)(LeBien & Tedder, 2008). The main function of B cells has classically been viewed as antibody production following their terminal differentiation to plasma cells, but we now know that B lymphocytes have a number of other roles.

Early B cell development in the bone marrow involves the re-arrangement of immunoglobulin gene segments encoding immunoglobulin heavy chains (V_H, D_H and J_H) and light chains (V_LJ_L) (Pieper, Grimbacher, & Eibel, 2013). This

incredible process is capable of producing a B cell repertoire that can recognise millions of antigens. At the pre-B cell stage the nascent IgM molecule is only found in the cytoplasm, moving to the cell surface in the immature B cell which then leaves the bone marrow to circulate in the blood to secondary lymphoid tissues (the spleen and lymph nodes mainly but also mucosal tissues, Peyer's patches and possibly the meninges) where they differentiate into naïve, follicular or marginal zone B cells (Pieper et al., 2013). Chemokine and cytokine gradients drive subsequent movement of B cells back into circulation (e.g. sphingosine-1-phosphate) or back into lymph nodes or germinal centres (e.g. CXCL13). Figure 1-1 gives a broad overview of this process, showing the major developmental points, from an immature B cell to a transitional B cell (which is also one of the B cell subsets that produces the regulatory cytokine IL10). Subsequently, the B cell may become a follicular B cell where upon encountering antigen and co-stimulatory signals from follicular T helper cells (including CD40L/CD40, ICOS-ICOSL and CD28/CD86) it can enter the germinal centre reaction where, via a process of clonal selection and somatic hypermutation, more specific antibodies are generated to the antigen (with subsequent class switching from IgM to IgG, IgA or IgG). The B cells then either differentiate into long lived plasma cells (homing back to bone marrow) or to memory B cells which retain the capacity to recognise antigen and proliferate in response to re-challenge for decades (at least in humans)(see Figure 1-1) (Clatworthy, 2014).

Figure 1-1

B cell maturation and development

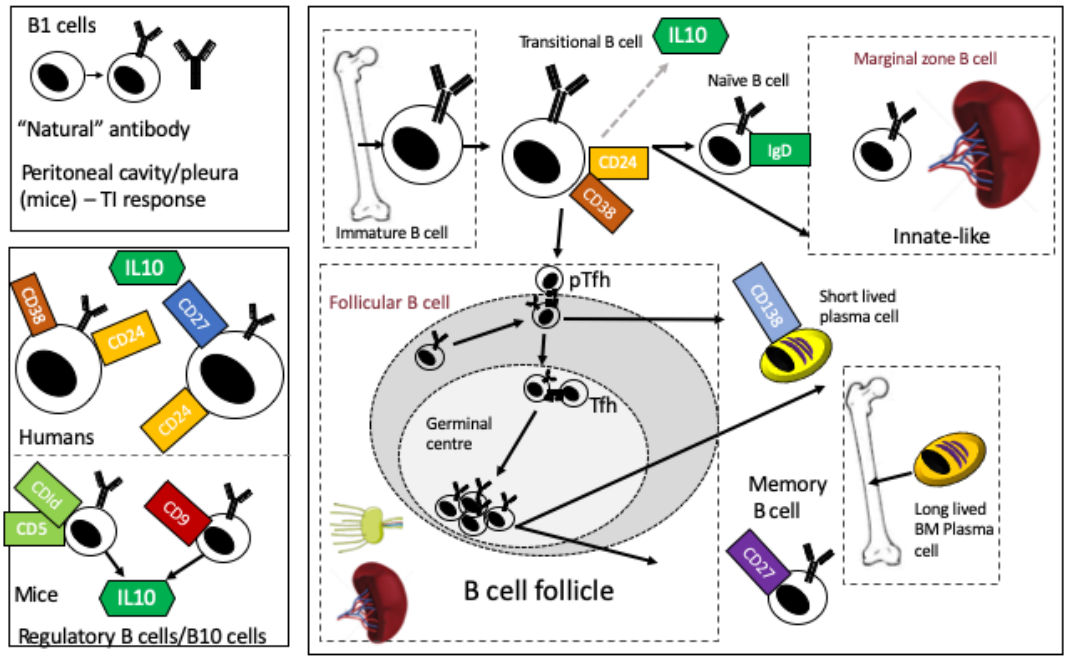

Figure 1-1 B1 cells are found in the peritoneum and in the pleura where they have been described in mice, producing low affinity 'natural' antibodies to T-independent antigens (such as polysaccharides). The remainder of B cells are considered "B2" cells. Immature B cells will move from the bone marrow into the circulation, becoming transitional B cells (shown here as CD24HICD38HI cells) (some of which are capable of producing IL10). They then go to lymphoid tissue becoming naïve (characterised by surface expression of IgD), follicular or marginal zone B cells. After encountering antigen follicular B cells will move to the T-B border in lymph nodes or the spleen and present antigen to T cells (pre-T follicular helper cells pTfh). The B cell will then either become a short lived plasma cell or enter a germinal centre reaction helped by T follicular helper cells (Tfh), going through somatic hypermutation leading to class switching (from

IgM to IgG, IgA or IgE) to form a long lived memory B cell (identified by surface expression of CD27 in humans) or a plasma cell (identified by CD138 and CD38). Regulatory B cells may be derived from transitional B cells or can be induced by cytokine stimulation and are defined by different markers in humans and mice (CD38HICD24HI in humans and CD5+CD1d+ or CD9 positive cells in mice).

1.4.2 Potential mechanisms underlying antibody generation in PD

B lymphocytes can produce antibodies via T cell-independent (TI) and T cell-dependent pathways (TD) (see Figure 1-2) . TI pathways involve the recognition of multimeric carbohydrate and lipid antigens by the B cell receptor (BCR) or by toll-like receptors (TLR) on the cell surface of "B1" cells (or marginal zone B cells in the spleen). This leads to the production of polyreactive IgM that binds with low affinity and can facilitate the removal of blood borne encapsulated organisms (LeBien & Tedder, 2008). Antibodies produced in this context are called 'natural antibodies'. Most of the literature on alpha synuclein antibodies suggests that these are natural antibodies (Besong-Agbo et al., 2013; Brudek et al., 2017; Heinzel et al., 2014; Kronimus et al., 2016). Natural antibodies are part of innate immune surveillance against pathogens or cell damage and are present from an early point in development (Panda & Ding, 2015). They are predominantly IgM but IgG and IgA natural antibodies have also been described (Panda & Ding, 2015). Antibodies to alpha synuclein epitopes could be generated via this process.

The recent description of alpha synuclein specific T cells in patients with PD (Sulzer et al., 2017) supports the thesis that alpha synuclein antibodies may also be generated by a TD response. These antibodies recognise protein antigens and their production requires a cognate interaction between "B2" cells and CD4 T

cells. This facilitates iterative rounds of somatic hypermutation and clonal selection within a germinal centre reaction to generate class-switched, long lived plasma cells or memory B cells capable of initiating a secondary response upon further encounter of the antigen (Panda & Ding, 2015). The plasma cells that arise from this process are able to produce large quantities of specific, high affinity class-switched antibodies (LeBien & Tedder, 2008). Humoral responses to self-antigen are limited by negative selection of self-reactive clones during B cell development.

However, if the self-antigen is modified sufficiently, as in the case of alpha synuclein toxic species, and is present in an immunogenic context, such as cell death, some B cell clones may be activated to produce alpha synuclein antibodies. Such an antibody response might change over time; firstly IgM may dominate, but with progression of the germinal centre reaction, there is class switching to IgG or IgE. Secondly, with persistent exposure to neo-antigen, clones with higher levels of somatic hypermutation and higher affinity antibodies would be selected. Thirdly, the overall level of alpha synuclein antibody might change with age, as older age is associated with decreasing antibody response to antigens (e.g. vaccines) and immunosenescence of the B cell compartment (Aw, Silva, & Palmer, 2007).

Figure 1-2

Possible mechanisms of antibody generation in PD

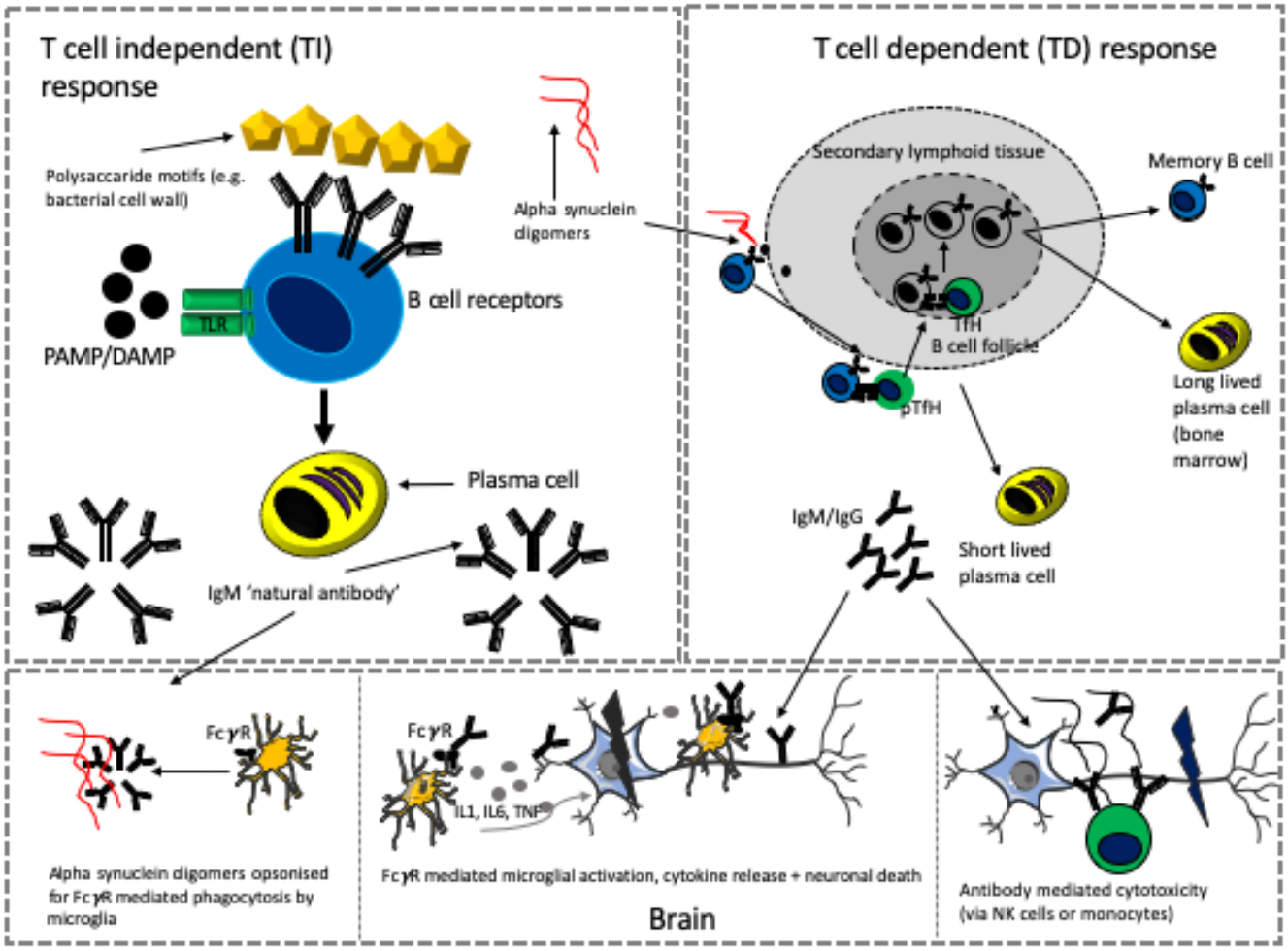

Figure 1-2 A modified version of this figure has been published in (Scott et al., 2018). It illustrates TI and TD dependent mechanisms of antibody generation and subsequent neuronal cell death after Fc gamma receptor medication phagocytosis, Fc gamma receptor mediation microglial activation and subsequent cytokine release (IL6/TNFalpha are neuro-toxic) and antibody mediated cytotoxicity towards neurons opsonised by antibody.

B cell activation to generate plasma cell-producing antibodies generally occurs within secondary lymphoid organs (lymph nodes and spleen) but may also occur in tertiary lymphoid follicles that develop in inflamed tissues. The site of B cell activation to generate alpha synuclein-specific responses is unclear and may be peripheral or within the CNS. Follicles have been described in the meninges of patients with multiple sclerosis (Magliozzi et al., 2006), with the potential to generate CNS localised antibodies, but whether such structures exist in PD is unknown.

The most common circulating antibody isotype is IgG, that can readily initiate and propagate inflammation by activating complement and engaging cell surface antibody receptors (Fcγ receptors (FcγR)) that are expressed by most innate immune cells. Antibodies bind non-specifically to Fcγ receptors on other immune cells (e.g.phagocytes, monocytes, dendritic cells) or via engagement of their Fc region with complement components (Willcocks, Smith, & Clatworthy, 2009). Different subclasses of IgG (IgG1, IgG2, IgG3 and IgG4) have different affinities for the FcγR on cells which can be either activating or inhibitory (see (Willcocks et al., 2009). There is evidence that FcγRI and FcγRIIB/C are required for uptake of alpha synuclein by CNS derived cells (human neuroglioma) in culture and that this is mediated by the presence of alpha synuclein specific antibodies (Gustafsson et al., 2017). One recent paper suggested that FcγRIIB (a low affinity inhibitory Fc receptor) is not only responsible for the inhibition of phagocytosis of alpha synuclein fibrils (via low affinity binding with the fibrils themselves) but also mediates cell to cell transmission of alpha synuclein (Choi et al., 2018). In addition, the glycosylation status of immunoglobulin also affects downstream binding and effector function (Jennewein & Alter, 2017). A study investigating the IgG glycome in PD showed significant differences between patients and controls, with the authors concluding that the changes observed in PD may result in enhanced Fcγ RIIIa-mediated antibody-dependent cellular

cytotoxity (with the potential to contribute to chronic inflammation) (Russell et al., 2017). Our group found recently that autologous serum significantly increased monocyte phagocytosis (which was increased in early moderate PD compared to controls)(Wijeyekoon et al., 2018). It is possible that this was due to the presence of antibodies in the serum but this requires further confirmation.

The presence of alpha synuclein specific antibodies in early PD could potentially contribute to pathology by exacerbating local inflammation in the brain, promoting neuronal damage and causing disease progression. Consistent with this hypothesis, IgG isolated from PD patients and injected into the rat substantia nigra causes selective dopaminergic cell death that was absent in animals receiving control IgG (Chen et al., 1998). There is also attenuation of disease in Fcγ receptor knockout mice receiving PD IgG, confirming that activation of microglia by PD IgG is pathogenic (He et al., 2002). Approximately 30% of dopaminergic cells in the substantia nigra of post mortem human PD brains were bound by IgG highlighting that immunoglobulins do cross the blood brain barrier in PD and may play a role in disease (Orr et al., 2005). Alternatively, alpha synuclein auto-antibodies may play a protective role, facilitating the clearance of toxic protein species by opsonizing alpha-synuclein for FcγR-mediated uptake by phagocytes. Consistent with this hypothesis, the passive peripheral transfer of alpha-synuclein specific antibodies in some mouse models of PD improved disease outcomes (Masliah et al., 2005). Trials of both passive and active immunization therapies targeting alpha synuclein are underway (Takamatsu et al. 2017).

1.4.3 B lymphocytes: antibody independent functions

Regulatory B cells

Like other arms of the immune system, B lymphocytes can be divided into immune effectors and immune inhibitors . The inhibitors, or "regulatory" B cells provide a brake on immune activation. Unlike their well described counterparts, T regulatory cells they are not defined by a single transcription factor (FoxP3 in the case of Tregs) and work via several different pathways to inhibit either T cell or innate immune activation. Several subsets of B cells are able to act as immunoregulatory cells (Blair et al., 2010; DiLillo, Matsushita, & Tedder, 2010; Iwata et al., 2011; Mauri & Bosma, 2012). They primarily exert their effect via the production of IL-10 and are therefore called sometimes referred to as "B10" cells or more generally as regulatory B cells. IL10 produced by B cells is able to induce T regulatory cells, to attenuate monocyte and macrophage activity and to decrease CD4 cell activation in co-culture assays and in disease model mice (e.g. in particular TH_1 type responses in collagen induced arthritis and in experimental autoimmune encephalitis EAE)(Mauri & Menon, 2015). There are an increasing number of B cell subsets and markers that have been described as regulatory B cells (which act via several pathways in additional to IL10). In mice, the most commonly used surface markers are CD1d and CD5 but studies have also described IL10 producing, marginal zone B cells, TIM-1+ B cells, plasmablasts, plasma cells (also acting via IL-35) $PDL1^{hi}$ cells (acting via PDL1). In humans, the IL10 producing subset is usually identified by an immature transitional subset (CD27-) $CD24^{hi}$ $CD38^{hi}$ (acting via PDL1 or IL10), or as B10 cells $CD24^{hi}$, CD27+ (IL10) but also as being $CD25^{hi}$, $CD71^{hi}CD73^{lo}$ (acting via both IL10 and IgG4) (markers in both humans and mice are reviewed in (Mauri & Menon, 2015). As one might expect, deficiencies of regulatory B cells in mouse models and human disease are associated with increased severity of auto-immune or inflammatory diseases (e.g. systemic lupus erythematosus and

rheumatoid arthritis) whilst offering some protection from infection (Mauri & Bosma, 2012; Mauri & Menon, 2015).

Apart from their role in regulation, B lymphocytes are also able to produce pro-inflammatory cytokines such as IL6 (Barr et al., 2012), stimulate the innate immune system (via the production of granulocyte macrophage colony stimulating factor GM-CSF (Rauch et al., 2012) and are required for the maintenance of sub-capsular sinus macrophages (Moseman et al., 2012). B1 B cells respond to pathogen associated molecular motifs (PAMPs), acting like innate immune cells (mainly in the peritoneum in mice).

There is also evidence that there are changes in the B lymphocytes that accumulate with age including impaired vaccine responses, a decrease in B cell diversity and an increase in memory B cells reflecting increase antigen exposure over a life time (Frasca, 2018). This is also reflected in an increase in a group of B cells that are terminally differentiated and adopt a 'senescence associated secretory profile' (SASP) (increased secretion of IL-6, IL-8 and TNFα) and identified by a 'double negative' phenotype (CD27-IgD- B lymphocytes)(Frasca, 2018). In mouse and humans, a separate subset, age associated B cells (ABC's) have been identified by their expression of the transcription factor T-bet and surface markers CD11c, CD80 and CD86. (Karnell et al., 2017; Rubtsov et al., 2011; Rubtsova, Rubtsov, Cancro, & Marrack, 2015). These are associated with auto-immune disease, infection and increasing age (Karnell et al., 2017) but have not been described in neurodegenerative disease or PD.

B lymphocytes are therefore an important branch of the immune system, performing multiple roles in interaction with T cells and the innate immune system and that may change during the aging process. Differences in B cell subsets and function have not been described in Parkinson's disease.

1.4.1 Examples of the involvement of B lymphocytes in other diseases

In the past autoimmune and inflammatory disorders were categorised as either antibody mediated (mainly involving B cells) such as Graves' disease or systemic lupus erythematosus (SLE) or T cell mediated (Multiple Sclerosis, type I diabetes or rheumatoid arthritis). More recently, it has emerged that this dichotomy is an oversimplification as there is in fact a complex interplay not only between B lymphocytes and T lymphocytes but also between the adaptive and innate branches of the immune system. All of the B cell functions described above can contribute to auto-immunity or inflammation not just antibody production.

Systemic lupus erythematosus has been traditionally thought of as a classic B cell antibody mediated disease (Hampe, 2012). B cells play a role in disease primarily by the production of antibodies to nuclear components including double stranded DNA, RNP particles (anti-Ro, anti-La and anti-Sm) and histones. There are several alterations in B cell subsets in addition to this: increased memory B cells (with a lower activation threshold) and exaggerated b-cell receptor (BCR) responses (Karrar & Cunninghame Graham, 2018). Immune complexes become deposited in tissues such as the kidney where they bind to Fc receptors and activate complement, recruiting neutrophils and NK cells and leading to further inflammation and ultimately organ damage. Serum transfer from affected animals in mouse models of lupus causes disease to previously unaffected animals (nephritis)(Cheng et al., 2013) providing direct evidence for the pathogenicity of the antibody. However, another study used mice expressing a transgene allowing surface expression of immunoglobulins but not circulating immunoglobulins (ie.no antibody production). The mice still developed disease (again, nephritis) suggesting that other aspects of the B cell response were involved (possibly antigen presentation to T cells or local cytokine secretion)(Chan et al., 1999). B cell depletion in SLE was less effective than

expected with depletion occasionally worsening symptoms and two trials of rituximab (an anti-CD20 monoclonal antibody) failed to meet their primary endpoints (although belimumab, a humanised monoclonal antibody to BAFF is now licensed as a treatment in refractory SLE)(Hampe, 2012; Thaunat, Morelon, & Defrance, 2010). This may be to do with the selection of patients, timing and how the balance between regulatory and effector arms of the B cell response is affected.

In Parkinson's disease, the involvement of B cells is likely to be a secondary phenomenon that then contributes to ongoing disease progression rather than being a primary auto-immune disorder like SLE. As described previously, PD may share some mechanisms with SLE, such as non-specific Fc receptor activation and subsequent local inflammation due to immunoglobulins bound to neurons or alpha synuclein in the brain (see previous section).

Type I diabetes (T1DM) on the other hand was viewed until recently as a primarily T cell mediated disorder. However, it has now been shown that B cells present beta cell antigens to T cells. Mouse models deficient in B cells do not develop diabetes and mice with MHC Class II deficient B cells are also protected, reviewed in (Hampe, 2012). It has now also been shown that B cell depletion is an effective treatment in T1DM (Pescovitz et al., 2009). The current model for disease pathogenesis is that pancreatic beta cell antigens are recognised and taken up by the BCR on B cells and then presented to CD4+ T cells via MHC Class II. These activated T cells then provide further T cell help to the B cells facilitating the differentiation into plasma cells and secretion of autoantibodies. These then bind to Fcγ receptors on other immune effector cells causing further inflammation and tissue destruction.

These examples highlight the fact that B lymphocytes play very different roles in different inflammatory diseases (and even different roles at different time points in the same disease). One common criticism of my work from other neurologists is that PD does not look like MS (clinically, demographically, pathologically or in the expression profile of post mortem brains (Filiou et al., 2014) and therefore 'inflammation' cannot be involved in its pathogenesis. I have argued that we are seeing a different inflammatory response in PD (compared to MS) which is still harmful and important to address. Given that the immune response is different even within canonical inflammatory or auto-immune conditions, it is not unreasonable to look for an inflammatory response unique to or more typical of neurodegenerative disorders.

1.5 Meningeal immunity

During my PhD, meningeal lymphatics were re-discovered having been originally described by an 18th century Italian neuroscientist who was then forgotten (Aspelund et al., 2015; Da Mesquita, Fu, & Kipnis, 2018; Louveau et al., 2018). Mass cytometry using CyTOF has shown that B lymphocytes form a significant proportion of meningeal immune cells (Korin et al., 2017). Meningeal lymphatics have now also been described in human imaging studies using MRI (Kuo et al., 2018). In addition, there is evidence that the skull bone marrow niche harbours a subset of cells that are responsive to immune signals from the brain and can communicate with the brain parenchyma and meninges via tiny channels in the bone (Herisson et al., 2018). Ablating the meningeal lymphatics, presumed to be draining the CNS results in worsening disease in amyloid, tau and alpha synuclein mouse models of neurodegenerative disease (Da Mesquita, Louveau, et al., 2018; Louveau et al., 2018; Patel et al., 2019; Zou et al., 2019). Improving lymphatic drainage with vascular endothelial growth factor rescued these deficits in a model of AD (Da Mesquita et al., 2018). This compartment is

likely to be relevant to all diseases affecting the CNS. Given the substantial representation of B cells within the meningeal immune compartment, they are likely to play a key role.

1.6 Overall hypothesis

B lymphocytes play a critical role in driving disease progression in PD by contributing to a pro-inflammatory milieu in the periphery which in turn alters microglial and neuronal homeostasis (via signals received from the meningeal B cell population) resulting in increased destruction of dopaminergic and other neurons in the brain, contributing to ongoing disease progression. This B lymphocyte response is likely to be, at least in part, antigen specific given that there is pathological aggregated alpha synuclein present in the periphery (the gut) and the CNS. Some subsets of B cells may also play a regulatory role via IL10 production.

Figure 1-3

Simplified schema showing the hypothesised relationships between peripheral and central inflammation

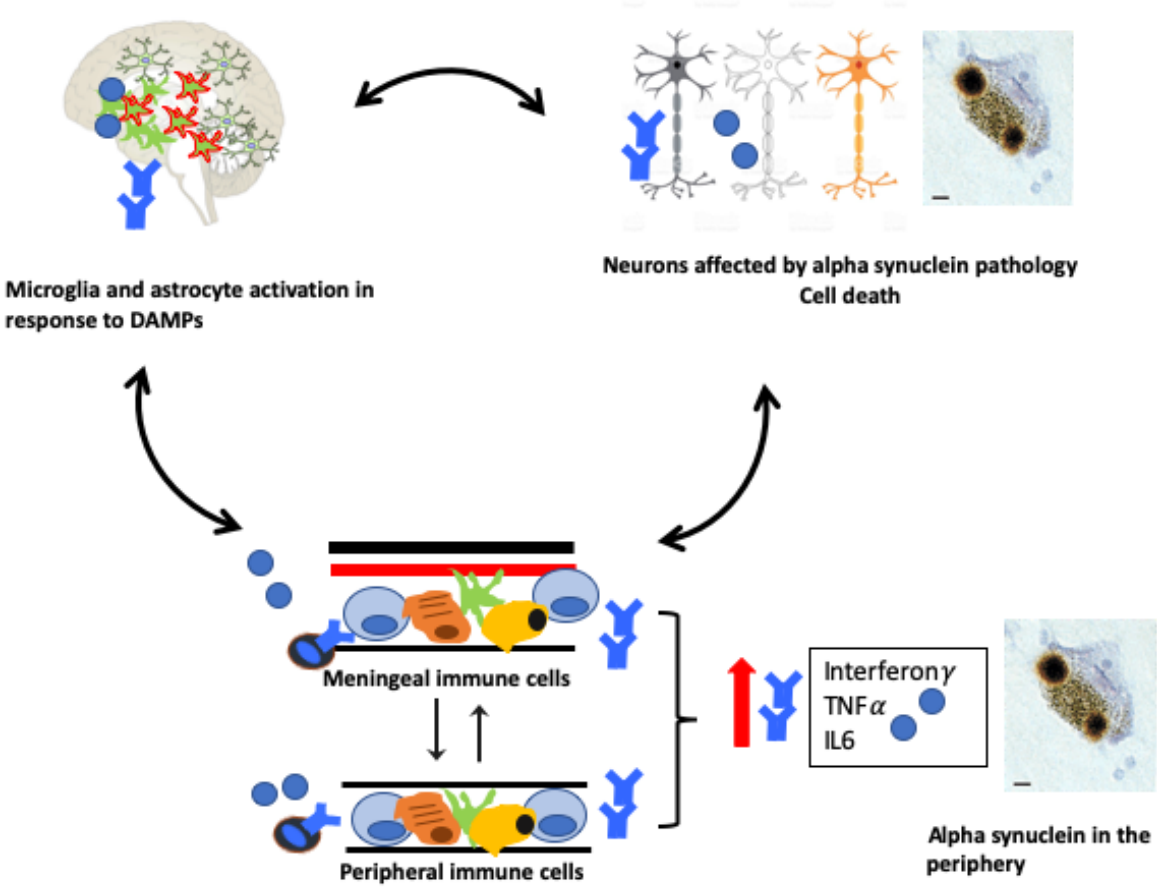

Figure 1-3 shows an overview of my overall hypothesis linking peripheral immune activation (shown here as increased levels of pro-inflammatory cytokines) in association with alpha synuclein pathology (e.g. in the gut). This is associated with (and possibly drives) microglial activation in the brain which contributes to ongoing neuronal cell death (again associated with alpha synuclein pathology). B cells specifically are likely to contribute to the peripheral immune activation via the production of cytokines and antibodies which cross the blood-brain barrier, contributing to a pro-inflammatory milieu in the brain that drives disease progression.

2 B LYMPHOCYTES IN PD

2.1 Chapter abstract

Background
Previous studies suggest there may be a decrease in the number of circulating B lymphocytes in PD. Whether this is of pathogenic significance is unknown.

Hypotheses:
There will be evidence of increased activation in the B lymphocyte compartment in PD patients compared to controls and in patients at high risk of dementia versus those at lower risk

Aims
To establish whether there is an alteration in the B lymphocyte number or phenotype of circulating B lymphocytes in patients with PD compared to matched controls
To investigate whether B lymphocyte phenotype correlates with any measures of disease severity.
To perform a pilot study looking for B lymphocytes in the cerebrospinal fluid (CSF)of patients and controls

Methods
Patient studies were done across three cohorts (see Figure 2-1). Peripheral blood mononuclear cells were extracted from blood samples from a total of 79 patients and 65 controls with early PD. CSF samples were available from 18 PD patients and 4 controls. Immunocytochemistry and flow cytometry were used to identify major B lymphocyte subsets using cell surface markers. Cryopreserved cells from a subset of patients were stimulated in vitro and intracellular production of cytokines (IL6 and IL10) was assessed by flow cytometry. Patients were stratified according to their risk of dementia using three biomarkers (MAPT haplotype, pentagon copying score and semantic fluency from the Addenbrooke's Cognitive Examination-Revised (ACE-R).

Results
The proportion of circulating B lymphocytes was reduced when comparing 41 patients to age, gender and genotype matched controls (cohort 1: controls mean 5.7% [SD 2.8], PD mean 4.6% [SD 2.6]; cohort 1, paired t-test $t[34] = 2.08$, $p = 0.04$) as described in other studies. This difference was largely driven by the group at high risk of dementia (Paired t-test for N=7 pairs, ($t[6] = 3.42$, $p = 0.01$). Cells from high risk patients produced more cytokines than those from the other risk groups (mixed measures ANOVA, IL10 $F[2,25 = 3.6$, $p =0.041$, IL6 $F [2,25] = 3.49$, $p = 0.046$). Data from two cohorts showed that transitional B cells (defined by CD27-CD24HICD38HI), a population enriched for IL10 producing B cells were associated with better motor outcomes on the UPDRS ($p = 0.0009$). This subset has been described as regulatory. The phenotype of B lymphocytes in the CSF was skewed towards a memory phenotype compared to the peripheral circulation.

Conclusions
Abnormalities in the B lymphocyte compartment are associated with disease susceptibility and severity. These results are consistent with the conclusion that B lymphocytes play a protective role in PD. In particular, having a larger transitional B cell pool appears protective. Testing drugs that expand this population would be an interesting therapeutic strategy to pursue. .

Figure 2-1

Clinical studies summary diagram

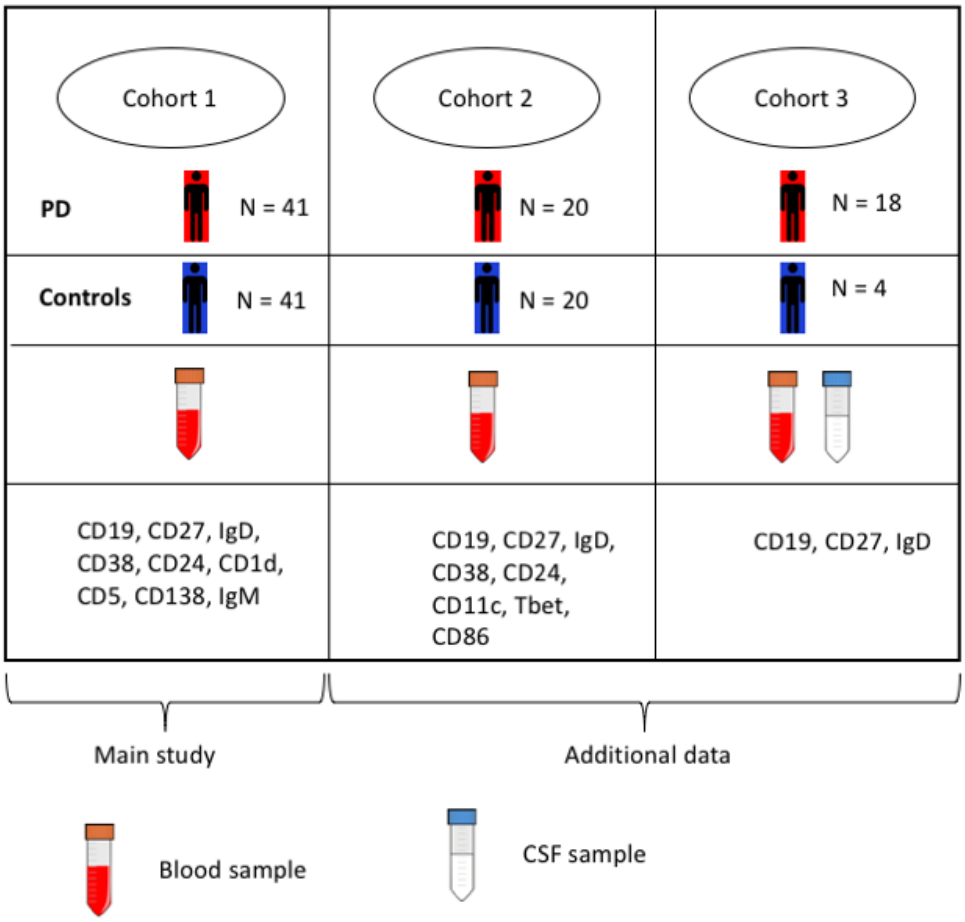

Figure 2-1: Overview of clinical studies by cohort. Cohort one patients and controls were specifically matched for age, gender and genotype and all assays were carried out in control/patient pairs to minimise the effect of inter-assay variability on group differences. The other cohorts were matched overall. The bottom panel shows the cell surface markers used in each study. CD19 is a surface marker identifying B cells, CD27 and IgD are used together to identify naïve B cells (characterised by surface expression of IgD, negative for CD27) and memory B cells (CD27 positive, IgD negative). IgM is also a surface immunoglobulin on mature naïve B cells. CD38 and CD24 are used to identify

transitional B cells (which are thought to be one of the IL10 producing subsets) (CD27-CD24HICD38HI). CD1d and CD5 were chosen as these mark an additional subset of regulatory B cells in mice (but this is not consistently the case in clinical samples). CD138 was chosen along with CD38 to identify plasma cells (which are infrequent in circulating blood). In cohort 2, additional markers were used to identify age associated B cells (Tbet, CD11c, CD86). Cohort 3 was a pilot study to look at whether it is possible to identify B lymphocytes in the cerebrospinal fluid (CSF) of patients and controls.

2.2 Methods

2.2.1 Participants (Cohort 1, Immune study in PD)

The study was approved by the Cambridgeshire Research Ethics Committee (03/303). Written, informed consent was obtained from all participants in accordance with the Declaration of Helsinki.

Inclusion criteria were fulfilment of the UK PD Brain Bank Criteria for a diagnosis of definite PD (made by neurologist), age 55-80 years and early stage disease (Hoehn and Yahr stage ≤ 2). Exclusion criteria included the presence of other neurodegenerative disorders, chronic inflammatory of autoimmune disorders, current clinically significant infection, surgery in the last month, vaccinations in the previous 3 weeks or recent use of anti-inflammatory or immunomodulating medication (steroids in the previous three months, high dose aspirin >75mg in the previous 2 weeks, ibuprofen and other non-steroidal anti-inflammatory drugs in the previous 2 weeks or any long term immunosuppressant drugs such as azathioprine, mycophenolate, methotrexate, rituximab or other biological therapies in the last year).

An interim power calculation was performed based on pilot results from 5 patients and 5 controls with the results suggesting that 23 partipants were required in each group to obtain 80% power. Given likely variability and the possibility of assay failure we aimed to recruit 40 in each group to ensure that the study was adequately powered.

The patients were stratified into groups at high, intermediate and low risk of dementia using predictive factors identified in a longitudinal cohort study (Williams-Gray et al., 2009). The stratification was done on the basis of their MAPT (tau) genotype, pentagon copying ability and semantic fluency score (the

high risk group was defined as MAPT H1/H1 genotype and any one of either semantic fluency <20 in 90s or pentagon copying score <2, the intermediate group had any one of these factors and the low risk group had none)(as in (Williams-Gray et al., 2018). Their overall probability of a 'poor outcome' (either dementia, postural instability or death) was also calculated using a combination of age, UPDRS axial score and semantic fluency score (Velseboer et al., 2016).Dementia in this context is used as a proxy to measure disease progression (as it suggests involvement of brain regions outside the substantia nigra and impairments involving other neuronal populations beyond dopaminergic cells where the pathology is thought to start).

Age, gender and MAPT-genotype matched controls were recruited from the NIHR Cambridge Bioresource (http://www.cambridgebioresource.org.uk/). Controls had no history of neurological disease, memory problems or depression. Exclusion criteria were the same as for the PD patients. Samples from matched patient and control pairs were processed on the same day with collection occurring in the morning (between 9 and 11am).
All patients went through a full clinical assessment including medical history and co-morbidities, the Movement Disorder Society Unified Parkinson's Disease Rating Scale (MDS-UPDRS), the Addenbrooke's Cognitive Examination (ACE-R), assessment of semantic fluency (animal naming in 90s), pentagon copying and the Beck Depression Inventory (BDI). The overall probability of a bad outcome (either postural instability or dementia) was calculated using a validated tool which uses axial components of the UPDRS, age and animal fluency (Velseboer et al., 2016).

Up to 50mL of venous blood was collected from each patient or control using a combination of lithium heparin tubes for peripheral blood mononuclear cell (PBMC) isolation, clotted tubes for serum collection and

ethylenediaminetetraacetic acid (EDTA) tubes for full blood counts. Clotted samples were left at room temperature for 15 minutes before centrifuging at 2000RPM for 15 minutes. Serum was collected and stored in 200µl aliquots at -80°C for subsequent use. Patients attended three times over a 4-5 week period in order to obtain repeat serum samples to validate baseline cytokine levels and to provide serum for subsequent analysis looking at auto-antibodies.

2.2.2 PBMC extraction, immunocytochemistry and flow cytometry

Peripheral blood mononuclear cells (PBMC) were isolated from heparinised blood using a Ficoll gradient within 2 hours of phlebotomy. The PBMC layer was removed and washed twice with PBS. Depending on the total number of cells, excess cells were frozen in freezing medium (90% foetal calf serum [FCS, Sigma Aldrich F7524] and 10% dimethyl sulfoxide [DMSO, Sigma Aldrich D8418]) and placed in a cryopreservation chamber at -80°C.

Surface staining was done on both fresh and frozen cells initially as part of the optimisation of the protocol. Frozen cells were placed on ice and allowed to warm up after being diluted with foetal calf serum (FCS) and subsequently placed in a 15mL Falcon tube. To reduce variation due to batch effects, I had planned to use frozen cells stained in batches. Due to some variability in staining of some of the surface markers and variable yield of live cells from frozen aliquots I then continued using only freshly obtained ex vivo cells for the final protocol (data not shown).

Cells were resuspended at a concentration of 1 x 106 per 100µl of FACS buffer for staining plus 2% mouse serum (0.1% BSA, Probumin. Millipore, cat. no. 82-045-1, 0.01% sodium azide, Sigma Aldrich, cat. no. S2002 made up in Phosphate Buffered Saline [PBS], mouse serum Sigma Aldrich, cat. no. M5905). Cells were

left to block for 10 minutes at 4°C. In the final protocol, 0.5µL of zombie acqua was added after blocking and left to incubate for 15 minutes prior to the addition of surface staining antibodies.

Antibodies were added in appropriate concentrations after titration experiments. The final surface staining panel is below (see Table 2-1 and Appendix II for details). Antibodies were incubated with the cells at 4°C. centigrade in the dark for 20 minutes. The cells were subsequently spun and washed twice in FACS buffer before being fixed in 2% paraformaldehyde (PFA) for 20 minutes. Cells were then washed twice with FACS buffer prior to being placed in FACS tubes for analysis. Flow cytometry was run within 2-4 hours of staining for all samples. Isotype controls were used for all panels to asses non-specific binding and to confirm gating of cell populations. FCS output files were imported into FlowJo software (version 10.5.0) which was used for initial gating of the cell populations which was done blinded to group.

Table 2-1

Final antibody combinations for surface staining of human PBMCs

Staining antibody	Volume (µL)	Compensation antibody	Volume (µL)
BV786 CD19	3	BV786 CD19	3
FITC CD5	2	FITC CD19	4
BV605 CD24	5	BV605 CD19	2
BUV 395 CD27	3	BUV395 CD27	3
APC CD38	10	APC CD19	2
PE IgM	10	PE CD19	2
V450 CD138	5	V450 CD19	3
APC H7 IgD	2	APCH7 IgD	2
PerCp Cy5.5 CD1d	3	PerCp Cy5.5 CD19	3
Live dead zombie aqua	0.5	Live dead zombie aqua	0.5

2.2.3 Alpha synuclein measurement

Alpha synuclein was measured using Meso Scale Discovery (MSD) human alpha synuclein kit (K151TGD-2) following the manufacturer's instructions. Serum samples were defrosted and handled on ice before being used immediately. Calibrators were prepared using solutions of known concentration to create a 7 point calibration curve with four fold serial dilution and a zero calibrator blank. All samples and calibrators were run in duplicate. Samples were diluted using the manufacturer provided diluent (8 fold dilution). The plate was blocked with proprietary diluent (number 35) and incubated with shaking for one hour. The plate was then washed three times with 150µl of PBS-tween 20 (Sigma Aldrich P1279) (PBS-T)(0.05%). Detection antibody solution was added at a volume of 25µl. Sample or calibrator solutions were then added at a volume of 25µl. The plate was sealed and incubated at room temperature with shaking for 2 hours. After incubation, the plate was washed with PBS-T three times and then 150µl of read buffer was added and the plate was read on an MSD plate reader (Sector S 600). The concentrations were calculated from the standard curve using a least squares fitting algorithm generated by Discovery Workbench Software (MSD).

2.2.4 B cell activating factor (BAFF) ELISA

Serum samples were collected as described above and stored at -80 degrees centigrade. Samples were defrosted on wet ice and the ELISA was run within 24 hours. BAFF was measured using the Abcam BAFF Human ELISA kit (ab119579) as per the manufacturer's instructions. Briefly, standards were prepared by using a 10ng/ml stock solution of recombinant human BAFF which was diluted to a final concentration of 4,000pg/mL for standard 1. Subsequent standards were

made using serial four fold dilutions. The last standard was blank. Serum samples were diluted 1:1 with sample diluent. 100µl of either sample or standards were added to the plate and incubated at 37 degrees centigrade for 90 minutes. The contents of the well were then discarded and 100 µl of biotinylated anti-human BAFF antibody was added and incubated for 60 minutes at 37 degrees centigrade. The plate was then washed three times with PBS. After washing, 100 µl of Avidin-Biotin-peroxidase complex solution was added to each well and incubated at 37 degrees for 30 minutes. The plate was then washed five times with PBS. TMB colour developing agent was then added (90 µl) per well and the plate was incubated at 37 degrees for 20 minutes. 100 µl od TMB Stop solution was added after incubation and the optical density (O.D) absorbance was read at 450nm using a microplate reader. Serum concentrations were estimated based on the standard curve generated for each plate. Serum from one control individual was run on all plates for the purposes of normalising the data across plates.

2.2.5 B lymphocyte stimulation

I selected standard reagents used for B lymphocyte stimulation (also described in (Wagner et al., 2004)). CpG DNA is a pathogen associated molecular motif (PAMP) recognised by toll-like receptor 9 which is predominantly expressed on B lymphocytes. CD40 ligand is expressed on a number of cells (T cells, B cells, dendritic cells and macrophages) and is known to activate B cells, inducing proliferation, class switching and antibody secretion (Wykes, 2003). Phorbol 12-myristate 13-acetate (PMA) and ionomycin are non-specific immune activators that work by increasing intracellular calcium. Brefeldin inhibits transport of protein from the endoplasmic reticulum to the golgi apparatus thereby preventing the secretion of cytokines.

PBMC's were obtained as for surface staining. As part of the optimisation of this protocol, initially the stimulations were performed on ex vivo cells and subsequently on frozen PBMC's to allow for larger batches to be done at the same time. For the clinical study, PBMC's were aliquoted into 1 x 10^7 aliquots and resuspended in 1ml of 10% dimethyl-sulfoxide (DMSO) (DMSO, Sigma Aldrich D8418]) in fetal calf serum (FCS). They were placed into a Mr. Frosty for 48 hours and subsequently stored at -80 degrees centigrade.

Alpha synuclein preparation

Alpha synuclein monomers (from rPeptide, S-1001-2) were suspended in MilliQ water. Using the Amicon Ultra 3K, samples were concentrated and resuspended to make a solution of 10mM Tris-HCl, pH 7.6, 5µg/µl concentration. Lastly the tubes were placed in a 37°C thermomixer and shaken for 7 days at 1,000 RPM. Preparation of alpha synuclein fibrils was kindly done by William Kuan, a post doc in the Barker lab. Fibrils were stored in aliquots of 20µl at -20°C. Prior to use, they were defrosted and sonicated with 60 pulses and 10% power to ensure that the aggregates were not too large.

Final protocol

PBMCs were removed from the freezer and placed on wet ice with 1mL of 10% FCS until thawed enough to be transferred to a 15ml Falcon tube containing 10% FCS. The tubes were centrifuged at 400g for 10 minutes and then resuspended in 5mL of 10% FCS for cell counts. The tubes were then spun again at 350g for 5 minutes and resuspended in RPMI cell culture media with glutamine (Gibco 21875-034) with 10% heat inactivated foetal calf serum to a concentration of 0.25 x 106 cells per 200µl. Cells were cultured in 200 µL in a 96 well round bottom

plate. The test wells were stimulated with either CpG DNA (1:10000) ((Cambridge Bioscience #Hycult HC4039) and CD40 ligand (1:5000) (R and D systems, 6245-CL-050) or alpha synuclein fibrils for 48 hours.

Five hours prior to removal from culture, Phorbol 12-Myristate 13-Acetate (PMA)(50ng/ml) (Sigma-Aldrich #P8139), ionomycin (500ng/ml) (Sigma-Aldrich #I0634) and brefeldin (5µg/ml) (BioLegend #420601) were added to the CD40L/CPG wells and to separate intermediate (PIB) wells (see figure). Brefeldin was added to the alpha synuclein and unstimulated (BFA) wells at this time point too.

Optimisation of the protocol

Given variable cell yields post freezing, the initial protocol using 1 x 10^6 cells per well was changed to 0.25 x 10^6 as this gave similar results. Using less cells necessitated a change from a 48-well flat bottomed plate to a 96 U bottomed plate (which was then used for staining subsequently, decreasing washes and related cell loss). The alpha synuclein culture condition was added part way through the experiment following results from another member of the lab. A number of cell surface markers were trialled and then dropped from the final protocol either because of a lack of expected differences post culture (CD27, CD38, IgD) or because there was no difference in readouts after stimulation (TIM1, CD71, CD73) despite recent literature suggesting that this might be the case (Aravena et al., 2017; van de Veen et al., 2013). An intermediate stimulation condition using only PIB was removed to streamline processing and save antibody (no differences observed in a subset of the data).

Figure 2-2

Schematic showing 96 well plate lay out for each assay.

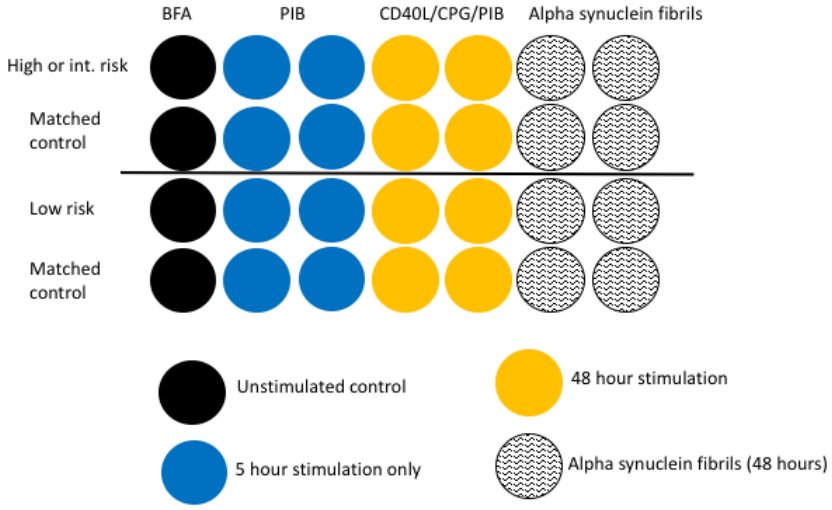

Figure 2-2 legend: Each run of the assay contained a low risk patient (and matched control) and either a high or intermediate risk patient (and matched control) to reduce the effect of inter-assay variability on between group comparisons. CD40L = CD40 Ligand, CPG = CPG DNA, PIB = Phorbol 12 myristate 13 acetate, ionomycin and brefeldin A (BFA).

Cells were removed from culture at 48 hours at spun at 350g for 5 minutes. The supernatants were removed and placed in cryovials at -80 degrees centigrade. Surface staining was done as per the protocol above excluding the fixation step (see section 2.2.2). Cells were fixed and permeabilised prior to intracellular staining using the eBiosciences fixation and permeabilisation kit (Fix/Perm concentrate (00-5123-43) Fix/Perm Diluent (00-5223-56) and 10X Perm buffer (00-8333-56)). Cells were incubated with antibodies for 45 minutes (at room temperature) and subsequently washed before being suspended in FACS buffer.

Flow cytometry was run within 2-4 hours using a BD LSR Fortessa cell analyser. A minimum of 5,000 B cells were collected per tube.

Table 2-2

Antibody panel for stimulated cells post culture

Antibody	**Vol(µL)**	**Compensation antibody**	**Vol (µL)**
BV786 CD19	3	BV786 CD19	3
FITC IL10*	5	FITC CD19	4
BUV 395 CD25	2	BUV395 CD27	3
APC CD38	10	APC CD19	2
PE IL10*	5	PE CD19	2
AF700 MHC Class II	2	AF700 MHC Class II	2
V450 CD138	5	V450 CD19	3
Live dead zombie aqua	0.5	Live dead zombie aqua	0.5

Table 2-2 Vol refers to volume per 100µl of staining buffer. See Appendix II for the manufacturer's details on antibodies

2.2.6 Statistical analysis for the peripheral immune study in PD

Demographic and clinical data and were collected in an Excel spreadsheet (Microsoft Office, version 16.5) and initial graphs were generated using FlowJo (version 7 for Mac OS). Population statistics were exported into a separate Excel spreadsheet that was then merged with the clinical data. Subsequent data analysis was performed using IBM SPSS version 25. Patient and control demographic variables were compared using paired t-tests for continuous parametric variables (or non parametric equivalents where appropriate) and chi-squared tests for categorical variables. The study was primarily designed to facilitate paired comparisons between the risk groups (high, intermediate and low) and their matched controls. An independent samples t-test was considered inappropriate in this context as it assumes complete independence of the two groups where characteristics in one group should not affect selection in the other. The control group was specifically matched to the patient group (for genotype, age and gender with assays carried out at the same time) and a paired analysis was therefore chosen for this reason. Matching groups in this way and using paired statistical tests is described elsewhere(Niven et al., 2012).

The Kolmogorov-Smirnov test was used to compare the data to a normal distribution. Clinical variables were compared across the three defined risk groups (high risk, intermediate and low risk) using a one way analysis of variance (ANOVA). Post hoc t-tests were carried if appropriate. Figures show the mean and SD unless stated otherwise. Graph Pad Prism (version 7 for Mac) was used to make graphs. Heat maps were generated using the gplot function in R.

To make representative images at a single cell level in multidimensional space, fcs files from each patient were merged using the concatenate function in FlowJo. File sizes were decreased by using the 'downsample' plugin which takes a representative sample of the original file at a small file size for downstream processing (in this case, the file size was reduced to 6000 cells). The tSNE (T-distributed stochastic neighbour embedding) algorithm was then run on the downsampled files for each group (patients versus controls, individual risk groups). This is a visualisation algorithm is designed to make images of multidimensional data (e.g. multiple flow cytometry markers) in a two dimensional space by showing cells that are similar to each other close together and those that are different further apart.

For the stimulation experiment, between group comparisons were made either using paired t-tests (or non parametric tests where appropriate) for patient versus control comparisons or unpaired t-tests between risk groups. Mixed measures ANOVAs were used to explore variation in each stimulation condition with IL10, IL6 and CD25 as the repeated measures (three levels: unstimulated, stimulated and alpha synuclein) and risk group as the independent variable. A correlation matrix was also constructed to explore relationships between measured variables and outcome measures (as in the previous study).

2.2.7 Age associated B lymphocytes pilot study (cohort 2)

Newly diagnosed participants were recruited from the Parkinson's disease research clinic as for the previous study under the same ethical approval and underwent the same clinical assessments, blood sampling, PBMC extraction and immunocytochemistry as the participants in the previous study. Controls were recruited opportunistically from the spouses or relatives of patients attending the research clinic.

B lymphocyte surface staining was done using a modified staining panel shown in Table 2-3 with an additional intranuclear staining step in order to stain for the transcription factor, T-bet (one of the markers used to identify age associated B cells). Intranuclear staining was done following fixation and permeabilization using the eBioscience Foxp3 transcription factor staining buffer set (cat number 00-5523-00). Subsequent washes were done using the permeablisation buffer provided with the kit. Prior to being run on the flow cytometer, cells were resuspended in FACS buffer as with the previous study.

Table 2-3

B lymphocyte staining for Age associated B cell study

Antibody	Volume (µL)	Compensation antibody	Volume (µL)
BV786 CD19	3	BV786 CD19	3
FITC CD11c	1	FITC CD19	4
BV605 CD24	5	BV605 CD19	2
BUV 395 CD27	3	BUV395 CD27	3
APC CD38	10	APC CD19	2
PE Tbet	1	PE CD19	2
APC H7 IgD	2	APCH7 IgD	2
PerCp Cy5.5 CD86	3	PerCp Cy5.5 CD19	3

Table 2-3 Volume refers to volume of antibody per 100µL of staining buffer. See Appendix II for manufacturer's details.

2.2.8 Statistical analysis for age associated B lymphocyte study

Data were collected and organised as described above. Patient versus control comparisons were made using unpaired t-tests or non-parametric equivalent (Mann Whitney U).

A correlation matrix was constructed to identify significant bivariate correlations between B lymphocyte related parameters, alpha synuclein and clinical parameters using data from both cohort 1 and cohort 2. Significant associations identified in the correlation matrix were taken forward into multiple regression models using either motor UPDRS or the probability of a bad outcome as dependent variables. All independent variables were entered into the model simultaneously. Prior to inclusion in the model, scatterplots were inspected to ensure that the associations were not driven by significant outliers. Scatterplots shown in the results section show the linear regression line and 95% confidence interval unless specified otherwise.

2.2.9 Pilot study: B lymphocytes in human cerebrospinal fluid (cohort 3)

CSF samples and PBMCs from PD patients and controls were available from a parallel study (NET-PDD) running in the Williams-Gray lab.
Patients were recruited from the research clinic at the Cambridge Centre for Brain Repair. Recruitment was done entirely by AK and CWG. Separate ethical approval for the study was obtained. Controls matched for MAPT genotype were recruited from the Cambridge bioresource. Recruitment was ongoing at the time of writing and therefore the results are from a subset of patients recruited prior to August 2018.

Participants attended the Cambridge Centre for Brain Repair for lumbar puncture and venepuncture. Clinical assessments were performed as for cohorts 1 and 2. CSF was collected in a sterile tube which was spun at 300g for 10 minutes. The supernatant was removed and frozen in 200µl aliquots. The cell pellet was resuspended in 100µl of 2% mouse serum in a 96 well plate and left for at least 20 minutes to ensure optimum blocking of non-specific antibody binding (as described for the previous cohorts). 50µl of 123 count ebeads (Invitrogen 01-1234-42) were also added to the well to facilitate the calculation of absolute cell counts. Venepuncture was performed as described for cohorts 1 and 2 including sending full blood counts. PBMCs were extracted as described in 2.2.2 and placed in three wells (unstained, isotype and test wells). Surface antibodies were then added to the CSF well and the test PBMC well as shown in Table 2-4 (see Appendix II for manufacturer's details). Once fixed cells were transferred to FACS tubes and run on the flow cytometer within 24 hours.

2.2.10 Statistical analysis for B lymphocytes in CSF study (cohort 3)

FCS files were gated in FlowJo (version 10.2) as for the other studies. Population parameters were exported to Microsoft Excel (version 16.16.1) and statistical analyses were performed using SPSS (IBM, version 25).
Between group comparisons were made using either one way ANOVAs (controls versus high versus low risk), independent t-tests or chi-squared tests as appropriate.

Table 2-4

Antibody panel for CSF study

Antibody	Volume (µL)	Compensation antibody	Volume (µL)
FITC CD16	3	FITC CD19	5
PerCP Cy5.5 CD57	2	PerCp Cy5.5 CD19	2
APC TLR4	1	APC CD19	4
A700 MHC Class II	1	A700 CD3	1
APC H7 IgD	2	APC H7 IgD	2
PE IgA	10	PE CD19	5
PE dazzle CD4	1	PE dazzle CD4	1
PE Cy7 CD3	1	PE Cy7 CD3	1
BV450 CD45	2	BV450 CD19	
BV510 CD8	1	BV510 CD8	1
BV605 CD28	2	BV 605 MHC Class II	1
BV650 CD14	1	BV650 CD14	1
BV711 TLR2	1	BV711 TLR2	1
BV786 CD19	3	BV786 CD19	3
BUV395 CD27	2	BUV395 CD27	2

Table 2-4 See Appendix II for manufacturer's details.

2.3 Results

2.3.1 Participant characteristics Immune study in PD (cohort 1)

41 patients and 41 controls were recruited (see Table 2-5). Patients and controls were matched for age (Mann Whitney U, Z = 0.33, p = 0.71) and gender (Chi-square = 0, p = 1 for patients versus controls, Chi-square = 1.1, p = 0.57 between risk groups). Disease duration, defined as time from diagnosis, was similar across the risk groups (One way ANOVA, F[2,38] = 0.05, p = 0.99). Samples were collected over an 18 month period.

There was a significant difference between groups in cognition as measured by the ACE-R (One way ANOVA F[2.38] = 20.14, p = 0.00001) with the high risk group having lower scores than the other two patient groups (t[21] = -3.9, p = 0.001 versus intermediate and, t[25] = -5.6, p = 0.000009 versus low risk) (Table 2-5). There were also significant differences in the levodopa equivalent daily dose between groups (One way ANOVA, F[2,38] = 4.5, p = 0.02) with the high risk group taking significantly less than the low risk group (t[25] = -2.9, p = 0.007 versus low) (see Table 2-5). There was no significant effect of risk group on the MDS-UPDRS motor score (One-way ANOVA (F[2,38] 3.01, p = 0.06) although there was a trend towards this being worse in the high risk group (Table 2-5).

Table 2-5

Participant demographic and clinical information

Variable	Controls (*n*=41)	PD (*n*=41)				P value
		All	High Risk (*n*=9)	Intermediate Risk (*n*=14)	Low Risk (*n*=18)	
Age	68.1(5.6)	68.4(6.3)	69.3(4.8)	70.4(6.7)	66.3(6.3)	0.74*
Gender (% male)	68.3	68.3	66.7	78.6	61.1	1*
Disease duration	N/A	4.24(1.2)	4.3 (1.1)	4.3(1.1)	4.23(1.3)	0.995
MDS-UPDRS motor score	N/A	35.23(12.3)	42.9(12.0)	35.43(12.7)	31(10.8)	0.06
ACE-R	N/A	93.0(8.3)	82(11.03)	95.1(4.5)	96.8(2.3)	0.000001
Levodopa equivalent daily dose (mg)	N/A	591.5(292.9)	389.2(268.7)	560.3(257.8)	717.0(279.3)	0.017

*show paired comparisons between patients and controls.

Full blood counts

Full blood counts were available for a subset of participants (n=20 patients and 20 matched controls). As shown previously in the literature, patients had lower lymphocyte counts than controls (PD mean 1.36, SD 0.41 and control mean 1.94, SD 0.62; paired t test, $t[3] = 2.87$, $p = 0.01$). There were no differences between patients and controls in the number of monocytes, neutrophils or eosinophils.

Figure 2-3

Cell counts in PD patients and matched controls

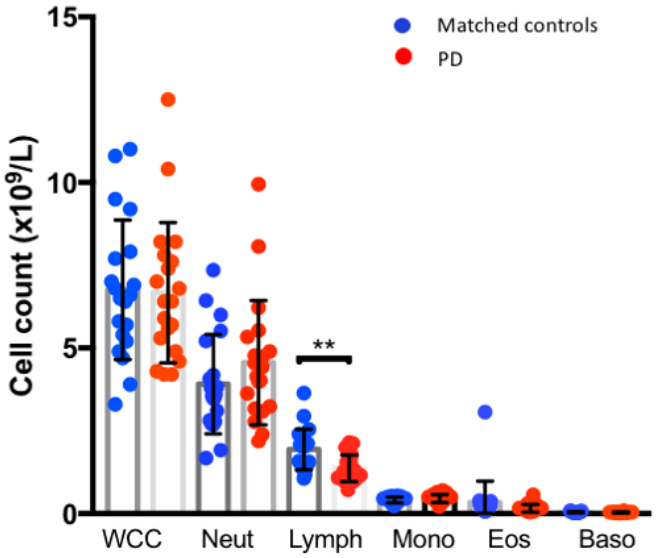

Figure 2-3 WCC white cell count, Neut neutrophils, Lymph lymphocytes, Mono monocytes, Eos eosinophils, Baso basophils.

2.3.2 Immunocytochemistry and flow cytometry

Gating of B cell subsets was performed as shown in Figure 2-4. All gating was done in batches that were processed at the same time with gates remaining consistent within each batch of patients and matched controls. I was blinded to group for all parts of the analysis.

Overall B lymphocyte numbers were decreased in patients compared to controls (paired t-test t[34]=2.08, p = 0.04). This appeared to be driven by the high risk group (see Figure 2-5). There were no differences in CD4 or CD8 T cell numbers between groups suggesting that the decrease in lymphocyte counts was driven by the B lymphocytes (data not shown).

Figure 2-4

Gating of B lymphocyte populations

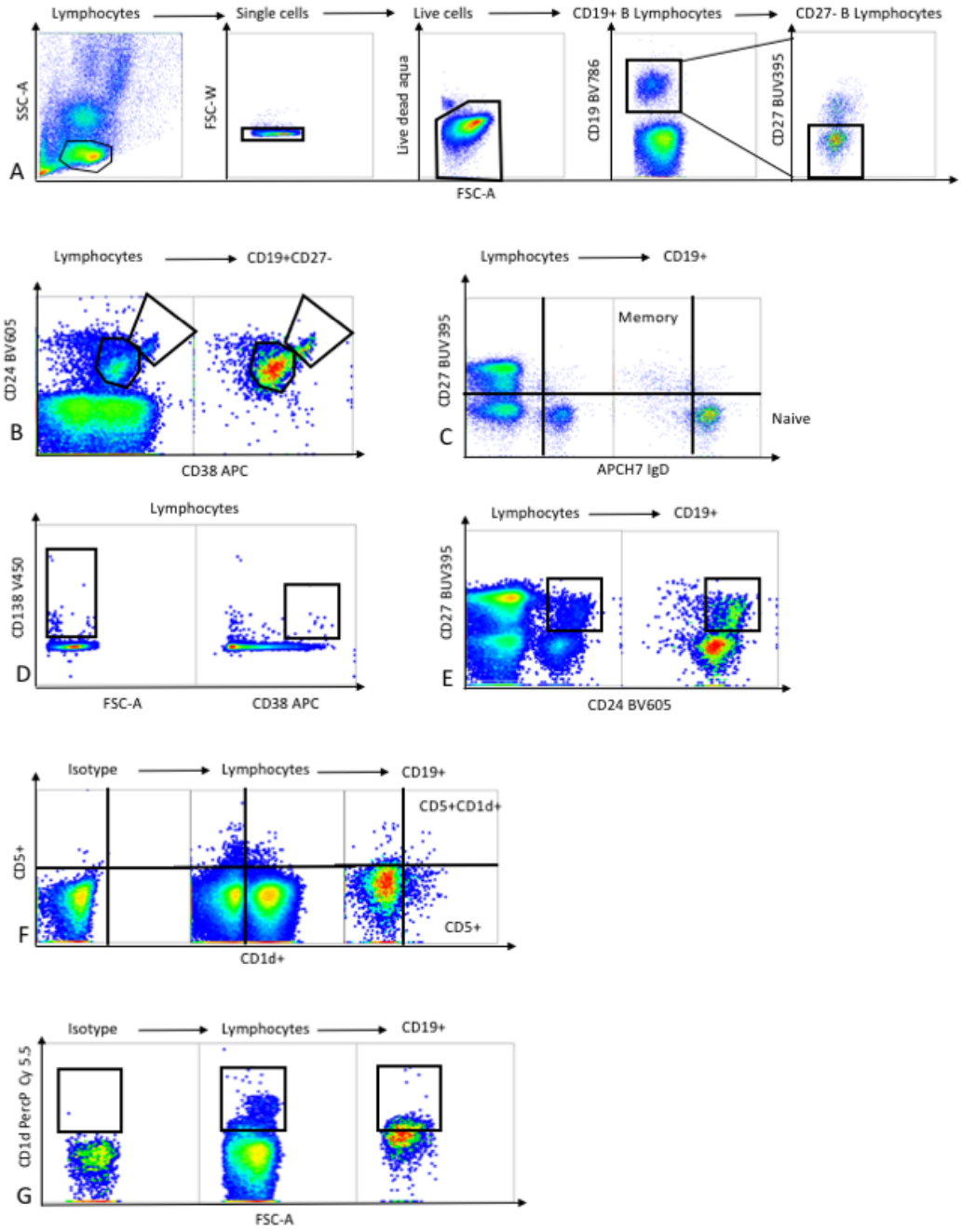

Figure 2-4 (see following page): B lymphocyte gating starting with lymphocytes, then single cells, then live cells and then CD19+ cells (A). The CD27+ and CD27- populations are then identified. From the CD27- population, the transitional cells are gated(CD19+CD27-CD38HICD24HI) (B). Other gates shown are for memory versus naïve B lymphocytes (C) and plasma cells (gated on live cells rather than CD19+) (D). CD5 and CD1d gates were applied initially using the lymphocytes as a whole as for CD27 and IgD (see C and F). CD1d positive cells were identified using the isotype control and the lymphocyte population as a whole (positive control) (G).

Figure 2-5

B lymphocytes are reduced in PD

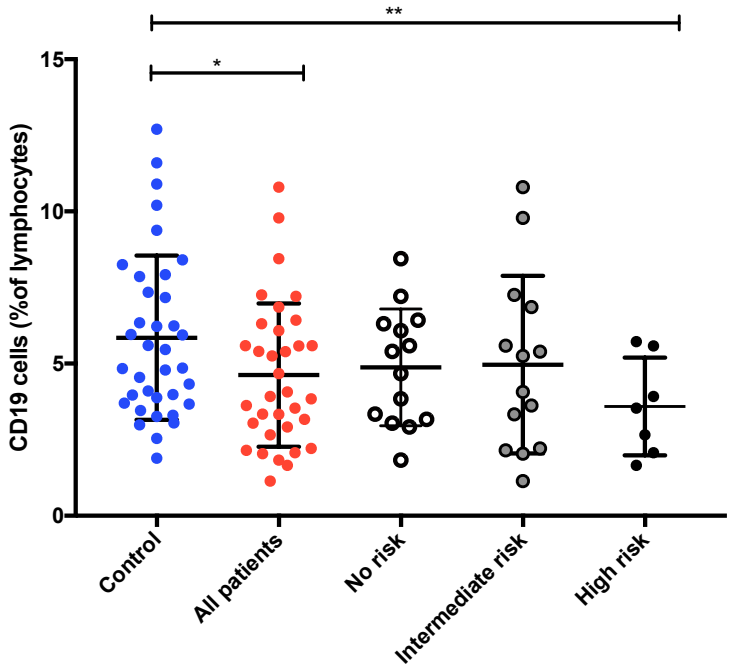

Figure 2-5: The percentage of B lymphocytes is reduced overall in patients compared to controls (paired t-test $t[34] = 2.08$, $p = 0.04$) Controls mean 5.7, SD 2.8; PD mean 4.6, SD 2.3; low risk mean 4.9, SD 1.9; intermediate risk mean 4.8, SD 2.8; high risk 3.5, SD 1.7. Paired t-tests between PD patients and matched

controls showed that there was a significant difference between high risk patients and their matched controls but not between the other groups and their matched controls ($t[6] = 3.42$, $p = 0.01$).

In order to determine whether the difference in B lymphocyte counts observed in the patient cohort was driven by a decrease in one subset of B lymphocytes or if it represented an overall decrease in B lymphocytes I next analysed the frequency of B lymphocyte subsets including naïve (CD19+IgD+CD27-), memory (CD19+IgD-, CD27+), transitional (CD19+,CD27-, CD24HI, CD38HI), plasma cells (CD138+ and CD38+CD138+), plasmablast-like (CD24+CD27+), CD5+ and CD1d+ cells.

Figure 2-6

Memory versus naïve B lymphocyte subsets in PD

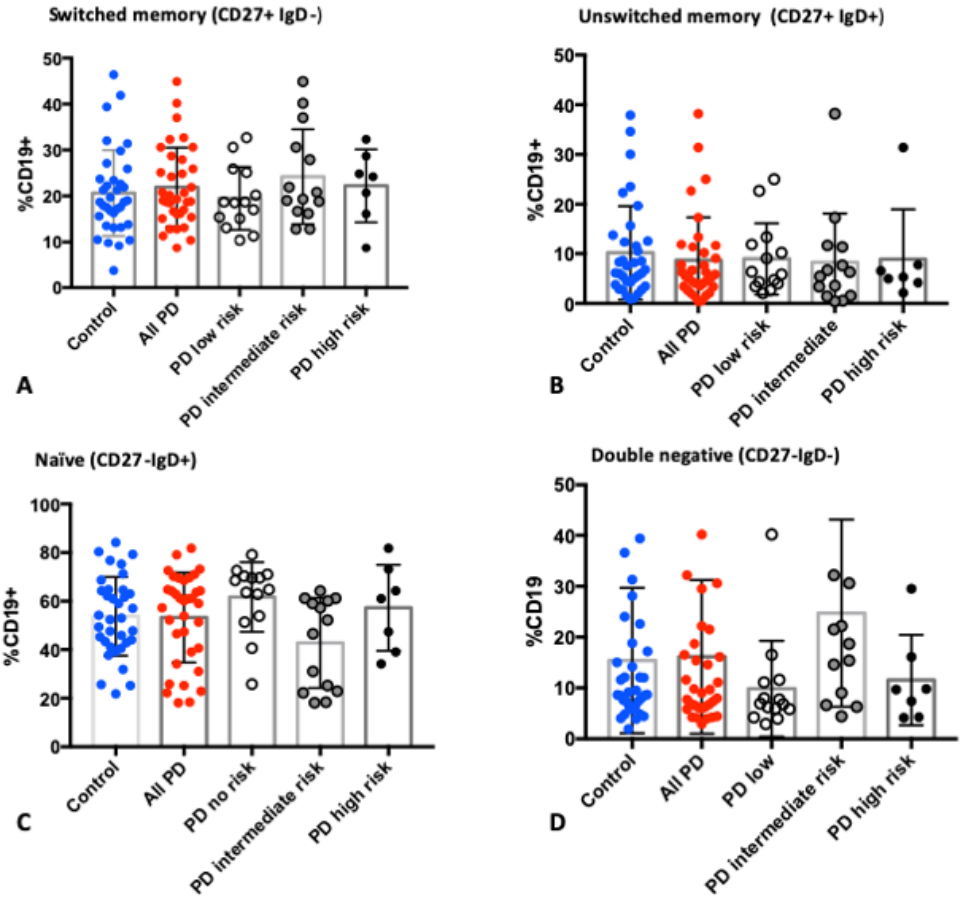

Figure 2-6 There were no paired control versus patient group differences in the overall percentage of switched memory, unswitched memory, naïve and double negative cells (statistics not shown). There were also no differences between the individual risk groups and their matched controls.

There were no differences between patients and matched controls across the naïve and memory subsets shown in

Figure 2-6 (see Table 2-9 for means and SD across each group, risk group data not shown).

Figure 2-7

Transitional and Plasma cell subsets

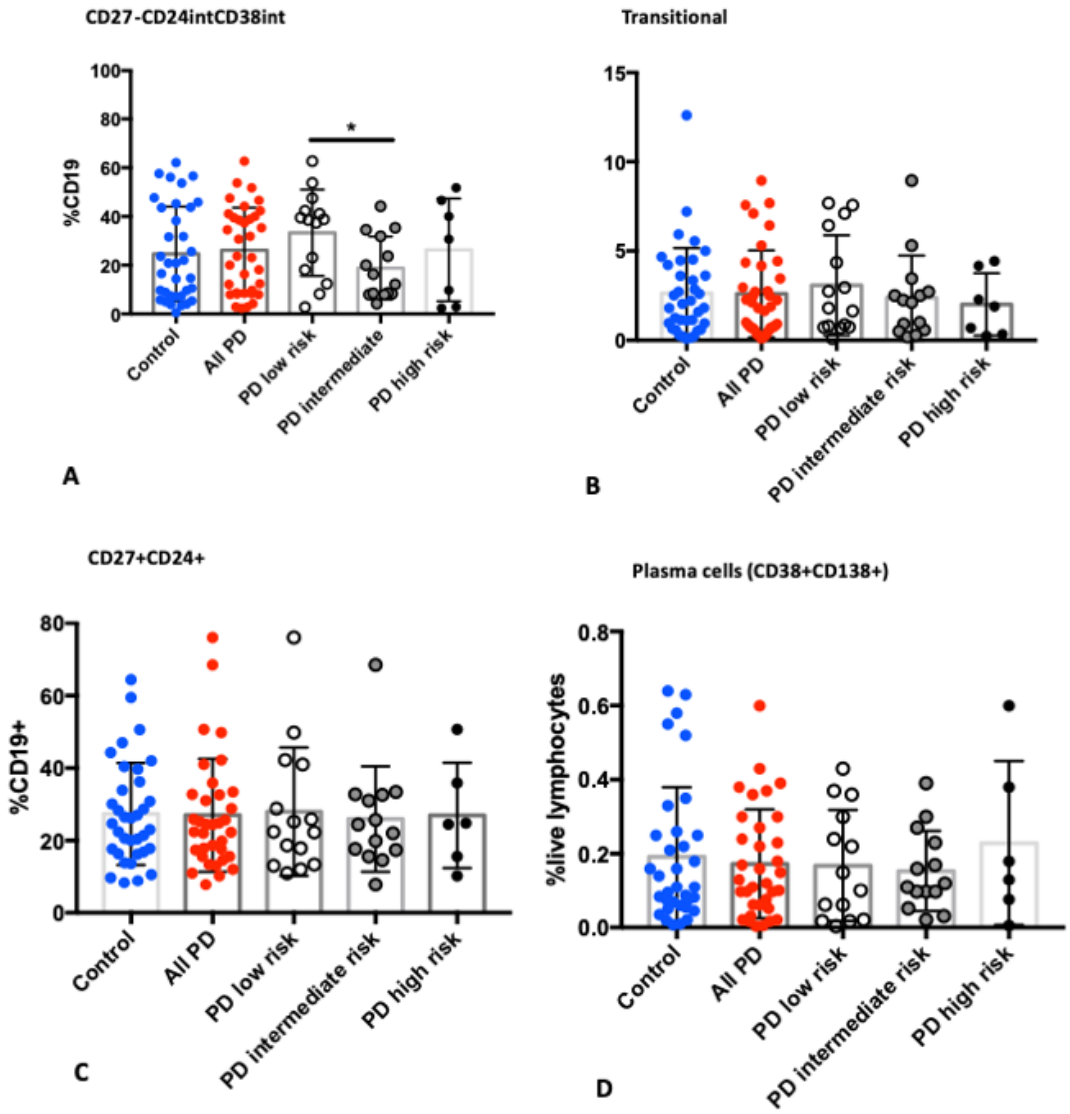

Figure 2-7 Transitional and intermediate populations, (A, B) and CD27+CD24+ ("regulatory") subset (C). Plasma cells are shown in D.

There were no overall paired control versus patient differences in either transitional (CD27- CD24HICD38HI) or intermediate transitional B cell subsets (CD27-CD24intCD38int), including paired comparisons between the individual

risk groups and their matched controls (data not shown). There were also no differences in plasma cells by two different gating strategies (see Figure 2-7 only CD38+ CD138+ shown). Exploratory post hoc analysis showed that there was a significant difference in the CD24intCD38int subset between those at low risk and those at risk (pooled) although this does not stand up to correction for multiple testing and is not validated by changes in the true transitional population.

There were no overall or risk group level paired patient versus control differences in CD5 positive, CD1d positive, CD5+CD1d+ groups or in the CD1d MFI ratio (versus the isotype control) (see Figure 2-8).

Figure 2-9 shows the t-SNE plots giving an overall representation of cell populations across patient and control groups. Figure 2-9 shows a smaller B lymphocyte population in the high risk group in particular.

Figure 2-8

CD1d and CD5 positive B lymphocytes

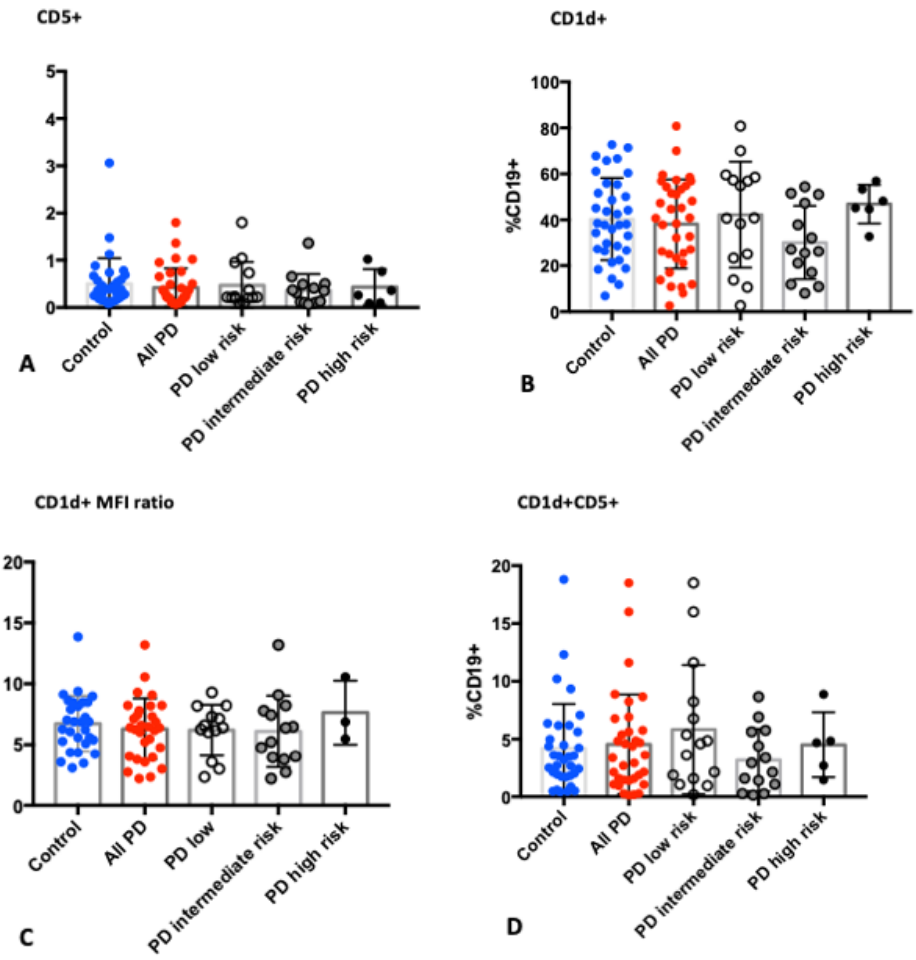

Figure 2-8 CD1d MFI ratio refers to the ratio between the MFI of the stained cells versus the MFI of the isotype control (and is not therefore dependent on gating of CD1d).

Figure 2-9

t-SNE plot showing decreased B lymphocytes in high risk group

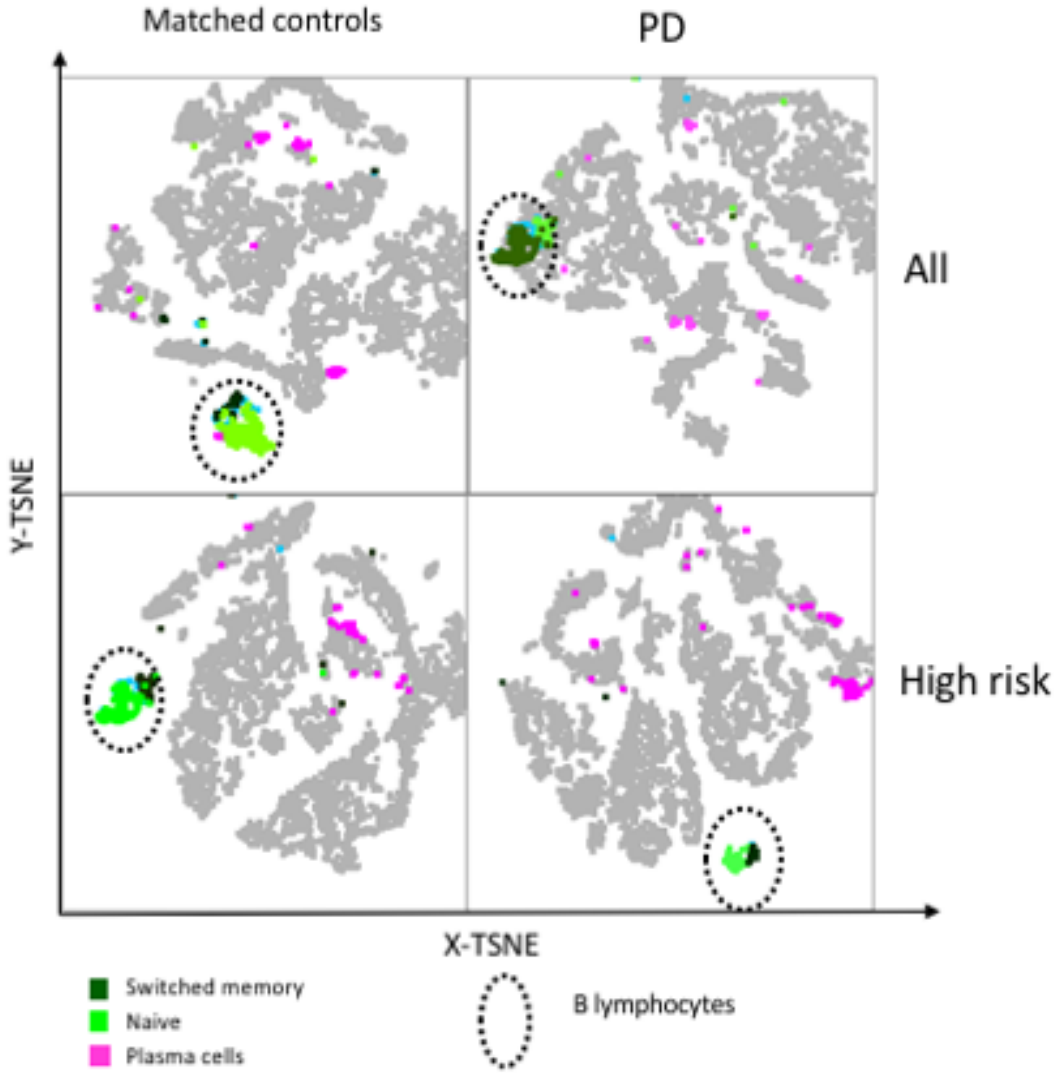

Figure 2-9 t-SNE plot showing representative individual cell data from pooled patient and control samples, illustrating the small B cell pool in the high risk patients. .

The correlation heatmap showed the expected relationships between clinical variables (see Figure 2-10). The ACE-R and the MMSE were highly correlated (r=0.97, p < 0.00001) with both of these tests being negatively correlated with UPDRS motor scores (r= -0.43, p = 0.005 and r = -0.39, p = 0.013 respectively). The ACE-R was also positively correlated with levodopa equivalent dose (LEDD) (r=0.34, p = 0.03). When two outliers on the ACE were removed this relationship remained (r=0.43, p = 0.008). The composite variable 'probability of a poor outcome' also showed the expected relationships with the related clinical variables (age; r = -0.61, p = 0.00003, MMSE; r= -0.56, p = 0.0002, ACE-R; r=-0.53, p = 0.001, UPDRS motor; r = -0.67, p = 0.000004).

The only B lymphocyte related parameter that correlated with the composite variable 'unfavourable outcome' was the percentage of CD1d+CD5+ cells (r=-0.40, p = 0.02). There were several B lymphocyte related variables that were negatively correlated with the motor UPDRS. That is, high proportions of these subsets were associated with a lower UPDRS score (which is an indicator of less severe disease). This included the percentage of CD24HICD38HI B lymphocytes (r = -0.34, p = 0.048), the percentage of CD1d+ lymphocytes (r=-0.35, p =0.042), the percentage of CD1d+CD5+ B lymphocytes (r=-0.39, p=0.024) and the CD1d MFI ratio (r=-0.46, p = 0.012). The scatterplots shown in Figure 2-11 confirm that this is not driven by isolated outliers. Other parameters associated with motor UPDRS were serum alpha synuclein (r=-0.41, p = 0.01), total white cell count (r = 0.45, p = 0.04) and neutrophils (r = 0.53, p=0.01)(see correlation heat map in Figure 2-10). These associations were not corrected for multiple testing. In order to look at relationships across variables in a more robust manner, a regression model was constructed using all of the B lymphocyte subsets that were negatively associated with motor UPDRS given that they were correlated with each other. All of the variables were entered into the model at the same time. Regression assumptions were not violated: scatterplots were examined for

linearity, the regression standardised residuals of the outcome (motor UPDRS) were normally distributed, there was independence of residuals as assessed by a Durbin-Watson statistic of 2.2 and there was homoscedasticity as assessed by inspection of the plot of standardized residuals against standardised predicted values. The model as a whole explained 37.6% of the variance in motor UPDRS (R^2 = 0.376, SE 10.6) and was overall a significant predictor of motor UPDRS scores (F [4,24] = 3.612, p = 0.019). The individual items were not significant predictors on their own.

Figure 2-10

Correlation matrix of both clinical and B lymphocyte related variables

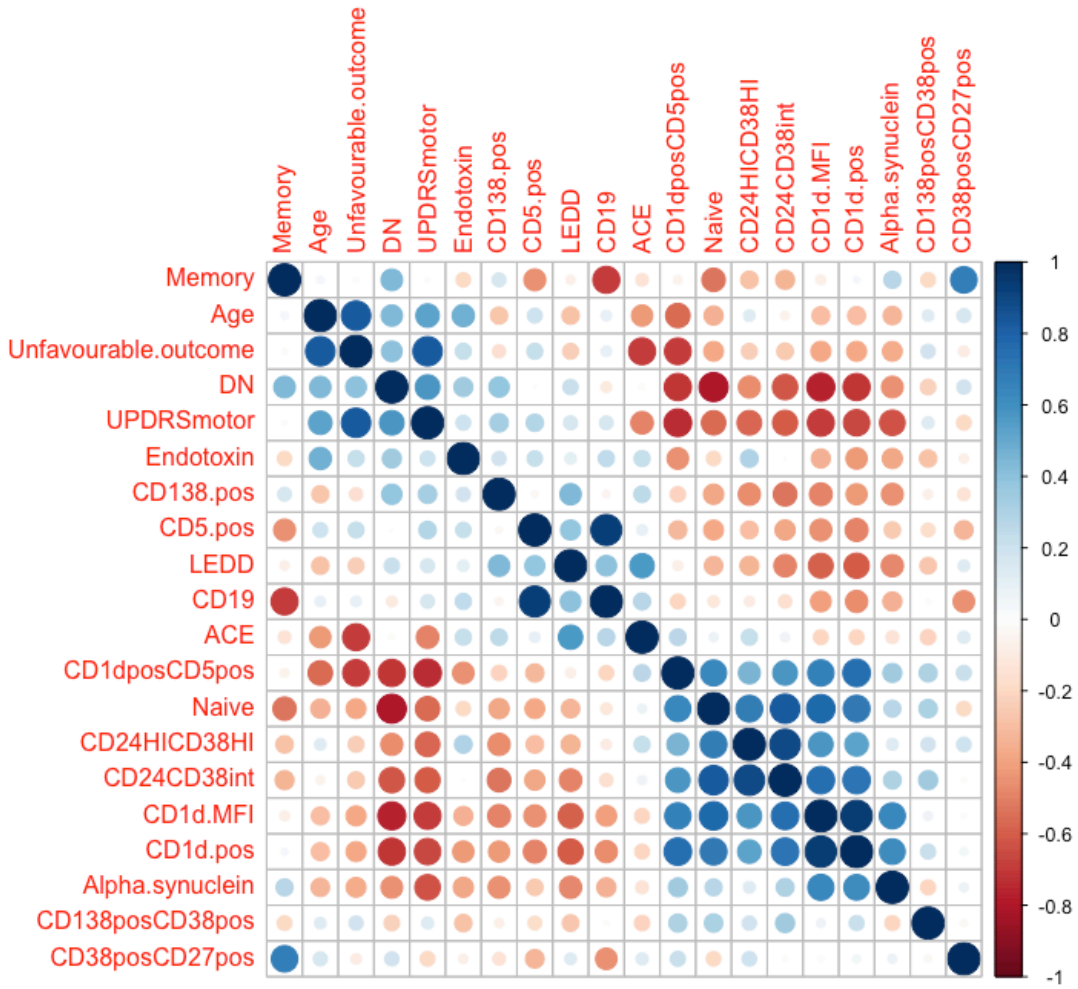

Figure 2-10 Correlation heatmap showing relationship between clinical and immune variables. Darker, larger circles indicated a higher correlation (positive in blue and negative in red).

Figure 2-11

Scatterplots showing the relationship between B lymphocyte subsets and motor UPDRS

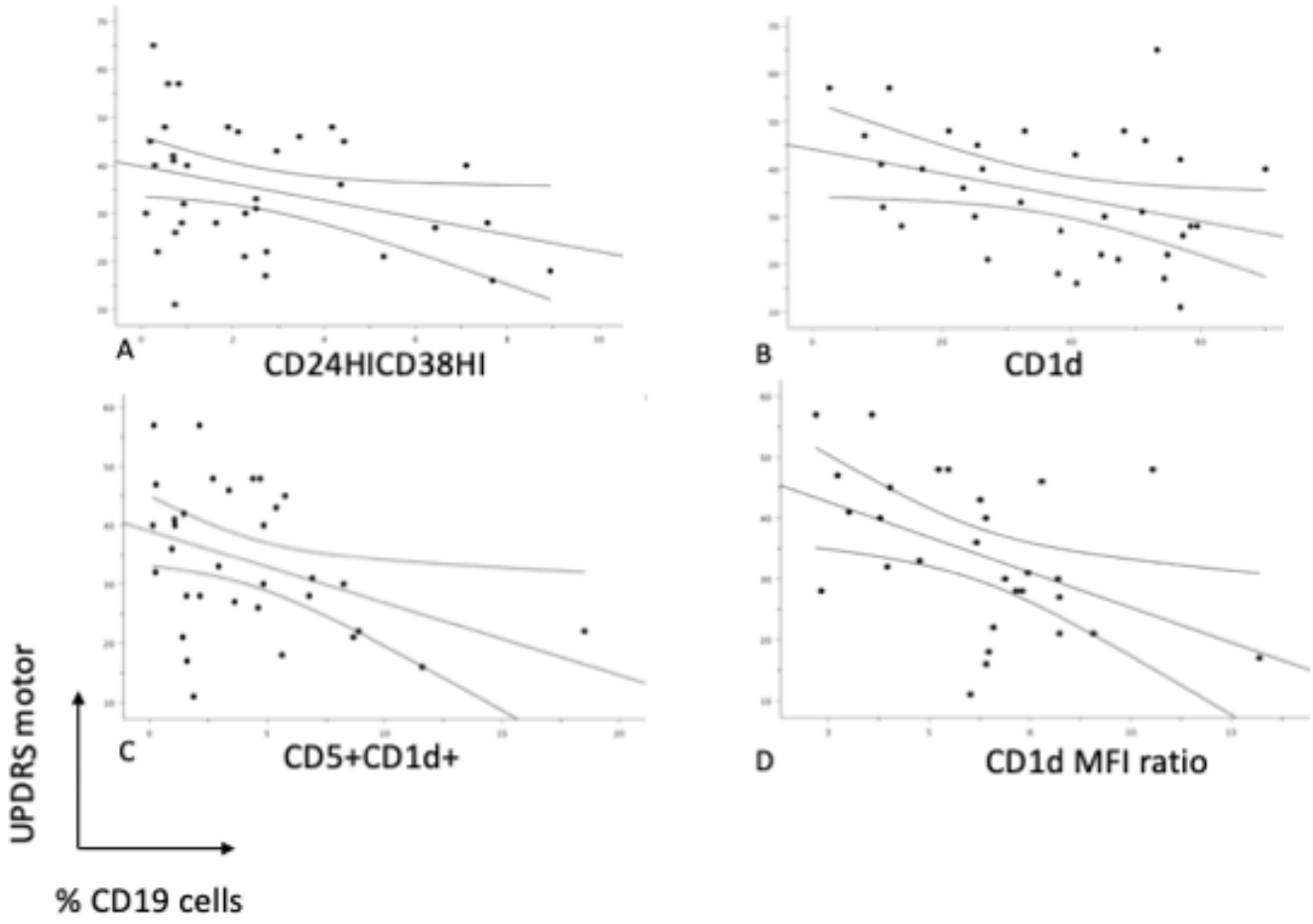

Figure 2-11 Associations between motor UPRDS score and B lymphocyte subsets; Transitional B lymphocytes (r = -0.34, p = 0.048).

2.3.3 Serum B cell activating factor (BAFF)

Serum BAFF was measured to see whether there was a compensatory increase in the high risk group (given the lower B lymphocytes in these patients). There was no statistically significant difference in paired comparisons between patients and no differences in paired comparisons between risk groups and matched controls (statistics not shown, see Figure 2-12). There was no correlation between serum BAFF and the percentage or absolute counts of CD19+ B lymphocytes (r = -0.0.01, r = -0.02, p = 0.9 respectively). There was a significant difference between serum BAFF in the high risk group versus the intermediate and low risk groups (unpaired t-tests high versus low t[23] = 3.08, p = 0.005; high versus intermediate t[20] = 3.86, p = 0.001).

Figure 2-12

Serum BAFF levels

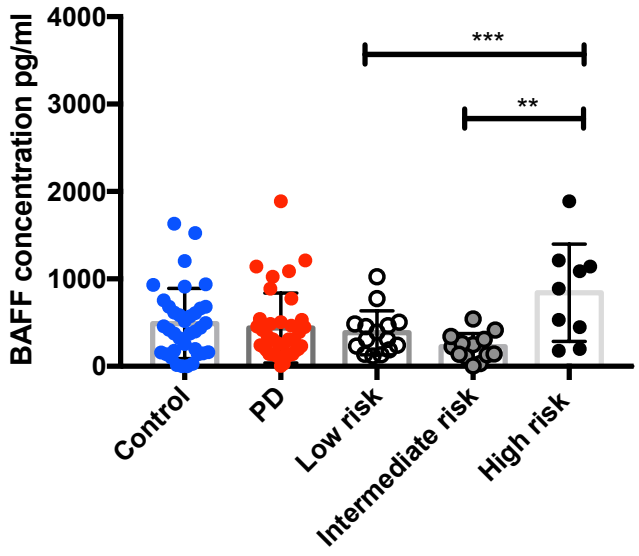

Figure 2-12 Control mean 489.5 (SD 401.7), PD mean 439.1 (SD 400.2), low risk mean 384.6 (SD 252.1), intermediate risk 223.4 (SD 152.7), high risk 841.3 (SD 557.9).

2.3.4 Participant characteristics B cell functional assay

Given the observed abnormalities in B cell numbers in patients with PD, we next sought to interrogate B cell function, specifically their capacity to secrete cytokines when stimulated *ex vivo*. Samples were obtained from participants in the same cohort as those included in the peripheral immune phenotyping study described above. Adequate numbers of frozen cells for *ex vivo* stimulation assays were only available in a subset of patients. The demographics of these patients are shown below and broadly reflect the trends seen in the main cohort (see Table 2-5 and Table 2-6). As in the main cohort the high risk patients were significantly more cognitively impaired (mean ACE-R 81.6, SD = 12.58 versus 95.6 (SD = 3.6) and 96.54 (2.0) in the intermediate and low risk groups respectively) (one way ANOVA F [2,27] = 13.00, p = 0.0001). Similarly, there were differences in levodopa equivalent dose (LEDD) across groups, with doses being lower in the high risk group than the low risk group (one way ANOVA F[2,27] = 4.43, p = 0.022). The trend towards worse motor UPDRS scores was also preserved in the high risk patients but this was no longer significant due to the smaller numbers involved (see Table 2-6). Importantly, the participants included in this sub-study remained matched for disease duration across groups and patients and controls were well matched.

Table 2-6

Participant demographics

Variable	Controls (*n*=30)	PD (*n*=30)				P value
		All	High Risk (*n*=7)	Intermediate Risk (*n*=10)	Low Risk (*n*=13)	
Age	68.5 (5.9)	68.23(5.14)	68.71 (5.47)	69.30 (7.17)	67.77(5.57)	0.85
Gender (% male)	18(60)	18 (60)	4 (57.1)	7 (70)	7 (53.8)	1.0
Disease duration	N/A	4.15 (1.17)	4.42 (1.22)	3.84 (1.08)	4.24 (1.24)	0.58
MDS-UPDRS motor score	N/A	34.8 (12.3)	43 (13.83)	31.5 (11.88)	32.54 (10.45)	0.116
ACE-R	N/A	92.8(8.79)	81.86 (12.58)	95.6 (3.60)	96.54 (2.0)	0.0001
Levodopa equivalent daily dose (mg)	N/A	578.82 (307.48)	406.17 (241.76)	480.38 (252.5)	747.50 (308.43)	0.02

Table 2-6: The table shows means and standard deviations (SD). P values refer to patient versus control comparisons for age and gender and to between group comparisons for the other variables.

2.3.5 Immunocytochemistry and flow cytometry

Gating of post culture cells was performed as shown Figure 2-13 and Figure 2-14.

Figure 2-13

Gating of post culture B lymphocytes showing activation markers

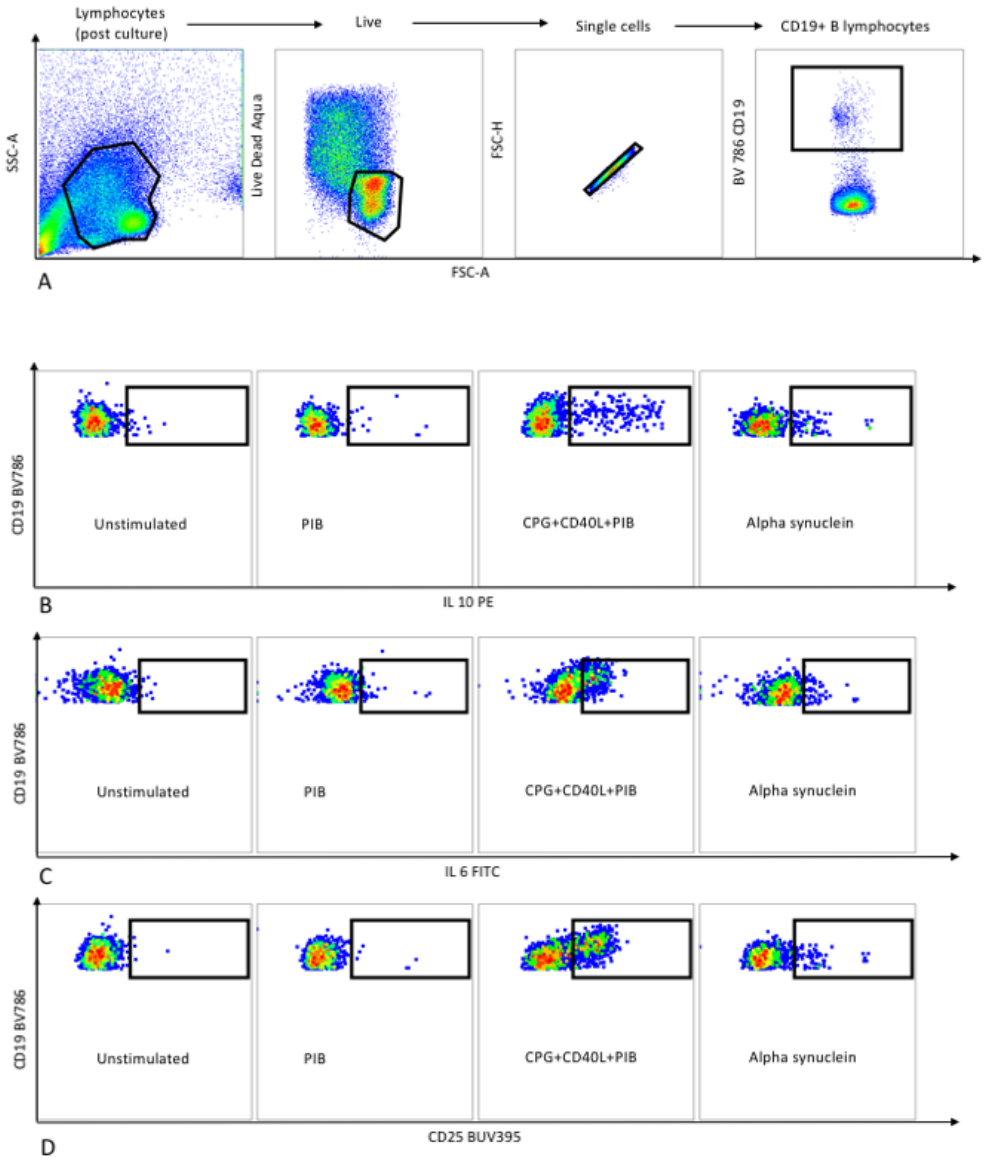

Figure 2-13 Post culture cells were gated using a wide lymphocyte gate followed by viability staining, single cell selection and CD19+ lymphocytes (A). Activation was assessed using intracellular stains for IL10 and IL6 with gates being set on unstimulated (brefeldin only) cells. An additional surface marker, CD25 was also used to assess activation with the gates set in a similar manner.

Figure 2-14

Gating of post culture B lymphocytes showing plasma cells

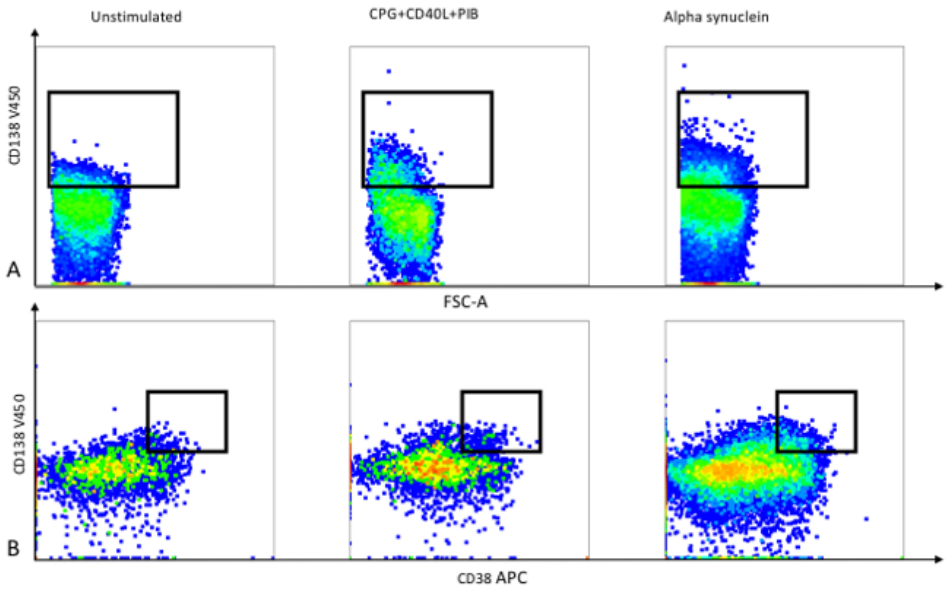

Figure 2-14 Plasma cells were gated from live, single lymphocytes using CD138 (A) and also CD38+ and CD138+ populations.

There were no significant differences overall in the percentage of either IL10+ or IL6+ cells between patients and controls (see Figure 2-15). There was a significant difference in the percentage of IL10 + cells between high risk patients and those at intermediate or low risk with those at high risk having significantly more (mean 6.56 [SD 3.39] in the high risk group versus 1.93 [SD 0.73] in the low risk group and 5.73 [SD 4.57] in the intermediate group) (Mann Whitney U high risk versus low risk = 12.00, p = 0.01, Mann Whitney U high risk versus intermediate = 14, p = 0.04). There were also no overall differences between the percentage of CD25+ cells in patients compared to controls. There was a significantly higher number of CD25+ cells in the high risk group compared to the low risk group (Mann Whitney U = 14, p = 0.039) (mean high risk group 5.67 [SD 3.9], mean intermediate group = 2.08 [SD 1.57], low risk group 1.56 [0.96]). A

correlation matrix was constructed of the activation markers which were highly correlated (apart from the MHC Class II MFI ratio) (see Figure 2-17).

Figure 2-15

Cytokine production in B lymphocytes in vitro

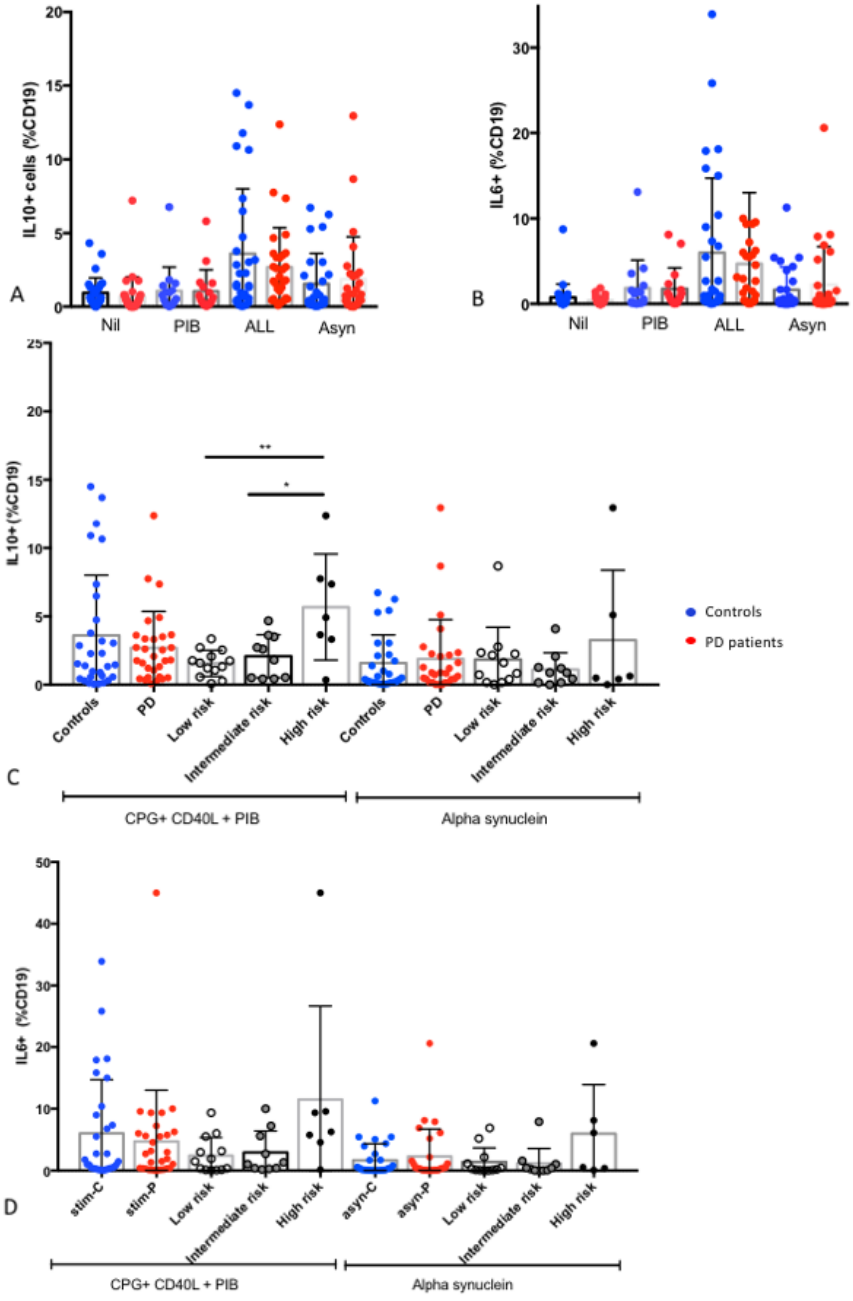

Figure 2-15 Differences in the percentage of IL10+ (A and C), IL6+ (B and D), Nil = unstimulated condition (brefeldin only), PIB = PMA, ionomycin and brefeldin and ALL = CPG + CD40L + PIB, Asyn = alpha synuclein. ** p=0.01, *p<0.05

Figure 2-16

Activation markers in B lymphocytes post culture

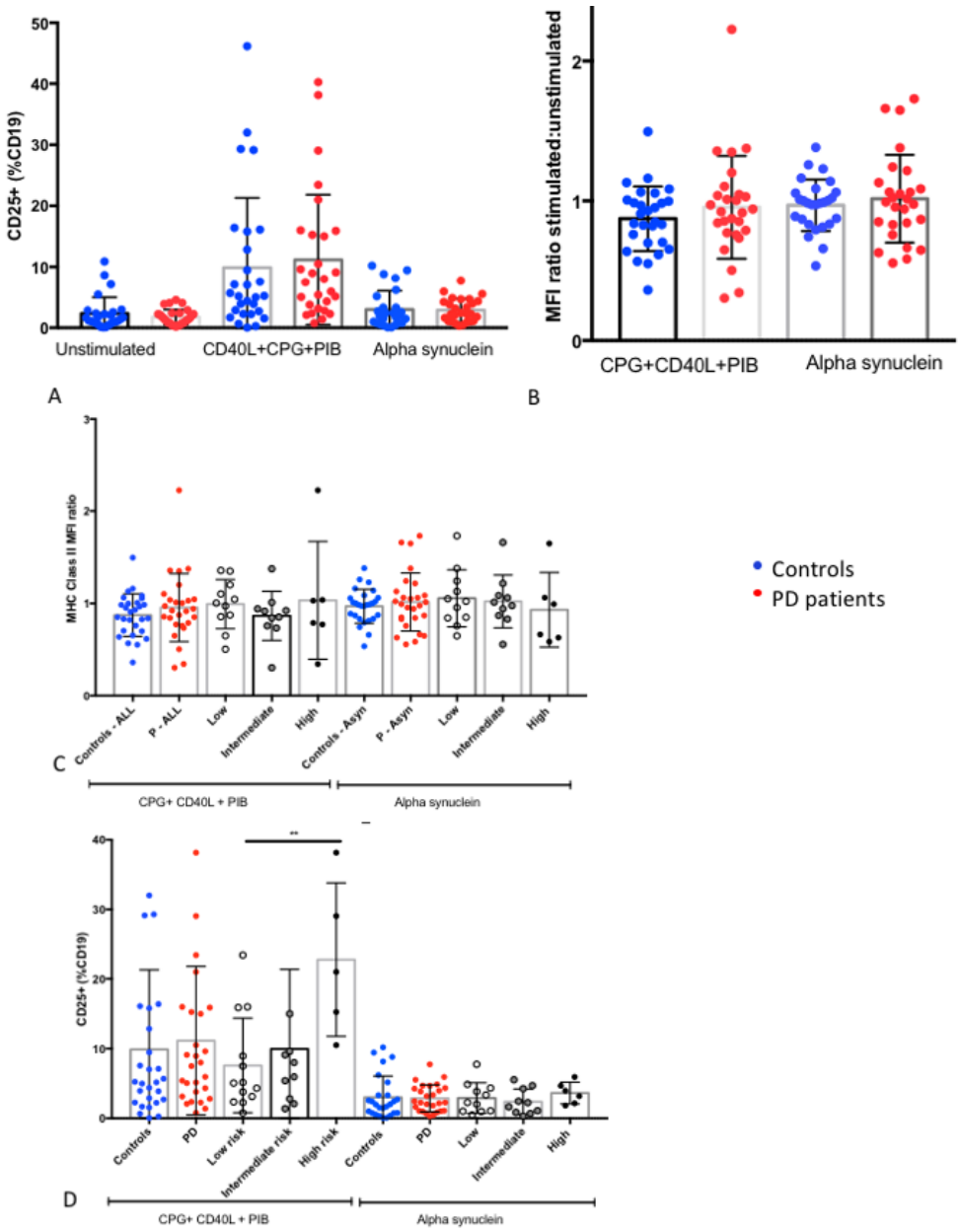

Figure 2-16 CD25 + (A and D) B lymphocytes are shown as well as the MHC Class II MFI ratios (stimulated:unstimulated) (B and C). Nil = unstimulated condition (brefeldin only), PIB = PMA, ionomycin and brefeldin and ALL = CPG + CD40L + PIB, Asyn = alpha synuclein. ** p=0.01, *p<0.05.

Figure 2-17

Correlation heatmap showing the relationship between chosen activation markers

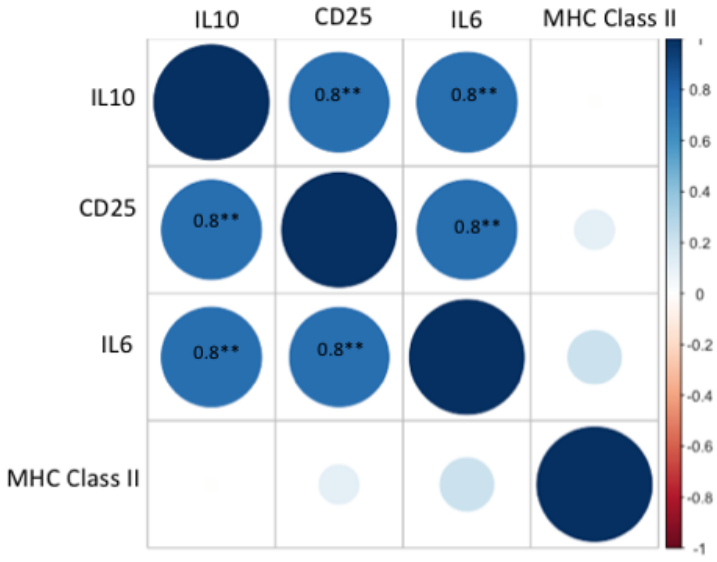

Figure 2-17 IL10, IL6 and CD25 refer to the proportion of cells that were positive for the respective marker. MHC Class II is the MHC Class II MFI ratio.

As the activation markers were so highly correlated they were converted into Z scores (standardised) and an overall activation score was calculated from the mean Z score (see Figure 2-18).

Figure 2-18

Standardised activation score across groups

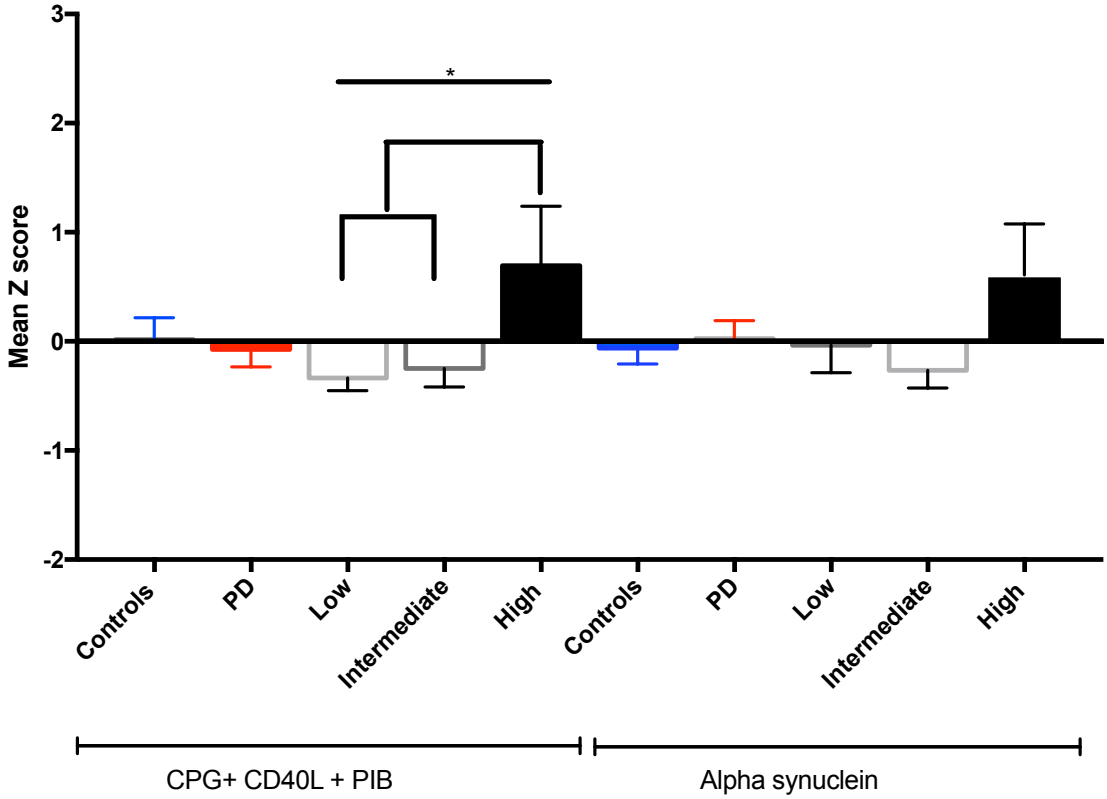

Figure 2-18 Figures shows mean standardised B cell activation scores across risk groups. The high risk group had a significantly higher mean standardised score in the CPG/CD40L and PIB condition than the low and intermediate groups (Mann Whitney U = 26, p = 0.02). There was also a trend towards a higher score in the alpha synuclein condition but this was not significant (Mann Whitney U = 30.5, p = 0.07). There were no differences in IL6:IL10 ratio between patients and controls or within patient groups (data not shown).

There were no differences between controls and patients (or between risk groups) in the number of CD138+ plasma cells. There were also no differences in CD38+CD138+ plasma cells (data not shown).

Figure 2-19

CD138+ plasma cells

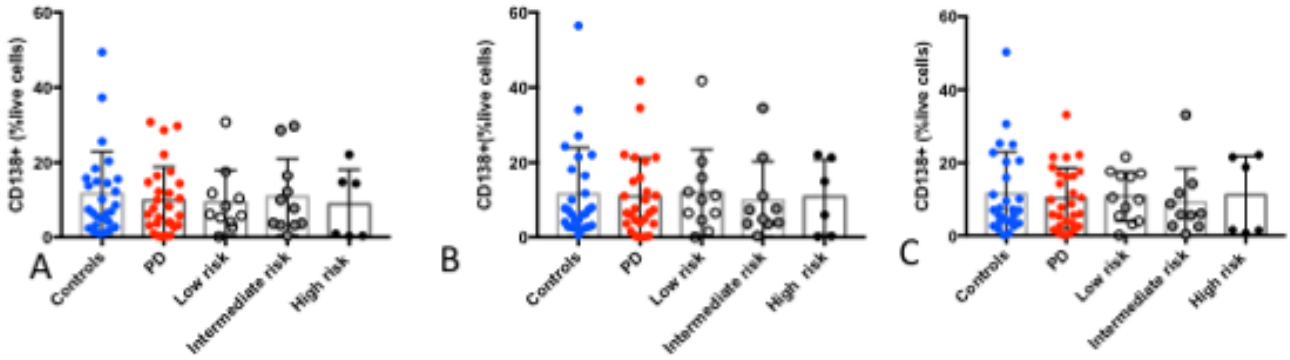

Figure 2-19 CD138+ plasma cells in (A) unstimulated (B) stimulated (CPG+CD40L + PIB) and (C) alpha synuclein conditions. There were no significant between group differences.

Three mixed measures ANOVAs were performed to confirm the between group differences within patients noted above (with IL10, IL6 or CD25 as the repeated measures variable with three levels, unstimulated, stimulated or alpha synuclein) and risk group (high, intermediate and low) as the independent variable. As expected there was a main effect of stimulation condition for all three outcomes ($F [1.4, 37.3] = 9.48$, $p = 0.001$; $F [1.2, 30.6] = 10.36$, $p = 0.002$, $F [1.04, 24.9] = 25.41$, $p = 0.00003$ for IL10, IL6 and CD25 respectively indicating that an appropriate change was seen with stimulation) (see Figure 2-20). As the assumption of sphericity was violated (according to Mauchly's test of sphericity) the Greenhouse-Geisser correction was applied to the degrees of freedom reported above with the p values adjusted appropriately. There was a main effect of risk group for IL10 ($F[2,25] = 3.6$, $p = 0.041$) and for IL6 ($F[2,25] = 3.49$, $p = 0.046$) but not for CD25 ($F [2,24] = 3.36$, $p = 0.052$) (see Figure 2-20). The interaction term (risk group x stimulation condition) was not significant for IL10, IL6 or CD25.

Figure 2-20

ANOVA plots showing the main effect of risk group and stimulus condition

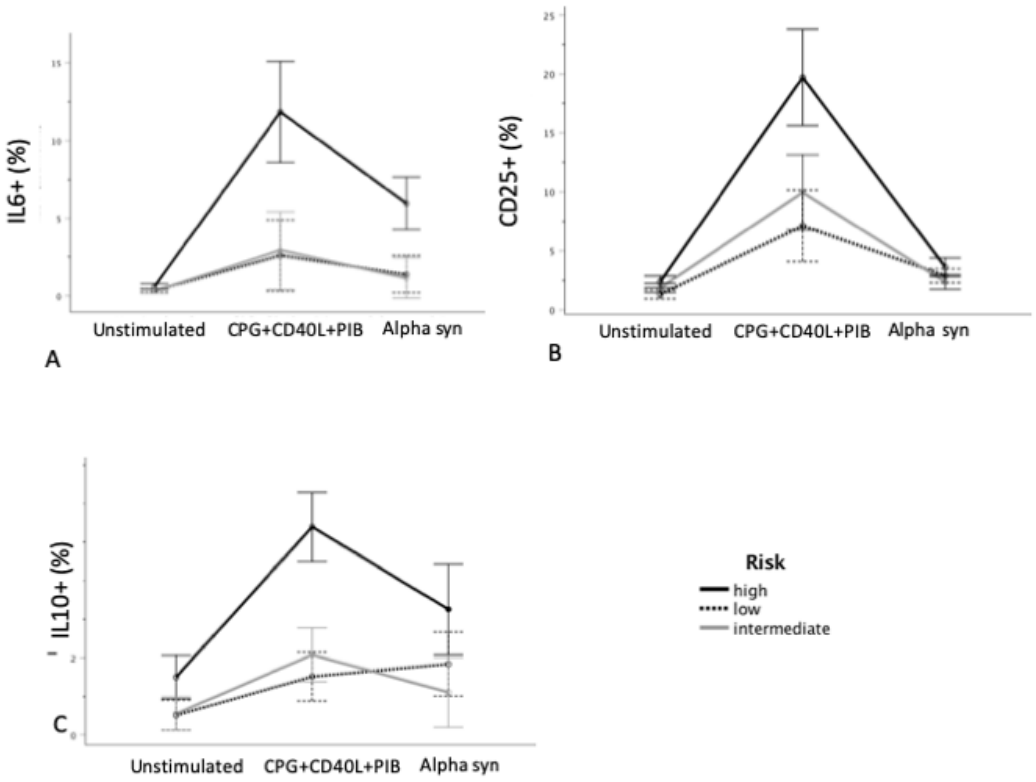

Figure 2-20: Plots show means and SE of the mean for IL6 (A), CD25 (B) and IL10 (C).

2.3.6 Age associated B lymphocytes pilot study (cohort 2)

We recruited 20 patients and 20 controls (see details for cohort 2 in Table 2-7, cohort 1 details are repeated for reference). There was no difference in age between PD and controls within cohort 2 (Mann Whitney U = 1.92, z=0.22, p = 0.82) or in the proportion of males (χ^2(1) = 2.51, p = 0.11). Cohort 2 was significantly younger than cohort 1 (Two way ANOVA with cohort and status [PD versus control] as independent variables, cohort: F [1,119] = 8.26, p = 0.005; status F[1,119] = 0.002, p = 0.97). Disease duration was also significantly less in cohort 2 than in cohort 1 (Mann Whitney U = 0.5, z = -6.3, p = <0.0001), motor scores were lower (MDS-UPRS t [58] = 2.15, p = 0.04) and levodopa equivalent dose was also lower (Mann Whitney U = 141.0, z = -4.15, p = 0.00003). There were no differences in cognition (ACE-R, t[59] = 0.03, p = 0.98) or the probability of a bad outcome (t[58]= -1.3, p = 0.2).

Table 2-7

Participant demographic and clinical details

Variable	Cohort 2		P value
	Control	PD	
Age	65.0(5.42)	64.7(7.6)	0.82
Gender (%male)	40	65	0.11
Disease duration	NA	0.78(0.52)	
MDS-UPDRS	NA	28.25(10.76)	
ACE-R	NA	92.90(4.52)	
LEDD (mg)	NA	302.9(152.56)	
Probability of a bad outcome	NA	0.52(0.21)	

Table 2-7 MDS-UPDRS = Unified Parkinson's Disease Ratiing Scale, LEDD = Levodopa equivalent daily dose, ACE-R = Addenbrooke's Cognitive Examination revised.

2.3.7 Full blood counts

As with the previous cohort absolute lymphocyte counts were lower in patients versus controls ($t[31.27] = -2.98$, $p = 0.006$). There were no between group differences in other full blood count parameters. The absolute B lymphocyte count was also reduced (Mann Whitney $U = 121.0$, $z = -2.14$, $p = 0.03$) (see Table 2-8 and Figure 2-22).

2.3.8 Immunocytochemistry and flow cytometry

Gating of cell populations was performed as shown in Figure 2-21. The major populations were identified as in the previous study. In addition, age associated B cells were identified using Tbet and CD11c. CD86 had been used as a third marker but there were so few cells that were triple positive that this was abandoned. There were no significant differences between patients and controls in the percentages of any of the B lymphocyte subsets including the age associated B cell subset (see Table 2-9). There was no correlation with age (due to the limited age range chosen).

Bivariate correlations were run using combined data from cohort 1 and 2 to see whether the associations with motor UPDRS in the initial cohort remained (see Figure 2-23). The significant negative correlation between the percentage of transitional B lymphocytes and UPDRS remained ($r=-0.35$, $p = 0.009$) and also between the intermediate transitional subset and UPDRS ($r = -0.326$, $p=0.015$). This would be consistent with the hypothesis that these regulatory subsets are protective. There was also a significant negative correlation between the motor UPDRS and the percentage of naïve B lymphocytes ($r=-0.279$, $p = 0.039$). Disease duration was negatively correlated with the percentage of transitional B lymphocytes ($r=-0.405$, $p = 0.002$) and positively correlated with the percentage of CD27-IgD- lymphocytes ($r=0.34$, $p =0.01$) (see Figure 2-24).

Table 2-9

Summary of B lymphocyte subsets across both cohorts

	Cohort 1		P value	Cohort 2		P value
	Control (N=41)	PD (N=41)		Control (N=20)	PD (N=20)	
Lymphocytes ($x10^9$ per L)	1.9(0.62)	1.3(0.4)	0.001	1.6(0.57)	1.23(0.35)	0.006
B lymphocytes absolute count median (IQR)	0.07(0.06)*	0.07(0.07)*	0.39	0.12(0.07)	0.09(0.06)	0.03
B lymphocyte percentage	5.7(2.8)	4.6(2.3)	0.04	7.5(2.7)	7.4(2.9)	0.86
Transitional B lymphocytes	3.36 (2.6)	3.2(2.5)	0.66	6.2(3.53)	5.2(3.11)	0.67
CD27+IgD- (switched memory)	20.6(9.3)	21.92(8.6)	0.61	20.17(5.8)	18.56(7.8)	0.55
CD27-IgD+ (unswitched memory)	53.8(16.2)	53.25(18.5)	0.87	56.72(10.9)	61.06(13.9)	0.35
Double negative	15.38(14.3)	16.14(15.11)	0.67	6.2(2.9)	6.64(4.2)	0.7
Age associated B cells (ABC)				2.9(2.4)	3.32(6.8)	0.47

*Full blood counts only available on a subset of patients and controls for cohort 1 excluding the high risk group (N=20 in each group). P values for cohort 1 reflect

paired t tests between patients and matched controls. P values for cohort 2 reflect independent t tests between patients and controls.

Figure 2-21

Gating strategy for cohort 2

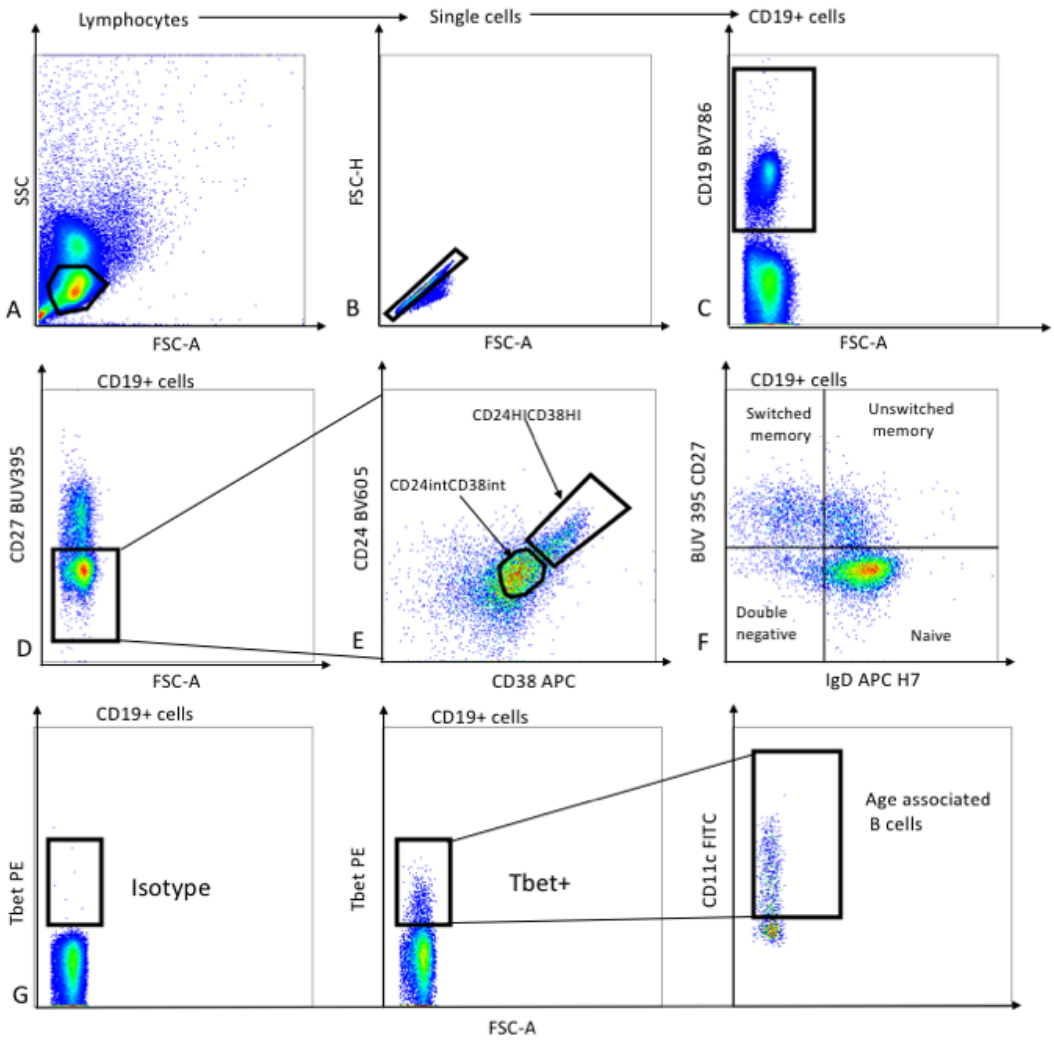

Figure 2-21 Representative plots showing the gating strategy used which was similar to that employed for cohort 1. Age associated B cells were identified using a two step strategy, first gating on Tbet positive B cells (G) then on CD11c positive cells. A PE isotype control was used for the Tbet gating.

Figure 2-22

Absolute lymphocyte counts and B lymphocyte counts

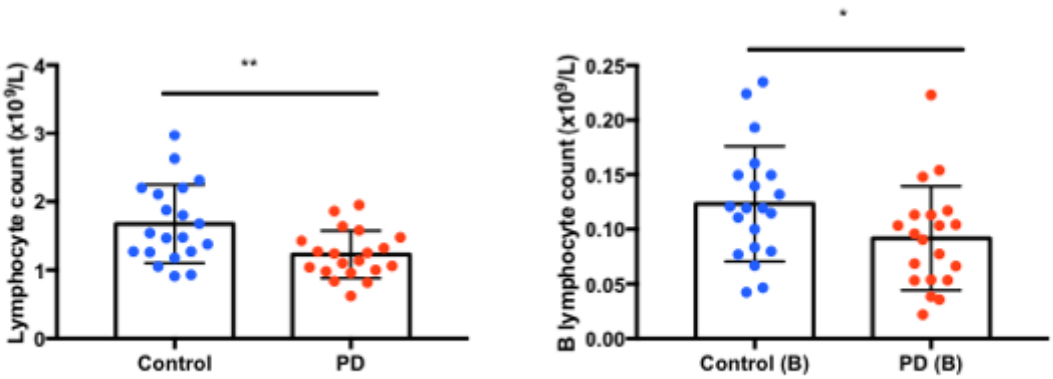

Figure 2-22 Comparison of absolute lymphocyte and B lymphocyte counts in cohort 2.

Figure 2-23

Correlation matrix showing relationships between B lymphocyte parameters and clinical outcomes using combined cohort 1 and 2 data (N = 55 patients) (*<0.05, **<0.01)

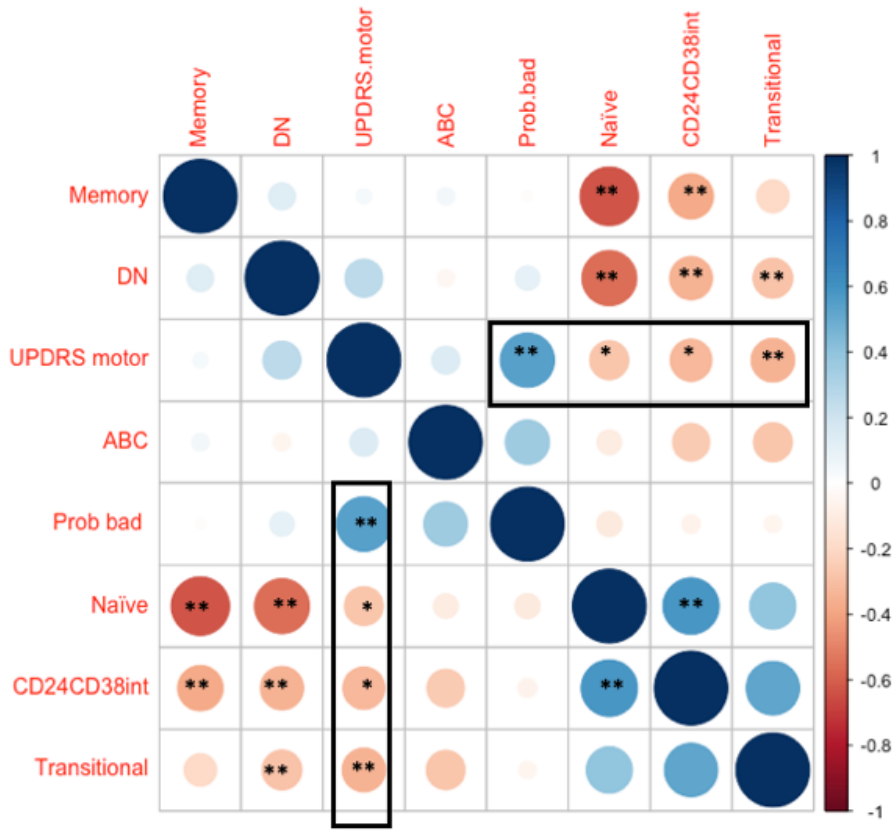

Figure 2-23 Boxes show relevant correlations with the UPDRS motor score. "Prob bad" probability of a bad outcome is correlated with the UPDRS score as it is derived from it. The other associations in the boxes are between the UPDRS and B lymphocyte subsets.

Figure 2-24

Scatterplots showing significant relationships between B lymphocyte subsets and motor UPDRS

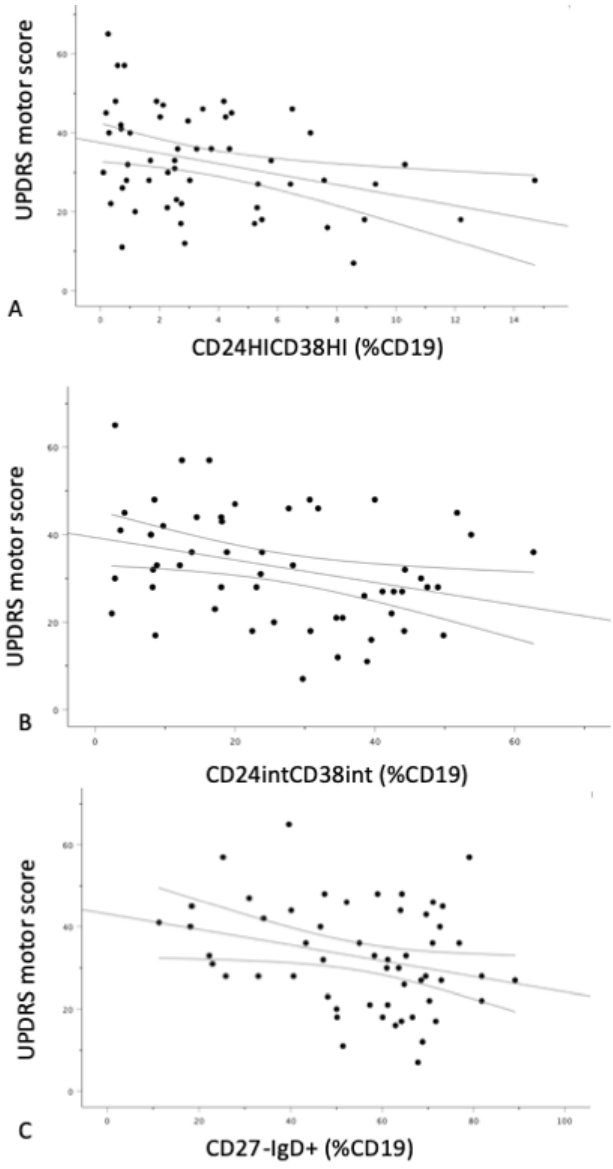

Figure 2-24: Motor UPDRS scores are on the y axis and B lymphocyte subset on the x axis, transitional (A), intermediate (B) and double negative (C).

I ran a multiple linear regression model using motor UPDRS as the dependent variable and CD27-IgD-, CD24HICD38HI and CD24intCD38int as the predictor variables. The first analysis was done using the enter method. Regression assumptions were met : the dependent variable was continuously distributed;, there were two or more independent variables; there was independence of residuals (Durbin-Watson statistic = 2.12), the relationships between variables were linear according to inspected scatterplots, there was homoscedasticity of residual error, there were no significant outliers and the residuals were normally distributed. There was some multicollinearity in that the predictors were correlated with each other.

The overall model was a significant predictor of motor UPDRS scores ($F[3,51] = 3.12$, $p = 0.027$) explaining 16.3% of the variance in motor UPDRS scores. Regression standardised coefficients for the individual predictor variables were not significant.

Due to the presence of multicollinearity in the data I ran a further regression model, this time using the 'stepwise' method which enters each variable in turn, keeping those that result in p values of $F < 0.05$ and removing those that have p values >0.1. The resulting model was highly significant, ($F[1.53]=7.32$, $p =0.009$) explaining 12.1% of the variation in UPDRS scores. It included only the CD24HICD38HI subset as adding the other variables did not significantly increase the percentage of the variance explained (Standardised beta = -0.348, t = -2.7, p = 0.009) and they were therefore removed from the model.

2.3.9 Participants B lymphocytes in CSF in PD and controls (Pilot study)

18 patients and 4 controls were recruited (see Table 2-10). There was no significant difference in age between the patients and controls (one way ANOVA

F[16,20] = 0.29, p = 0.97). At the time of writing, only male controls had been recruited (further recruitment is ongoing) (as shown in Table 2-10).

Table 2-10

Participant demographic and clinical details

	Controls (N=4)	**PD (N=18)**	**P value**
Age	68.0	65.61(7.61)	0.977
Gender (%male)	100	71.4	0.466
Disease duration	NA	1.23(0.73)	
MDS-UPDRS motor score	NA	24.17(9.93)	
ACE-R	NA	92.0(4.69)	
Levodopa equivalent dose (mg)	NA	290.39(153.57)	

2.3.10 Full blood counts

Full blood counts were available for all participants. There were no significant differences in the numbers of lymphocytes, neutrophils, monocytes, eosinophils or basophils between patients or controls (at the point of analysis the study was underpowered to detect such differences, these are only included to fully describe the cohort, see Table 2-11).

Table 2-11

Full blood counts CSF study

	Controls	PD (All)
Neutrophils	3.49(1.63)	3.8(1.51)
Lymphocytes	1.3(0.38)	1.36(0.30)
Monocytes	0.44(0.09)	0.39(0.1)
Eosinophils	0.15(0.01)	0.15(0.11)
Basophils	0.02(0.01)	0.04(0.02)

2.3.11 Immunocytochemistry and flow cytometry

The gating strategy for both peripheral blood mononuclear cells (PBMC) and cerebrospinal fluid cells (CSF cells) is shown below (see Figure 2-25). The same strategy was applied to both the peripheral and CSF cells in order to make direct comparisons. There were no significant differences in absolute cell counts between the controls and PD patients although there is a clear trend towards higher cell counts in the patients particularly in the CSF (see Figure 2-27 and associated legend, unpaired t-tests, statistics not shown).

There were no significant differences between controls and PD patients in the B cell phenotype (unswitched, memory, naïve versus double negative) (see Figure 2-28). There was a significant shift between blood and CSF across all participants with the majority of B cells being naïve peripherally and the majority being memory cells in the CSF (as shown in the radar plot in Figure 2-28, C) (Repeated measures ANOVA with 2 factors (tissue blood versus CSF) and phenotype (memory versus naïve), the interaction term was significant $F [1,16] = 30.19$, $p = 0.00005$).

Figure 2-25

Gating strategy for peripheral PBMCs and CSF cells (showing PBMCs)

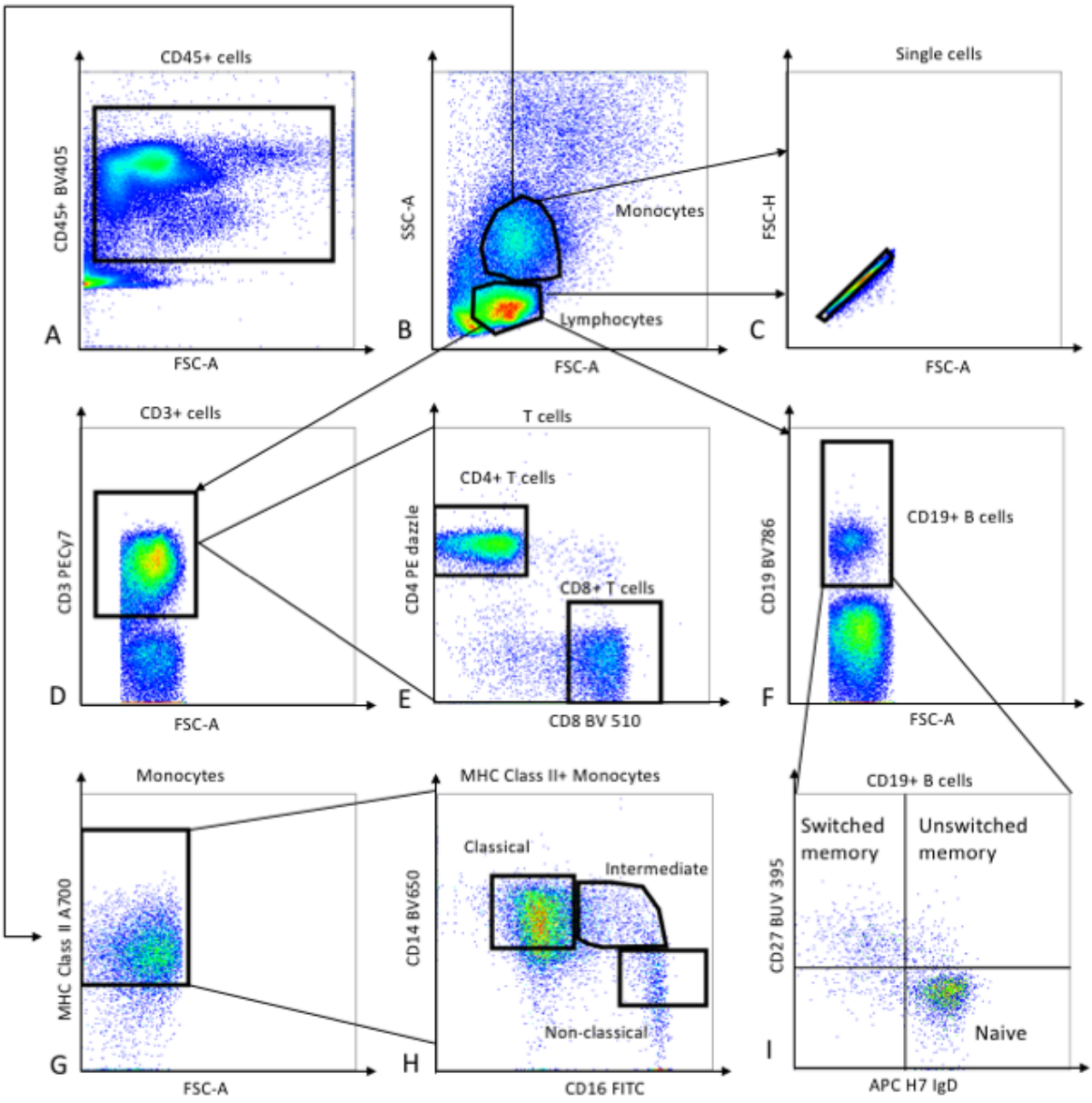

Figure 2-25: Initially CD45+ cells were identified (in order to exclude any non-immune cells from the CSF population) (A). Lymphocytes and monocytes were then identified using FSC and SSC (B). T cell populations and B cell populations were identified using CD3 (D), CD4 and CD8 (E) for T cells and CD19, CD27 and

IgD for B cells (F and I). Monocytes were identified using MHC Class II, CD14 and CD16 to ensure that CD16+ NK cells were excluded (G, H).

Figure 2-26

Gating strategy showing CSF cells

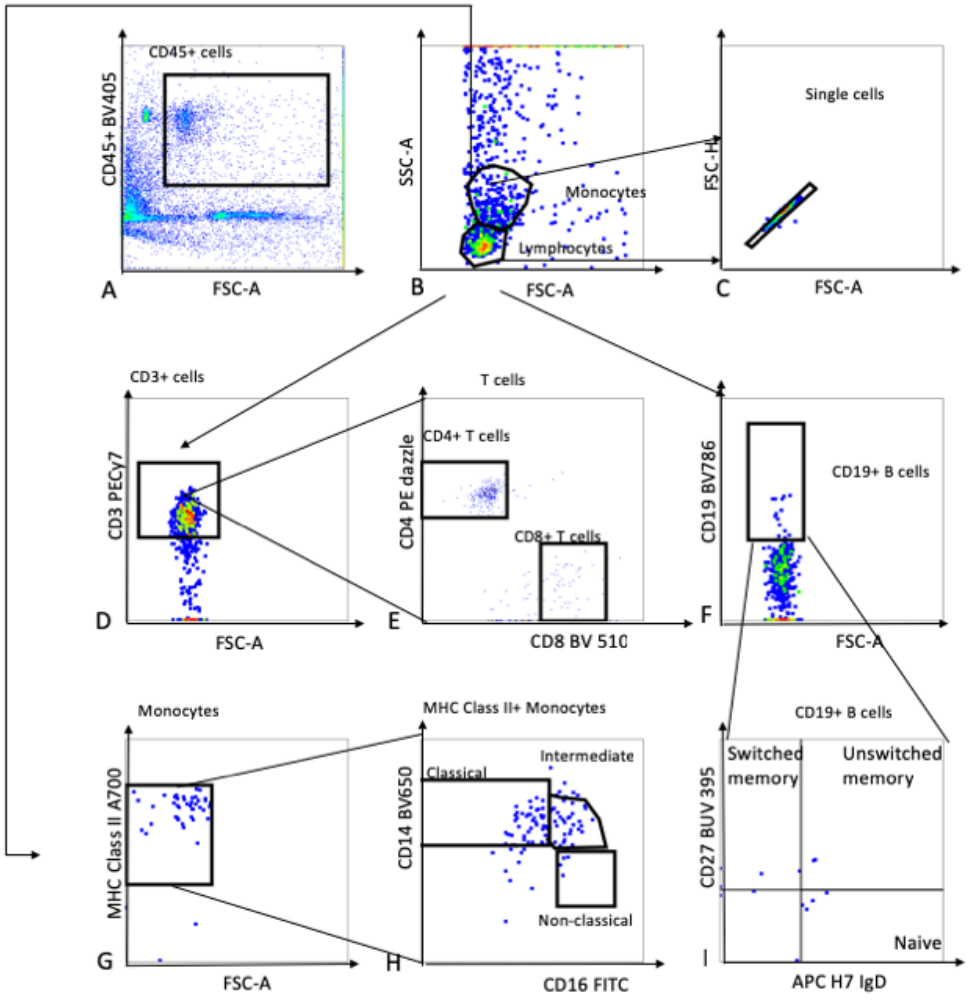

Figure 2-27

Cell counts in blood and CSF across patients and risk groups

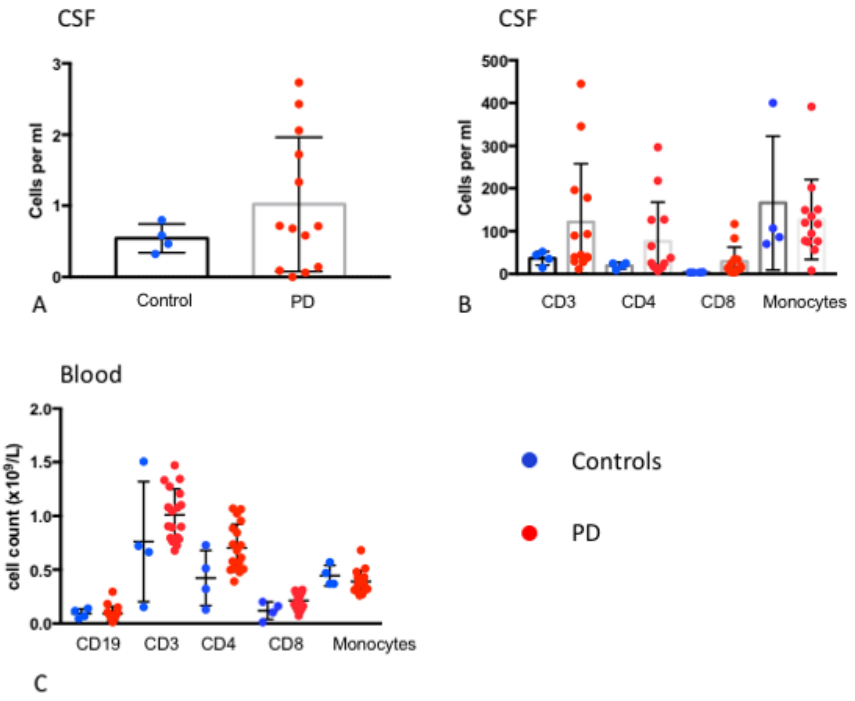

Figure 2-27 shows A) the number of B cells in the CSF B) the number of T cells and monocytes and C) the number of cell concentration in the peripheral blood of PD patients and controls.

Figure 2-28

B cell phenotypes in peripheral blood and CSF

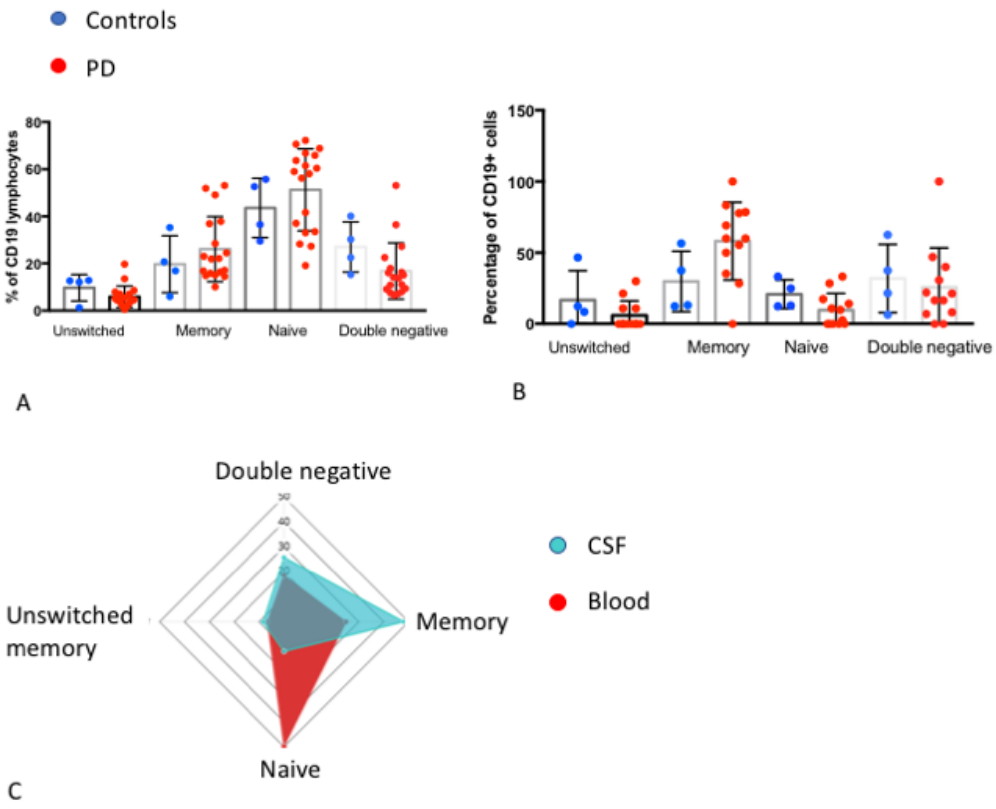

Figure 2-28 A) Memory and naïve cells as defined by CD27 and IgD in the blood and B) the CSF. C) shows a skew towards a memory phenotype in the CSF.

2.4 Summary of main findings

I have replicated previous findings of decreased B lymphocytes in PD compared to controls with a comparable sample size (N=40 patients and 40 matched controls)(Bas et al., 2001 (N=64 PD and 38 controls; Gruden et al 2011 (N=32 PD and 26 controls); Stevens et al., 2012 (N=88 PD and 77 controls)) and additionally shown that this effect is larger in those at risk of disease progression. The patient sample described in my thesis is unique in being matched to the controls for age, gender and MAPT genotype with all assays being run in parallel (patient and a matched control). I performed the first study detailing circulating B lymphocyte subsets and phenotypes in PD, including age associated B lymphocytes. There were no differences in B lymphocyte subsets between patients and controls that withstood correction for multiple comparisons suggesting that it is not one particular subset driving the observed differences. I also showed for the first time, a robust negative correlation between motor UPDRS scores and B lymphocyte subsets that are enriched for regulatory B cells, raising the possibility that these cells may play a protective role in disease. There is also a negative association with expression of CD1d which is known to present lipid or glycolipid antigens to natural killer cells (NK) in particular (Chaudhry & Karadimitris, 2014).

I performed ex vivo stimulation assays on peripheral B cells, showing that cells from patients at high risk of progression to dementia are more responsive to stimulation in vitro, producing more cytokines than the other PD risk groups. As expected, given the decreased number of B lymphocytes, this group also had higher baseline levels of BAFF compared to patients at lower risk. I have also identified B lymphocytes in the CSF of both patients and controls, with a trend towards increased numbers in patient CSF (but the small number of controls limits the robustness of this data). I have also described for the first time that

CSF B lymphocytes are skewed towards a memory phenotype, suggesting that they are antigen-experienced cells which is likely to be relevant in PD where there is a putative antigen in aggregated or misfolded alpha synuclein).

2.5 Chapter discussion

My initial hypothesis was that there may be an increase in pro-inflammatory B cells or memory B cells in patients with PD compared with controls. This includes the CD27-IgD- subset which have been reported in other studies (summarised in (Frasca, 2018)) which are highly pro-inflammatory (exhibiting a senescence associated secretory profile or SASP consisting of TNF-alpha, IL6 and IL8, inflammatory microRNAs such as miRs, miR-155/16/93 and a high level of expression of the cell cycle regulator p16INK4) but with a poor ability to differentiate or proliferate in response to stimuli. There was no significant change in the proportion of these 'late memory' (also known as exhausted memory or terminally differentiated memory B cells (Frasca, 2018) but the functional studies stimulating B lymphocytes in vivo did show that, at least in the PD subgroup at high risk of disease progression, there was increased production of cytokines and activation markers following stimulation than in the lower risk subgroups. This is consistent with previous work by our group in a large multicentre longitudinal study of 213 PD patients (and 93 controls) (Williams-Gray et al., 2016) which showed that patients with a more pro-inflammatory circulating cytokine profile had faster motor progression over a 36 month period and lower MMSE scores. The pro-inflammatory profile was derived from a principal components analysis (PCA) and consisted of TNF alpha, IFN gamma, IL2 and also IL10 (the latter cytokine does not fit neatly into the 'pro-inflammatory' category).

During my PhD I contributed to another study looking at T cell replicative senescence (Williams-Gray et al., 2018) where we found that CD8 T cells in PD patients did not develop an age associated senescent phenotype in response to CMV infection unlike in controls suggesting that there is an aberrant response to CMV infection (or aging) in PD patients. .We had hypothesised initially that PD patients would show accelerated (rather than absent) 'inflammaging' (or immunosenescence), a process related to aging that involves chronic low grade sterile inflammation (Franceschi, Garagnani, Parini, Giuliani, & Santoro, 2018). Senescent immune cells have a terminally differentiated phenotype, they do not replicate and show increased secretion of pro-inflammatory cytokines such as IL-6 and TNFalpha (Nikolich-Žugich, 2018). In line with this finding, I also hypothesised that I would see less age associated B cells (defined by CD11c+ and tbet+ B lymphocytes or by CD27-IgD- B lymphocytes). Neither of these cell subsets were different, suggesting that there is not a differential or aberrant response to aging that is specific to the B lymphocyte compartment in PD.

A T cell phenotyping study with 113 patients and 96 age and gender matched controls noted that there was an increase in T effector memory cells (CD45RO+ and FAS+) in PD patients with higher motor UPDRS scores (>31) compared to those with lower UPDRS scores (1-20) and controls (Saunders et al., 2012). At the same time there was a decrease in the proportion of CD31+ Treg cells (CD4+CD25+CD127-) in the patients with the higher UPDRS scores. Functional T cell assays showed impaired Treg suppression of T effector function in PD patients versus controls. This finding is not entirely consistent in the literature (as reviewed in (Z. Chen, Chen, & Liu, 2018) but in the light of this and other studies showing a protective effect of Treg cells in neurodegeneration (F. He & Balling, 2013), there has been a phase I trial demonstrating that the recombinant granulocyte macrophage colony stimulating factor (GM CSF), sargramostim is able to increase the proportion of T regs in PD patients and this was associated

with some improvements in motor outcomes (although the study was not powered to identify differences in motor outcomes)(Gendelman et al., 2017). Larger trials are awaited. The study did not look specifically at B lymphocytes or regulatory subsets. It is known that B cells themselves are able to produce GM-CSF(Rauch et al., 2012) and this may also be an avenue for further exploration. It is difficult to understand the rationale specifically for the use of GM-CSF when there are other drugs that expand this population. GM-CSF has a wide range of effects on many immune cells including monocytes and macrophages which were not specifically measured or accounted for in this study.

The negative association between the proportion of regulatory B cells and UPDRS motor scores that I have described further expands these findings, supporting the view that an imbalance between effector and regulatory functions in the lymphoid compartment is associated with worse disease outcomes and suggesting that, at least theoretically, attempting to boost regulatory T or B lymphocytes is a worthwhile therapeutic strategy to prevent disease progression. Ultimately doing a clinical trial of such an agent is the best experimental strategy for demonstrating proof of principle as observation studies will only confirm an association. For example low dose IL2 is able to induce both T regulatory cells (Ye, Brand, & Zheng, 2018) and B regulatory cells (Akimichi Inaba (Clatworthy Lab), personal communication based on unpublished data). Fingolimod, a drug currently licensed for the treatment of relapsing and remitting multiple sclerosis has also been shown to increase the proportion of circulating regulatory B lymphocytes (identified by surface markers and by in vitro production of IL10) (Blumenfeld, Staun-Ram, & Miller, 2016; Grützke et al., 2015), with the former study additionally showing an increase in CSF regulatory B lymphocytes and increased transmigration of the regulatory B cells in an in vitro model of the blood brain barrier (Grützke et al., 2015). There is also some evidence that fingolimod is protective in toxin based animal models of PD (Zhao et al., 2017).

Another licensed multiple sclerosis drug, glatiramer acetate (Copaxone) is also able to induce T reg populations (J. Haas et al., 2009) with an unknown effect on regulatory B lymphocyte populations. Belimumab, a monoclonal antibody against BAFF has also been shown to expand regulatory B lymphocyte populations(Banham et al., 2018) and would be a further potential option.

I also noted a negative association with CD1d positivity and expression on B lymphocytes. CD1d has not been studied in the context of Parkinson's disease and was initially included in the phenotyping panel because of its use as a marker of regulatory B lymphocytes in mice along with CD5 (primarily defined by their ability to produce IL10)(Mauri & Menon, 2015). In both mice and humans it has an additional role in presenting lipid and glycosphingolipid antigens to a specific subset of natural killer T cells (NKT)(Chaudhry & Karadimitris, 2014; Nair et al., 2015; Oleinika et al., 2018).

Invariant NKT cells can be activated following presentation of antigen and can assume a Th1, Th2 or Th17 profile or provide help to the presenting B cells to trigger a germinal centre reaction(Chaudhry & Karadimitris, 2014). Perturbations of the B cell-iNKT axis can therefore skew the peripheral immune response. In SLE patients with active disease there is decreased CD1d expression on B cells and also decreased iNKT cells. Once they have reconstituted their B lymphocyte population following depletion this disappears in association with a clinical response(Oleinika et al., 2018). Human β-glucosylceramide and glucosylphingosine specific iNKT cells can activate B cells in vitro and the frequency of these cells in mouse models and patients is associated with treatment response in lupus (Nair et al., 2015) There is also more recent evidence that CD1d expressed on B cells is able to induce a population of suppressive iNKT cells capable of suppressing Th1 and Th17 responses and it may

be this regulatory effect that acts in concert with the other regulatory B cells to decrease the deleterious Th1 response (Oleinika et al., 2018).

Limitations of this work

To confirm the abnormalities in B cell subsets and function that I have described in patients with PD, one would ideally replicate these findings in a larger cohort using a matched design as for cohort 1. Increasing the cohort size was limited by the time available to recruit patients to this study and the practical challenges of completing the assessments and assays limit on a large number of patients, which would ideally require a large team of investigators and high-throughput, automated assays. The negative association with the CD1d positive cells could be an artefact of the gating which was based on isotype controls but which did not give two defined populations. In order to avoid bias introduced by the gating, I used the CD1d MFI ratio (ratio of the MFI in the relevant channel to the unstained sample run at the same time) which was not affected by gating and the effect remained suggesting that it is genuine.

There were also significant batch effects in the B lymphocyte stimulation study due to differences in duration of cryopreservation. This problem was offset by the fact that I ran the assays with matched high or intermediate risk patient, low risk patient and their respective controls in each batch ensuring this confounding factor did not affect one group more than others.

When investigating patient peripheral immune cell phenotypes, there are often concerns that any observed differences may be mediated by differences in medication. The high risk group in cohort 1 was on the lowest dose of levodopa rather than the highest. The levodopa equivalent dose was not directly correlated with any of the B lymphocyte subsets suggesting at the very least that

there is no dose response effect. Similarly, in Cohorts 2 and 3, LEDD was not associated with B lymphocyte subsets or any other parameters measured. In a study looking at T cells in 53 treatment naïve patients and 28 healthy controls there were differences between patients and controls in response to alpha synuclein *in vitro* suggesting that at least some of the effects observed in lymphocytes occur in the absence of drug treatment (Kustrimovic et al., 2016). Other studies have found that l-dopa and dopamine agonists can decrease cytokine production in healthy young subjects (Rocha et al., 2018).

Figure 2-29 Graphical summary of main findings

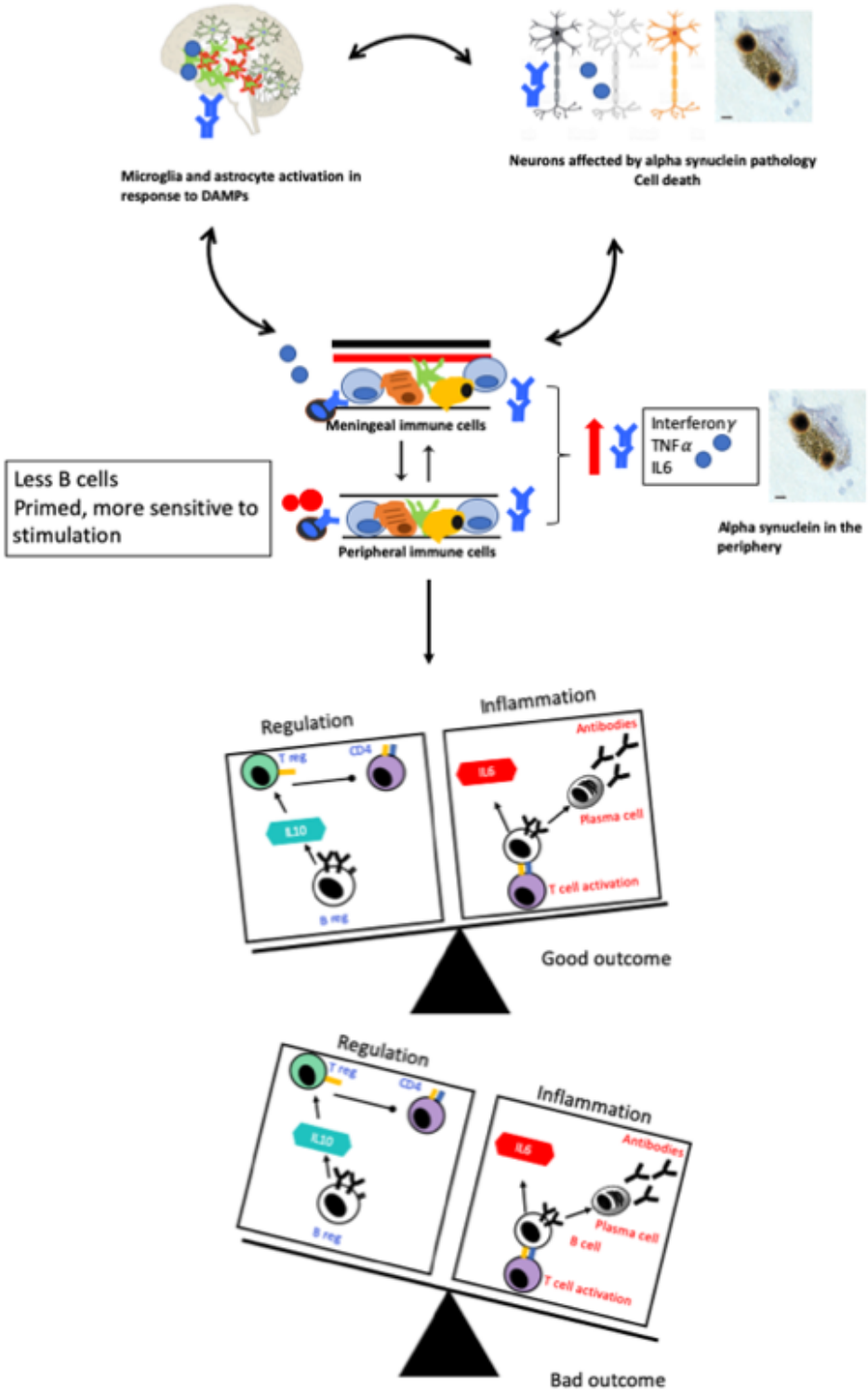

Figure 2-29 I showed that there were less B lymphocytes in the periphery, driven mainly by the high risk group and that these B cells produced more cytokine on stimulation. A greater proportion of regulatory B cells was associated with better motor outcomes in a cross-sectional study.

2.6 Future directions

There are a number of avenues of research which could be pursued, based on my findings:

i) Characterisation of CSF B lymphocytes. I have identified the presence of predominantly memory B cells within the CSF, with potentially higher numbers in patients with PD. This observation needs to be validated with the inclusion of larger numbers of control CSF samples. In addition, the use of single cell RNA sequencing would allow these cells to be transcriptionally characterised and would facilitate the identification of specific clones (which may be specific for alpha synuclein in PD patients) and allow their comparison to circulating B cells. This could potentially include the sequencing of B and T cell receptors building on the work by (Sulzer et al., 2017) and is now underway in the Barker/Clatworthy Labs.

ii) Extend the assessment of B cells in PD to include the meningeal compartment. There is an increasing appreciation of the complexity of immune cell subsets within the meninges, and meningeal B cells are evident in mice. Therefore, it would be of interest to investigate B lymphocytes in human dura, examining for evidence of B cell follicle formation in association with disease and further defining the phenotype and role of these cells. It is possible to obtain dural samples in the context of patient's having brain biopsies for other

conditions and in patients with PD who are undergoing the insertion of deep brain stimulators. Such experiments rely on opportunistic sampling where it is difficult to remove other confounding factors but can nevertheless supply relevant in vivo information in humans, and are also a line of investigation being pursued in collaboration with Mr Adel Helmy. The decrease in peripheral B lymphocytes may be associated with recruitment of B lymphocytes to the meninges and this could be shown using mouse models and by looking at human dura.

iii) The application and investigation of the effects of different immunomodulatory therapies on patients with PD. To build on these findings experimentally in patient cohorts, therapeutic strategies aimed at boosting regulatory B lymphocytes may be beneficial and would provide definitive experimental proof that the associations I have observed are causal. Specifically taking forward repurposed drugs such as low dose IL2, glatiramer acetate or fingolimod in order to show that it is possible to boost regulatory B lymphocytes in our patient populations and that this effect is associated with improved disease outcomes. Fingolimod is available in an oral once daily preparation that is likely to be more acceptable to our patients than the IV or subcutaneous administration required from both of these other drugs suggested. Demonstrating a change in disease outcome is often difficult in Parkinson's disease trials due to the slow progression of the disease and the heterogeneity of clinical outcomes. Choosing an enriched population of patients such as those at high risk of disease progression (identified by the multi-parameter risk score) would be one strategy that would potentially allow for the demonstration of a proof of principle over an appropriate time period that is within the limits of feasibility for a drug trial (for example change in UPDRS motor scores or cognition over a 2 year follow up period). The disadvantage of a high risk population of patients is that these patients are harder to recruit and will tend to

be older and frailer thereby being more vulnerable to infections secondary to the drug and also to the cardiovascular side effects which include first dose bradycardia (requiring in-patient administration of the first dose). An alternative strategy would be to use a high risk prodromal cohort which represent an earlier time point in disease pathogenesis. For example, using a cohort of patients with REM sleep behaviour disorder (as described in (Postuma, Gagnon, Bertrand, Génier Marchand, & Montplaisir, 2015). One could enrich for participants at a high risk of progression to clinically overt Parkinson's disease and thereby test the hypothesis that modulating B lymphocyte function can slow disease progression (as measured by a standard clinical trial outcome such as the change in motor UPDRS).

iv) Investigate B lymphocytes in Gaucher's cohorts and in carriers (and monitor conversion to PD in a longitudinal cohort)

There is a well described association between Gaucher's disease (GD) and dysfunction in the B lymphocyte compartment (in the form of an increased risk of myeloma and B cell lymphoma) (Mistry, Taddei, vom Dahl, & Rosenbloom, 2013). One could therefore hypothesise that part of the mechanism underlying the association of Gaucher's disease with PD is related to altered function in the B lymphocyte compartment leading to chronic inflammation, but this will require further investigation.

There is evidence in both human and mouse cell lines that glucosylsphingosine (which accumulates in GD) stimulation is able to induce aggregation of alpha synuclein *in vitro* (Taguchi et al., 2017). There is also a negative association between GBA enzyme activity and the levels of plasma alpha synuclein oligomers with lower enzymatic activity being associated with higher levels of plasma oligomers (Pchelina et al., 2016). One could therefore hypothesise that part of the association between GBA mutations and PD is driven by increased

aggregation of alpha synuclein and decreased antigenic presentation (and therefore reduced clearance). This may be associated with reduced activation of a regulatory subset of invariant NKT cells. This then contributes to a more pro-inflammatory environment that increases the risk of PD and subsequent progression.

2.7 Conclusions

There are changes in the B cell compartment associated with Parkinson's disease and its progression. In particular, cells from PD patients at high risk of an early dementia produce more cytokines after stimulation. Higher proportions of regulatory B lymphocytes are protective in a cross-sectional cohort. Boosting this subset may be a therapeutic strategy.

3 ALPHA SYNUCLEIN AUTO - ANTIBODIES IN PD

3.1 Chapter abstract

Background
In the previous chapter, I have described alterations in the B cell compartment associated with Parkinson's Disease (PD). In this chapter I aimed to demonstrate that this response is at least in part an antigen specific response to alpha synuclein.. Alpha synuclein binding antibodies have been described in Parkinson's Disease but there is conflicting evidence as to whether these are actually associated with disease or its severity.

Hypotheses:
There is an increase in alpha synuclein antibodies in early PD, reflecting an antigen specific response to disease. This response is greater to pathological forms of alpha synuclein such as S129D, fibrils or the more recently described Y39 peptide.

Aims
To perform a systematic review and meta-analysis to see whether such an association exists in the published studies to date
To develop an assay to measure antibodies to different forms of alpha synuclein
To measure alpha synuclein antibodies in a cohort of patients and matched controls

Methods
I carried out a systematic review and meta-analysis, searching pubmed, Medline, Cochrane database, Keele web of science and google scholar for terms including antibody, Parkinson's disease and alpha synuclein. Reference lists of identified papers were hand searched to ensure that studies were not missed. Relevant manuscripts were taken forward for meta-analysis if they were of adequate quality and power using the metafor package in R .

I designed custom Mesoscale discovery assays (MSD) to measure serum antibodies to monomeric alpha synuclein, fibrils, two peptides of alpha synuclein known to be associated with disease (S129D peptide and Y39 peptide). I also used tau in this assay system as an alternative disease relevant protein. Figure 3-1 gives an overview of the antibody studies. I piloted these assays in a small sample of patients and controls.

Results
The systematic review and meta-analysis suggested that there is evidence in early disease to suggest an increase in the antibody response to alpha synuclein in PD. There was also significant clinical heterogeneity both between and within studies that was sometimes poorly described. This was additionally complicated by assay variability.

Initial testing of the antibody assays that I developed in a small cohort of patients showed no difference between patients and controls overall. There was an increase in Y39 antibodies in the group at high risk of an early dementia compared to controls. This was driven by a few individuals and requires further validation but is consistent with a recent study showing that T cells produce IL5 and IFN gamma after exposure to this alpha synuclein epitope.

Conclusions
The published studies to date collectively support the conclusion that there is an alpha synuclein specific response in early PD. Further samples are required to see whether I can replicate this with my antibody assay. This work is ongoing.

Figure 3-1

Alpha synuclein antibody studies overview

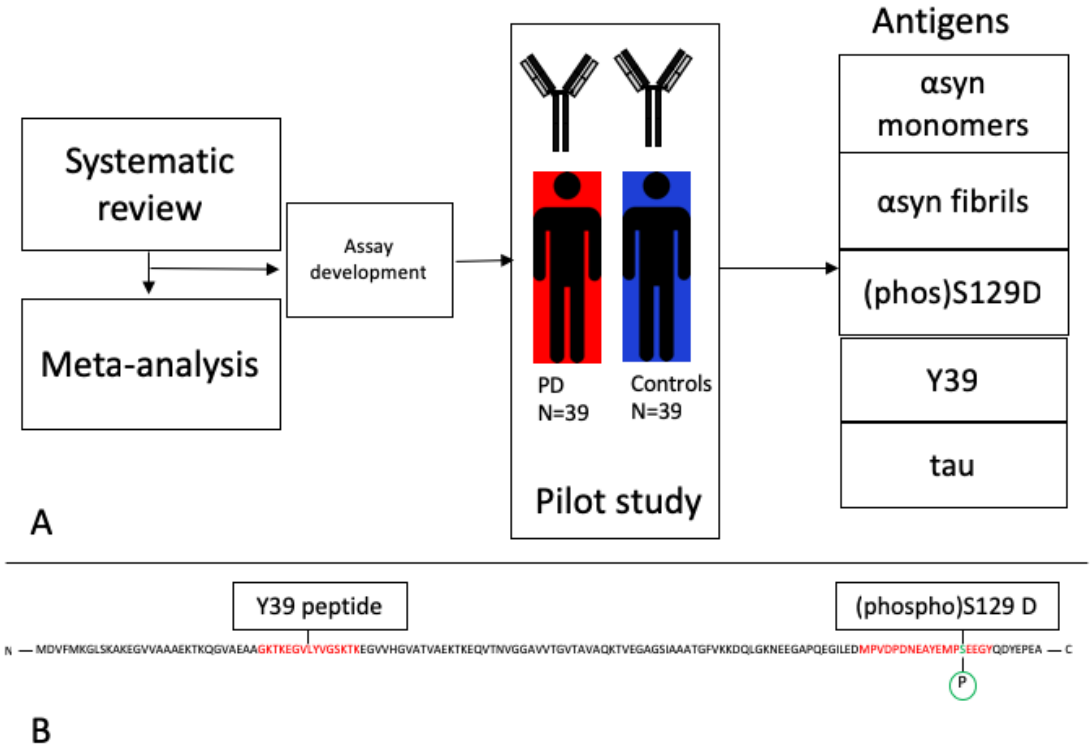

Figure 3-1 A shows an overview of antibody studies, highlighting the antigens used to identify serum antibodies in a pilot study using cohort 1 described in Chapter 2 (controls matched to PD patients for age, gender and genotype). B shows the amino acid sequence of alpha synuclein, highlighting the sequence for the Y39 peptide (described in (Sulzer et al., 2017) and the peptide including the pathologically phosphorylated serine, S129D.

3.2 Systematic review and meta-analysis of auto-antibodies to alpha synuclein in Parkinson's disease

It is critical to have a better understanding of how alpha synuclein autoantibodies relate to PD and its progression. In particular, there is a need to discern whether they constitute a useful diagnostic or prognostic biomarker or may have potential therapeutic relevance. In this chapter, I will present a systemic review and meta-analysis of antibody studies in PD cohorts, critically discuss the value and limitations of existing data and make recommendations for future studies. As noted in the acknowledgements section, this work has been recently published (Scott et al., 2018).

3.3 Methods

3.3.1 Systematic review of alpha synuclein antibody studies in PD

I searched the literature for studies published prior to 1st June 2018 using Pubmed, Medline, Cochrane database, Embase, Google scholar and Keele Web of Science. I used the following search terms: "Antibody and Parkinson's Disease", "Auto-antibody and Parkinson's disease", "Alpha synuclein antibody", "Alpha synuclein auto-antibody". To ensure complete study capture I also searched using "Auto-antibody dementia" "Antibody dementia". Reference lists of the selected papers were also manually searched to identify additional studies. Papers were excluded if they did not involve PD patients, if they did not measure alpha synuclein antibodies and if there was no control group. Otherwise all papers measuring antibodies to alpha synuclein or its epitopes in Parkinson's disease patients were included in the systematic review. The literature searches were done between 1 May 2018 and 6 June 2018. Summary information from each study was compiled into a table .

In order to assess whether studies were adequately powered, mean alpha synuclein antibody titres (or optical density) in each group and standard deviations were recorded and used to calculate the required sample size to detect a difference of the magnitude reported. The following formula was used to calculate sample size (modified from (LLC, 2018).

$$nA = \kappa nB \; and \; nB = (1 + \frac{1}{\kappa})(Swithin \frac{z1 - \frac{a}{2} + z1 - \beta}{\mu A - \mu B})^2$$

Where:

K = nA/nB (matching ratio between groups – nA = PD patients, nB = controls)

Swithin = pooled standard deviation across groups

α = Type I error (set at 0.05)

β = Type II error (1-β = power, set at 0.8)

The pooled within sample standard deviation was calculated to overcome differences in variation between the groups (from (Borenstein, Hedges, Higgins, & Rothstein, 2009):

$$Swithin = \sqrt{\frac{(n1 - 1)S1^2 + (n2 - 1)S2^2}{n1 + n2 - 2}}$$

n1 = sample size (SS) in patients, n2 = SS in controls

S1 = SD in patients, S2 = SD in controls

3.3.2 Meta-analysis of alpha synuclein antibody studies in PD

I undertook a meta-analysis, stratified by disease duration given the suggestion in the literature that this is a relevant factor (e.g. (Yanamandra et al., 2011). Studies with mean disease durations of 5.9 years and less were included in an "early disease" meta-analysis and those with disease durations of 7 years or more

were included in a "later disease" meta-analysis given the trends noted in the review above and in table 1.

More stringent data quality criteria were adopted for the meta-analysis than for the systematic review described above.

Inclusion criteria:

i) The study measured antibodies to full length alpha synuclein
ii) The antibodies were measured using titres (either relative or absolute) as a continuous measure
iii) The study included both idiopathic PD patients and controls
iv) The study stipulated a measure of disease duration for the cohort
v) The controls were age and gender matched to the patients
vi) Antibodies were measured in either serum or plasma

If a study had not published appropriate statistical tests to determine whether the controls were matched appropriately to the patients this was performed (independent samples t-test for age; chi-squared test for gender). The study estimates were extracted from the included papers according to the protocol below.

Study estimate extraction:

(i) Means and standard deviations were used as the basis for the study estimates, if reported.

(ii)If these were not reported, then the median and interquartile ranges were extracted and converted into means and standard deviations using the methodology described in (Wan, Wang, Liu, & Tong, 2014) and an online calculator.
(http://www.comp.hkbu.edu.hk/~xwan/median2mean.html)

(iii)If the above estimates were not described in the text then they were estimated from the boxplots or graphs published in the text.

As all studies used different assays and units of measurement, it was not possible to do a direct comparison using the raw unstandardised mean difference. The study estimates were therefore used to calculate the standardised difference and the associated variance (yi and vi respectively) using the metafor package for R in R studio (version 1.0.153), and the following formulas: (Borenstein et al., 2009)

$$yi = \frac{\overline{X}1 - \overline{X}2}{Swithin}$$

Where yi = standardised mean difference (d)

$\overline{X}1$= sample mean in PD patients

$\overline{X}2$ = sample mean in controls

S*within* = within groups standard deviation, pooled across groups (as used above for the power calculation)

$$Swithin = \sqrt{\frac{(n1-1)S1^2 + (n2-1)S2^2}{n1+n2-2}}$$

S1 = standard deviation in PD group

S2 = standard deviation in controls

A random effects model was used to assess the overall difference between patients and controls. Forest plots were generated to show the results graphically. Funnel plots were generated to plot standardised mean difference (x axis) against standard error (y axis) to assess the impact of publication bias and heterogeneity.

The variance of d (referred to as vi) is given by the following formula (see (Borenstein et al., 2009) page 27):

$$vi = \frac{n1+n2}{n1n2} + \frac{d^2}{2(n1+n2)}$$

3.4 Results

3.4.1 Systematic review

A total of 17 papers met the inclusion and exclusion criteria for the systematic review (Table 3-1). Eight studies found a statistically significant increase in alpha synuclein antibodies in idiopathic PD patients compared to controls (Bryan, Luo, Forsgren, Morozova-Roche, & Davis, 2012; Caggiu et al., 2016; Gruden et al., 2011, 2012; Horvath, Iashchishyn, Forsgren, & Morozova-Roche, 2017a; Shalash et al., 2017; Q. Xu et al., 2014; Yanamandra et al., 2011). These studies included a total of 305 patients and 198 controls but two of the papers appear to use overlapping patient samples with identical demographic tables and results figures and so the second of these was excluded (Gruden et al. 2012; Gruden et al. 2011).

Three papers found raised alpha synuclein antibodies in sub-groups of PD patients, either in familial PD (Papachroni, Ninkina, Papapanagiotou, & Georgios, 2011), pre-manifest LRRK2 carriers (Alvarez-Castelao, Gorostidi, Ruíz-Martínez, López de Munain, & Castaño, 2014) or only in CSF and not serum (Akhtar et al., 2018). Four studies reported no difference in peripheral anti-alpha synuclein antibodies (Smith et al. 2012; Maetzler, Pilotto, et al. 2014; Heinzel et al. 2014; Woulfe et al. 2002) and two studies found that alpha synuclein antibodies were decreased in patients versus controls (Besong-Agbo et al., 2013; Brudek et al., 2017). Importantly the Brudek et al. paper focused on high affinity antibodies only which may explain the difference in findings.

Table 3-1

Summary of studies measuring alpha synuclein antibodies in PD

Table legend: Numbers refer to mean and standard deviation unless otherwise specified. The table is ordered according to disease duration. Patient and controls groups were considered "matched" if there were no significant between-group differences in age and gender distributions. One paper was removed due to cohort overlap (Gruden et al., 2012). N/A was recorded in the sample size column if there was not sufficient data to do the power calculation. *Range **SEM ***author overlap ^^ in each group DD Disease duration.

*Range ** SEM ***author overlap ^^in each group DD = Disease duration

	Paper	Method	Fluid	N (HC = healthy controls)	Matched	Mean age of PD (SD)	Disease duration years (SD)	H & Y (SD)	Finding (in PD versus controls)	Required N^^
<=5 years DD	Xu 2014***	Electrochemical impedance spectroscopy	Serum	60 PD, 29 HC	Yes	69.4 (SD10.8)	1.4 (1.44)	20 H&Y1, 20 H&Y2, 20 H&Y3	↑ in PD, more in H&Y 1 and 2 than controls, no diff betweeen stages	382
	Horvath 2017***	indirect ELISA	Plasma, CSF	20 PD, 20 HC	Yes	Mild: 65.5 (38-79*) Moderate: 67.2 (56-77*)	2.8 (1-8*) months (<1 year)	1.5 to 2	↑ in PD versus HC in CSF and plasma Decreased in moderate versus mild disease	N/A
	Smith et al 2012	ELISA	Serum	14 PD, 11 PD syndrome, RBD 10, 9 HC	Yes	RBD 58 (SD 9), PD 63 (9)	Median 3.5 (1-12*)	1.3 (range 1-3.5)	No difference	N/A
	Gruden 2011***	ELISA	Serum	32 PD, 26 HC	Yes	60.8 (2)**	8.6 (3.4) ** Subgroup <5	2.1 (0.6)	↑ in PD versus HC, greater difference with monomers than oligomers	23
	Shalash 2017	ELISA	Serum	46 PD, 20 HC	Yes	56.26 (SD12.26)	5.2 (3.36)	3 (1.5-3.5 range)	↑ in PD versus HC	N/A
7-10 years DD	Akhtar 2018	ELISA	Serum, CSF	Serum: 53 PD, 16 HC CSF: 93 PD, 52 HC Both CSF and serum for 24 participants	No	Serum 70.9 (7) CSF 67.1 (9.4)	7.9 (5)	3 (1-4) (median + range)	CSF ↑, serum →	77
	Brudek 2017	ELISA, MSD	Plasma	46 iPD, 46 HC	No	62.4 (6.7)	7.9 (5)	2 (median)	↓ in PD versus HC	126
	Papachroni 2007	Immunoblot	Serum	31 iPD, 20 FPD, 26 HC	Yes	Idiopathic: 65.1 (11.6) , Familiial: 66.1 (12.7)	Calculated - 7.2 iPD, 9.4 FPD	2.4 (FPD), 2.5 iPD	↑ in FPD versus PD or controls	N/A
	Yanamandra et al 2011***	Elisa, western blot, biocore surface plasmon resonance	Serum	39 PD, 23 HC	Yes	55.7 (10)	7.7 (5.6)	H&Y1-2 27, H&Y 2.5-4 12	↑ PD versus HC	N/A
	Caggiu et al. 2016	ELISA	Serum	40 PD, 40 HC	Yes	69.8 (7.95)	8.42(4.29)	3.01 (0.88)	↑ in PD versus controls to 3 peptides (similar to HSV)	N/A
	Maetzler 2014	ELISA	Serum	93 PD (demented subgroup 31), 194 controls	No	68.5(SD9) PDND, 76.7 (SD8) PDD	9.5(1-26*)	2(1-4)	No difference	N/A
10-12 years DD	Alvarez-Castelao 2014	ELISA immunoblots	Plasma	55 iPD, 104 LRRK2 carriers, 85 HC	No	67.8 (9.9) iPD 68.37 (10.2) LRRK2	12 (8.7) iPD 13 (11) LRRK2	2.44 (0.8) iPD, 2.55 (0.88) LRRK2	Controls and iPD no difference Using stringent criteria ↑ antibodies in LRKK2 pre-manifest	N/A
	Besong-Agbo 2013	ELISA	Serum	62 iPD, 46 HC	Yes	68.6 (9)	10.2(6)	>3	↓ in PD versus HC	60
Unknown DD	Bryan 2012	Electrochemical impedance spectroscopy	Serum	30 PD, 14 HC	No	Not reported	Not reported	1 to 3	↑ in PD versus HC, increasing up to H&Y 2 then decreasing for H&Y 3.	N/A
	Heinzel 2014	ELISA	Serum, CSF	66 PD, 69 HC (CSF 59 PD and 46 controls)	Yes	No ages reported	Not reported	2	No difference	214
	Woulfe 2002	ELISA	Serum	Serum: 28 PD, 19 HC CSF: 4 PD, 5 controls	Not reported	Not reported	Not reported	Not reported	No difference	N/A

Three studies investigated antibodies in CSF as well as in plasma or serum (Akhtar et al., 2018; Heinzel et al., 2014; Horvath et al., 2017a) with two of these finding raised alpha synuclein antibodies in the CSF ((Akhtar et al., 2018; Horvath et al., 2017a).

All studies investigated the antibody response to full length alpha synuclein apart from the Caggiu et al study that assessed the response to specific epitopes deemed to be relevant due to their similarity to EBV (Caggiu et al 2016).

Clinical heterogeneity

There is wide variation in disease stage and duration across studies (see Table 3-1). Previous studies have noted an increase in early disease e.g.(Gruden et al., 2012). Of the five papers reporting a mean disease duration of 5 years or less (see table 1), four report an increase in alpha synuclein antibodies in patients compared to controls (representing a total of 196 patients and 121 controls excluding the first Gruden et al paper as described above)(Xu et al. 2014; Horvath, Igor A Iashchishyn, et al. 2017; Smith et al. 2012; Gruden et al. 2012; Yanamandra et al. 2011; Shalash et al. 2017). Only the smallest of the studies in early PD showed no PD-control difference (N=14 PD patients and 9 controls)(Smith et al. 2012). Even taking a conservative interpretation of these results, the larger studies are consistent in reporting an increase in alpha synuclein antibodies in early disease. An additional study for which disease duration was unavailable reported an association with HY disease stage with increasing titres from HY stage 1 to 2, decreasing at stage 3 (Bryan et al., 2012). Alvarez-Castelao et al. found increased alpha synuclein antibodies in LRRK2 carriers versus controls but not in patients with longer disease durations (>10 years)(Alvarez-Castelao et al., 2014). Other studies have also reported a similar

association with HY staging (Shalash et al., 2017; Y. Xu et al., 2012). Of six studies with mean disease durations between 7 and 10 years, two studies report a clear increase in patients versus controls(Caggiu et al., 2016; Yanamandra et al., 2011). Two further studies show an increase in a subgroup, in familial PD versus controls (but not idiopathic PD)(Papachroni et al., 2007) in one study and in CSF only and not serum in another (Akhtar et al., 2018). The two studies that showed either no difference (Maetzler, Apel, et al., 2014) or a difference in the opposite direction (Brudek et al., 2017) did not have age and gender matched control groups. In the two studies with disease duration beyond 10 years there was either no difference (Alvarez-Castelao et al., 2014) or a decrease in patients compared to controls (Besong-Agbo et al., 2013).

Patient age also varies between study cohorts, ranging from a mean of 55.7 (Yanamandra et al., 2011) to 69.8 (Caggiu et al., 2016)(table 1). Antibody responses vary with age and gender (Candore et al., 1997). It is therefore also critical to ensure that patient and control groups are well matched. Of the 17 studies reviewed, 7 either did not report appropriate demographic information or the control group was not matched to the patients.

Assay variability

Most studies have made use of custom ELISAs with one study using a commercial ELISA for serum anti-alpha synuclein antibodies (Shalash et al., 2017). Two positive studies by the same group in different patient cohorts used electroimpedence spectroscopy (Bryan et al., 2012; Q. Xu et al., 2014). Several others used immunoblots or western blots (Alvarez-Castelao et al., 2014; Papachroni et al., 2011; Yanamandra et al., 2011). ELISAs are limited by many factors including the requirement for two independent binding events and

problems with non-specific binding (Q. Xu et al., 2014) There is also variation in conditions between studies such as buffers used, protein coating concentration and temperature of the assay which are particularly relevant for an intrinsically disordered protein such as alpha-synuclein.

Most of the alpha synuclein for the use in ELISAs was generated in E.coli in-house, and therefore may not include post-translational modifications present in mammalian cells (Akhtar et al., 2018; Bryan et al., 2012; Horvath et al., 2017a; Maetzler, Pilotto, et al., 2014; Papachroni et al., 2011; Q. Xu et al., 2014; Yanamandra et al., 2011)(with other papers obtaining commercially generated protein). Alvarez-Castelao et al. attempted to replicate their ELISA findings using immunoblots and identified that some of the ELISA positive samples were recognising something other than alpha synuclein (Alvarez-Castelao et al., 2014). This effect disappeared when they introduced an additional purification step suggesting the possibility that at least some of the findings in the literature may be due to interfering antibodies to bacterial toxins rather than to alpha synuclein itself. Antibodies present in serum may also be bound to serum protein (either specifically or non-specifically) which may interfere with antibody detection (Maetzler, Apel, et al., 2014). Most of the papers investigated antibody responses to monomeric alpha synuclein (which is not necessarily the disease relevant species) with only a minority assessing responses to fibrils, mutated alpha synuclein (Alvarez-Castelao et al., 2014; Gruden et al., 2012; Yanamandra et al., 2011), oligomers or other pathological forms (e.g. phosphorylated alpha synuclein (Brudek et al., 2017) or specific peptides (Caggiu et al., 2016). The Brudek et al. paper focused on high affinity antibodies and found that these were decreased in patients compared to controls which is consistent with them having a role in alpha synuclein clearance. As other studies have investigated the overall antibody response it is not useful to directly compare these.

Lastly, some of the variation between studies may be due to the use of either serum or plasma (although only two studies used plasma rather than serum, see table 1). It is possible that factors present in plasma but not in serum (e.g. alpha synuclein produced by platelets) may affect subsequent results and therefore it would be wise to standardise the use of serum across studies.

Power

Lack of adequate power may be an important factor leading to false negative findings in a number of studies. The largest study included 93 PD patients and 194 controls (Maetzler, Pilotto, et al., 2014) but unfortunately the controls were not age and gender matched to the patients (see Table 3-1). Of the 17 studies, 7 included appropriate information to calculate power. Of those with incomplete information, this was usually because the data were presented as graphs or as medians and IQ range. The estimated sample sizes required to detect the differences reported ranged from 23 to 382, with a mean of 147 per group (see Table 3-1). The only study that was adequately powered was that by Gruden et al. that reported much larger differences between controls and patients than other studies and is therefore an outlier. Excluding this study, the estimated required sample size per group is between 60 and 382.

3.4.2 Meta-analysis

All of the "early disease" papers shown in Table 3-1 met the inclusion criteria (see also flow plot in Figure 3-2). Means and standard deviations were available from two of the studies (Gruden et al. 2011; Xu et al. 2014). The means and standard deviations from Horvath et al. (Horvath, Iashchishyn, Forsgren, & Morozova-Roche, 2017b) were estimated based on the reported medians and interquartile

ranges. The medians and interquartile ranges from the other two papers were estimated from boxplots and subsequently converted to means and standard deviations as described in the methods (Shalash et al. 2017; Smith et al. 2012). Study effect size estimates and model results are shown in Table 3 2. Overall, there is a significant increase in antibodies in patients versus controls across studies (see forest plot in Figure 3 3) but the effect size is modest (0.88, 95% CI 0.05-1.71, p value = 0.036). There was significant heterogeneity across studies (I^2 = 89.32%).

Figure 3-2

Flow diagram showing inclusion and exclusion of the studies in the meta-analysis

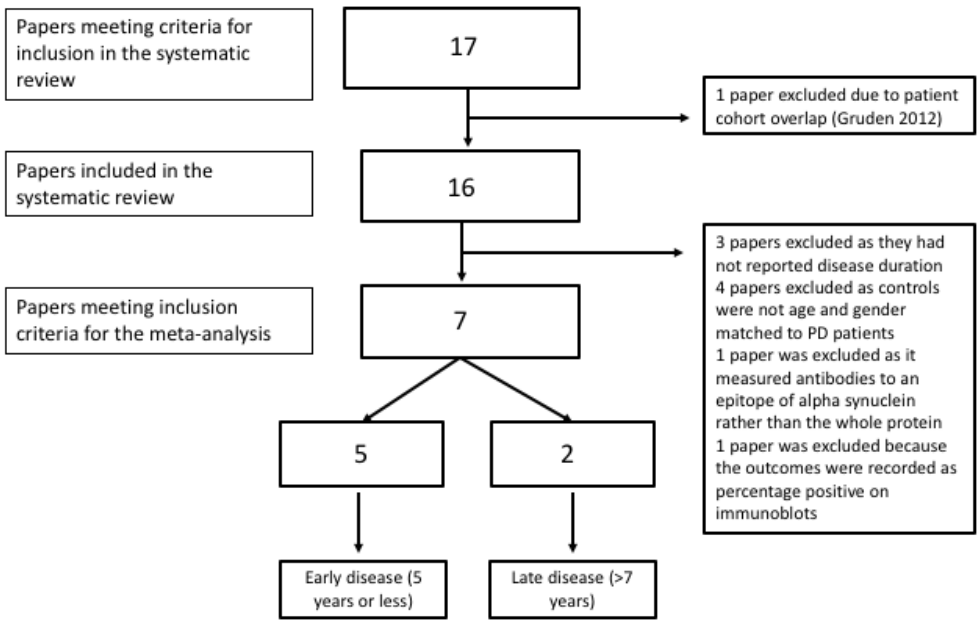

Table 3-2

Study estimates, standardised effect sizes (yi) and variance (vi) ("early disease" <5.9 years disease duration).

	Year	Controls			PD			yi	vi
		Mean	SD	N	Mean	SD	N		
Gruden	2011	25.00	50.99	26	310.00	452.55	32	0.83	0.08
Xu	2012	1.24	1.44	29	1.62	2.04	60	0.20	0.05
Smith	2012	0.83	1.13	9	1.06	1.81	14	0.14	0.18
Horvath	2017	5.00	0.67	20	6.50	2.72	20	0.74	0.11
Shalash	2017	0.49	0.69	20	4.39	1.78	46	2.50	0.12

Table 3 2 Model results: Estimate = 0.88 (95% CI 0.005-1.17), SE = 0.42, Z = 2.09, p = 0.036, I^2 = 89.32%, Q(df = 4) = 33.71, p = 0.0001.

Figure 3-3

Forest plot showing study effect sizes in early disease (<5.9 years)

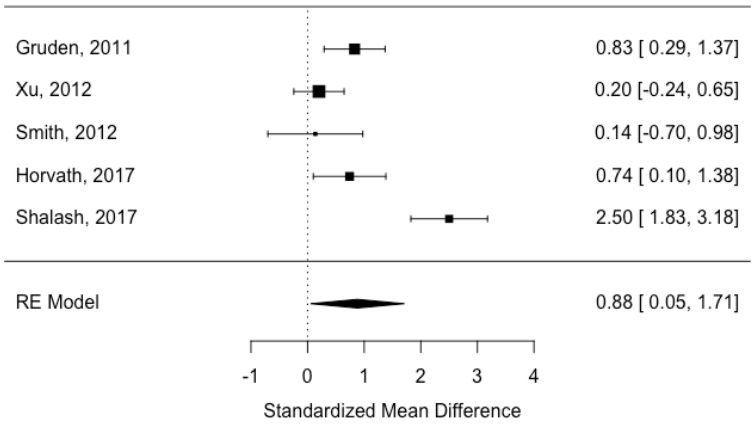

Only two of the "later disease" studies (mean disease duration >7 years) met inclusion criteria ((Besong-Agbo et al., 2013; Yanamandra et al., 2011). Means and standard deviations were published in the Besong-Agbo study and therefore used to calculate study estimates. Medians and interquartile ranges were estimated from boxplots in the Yanamandra study which was divided into two subgroups (mean disease duration 6.7 years and mean disease duration 9.7 years as there was no available data for the patient group overall). Means and standard deviations were then derived from this data.

Three studies were excluded due to a lack of reported disease duration (Bryan et al., 2012; Heinzel et al., 2014; Woulfe et al., 2002); four studies were excluded due to a lack of age and gender matching between patients and controls (Akhtar et al., 2018; Alvarez-Castelao et al., 2014; Brudek et al., 2017; Maetzler, Apel, et al., 2014). The Alvarez-Castelao paper did not include published significance testing of the age difference which was therefore done as part of this review. There was a significant difference in age between patients and controls according to an independent samples t-test (idiopathic PD mean 67.81, SD 9.98 and controls mean 61.4, SD 14.7), $t\ [136] = 2.83$, $p = 0.005$). One study was excluded as it only measured antibodies to specific epitopes of alpha synuclein rather than the entire protein (Caggiu et al., 2016) and one other study was excluded because outcomes were recorded as percentage positive on immunoblots (Papachroni et al., 2007).

The study estimates are shown in Table 3-3 and the overall random effects model is shown in the forest plot in Figure 3-4. There was no overall difference between groups in this small sample (estimate = 0.34, 95% CI = -0.57-1.24, $p = 0.46$) and there was also significant heterogeneity ($I^2 = 87.67\%$).

Given the significant heterogeneity, funnel plots were generated plotting standardised mean difference on the x axis against standard error on the y axis for studies in the "early disease" group (there were too few in the later disease group to make interpretation of these plots meaningful). The plot is symmetrical around the effect size of 0.88 (z = 0.20, p = 0.84) but shows that 2 of the studies fall outside of the 95% CI of an assumed true effect (see Figure 3-5). One of the many explanations for the shape of this plot is the presence of true heterogeneity between studies (both clinical and assay related factors discussed above). If we were able to include more studies in the analysis one would expect, assuming the same true effect, that effect estimates from smaller studies would spread widely along the bottom with those from larger, more powerful studies appearing at the top (see Figure 3-5). One cannot fully discount the role played by publication bias in this context as positive findings in this field will be more likely to be written up and published than negative results particularly in the context of smaller studies.

Table 3-3

Study estimates, standardised effect sizes (yi) and variance (vi) ("later disease", >7 years disease duration)

Study	Year	Controls			PD			yi	vi
		Mean	SD	N	Mean	SD	N		
Yanamandra 6.7 years	2011	108.67	126.43	23	696.44	821.82	27	0.95	0.09
Yanamandra 9.7 years	2011	108.67	126.43	23	313.11	490.58	12	0.66	0.13
Besong-Agbo	2013	153.5	103.77	46	105.40	85.83	62	-0.51	0.04

Figure 3-4

Forest plot showing study effect sizes in later disease (>7 years)

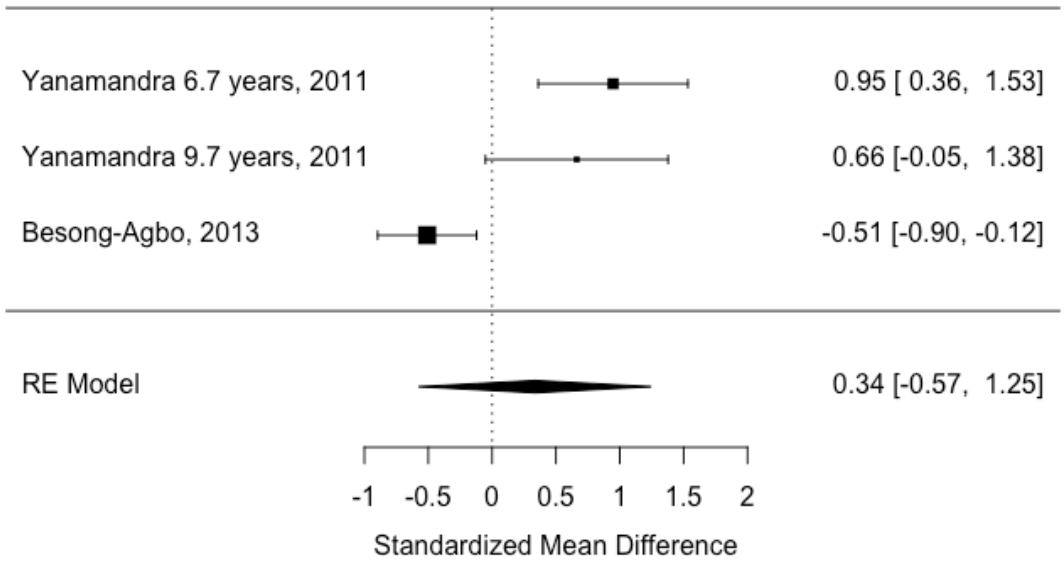

Figure 3-5

Funnel plot showing standard error versus standardised mean difference in early disease

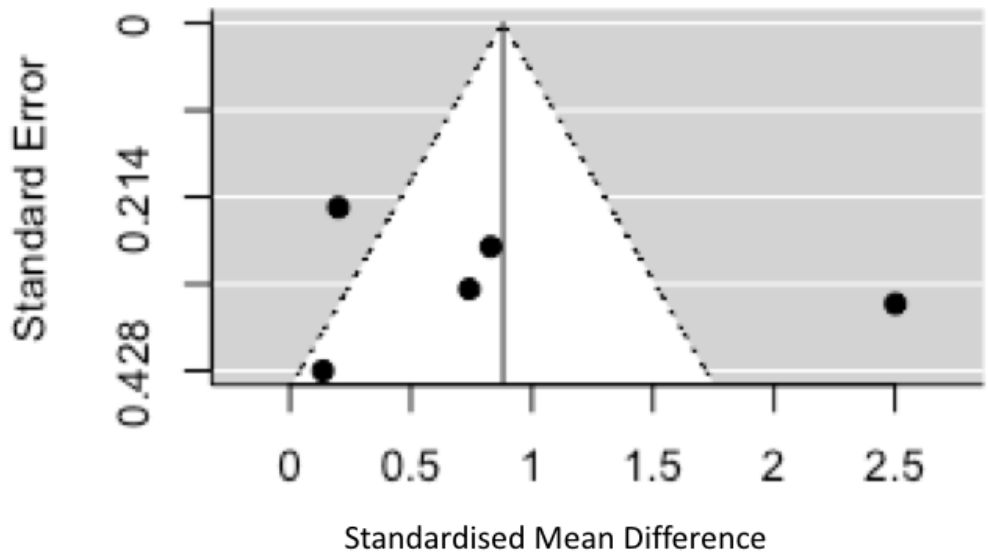

3.5 Conclusions and recommendations for future studies

Whilst the available data does not suggest elevation of alpha synuclein antibodies universally across all stages of PD, it is consistent with the hypothesis that there is an increased antibody response in early disease that wanes during disease progression, which is biologically plausible. According to our meta-analysis the effect size is modest in early disease but the analysis is limited by significant study heterogeneity.

There are many caveats to this conclusion based on both the systematic review and the meta-analysis, including the limitations of the assays used, the clinical heterogeneity of cohorts, the lack of any longitudinal data and poor matching of controls to patient groups, meaning that the overall quality of evidence is poor

(for example, 7 of 9 studies in later disease did not meet the inclusion criteria for the meta-analysis making it difficult to draw any firm conclusions from this aspect of the study) . Hence the value of alpha synuclein auto-antibodies as a diagnostic or prognostic biomarker remains uncertain. Further studies are needed to demonstrate a consistent, reproducible effect in early PD cases versus controls (or indeed between different groups of PD patients), to investigate the specificity of raised antibody titres in PD versus other alpha-synucleinopathies, and to track longitudinal changes in antibody titres and their relationship to disease onset and clinical disease progression. The possible utility of using antibody based biomarkers for identifying patients who would potentially benefit from either immune modulating or antibody based therapies is also unknown.

There is a clear need for further studies in this field and I therefore have developed the following recommendations:

1. Appropriate sample size with more than 30 in each group (based on approximate power calculations from existing studies)
2. Well characterised clinical cohorts with appropriately matched controls using both serum and CSF if possible
3. Longitudinal assessment to measure changes in antibody levels over the course of the disease and relationship with clinical disease progression
4. Study of prodromal PD cohorts to establish whether the antibody response is truly an early feature of the disease
5. Using a robustly validated method (ideally with validation using a second method in the same samples) to measure antibodies including standardisation and testing of different coating concentrations, buffers and assay temperature.
6. Study of epitope-specific antibodies and Ig subclasses to allow a fuller understanding of the adaptive immune response to PD.

3.6 Overview of auto-antibody assays in PD

In order to investigate alpha-synuclein antibodies in the PD cohorts at the John Van Geest Centre for Brain Repair, I developed a set of custom designed Meso-Scale Discovery (MSD) assays to measure antibodies to a selection of alpha synuclein species and tau (as a non alpha synuclein disease relevant antigen). I chose this system because there is some evidence that it has increased sensitivity and lower background than traditional ELISA based methods (Bastarache, Koyama, Wickersham, & Ware, 2014) but also because of the experience in the lab with using MSD based systems for measurement of cytokines and alpha synuclein (Williams-Gray et al., 2016). Figure 3-6 shows an overview of the assays that I used. The initial step involves binding of biotinylated protein to a streptavidin coated plate (MSD, L15SA). Serum antibodies then bind to the protein after a blocking step. Finally a detection antibody is added that binds to the serum antibody and a final read buffer is added. When the plate is placed in the reader an electri-chemiluminescent signal is generated that is in proportion to antibody concentration which is calculated using a set of standards.

.

Figure 3-6

Overview of MSD assay set up

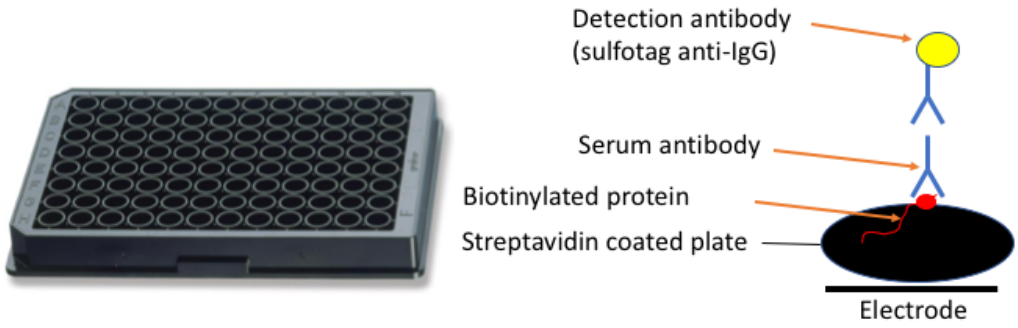

The target antigens were two species of alpha synuclein, alpha synuclein fibrils and alpha synuclein monomers. I also used two alpha synuclein peptides; S129D, a peptide containing a phosphorylated serine at position 129 known to be pathogenic in PD(Anderson et al., 2006) and Y39 which was a custom designed peptide based on a recent paper showing that this epitope activated T cells in PD (Sulzer et al., 2017). Lastly, I included tau as an alternative disease relevant protein. There is one study showing an association with PD dementia and anti-tau antibodies (Kronimus et al., 2016) suggesting that an immune response to tau may also be relevant to disease progression.

3.7 Methods

3.7.1 Participant recruitment

For this study, serum samples from the participants recruited for the immune study in PD (cohort 1) were used (as described in 2.2.1). Inclusion criteria were fulfilment of the UK PD Brain Bank Criteria for a diagnosis of definite PD (made by neurologist), age 55-80 years and early stage disease (Hoehn and Yahr stage ≤ 2). Exclusion criteria included the presence of other neurodegenerative disorders, chronic inflammatory of autoimmune disorders, current clinically significant infection, surgery in the last month, vaccinations in the previous 3 weeks or recent use of anti-inflammatory or immunomodulating medication (steroids in the previous three months, high dose aspirin >75mg in the previous 2 weeks, ibuprofen and other non-steroidal anti-inflammatory drugs in the previous 2 weeks or any long term immunosuppressant drugs such as azathioprine, mycophenolate, methotrexate, rituximab or other biological therapies in the last year).

The patients were stratified into groups at high, intermediate and low risk of an early dementia using predictive factors identified in a longitudinal cohort study (Williams-Gray et al., 2009). The stratification was done on the basis of their MAPT (tau) genotype, pentagon copying ability and semantic fluency score (the high risk group was defined as MAPT H1/H1 genotype and any one of either semantic fluency <20 in 90s or pentagon copying score <2, the intermediate group had any one of these factors and the low risk group had none)(as in (Williams-Gray et al., 2018).

Age, gender and MAPT-genotype matched controls were recruited from the NIHR Cambridge Bioresource (http://www.cambridgebioresource.org.uk/). Controls had no history of neurological disease, memory problems or

depression. Exclusion criteria were the same as for the PD patients. Samples from matched patient and control pairs were processed on the same day with collection occurring in the morning (between 9 and 11am).
All patients went through a full clinical assessment including medical history and co-morbidities, the Movement Disorder Society Unified Parkinson's Disease Rating Scale (MDS-UPDRS), the Addenbrooke's Cognitive Examination (ACE-R), assessment of semantic fluency (animal naming in 90s), pentagon copying and the Beck Depression Inventory (BDI). The overall probability of a bad outcome (either postural instability or dementia) was calculated using a validated tool which uses axial components of the UPDRS, age and animal fluency (Velseboer et al., 2016).

Clotted blood samples were left for 20-30 minutes before being spun in a centrifuge at 2000RPM for 15 minutes. The serum was aliquoted into cryovials and frozen at -80°c.

3.7.2 Antigens

Alpha synuclein fibrils were produced using the method described in 2.2.1 by William Kuan, one of the post docs in the Barker laboratory (using monomeric alpha synuclein from rPeptide S-1001-2). The phosphorylated S129D peptide was obtained from Abcam (ab188826). The fibrils and S129D peptide were biotinylated using the EZ link Sulfo NHS biotin kit as per the manufacturer's instructions (21335). The proteins were dialysed after biotinylation to remove excess biotin using Slide-A-Lyzer dialysis cassettes (66205) and associated float buoys (Thermofisher 66430) as per manufacturer's instructions. Biotinylation status was confirmed using the Pierce biotin quantitation kit (28005). The tau protein and Y39 were obtained from Creative Biomart as custom biotinylated

protein/peptide (tau: MAPT-38H lot 290831, Y39: GKTKEGVLYVGSKTK lot 100281). Recombinant alpha synuclein was available in a biotinylated form commercially (alpha synuclein with biotin Anaspec AS-55581). The manufacturers of all the proteins confirm that the products are purified to remove endotoxin. The antigens were coated on the plates at a concentration of 0.15 picomole per well with the exception of tau which was coated at a concentration of 0.3 picomole per well. The antigens were diluted in 1% BSA (Probumin. Millipore, cat. no. 82-045-1). Prior to finalising the protocol, all antigens were tested at two different coating concentrations (0.15 picomole per well and 0.3 picomole per well).

3.7.3 Standard curves

Seven point standard curves were constructed using known duplicate concentrations of commercial mouse or rabbit antibody to the protein or peptide in question. All plates included 2 blank wells. For the alpha synuclein fibrils and recombinant alpha synuclein, mouse anti-alpha synuclein (Abcam, ab1903) was used at a starting concentration of 2000ng/ml with serial 1 in 5 dilutions. For the tau protein, mouse anti-tau antibody (Abcam, ab80579) was used at a starting concentration of 2000ng/ml with serial 1 in 5 dilutions. For the S129D peptide, a rabbit anti S129D antibody was used (Abcam, ab51253) at a starting concentration of 2840 ng/ml with serial 1 in 7 dilutions. There was no commercial antibody to Y39 and therefore it was not possible to generate a standard curve for this antigen. Instead, raw signal intensity scores were normalised to a standard serum sample which was the same across assays. The concentrations of antibodies for the standard curves were optimised prior to running the test assays on patient samples.

3.7.4 Assay protocol

Streptavidin plates were blocked with 150µl of 3% BSA (Probumin. Millipore, cat. no. 82-045-1) for 1 hour on a shaker at 4000RPM. They were then washed three times with 150µl 0.05% Tween 20(Sigma Aldrich P1279)-PBS. The plates were then coated with 25µl of antigen and incubated overnight at 4 degrees centigrade. There were 5 plates per lot of samples defrosted (one plate per antigen with 40 samples run in duplicate).

Serum samples stored at -80 degrees centigrade were taken out of the freezer the following morning and thawed on wet ice. Serum was diluted 1:25 in 1% BSA based on experiments with different concentrations. Calibrator antibodies were prepared as described above.

The plates were then washed three times with 0.05% Tween 20 PBS. Diluted serum or calibrator was added in volumes of 25 µl. Plates were incubated for 1 hour at room temperature on a shaker at 4000RPM. They were then washed again with 0.05% Tween 20 PBS three times.

The detection antibodies were then added. MSD sulfotag anti-human antibody was added to the test wells and MSD sulfotag anti-mouse or anti rabbit to the calibrator wells at a concentration of 1:500. The plates were then incubated at room temperature for an hour on a shaker at 4000 RPM.

After incubation, the plates were then washed three times with 0.05% Tween 20 PBS and 150µl of 1x read buffer was added . The plates were then read on an MSD plate reader (Sector S 600). Absolute concentrations were calculated from the standard curve as described above (2.2.3).

3.7.5 Human total IgG

The MSD human total IgG panel (K15203D) was used to measure total IgG in the serum samples as per the manufacturer's instructions. Briefly, samples were diluted with the proprietary diluent 100 to a dilution of 1:250000 by performing serial dilutions. Calibrators were prepared to produce a 7 point standard curve. The plate was washed three times with 0.05% Tween 20 PBS. 25µl of diluted serum or calibrator was added, the plate was sealed and incubated at room temperature for 2 hours. The plate was then washed three times with 0.05% Tween 20 PBS. 25µl of detection antibody was then added (sulfo-tag anti-human IgG) at a concentration of 1:500. The plate was incubated at room temperature for a further 2 hours. After incubation, the plate was washed three times with 0.05% Tween 20 PBS and then 150µl of 2x read buffer was added before reading the plate on the MSD plate reader as above. Absolute concentrations were calculated using the MSD Discovery workbench software as described above.

3.7.6 Statistics and data handling

The MSD reader outputs a text file which is then manipulated using the MSD Discovery Workbench software in order to generate the standard curve and interpolate the calculated titres which were exported into Excel (version 16.16.2). Samples with unacceptably high co-efficients of variation (CV) were removed from the analysis (CV >20%). Sample CV was calculated using the following formula:

$$Sample\ CV = \frac{\sigma}{\mu}$$

Where σ = the standard deviation of the two duplicates and μ is the mean.

The overall plate CVs are reported after removing samples above the cut-off. Coefficients of variation (CV) were calculated by dividing the standard deviation by the mean. Percentage recovery was calculated using the standards of known concentration.Statistical analysis was carried out using SPSS (IBM, version 25) and graphs were generated using graphpad prism (version 7 for Mac OS). Paired t-tests or non-parametric equivalent were used for PD versus control comparisons (given that participants were recruited as age/gender and genotype matched pairs with assays and sample collection run in parallel). Unpaired t-tests (or non parametric equivalent) were used to compare the risk groups. Bivariate correlations were explored using a correlation matrix. A correlation heatmap was produced using the corrplot package in R studio (version 1.0.153)..

3.8 Results

3.8.1 Participant characteristics

Participant characteristics for this initial study are described in 2.3.1. For optimisation of the assay, sub-groups of samples were used (as described below).

3.8.2 Assay optimisation

Antigen coating concentration and development of standard curves

All antigens were tested at concentrations of 0.15 picomole per well and 0.3 picomole per well (the maximum protein concentration advised by the manufacturer). For most of the antigens binding of the control antibodies was the same for both concentrations and therefore the lower concentration was

chosen for subsequent assays. The concentration of the standards was optimised to give readings across the full range of the assay (see Figure 3-7, Figure 3-8, Figure 3-9, Figure 3-10). There was no commercially available antibody for the custom designed Y39 peptide. The mouse monoclonal antibody (abcam, ab1903) used for the alpha synuclein and fibril standards was therefore tested but did not show consistent binding (see Figure 3-11).

Serum dilution

Initially a serum dilution of 1:500 was tested (in line with the methodology employed in a similar study (Brudek et al., 2017). The resulting values were at the lower limit of detection of the assay (see Figure 3-13)and were therefore also tested at 1:50. An eventual concentration of 1:25 was used for the final protocol as described in the methods.

Figure 3-7

Optimising standard and antigen coating concentrations (alpha synuclein antibody plate)

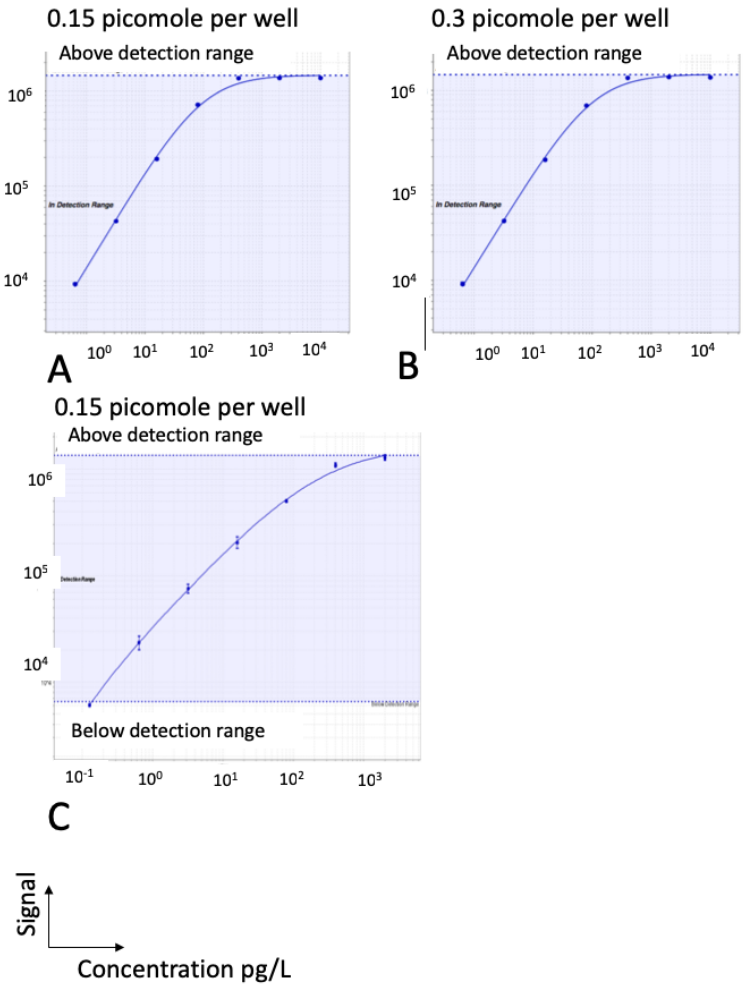

Figure 3-7 legend: A and B show antigen coating concentrations of 0.15 picomole and 0.3 picomole respectively. The highest standard for these curves was 10,000ng/ml with 5 fold serial dilutions. The curves did not adequately cover the lower end of the detection range and therefore the final highest concentration used was 2,000 ng/ml shown in C (with 5 fold serial dilutions), covering the entirety of the detection range.

Figure 3-8

Optimising standard and antigen coating concentrations (alpha synuclein fibril antibody plate)

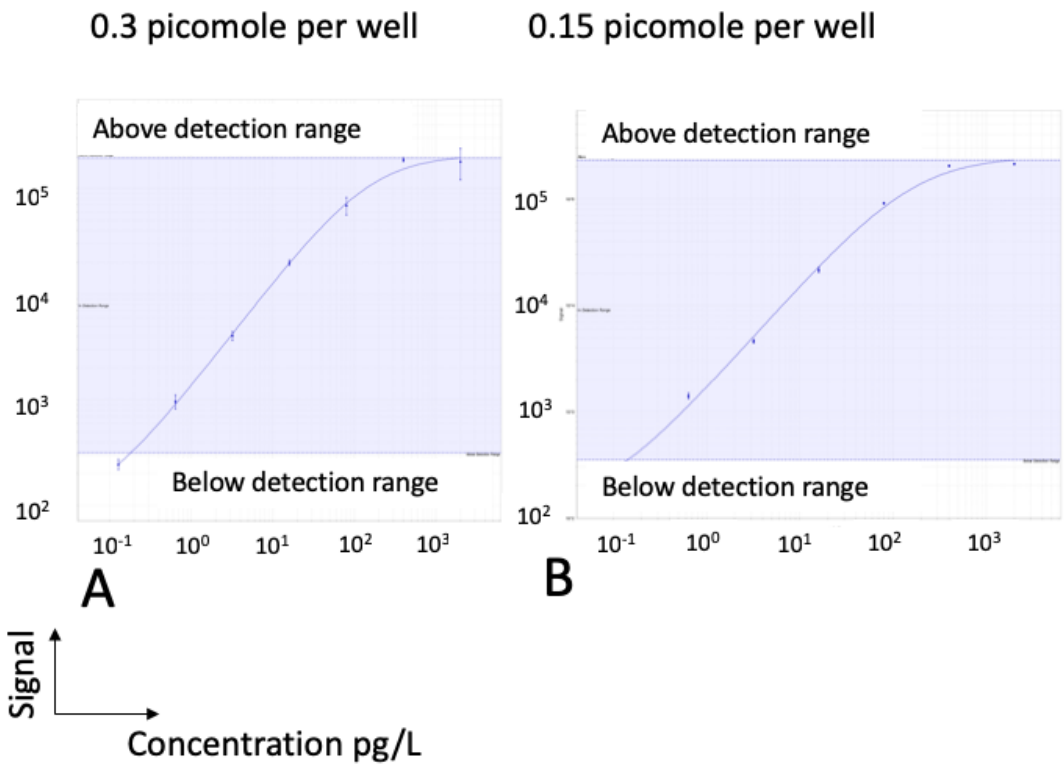

Figure 3-8 legend: The same standards were used for the alpha synuclein fibrils plate as for the alpha synuclein plate (highest concentration 2,000ng/ml with 5 fold serial dilutions to create 7 standards). The lower coating concentration was adequate.

Figure 3-9

Optimising standard and antigen coating concentrations (S129D antibody plate)

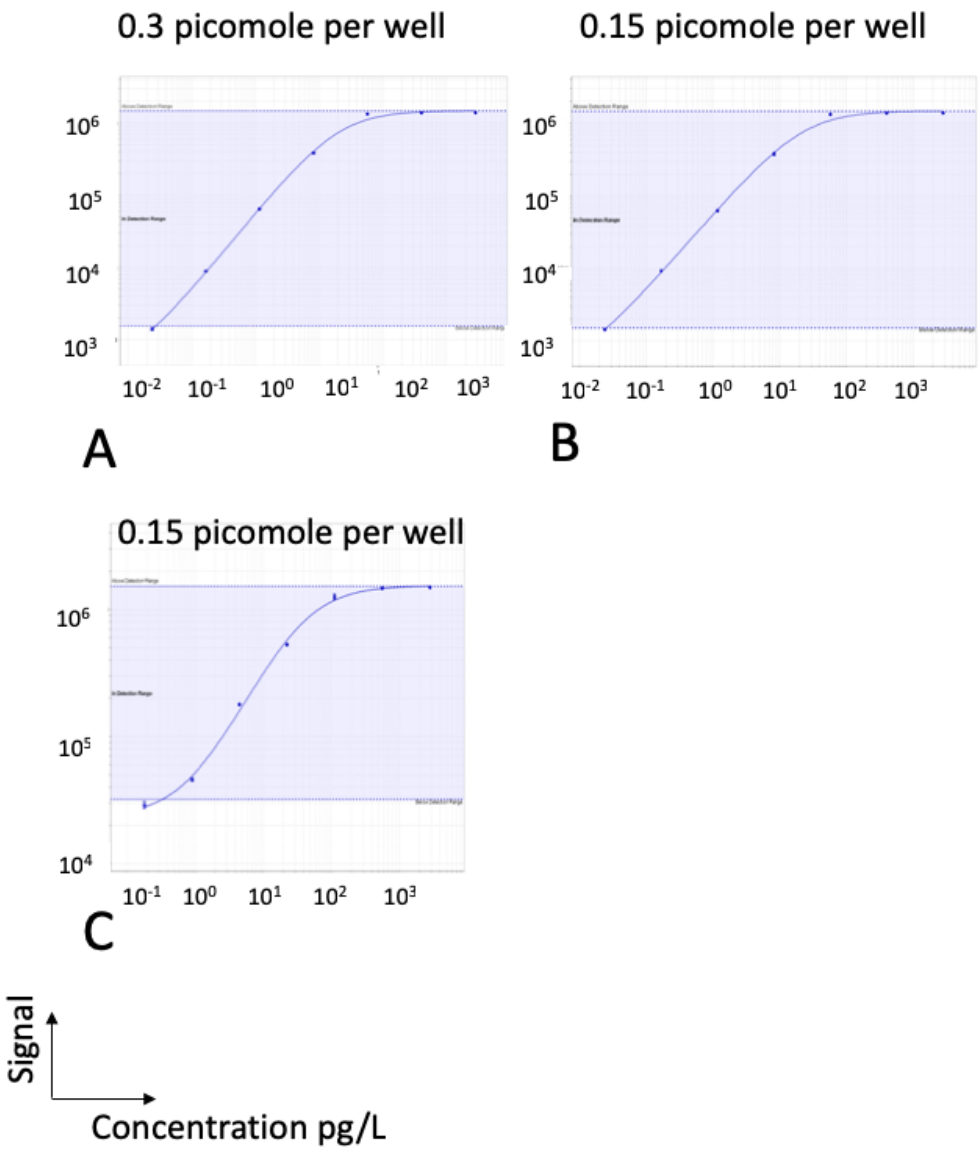

Figure 3-9 legend: A and B show standard curves generated using a starting standard at 284ong/ml with subsequent 7 fold serial dilutions at either 0.3 or 1.5 picomole antigen coating per well as shown. C shows a 5 fold serial dilution curve which was similar to A and B.

Figure 3-10

Optimising standard and antigen coating concentrations (tau antibody plate)

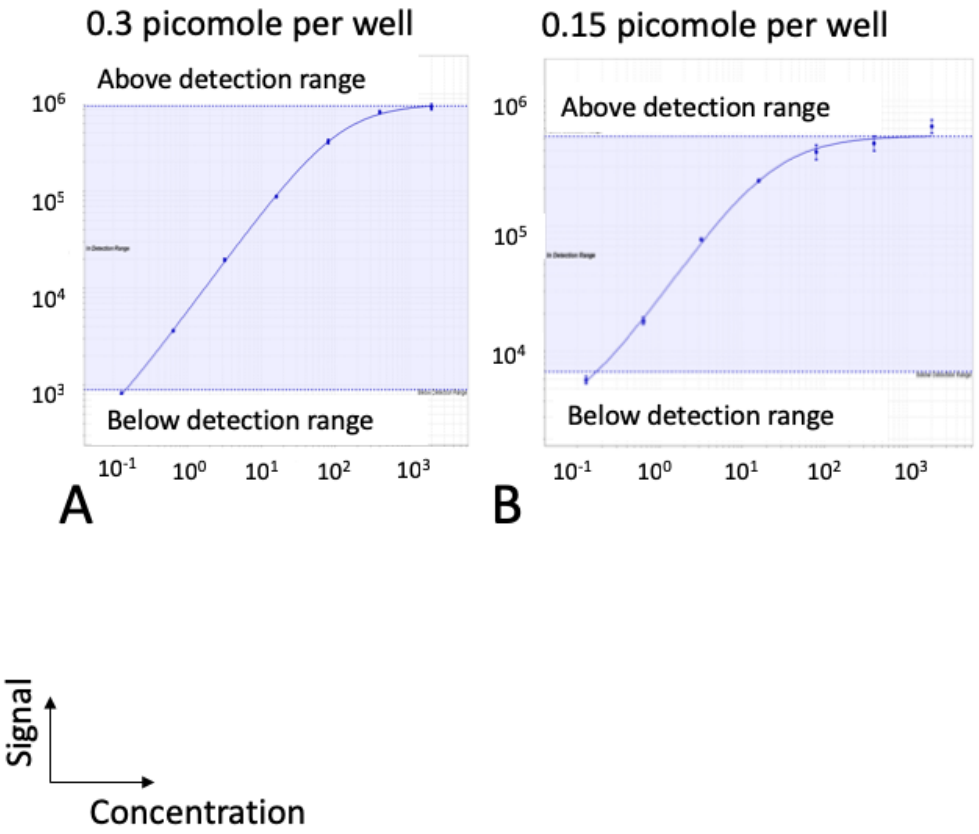

Figure 3-10 legend: Standard curves for tau protein plates showing that the standard curves are similar for the two coating concentrations.

Figure 3-11

Optimising standard and antigen coating concentrations (Y39 antibody plate)

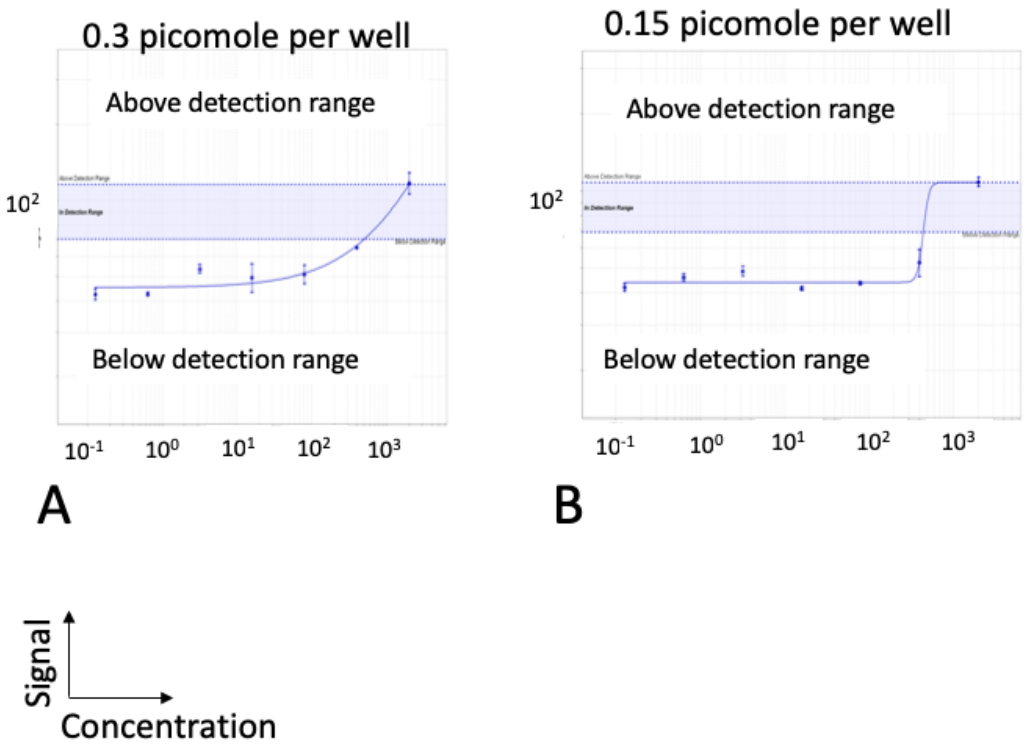

Figure 3-11 legend: The mouse anti alpha synuclein antibody only bound to the Y39 antigen at the highest concentrations and was therefore not useful as a standard for the assay.

The alpha synuclein antibody (ab1903) used as a standard for the monomer and fibril assays did not bind to the Y39 peptide therefore instead of going forward with the standards all samples were normalised to a control sample that was included in all plates.

Pilot study 1 demographic and clinical details

A subgroup of patient and matched control samples was selected for a pilot study (N=15 in each group). The demographic and clinical details of the sample are shown below (see Figure 3-12). This sub-group was representative of the larger cohort and PD patients were well matched to controls for age and gender (Age t[14]=0.29, p=0.77, Gender chi-square[1] = 0.0, p=1). There was no difference in disease duration or age between low dementia risk and high dementia risk groups (disease duration t[13] = 0.28, p = 0.78, age t[13] = 2.14, 0.056). There were differences between these groups in their ACE-R scores (t[13]=-3.8, p = 0.012) and LEDD (t[13] = -2.6, p = 0.02) as noted for the larger cohort (with the high risk group having a lower LEDD and lower ACE-R than the low risk group).

Assay parameters

The standard curve derived from this experiment is shown in Figure 3-7 C. The mean percentage recovery as calculated from the standards was 113% (SD 24.50, range 74.4-157.0). The percentage co-efficient of variation was 17.8%. The distribution of calculated concentrations is shown in Figure 3-13 with the majority of samples falling in the lower end of the standard curve. All samples were within the detectable range of the assay.

Pilot study results

The antibody titres are shown in Figure 3-14 with associated means and standard deviations. Paired comparisons between patients and matched controls were not significantly different. There was a significant difference between high risk and low risk groups on post hoc analysis (see Figure 3-14 legend).

Figure 3-12

Participant clinical and demographic details for pilot study

Variable	PD				P
	All	High (N=8)	Low (N=7)	Controls (N=15)	
Age	67.93 (6.3)	67.75 (6.6)	68.14 (6.5)	67.73 (5.6)	0.77
Gender (%male)	68.8	75.0	57.1	68.8	1
Disease duration	4.28(1.25)	4.48(0.97)	4.24(1.62)	-	0.78*
MDS-UPDRS motor score	34.53 (11.05)	40.13 (9.25)	29.33 (10.17)	-	0.06*
ACE-R	89.47 (10.39)	83.38 (10.4)	96.67 (2.58)	-	0.01*
Levodopa Equivalent Daily Dose (LEDD)	511.75 (285.8)	387.90 (287.2)	712.16 (177.6)	-	0.02*

Figure 3-12 legend: Numbers refer to means and (standard deviation). P values refer to paired t tests (PD versus controls), unpaired t-tests (High risk versus low risk) or to chi-squared tests (proportion of males). *comparisons between high versus low risk.

Figure 3-13

Scatterplot showing standards and samples

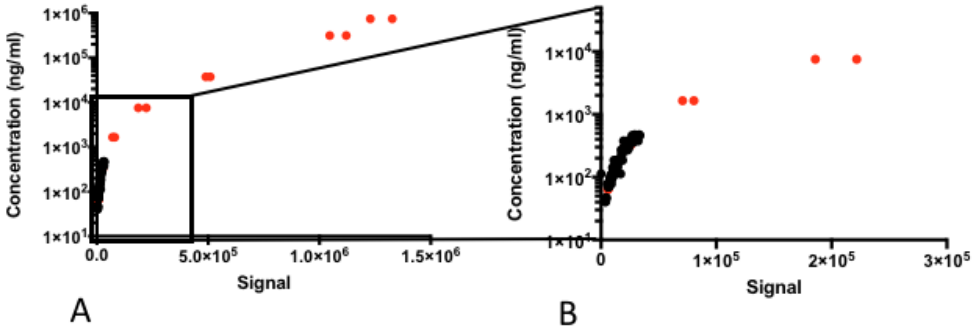

Figure 3-13 legend: Samples shown in black, duplicate standards shown in red. The whole distribution is shown in A, the linear phase is shown in B.

Figure 3-14

Antibodies to alpha synuclein – pilot study

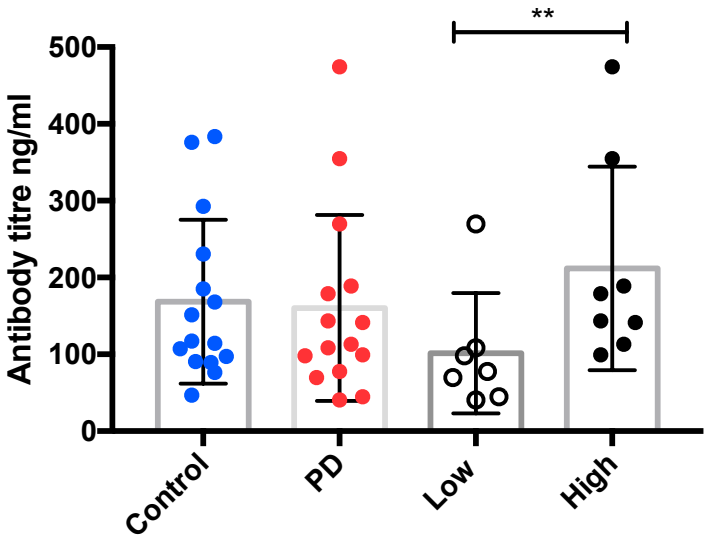

Figure 3-14 legend: Mean (SD) – control 168.5 (106.6), PD 160.3(121.1), low risk of dementia group 101.4 (78.3), high risk of dementia group 211.8 (132.5). Paired comparisons between PD patients and matched controls were not significantly different (either as a whole or within the risk groups). ** Mann Whitney U test =7, p = 0.01.

Pilot study 2

In order to test the performance of all 5 plates using serum, a further pilot study was run using 8 serum samples that were available due to excess storage of aliquots from cohort 1 (N=8, 3 PD and 5 controls, 3 males) . Two different serum dilutions were tested (1:500 and 1:50). Diluting samples to a greater extent decreases 'matrix effects' (the effect of unmeasured factors in the sample on the signal e.g. haemoglobin) but this is counterbalanced by the need to reduce variability which is greater at higher dilutions. There were a number of data points at the 1:500 dilution that fell below the detectable range of the assay (S129D = 4, Y39 = 1, fibrils = 2, alpha synuclein= 2, tau = 4). There were none below the detectable range at the 1:50 dilution which was still on the lower end of the standard curve. In addition, Figure 3-15 shows the greater variability using the 1:500 dilution but also highlights that it is important to maintain constant dilution ratios across assays as more dilute samples give higher estimates. For the final protocol, a dilution of 1:25 was therefore chosen as this was likely to ensure that all samples were within the limits of detection of the assay.

Figure 3-15

Concentrations of antibodies to each antigen across two different serum dilutions

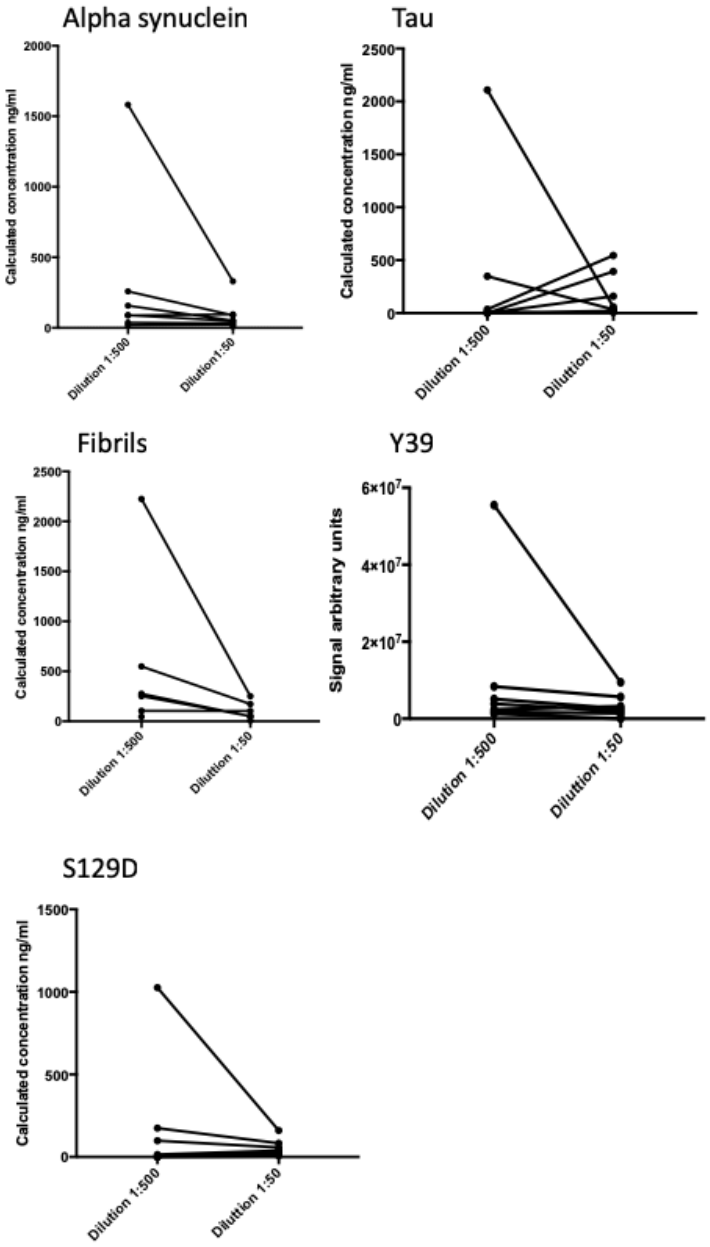

3.8.3 Serum antibodies in cohort 1

Samples were run in two batches (39 per plate in duplicate and one batch control serum sample that was run across all plates). PD patients and matched controls were run on the same plate. Further analysis using serum samples from our other cohorts is still ongoing and therefore not included in this chapter.

Assay performance

Samples were removed from subsequent analysis if the co-efficient of variation exceeded 20%. Table 3-4 shows the number of samples removed in each batch. There were larger numbers in batch 1. It is likely that this improved in batch 2 with further practice doing the assays. Intra-assay measures of variability are shown in Table 3-5 after removal of the samples described in Table 3-4. The usually quoted acceptable maximum for intra-assay variability is up to 15% (although some studies use a lower range). The standard curves all worked as expected and resembled example curves shown above (data not shown).

Table 3-4

Table showing the number samples removed due to unacceptable CV (>20%)

Plate	Samples removed (batch 1)		Samples removed (batch 2)	
	control	PD	control	PD
Alpha synuclein antibody	10	10	1	-
Fibrils antibody	10	9	-	3
S129D peptide antibody	4	6	-	1
Y39 peptide antibody	12	7	1	2
Tau antibody	6	11	1	2
IgG plate	4	3	4	5

Table 3-5

Co-efficients of variation (CV) and percentage recovery across both assays

	Batch 1		Batch 2	
Antigen	Mean CV(SD)	%recovery (SD)	Mean CV(SD) 2	%recovery (SD) 2
Alpha synuclein monomers	8.4(5.67)	81.7 (41.3)	5.38(4.2)	97.8(30.1)
Alpha synuclein fibrils	9.1(5.04)	148(155.2)	5.36(5.3)	112.8(56.7)
Tau	2.15(4.34)	152.7(102.4)	5.8(5.2)	102(6.9)
S129D	5.7(6.1)	97.5(64.9)	2.8(2.5)	142.4(66)
Y39	9.7(5.12))	-	7.1(4.6)	-
Total IgG	5.8(5.5)	207.3(170.6)	7.7(5.9)	123.4(64.2)

Inter-assay variation

Inter-assay co-efficients of variation were deduced using the calculated concentrations from the control sample that was run on both plates (alpha synuclein = 22.51%, fibrils 43.2%, S129D = 130%, Y39 normalised=16.9%, tau = 117%, IgG =16%). There was an 11 fold difference between the batch 1 and the batch 2 mean for the tau antibody plate. The batch 1 values were more variable and were therefore discarded entirely. These samples will be re-run.

Due to the variability between assays described above, the samples with acceptable CVs were normalised to the control sample run across all plates to allow comparisons across assays.

Results from cohort 1 samples

There were no significant differences between PD patients and age and gender matched controls in normalised titres of alpha synuclein antibodies, alpha synuclein fibril antibodies, S129D or Y39 peptide antibodies and tau antibodies (see Figure 3-16, Figure 3-17, Figure 3-18 and Table 3-6). There were also no differences in total IgG (normalised) between patients and controls (see Figure 3-18). Participants were stratified by their risk of dementia (low, intermediate and high). The only difference between risk groups and controls was in the normalised antibody titres to the Y39 peptide ($t [31] = 2.41$, $p = 0.02$).

Table 3-6

Table showing normalised antibody titres to five antigens

Antigen	**Controls**	**PD**			
		All	Low	Int	High
Alpha syn	2.54(1.76)	2.46 (1.88)	2.18(1.18)	2.91 (2.5)	1.71(0.68)
Fibrils	3.14(1.73)	2.54(1.73)	2.38(1.33)	3.10(2.29)	1.36(0.23)
S129	2.49(2.37)	2.31(2.10)	1.87(1.30)	2.49(1.85)	3.53(4.4)
Y39	5.14(5.72)	5.64(6.50)	3.40(1.72)	2.84(1.59)	11.98(10.16)*
Tau	4.27(2.63)	3.49(3.14)	3.90(1.46)	3.30(3.72)	-

Table 3-6 shows mean (SD) for normalised antibody titres (normalised to control standard run on each plate). Low = low dementia risk, Int = intermediate dementia risk, High = high dementia risk. *p< 0.02 versus controls.

Figure 3-16

Antibodies to alpha synuclein and alpha synuclein fibrils

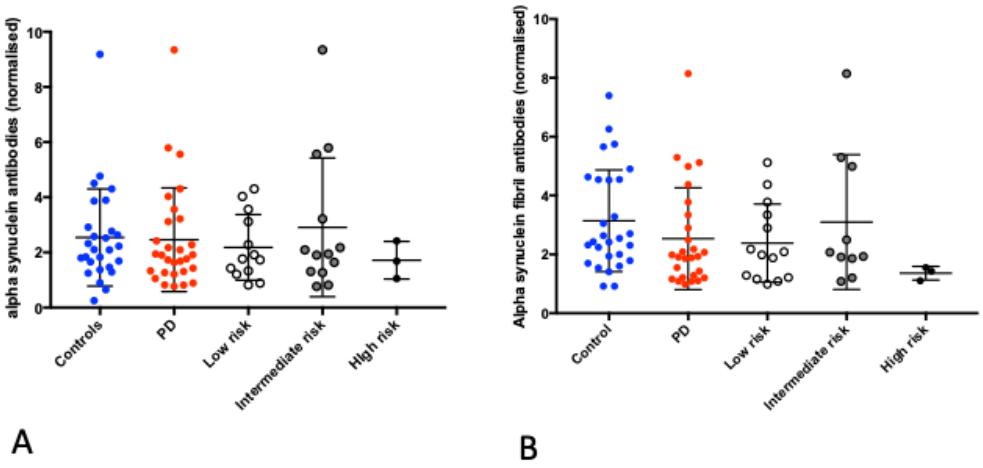

Figure 3-16 shows antibodies to A) alpha synuclein and B) alpha synuclein fibrils (normalised to control sample to allow inter-assay comparisons).

Figure 3-17

Antibodies to S129D and Y39 peptides

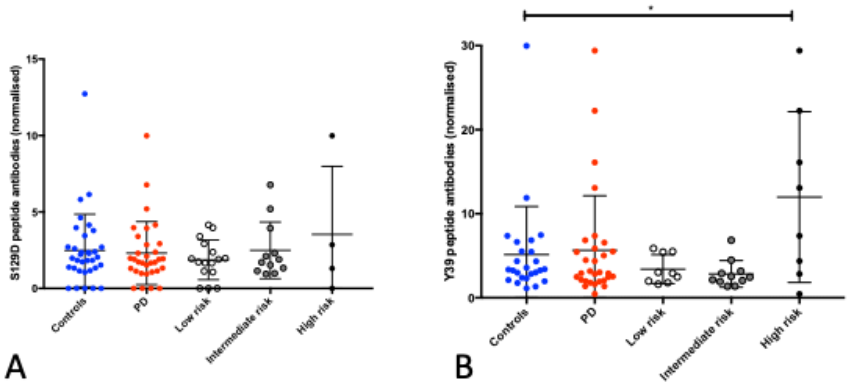

Figure 3-17 shows A) antibodies to the S129D peptide and B) to the Y39 peptide (normalised to control sample to allow inter-assay comparisons).

Figure 3-18

Antibodies to tau and total IgG

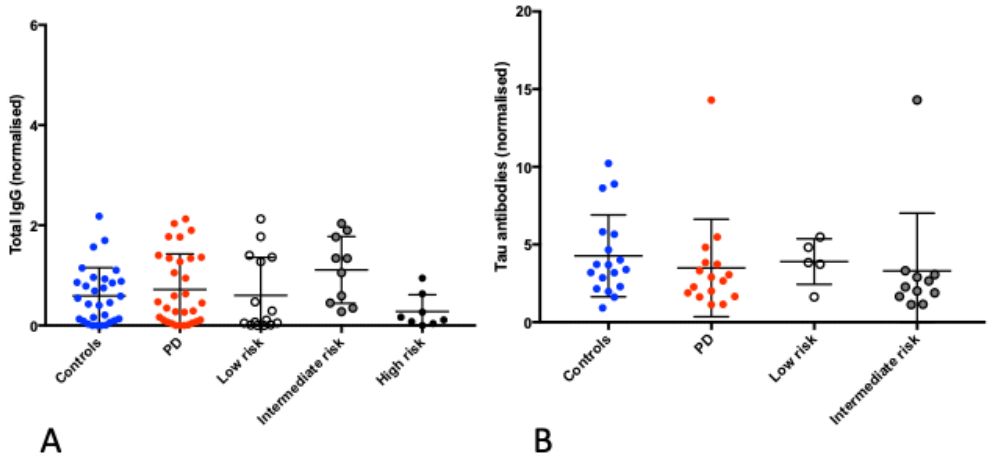

Figure 3-18 shows A) antibodies to tau and B) total IgG (normalised to the control sample to allow inter-assay comparisons).

The normalised antibody titres were highly correlated with each other (see Figure 3-19) but not with total IgG. There was a negative correlation between ACE-R scores and Y39 antibodies ($r = -0.50$, $p = 0.005$) and a positive correlation between the motor UPDRS (part III scores) and Y39 antibodies ($r = 0.39$, $p = 0.038$) (consistent with higher Y39 titres having a worse outcome overall). This was largely driven by 5 individuals with high Y39 normalised titres (who had worse ACE-R scores and higher motor UPDRS scores putting them in the high risk of dementia group as illustrated in Figure 3-17). A 3D scatterplot confirms that the outliers are driving the relationship (see Figure 3-20). Removing them removes the significant correlation (Y39 antibodies and ACE-R $r = -0.23$, $p = 0.25$, Y39 antibodies and motor UPDRS $r = 0.18$, $p = 0.36$).

Figure 3-19

Heatmap showing correlations between antibody titres and clinical variables

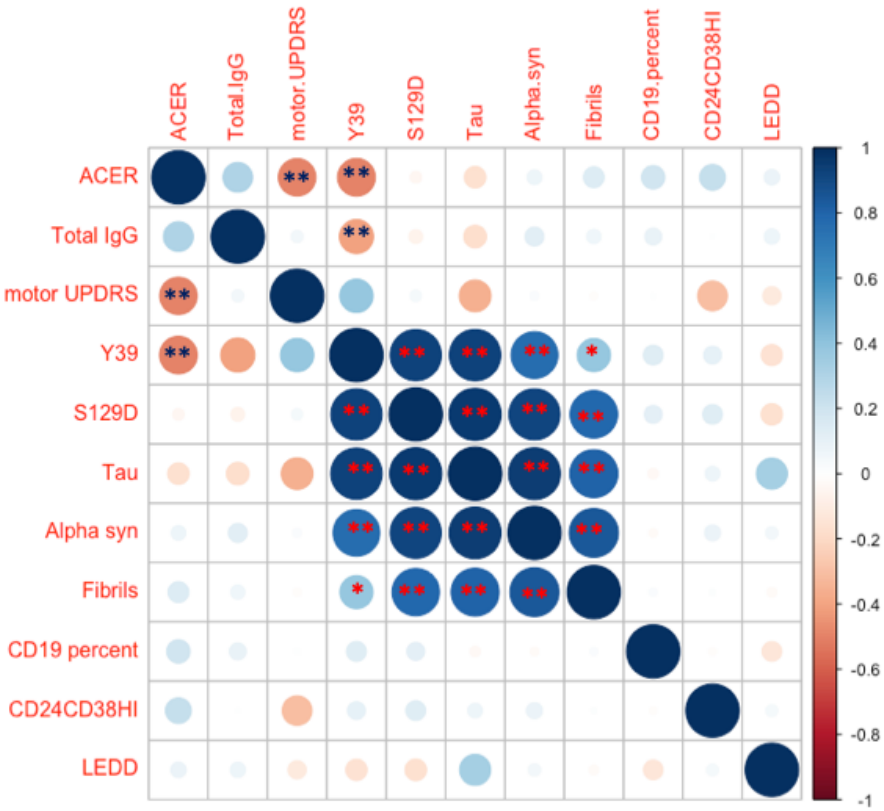

Figure 3-19 The heat map shows values for Pearson's R. Antibody titres to different antigens are highly correlated with each other * p<0.05, ** p<0.01. Addenbrooke's Cognitive Examination-Revised (ACE-R), y39 – antibodies to Y39 peptide, S129D – antibodies to S129D peptide, Tau – antibodies to tau, Alpha syn – Alpha synuclein antibodies, Fibrils – antibodies to alpha synuclein fibrils, CD19 percentage of total lymphocytes, CD24CD38HI – transitional B lymphocytes ("regulatory" B lymphocytes), LEDD levodopa equivalent daily dose.

Figure 3-20

3D Scatterplot showing relationship between Y39 antibody titres (normalised) and clinical parameters (ACE-R and motor UPDRS)

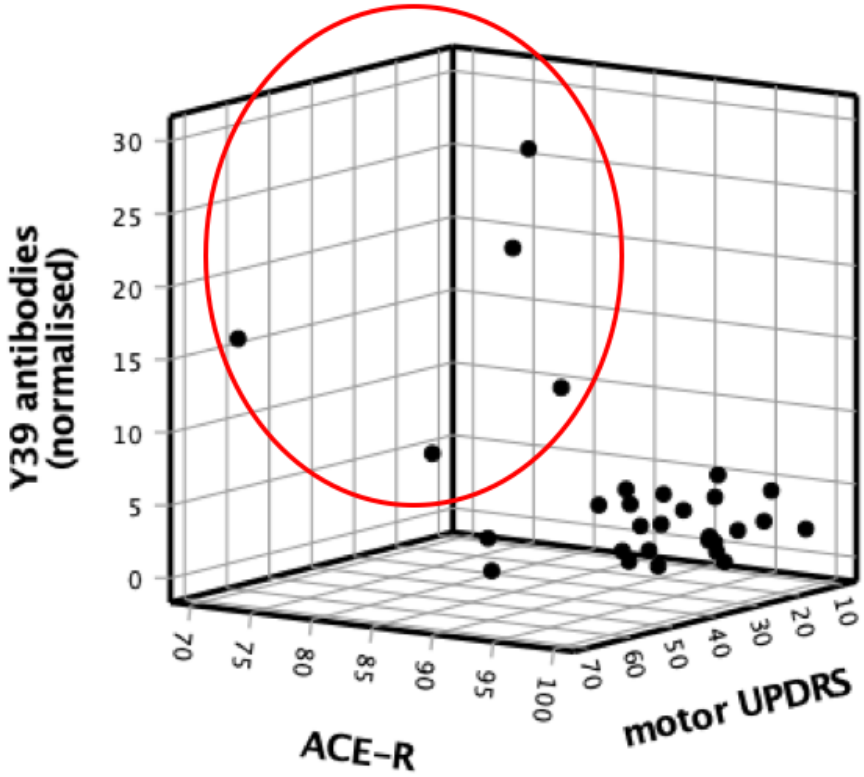

Figure 3-20 The red circle shows that the correlations observed in Figure 3-19 are largely driven by the 5 outliers with particularly high Y39 antibody levels and bad outcomes (lower ACE-R scores and higher motor UPDRS scores).

3.9 Summary of main findings

The systematic review and meta-analysis of studies looking at auto-antibodies to alpha synuclein found evidence that there are raised antibodies in early disease (less than 5 years). This would be similar to the picture in type 1 diabetes where the antibodies to self antigens in the pancreas are higher in the early stages of disease (where tissue damage and inflammation are greatest). This response then wanes subsequently(Lampasona & Liberati, 2016). It was also clear from reviewing the literature and from statistical measures that there is a lot of heterogeneity between and within studies that is likely to dilute any apparent signal. To move the field forward, I argued that there is a need for larger studies using robustly validated methods particularly focusing on the early stages of disease but also using longitudinal cohorts.

I subsequently went on to design a set of customised mesoscale discovery (MSD) assays to measure antibodies to five disease relevant antigens (monomeric alpha synuclein, alpha synuclein fibrils, tau and two disease relevant peptides, S129D and Y39). I have reported a number of experiments optimising some of the parameters of these assays. In particular, I have optimised the plate coating concentration, standards for each plate and the serum dilution. The co-efficients of variation (CVs) within batch 1 were unacceptably high for almost a quarter of the samples (which had to be removed from subsequent analysis). Batch 2 showed improved CVs which may have been due to an improvement in lab technique and practise with running multiple plates concurrently. There was also significant inter-assay variability. I have now resolved this problem by using a control sample run across plates which can then be used to normalise the other samples to facilitate comparisons.

I used the custom plates to measure antibodies in a cohort of patients and matched controls (the same cohort as cohort 1 in chapter 2). There were no

significant patient versus control differences in the normalised titres of alpha synuclein, fibril, tau, S129D or Y39 antibodies. When I looked specifically at the group at high risk of an early dementia there were significantly higher normalised Y39 antibody titres ($p = 0.02$). This effect was driven by 5 individuals in the high risk group. Scatterplots showed that these participants had lower cognitive scores (as measured on the Addenbrooke's cognitive examination revised, the ACE-R) and worse motor scores (on the motor Unified Parkinson's Disease Rating Scale).

3.10 Chapter discussion

The main limitation of the antibody study at the moment is the sample size as it is possible that there is a small effect that is masked by other variability, including inter-assay variability. The analysis of further samples is ongoing (see future directions).

There was marked inter-assay variability despite having previously optimised the assay. The intra-assay CVs improved in batch 2 and in subsequent plate runs in the lab suggesting that this was related to laboratory technique. I was assisted by two new lab members when I ran batch 1 due to the amount of pipetting required to run 6 plates concurrently. I did all the plate preparation and pipetting for batch 2 myself and have subsequently closely trained and supervised the rest of the team for further assays which has improved the intra-assay CVs. Other factors such as the age of the samples, time that they were defrosted and incubation periods were all similar across batches and I have ensured that all buffers are freshly made 24 hours in advance (even the PBS-tween which shouldn't alter with age). The use of a standard control across batches was useful as this facilitated normalisation of the samples which allowed for inter-assay comparisons. This also highlights the problem in the existing

literature around variability across assays measuring antibodies which can only really be counterbalanced by greatly increasing sample sizes.

The finding of increased normalised antibody titres to Y39 peptide in the high risk group compared to controls is potentially interesting and would support the findings from the (Sulzer et al., 2017) paper which found that this peptide induced a prominent class II-restricted IL5 and IFN gamma response in T cells. B cells may act as major antigen presenting cells, therefore the presence of cognate B cells that also recognise this peptide confirms the potential importance of this antigen in stimulating adaptive responses. This Y39-specific response was only robust in a few individuals (5 out of 39) and therefore requires further validation. These results are consistent with my previous data presented in chapter 2, showing that cells obtained from patients in this group produce more cytokine when stimulated *in vitro*, suggesting that patients at risk of progression have a more activated peripheral immune milieu and that this may be partly driven by an alpha synuclein-specific response, at least in a proportion of individuals. Antibodies to the S129D peptide, which was also shown to activate T cells in the Sulzer study, were not observed in the sera tested in my study.

The lack of differences between patients and controls in the antibody response to the other antigens investigated may reflect the clinical characteristics of the patients. The mean disease duration in this group was 4.24 years. Although this is still within the "early" side of a disease that can run for over 20 years, my hypothesis was that the antibody response would be greatest in early disease and therefore expanding the samples to include more recently diagnosed patients and those with prodromal PD (for example those with rapid eye movement sleep behaviour disorder, RBD) may increase the chance of finding relevant differences and identifying this alpha synuclein specific response before it starts to wane.

The preliminary finding that there are no other differences in the normalised titres of antibodies against the other antigens may reflect a genuine lack of difference between the two groups. Some other studies reported null findings (as described in the systematic review) and also there is likely to be publication bias. Studies reporting negative associations are less likely to be submitted and less likely to be accepted compared to ones reporting positive outcomes. However, it is too early to reach this conclusion at this stage as my study is currently underpowered.

Most studies to date, including this one, have been designed around identifying patient versus control differences rather than looking at whether alpha synuclein antibodies are associated with better outcomes cross-sectionally or longitudinally. The real utility of clinical biomarkers in this context is unlikely to be in relation to diagnosis (as there is enough published evidence to suggest that such tests are neither sensitive nor specific for PD) but potentially in identifying patients who have an increased peripheral immune response to alpha synuclein which in turn could potentially be driving microglial activation and neuronal degeneration in the brain. Such patients would be ideal candidates for taking forward into trials of immune modulating therapies.

A series of recent papers in mice have shown that meningeal lymphatics are required for the clearance of amyloid-B (Da Mesquita, Louveau, et al., 2018), tau (Patel et al., 2019) and alpha synuclein (Zou et al., 2019). Appropriate clearance of pathological forms of these proteins may be increased by microglial phagocytosis (Patel et al., 2019). Antibodies specific for alpha synuclein may be involved in this clearance when other mechanisms become saturated and there is a build up of aggregated alpha synuclein in the context of a more pro-inflammatory environment.

3.11 Future directions

Based on my initial data there are a number of additional directions that could be pursued.

i) The first priority for this study is to increase the sample size by including PD patients with a more recent diagnosis (and controls) and by looking at a prodromal cohort. I have obtained funding from the Michael J Fox Foundation to do this and I have obtained the samples and started to run the assays for an additional group of PD patients (N=20, disease duration <2 years), controls (N=20) and prodromal patients at high risk of disease conversion to PD obtained from collaborators in Oxford (N=50). There are a number of large Parkinson's Disease biobanks with stored serum samples from patient collected over time (e.g. the ProBAND study which has prospectively collected clinical data and serum samples for over 2,500 PD patients longitudinally). Assuming there is enough evidence to justify further investigation, assessing the predictive effect of the antibody response on disease outcome using the large numbers in such a cohort would provide a robust demonstration of the effect and its utility as a prognostic biomarker.

ii) As suggested in chapter 2, B cell and T cell receptor sequencing of both CSF and peripheral lymphocytes will also provide a more sophisticated means to identify whether there are specific clones in PD patients or in those with worse outcomes.

iii) Using animal models it is possible to further investigate the role of antibodies in clearance. The therapeutic effect of anti-alpha synuclein antibodies is well described in animal models but the relevance of the antibody response to clearance by the meningeal lymphatic system is not known. Immunological tools such as mice lacking a functioning meningeal lymphatic system are available (K14-VEGFR3-Ig mice as used in (Patel et al., 2019) and can show the accumulation of e.g. tau in a mouse model of Alzheimer's disease. Using such models to investigate the endogenous antibody response in models of alpha synucleinopathies and the efficacy of transferred antibodies may help to unpick why therapies aiming at removing aggregated protein (with antibodies) have so far not worked in human neurodegenerative disease (.e.g, crenezumab a monoclonal antibody trialled in Alzheimer's disease has now been withdrawn from trials due to futility). In the absence of a functioning lymphatic system it is possible that such therapeutic strategies are not likely to work and it is as yet unknown whether neurodegenerative disease affects the meningeal lymphatics.

3.12 Conclusions

A systematic review and meta-analysis of the existing literature suggests that there is an early alpha synuclein specific antibody response in PD. I have designed and optimised a series of assays to measure antibodies to 4 different types of alpha synuclein (monomers, fibrils and 2 peptides S129D and Y39). We have started work measuring these in a prodromal cohort.

4 MOUSE MODELS

4.1 Chapter abstract

Background:
The results from chapter 2 suggest that B lymphocytes, in particular, regulatory B lymphocytes may play a protective role in PD with lower circulating B cell numbers in patients with PD. Meningeal lymphatics, draining the CNS and rich in immune cells have recently been described in both mice and humans. Alpha synuclein transgenic mice and toxin based mouse models recapitulate some of the pathology of PD.

Hypotheses:
Depleting B cells will have a deleterious effect in mouse models of PD
The presence of B cells in the meninges will be associated with the response to disease

Aims:
To characterise peripheral B lymphocyte phenotypes in models of PD
To assess the effect of B cell depletion on disease outcomes (either using a genetically deficient mouse, μMT) or depletion by an anti-CD20 antibody
To describe the phenotype of B lymphocytes in the meninges in PD models and controls

Methods:
I used the 6-OHDA lesioned mouse model of PD and examined disease course by testing motor capacity in mice lacking B lymphocytes (μMT) mice and in wild type controls (C57bl/6). Dopaminergic cell counts and staining were compared. Motor function was tested using the rotarod. I used flow cytometry to phenotype circulating B lymphocytes in transgenic models (thy1 SNCA and MI-2 mice) compared to controls. I also phenotyped B lymphocytes in the lymphoid organs (spleen, lymph nodes) and bone marrow (tibia and skull) of these mice. I carried out a number of behavioural experiments using rotarod, Y maze, marble burying to identify a simple behavioural read out.

Results:
Alpha synuclein transgenic mice had decreased circulating B lymphocytes compared to appropriate controls. Mice lacking peripheral B lymphocytes developed a worse motor phenotype and showed more extensive loss of midbrain dopaminergic cells than wild type controls. Transferring IL10 producing B cells prior to surgery resulted in a non-significant improvement in motor scores. The phenotype and number of meningeal B lymphocytes was not different between PD models and controls but was significantly different from circulating B lymphocytes (less naïve B lymphocytes in the meninges) and similar to the phenotype of skull bone marrow B lymphocytes. Microscopy demonstrated clusters of meningeal B cells that increased with age and were present in both WT and Alpha synuclein transgenic mice.

Conclusions:
The results in the 6OHDA model are consistent with the hypothesis that B lymphocytes play a protective role in the neurotoxin induced loss of nigral dopaminergic neurons. The decrease in circulating B lymphocytes in PD models compared to controls suggests that this is associated with alpha synuclein pathology but the data does not support the hypothesis that these cells move to the meninges. The presence of clusters of B lymphocytes in the meninges is nevertheless likely to be relevant to disease and warrants further investigation.

4.2 Overview of rationale behind mouse experiments

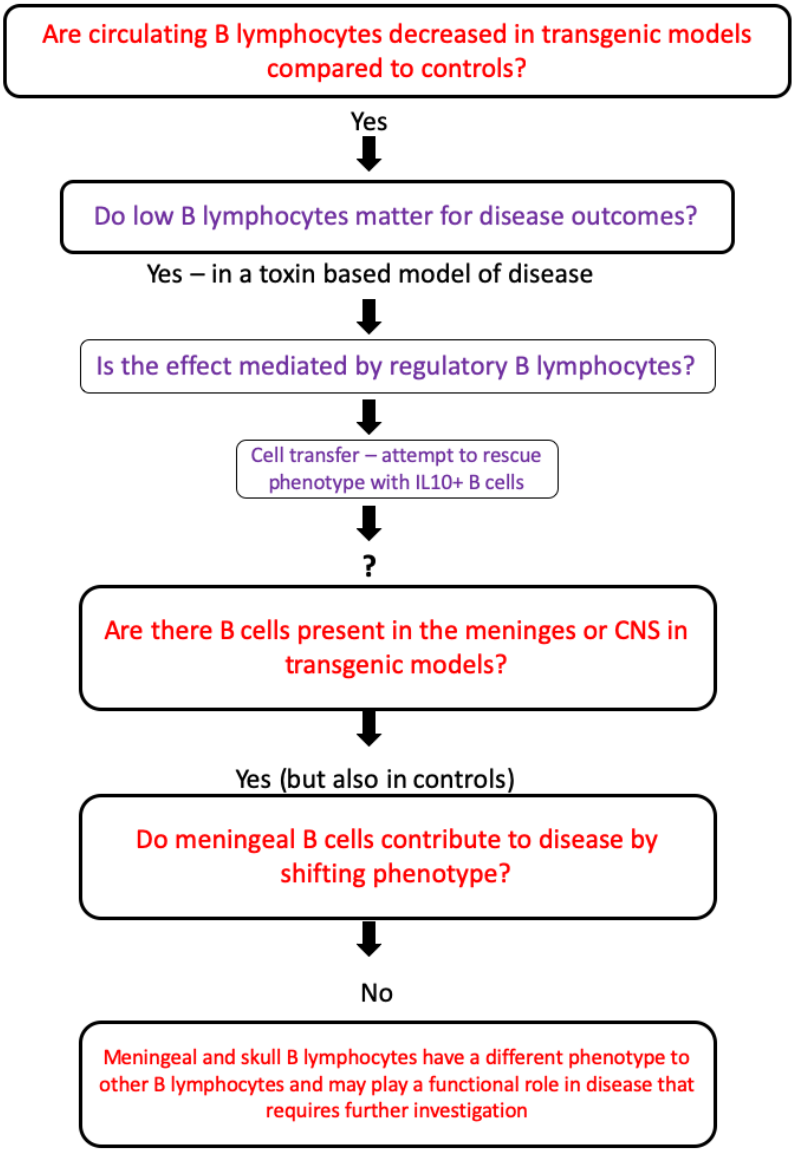

Purple lettering indicates experiments on 6OHDA mice, red lettering indicates transgenic experiments. Additional experiments attempting to worsen the phenotype in transgenic mice are not included in this overview.

4.3 Ethics statement

All animal experiments were done in accordance with the Animals (Scientific Procedures) Act (ASPA), 1986 and the protocols were reviewed by the University Animal Welfare and Ethical Review Body under the appropriate project licence (either the Clatworthy Lab license or the Barker lab license held by Pam Tyers). Each experiment was conducted under an approved study plan that was reviewed by the Named Animal Care and Welfare Officer (NACWO) of the relevant facility.

4.4 Introduction to mouse models

4.4.1 Toxin based mouse models

It is possible to induce selective dopaminergic cell death in rodents by either injecting toxins such as 6 hydroxydopamine (6OHDA) directly into the brain or administering them systemically (rotenone, MPTP [1-methyl-4-phenyl-1,2,3,6-tetrahydropyridine] or paraquat). The rationale for using these models related (i) to a known loss of dopaminergic neurons in PD and ii) with respect to MPTP, related to the discovery of a group of drug addicts in California who attempted to make their own heroin (Langston et al., 1999). They ended up injecting MPTP which caused a parkinsonian syndrome that responded to standard L-dopa treatment. Eventual examination of their post mortem brains showed that there was microglial activation as long as sixteen years after the initial insult suggesting that there was an ongoing neurodegenerative process (Langston et al., 1999). The 6OHDA model dates from the 1970's and was a standard model prior to MPTP (Bové, Prou, Perier, & Przedborski, 2005). In mice, 6OHDA is injected into the striatum or the medial forebrain bundle where it is transported (via the dopamine transporter) into the cytosol of cells causing intracellular oxidative stress that replicates some aspects of Parkinson's disease (Jackson-Lewis, Blesa, & Przedborski, 2012). Although 6OHDA does not result in

aggregates of alpha synuclein or Lewy bodies, there is some evidence that it interacts with alpha synuclein (Alves da Costa et al., 2006). The biggest limitation of these models is that the pathology develops rapidly over hours to days unlike human disease which progresses slowly over years probably on the background of genetic and environmental risk factors that have been present for an entire lifetime (Perry, 2012). The MPTP model is less rapid and has some element of reversibility over the 6OHDA model but involves the use of a neurotoxin that is highly damaging to humans if ingested.

4.4.2 Transgenic models and those overexpressing alpha synuclein

Mutations in the SNCA gene (coding for alpha synuclein) were the first to be linked to a rarer autosomal dominant form of PD (Polymeropoulos et al., 1997). There are now three known missense mutations in SNCA (A30P, A53T and E46T) that are linked to familial PD ((Vekrellis et al., 2011) and duplication or triplication of the normal variant also results in familial disease (Singleton et al., 2003)(Kara et al., 2014). As a result there are several transgenic mouse models involving mutated or overexpressed human or mouse alpha synuclein (Blesa & Przedborski, 2014). Unlike the toxin mediated models, these models do lead to neurodegeneration albeit to a very modest degree. The resultant phenotype and pathology is very dependent on the promoter and transgene used as well as the amount of alpha synuclein overexpression and the background of the mouse strain used (Blesa & Przedborski, 2014).

Transgenic mice expressing mutant alpha synuclein on the mouse or hamster prion promotor and PDGF-β (platelet derived growth factor) do not show cell loss in the substantia nigra, similarly the tyrosine hydroxylase (TH) promotor leads to dopaminergic cell loss in some studies but not others (Blesa & Przedborski, 2014)(Marie-Françoise Chesselet & Richter, 2011). Use of the Thy1

promotor (either human or mouse) has had slightly more success in that some of these models manifest abnormal aggregations of alpha synuclein and have behavioural deficits (Marie-Francoise Chesselet et al., 2012). Some of these lines have mainly motor neuron pathology which was not considered helpful for modelling PD. Unlike the TH promotor, transgenes driven off the Thy1 promotor are expressed throughout the brain not just in dopaminergic neurons (Marie-Francoise Chesselet et al., 2012). Table 4-1 shows the relative advantages and disadvantages of using toxin versus transgenic models.

A number of other transgenic models have been created as further genes causing monogenic PD are discovered. Such models include animals with modified or knocked out LRRK2, PINK1, PARKIN, DJ-1, MAPT (tau) (Blesa & Przedborski, 2014; Magen & Chesselet, 2010). Most of these models are limited in their recapitulation of only one aspect of disease and none of them develop alpha synuclein pathology characteristic of Parkinson's disease.

Alpha synuclein can also be overexpressed in the brain by injecting it with viral vectors (Van der Perren, Van den Haute, & Baekelandt, 2014). Viral vector models show better neurodegeneration and dopaminergic cell death than most of the transgenic models overexpressing alpha synuclein, possibly due to the acute nature of the insult(Blesa & Przedborski, 2014) but have largely been used in rats as the stereotaxic surgery is easier in larger rodents. There are examples of successful use of the model in mice (e.g. (Cao, Theodore, & Standaert, 2010). There are also multiple 'hit' models of PD where, for example, a transgenic model undergoes a further insult (e.g. the injection of LPS) that drives the pathology (Gao et al., 2011) and viral vector models may be combined with transgenic models to exacerbate pathology. More recently, other models have used alpha synuclein pre-formed fibrils (that are thought to act as a 'seed' to trigger alpha synuclein aggregation) either on their own or combined with

genetic overexpression of alpha synuclein or viral vector injection to better model PD in rodents (Thakur et al., 2017). Combination approaches such as this result in more obvious recapitulation of the relevant features of human disease including alpha synuclein aggregation, neuroinflammation (microglial and astrocyte activation) and cell death (Thakur et al., 2017).

4.4.3 Rationale for choice of animal models

In my PhD, I planned to use at least two different approaches to model PD. The 6OHDA model benefits from being well-characterised and being highly reproducible. There was also significant experience within the lab of using this model. The other toxin based models including MPTP (and also rotenone and paraquat) are also well-characterised but involve the systemic administration of the toxin which also is known to have effects on humans if accidentally ingested. There are therefore a number of safety concerns and the use is restricted. I therefore decided, mainly from a practical point of view, that I would use the 6OHDA model to explore the effects of B cell modulation on outcomes following dopaminergic cell loss. See Table 4-1 for a summary of the benefits and disadvantages of the mouse models I considered.

I also used a transgenic model, overexpressing alpha synuclein on the thy1 promotor. I chose this model as a behavioural phenotype had been described previously (with impaired performance on the balance beam and spontaneous alternation, tests of motor and non-motor function respectively)(Marie-Francoise Chesselet et al., 2012) and it appeared to recapitulate some aspects of disease (Marie-Francoise Chesselet et al., 2012; Delenclos, Carrascal, Jensen, & Romero-Ramos, 2014; Watson et al., 2012). Towards the end of my Phd, I also included a further model in mouse that expressed a truncated version of alpha

synuclein (that was prone to aggregation) on the TH promotor (Wegrzynowicz et al., 2018) . Given the finding that additional inflammatory 'hits' worsen alpha synuclein pathology e.g. (Gao et al., 2011) and that recurrent infections are associated with cognitive decline in AD (Holmes et al., 2009a), I also used a UTI model (local infection elsewhere in the body) and the systemic injection of LPS to add additional 'hits' to the thy1 SNCA model.

At the beginning of my PhD I did also attempt to use an adenovirus associated model that involved injecting AAV2-alpha synuclein into the substantia nigra. In a mouse it is technically challenging to accurately target the substantia nigra accurately and despite involving a research technician with years of experience of stereotaxic surgery we were successful at injecting the substantia nigra in less than a quarter of the mice. There was minimal spread of alpha synuclein outside the injection site and I therefore decided not to continue with this model (data not shown in the results section).

I also did not attempt to use pre-formed fibrils as an additional hit. A model involving pre-formed fibrils injected peripherally with a CNS trophic viral vector was being used in the lab in rats when I started my PhD (William Kuan, unpublished work). However, it had not been optimised in mice and the tools for looking at the rat immune system (in terms of monoclonal antibodies and transgenic strains manipulating the immune response) are more limited.

Table 4-1

Summary of the relative advantages and disadvantages of different mouse models of disease

	Advantages	Disadvantages
Toxin models	Pathology and cell death is induced very quickly and is irreversible	Rapid development of pathology does not mirror human disease
	Allows study of the microglial response to dopaminergic cell death	The behavioural phenotype in mice is subtle and does not progress over time (different to human disease)
	Relatively easy to assess the response of the model to intervention	Difficult to translate positive findings to human disease
	Provides a model of cell death Highly reproducible	Does not provide a model of PD pathology
Transgenic models	Better reflects human pathology with disease progression occurring over months (rather than days)	Despite the appearance of aggregates in many models, there is still minimal neurodegeneration and no lewy body formation
	May provide a good model of early clinical and sub-clinical disease in humans. As this is the period that is likely to provide a treatment window in humans, the models are useful for testing therapies.	Subtle phenotypes that require detailed testing to identify differences between transgenic and wild type animals.
	These models progress over time	Progression is often slow and one may need to wait up to a year to see any differences.
AAV viral vector models (overexpressing alpha synuclein)	There is neurodegeneration and cell death after a period of approximately 4 weeks Can target a number of different CNS sites with a disease relevant protein	This short time period does not reflect human disease course Disease lesion is different to that seen in patients where there is no overexpression of this protein Targeting smaller anatomical regions (e.g. substantia nigra) is technically challenging.

4.5 Methods

4.5.1 6-OHDA model

Mice were anaesthetised to a surgical depth using isofluorane (2L/min) (Baxter, Newbury, UK). Their fur was shaved and the underlying skin was cleaned to create a sterile field. They were placed in a stereotaxic frame. The needle was positioned to target the striatum (antero-posterior [AP] 0.5mm, medio-lateral[ML} 2mm, ventral [V} 3.0mm from bregma, see Figure 4-1) where 1µl of 6-hydroxydopamine (5µg/ µL) was injected at a rate of 0.5 µl per minute. Following surgery, the needle was withdrawn over 2-3 minutes and the animals were allowed to recover in a warmed cage with gel feed. Once recovered, they were returned to their home cages and monitored closely for the next seven days, including daily weights. They were given mash and Nutella for four days post-operatively to encourage them to eat as this model is associated with weight loss due to the effects on the lateral hypothalamus (and the drive to eat). They were given 1ml of sub-cutaneous fluid twice daily for forty eight hours following surgery.

4.5.2 Transgenic alpha synuclein models

Mice overexpressing alpha synuclein on the thy1 promotor (mThy1 -h SNCA, line 15 mice, see Figure 4-1) were obtained from the Jackson Laboratories (https://www.jax.org/strain/017682) (Ouyang Y. 2012. Direct Data Submission 2012/03/09 MGI Direct Data Submission MGI: J:181092). Mice for experiments were bred from a hemizygous carrier and a non carrier. All mice were genotyped using JAX protocols (available at https://www.jax.org/strain/017682). Wild type controls and transgenic littermates were co-housed where possible. Samples were also available from an additional transgenic mouse expressing a truncated

version of human alpha synuclein (h1-120) that is prone to aggregation (using the tyrosine hydroxylase promotor(Wegrzynowicz et al., 2018).

Figure 4-1

Summary of disease models used in experiments

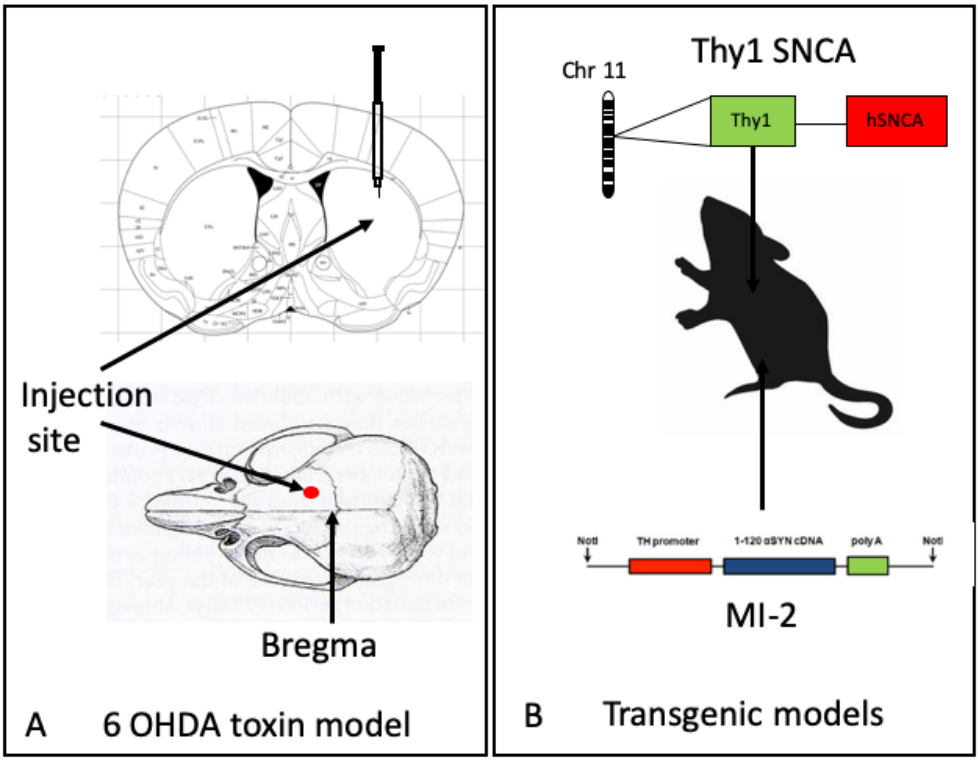

Figure 4-1 A) shows the location of the 6OHDA intra striatal injection. The pathology in this model is mainly in the nigro-striatal pathway affecting the dopaminergic cells with associated microglial activation and T and B cell infiltration B) shows the alpha synuclein transgenic mouse model where the transgene is expressed throughout the brain (thy1 SNCA) or in the tyrosine hydroxylase positive cells (MI-2 mouse, transgene on the TH promotor) 6OHDA 6 hydroxydopamine, hSNCA human alpha synuclein. Thy1 mouse Thy1 promotor. TH Tyrosine hydroxylase

4.5.3 Cell transfer experiments

I obtained spleens from donor mice which were either C57bl/6 or IL10KO mice. The spleen was mashed through a 70µm cell strainer with PBS. Red cells were lysed using red cell lysis buffer (155mM NH_4Cl, 12mM $NaHCO_3$ and 0.1mM EDTA) for 1 minute and then spun down for 5 minutes at 1300 RPM. The cells were counted using a manual cell counter. B lymphocytes were separated from the splenocytes using a magnetic separation pan B cell selection kit (MACS, Miltenyi Biotec, 130-104-443) as per the manufacturer's instructions. Mouse serum was obtained from C57bl/6 mice following cardiac puncture. Clotted blood was spun down at 2000RPM for 15 minutes and the serum removed and stored at -80°c.

4.5.4 µMT cell transfer

To attempt to rescue the worse outcomes noted in the µMT mice, I transferred either B lymphocytes (1×10^7 B lymphocytes per mouse in 200µl, N = 6 mice) or 200µl normal mouse serum one week prior to 6OHDA surgery (IV via the tail vein).

4.5.5 µMT UTI model

In order to see if the cytokine profile in the meninges was perturbed following infection elsewhere I used a model of urinary tract infection (hypothesising that B cell in the meninges become activated following systemic infection). This involves injecting uropathogenic E.coli (UPEC) directly into the bladder of mice aneasthetised to a surgical depth using isofluorane (2L/min) (Baxter, Newbury, UK).

The UPEC (UTI89) was a gift from Scott Hultgren (Washington University, USA). Bacteria frozen at minus 80°C in 20% glycerol were thawed quickly and grown in LB (Lysogeny broth) at 37°C until reaching the end of log-phase (OD600 ~ 1.0). Then, they were washed in PBS and passaged 1:200 into 200 mL of fresh LB. No more than five passages were performed before bacteria were used for animal inoculation. Under isoflurane anaesthesia, the perineum was cleaned, the urethra catheterized using 0.28 × 0.60 mm polyethylene tubing (Instech Laboratories, PA, USA) and 100 µL of UPEC (OD600 0.5) instilled. Mice were sacrificed after 48 hrs and organs immediately perfused with sterile PBS.

4.5.6 Lipopolysaccaride (LPS) or control IP injections

I also used LPS to add an additional inflammatory hit to the transgenic thy1 SNCA model (to recapitulate the effect of intercurrent infections in patients). Mice were injected intraperitoneally with either 200µl sterile phosphate buffered saline (PBS) or lipopolysaccharide (LPS) at a dose of 0.33mg/kg (Sigma Aldrich L5293 Ready Made Solution from *E. coli* 011:B4 1mg/ml). This dose has been found to elicit a pro-inflammatory cytokine response in the brain resulting in transient, mild sickness behaviour in adult mice (Henry, Huang, Wynne, & Godbout, 2009).

4.5.7 B cell depletion

Due to problems with survival of the transferred cells in the µMT model (see comments in the results section), I decided to deplete B cells using an anti-CD20 monoclonal antibody in vivo (mIgG2a, kind gift from Biogen). B cell depletion was done 2 weeks prior to surgery.

B cell depletion was performed using an anti CD20 monoclonal antibody (mIgG2a, kind gift from Biogen, 18B12). Mice were given a standard dose of anti CD20 antibody (10mg/kg) via the tail vein or control antibody at the same concentration (anti-human CD20 that has no cross-reactivity with mouse B cells, Truxima [Rituximab]). The Truxima was obtained from vials discarded within an hour after patient use in our hospital. For a 30g mouse this was 300µg in approximately 150µl of sterile normal saline. Previous studies have shown effective depletion at this dose that lasts 5-8 weeks (Bekar et al., 2010a).

4.5.8 Cell transfers following B cell depletion

Splenocytes were obtained from 10 female C57bl/6 mice (12 weeks old, obtained from Charles River/JAX) or from 10 female 12 week old IL10 KO mice (IL10 knockout B6.129P2-IL10 (tm1cgn)/JAX strain number 002251 obtained from Charles River/JAX). Tissue processing was done in a sterile hood using sterile reagents(category 1). The spleens were mashed through a 40µm cell strainer using a plunger from a 1ml syringe. The cell strainer was washed with additional PBS. They were then spun for 5 minutes at 1300 RPM. Red cell lysis was performed on spleen tissue using red cell lysis buffer for 1 minute (155mM NH_4Cl, 12mM $NaHCO_3$ and 0.1mM EDTA). The cells were washed with 1mL of PBS and filtered again using a 30µm pre-separation filter. B lymphocytes were separated from the splenocytes using negative magnetic separation (MACS, Miltenyi Biotec, Pan B cell separation kit, 130-104-443) as per the instructions from the manufacturer. CD20 depleted mice were injected with 1×10^7 B lymphocytes in 300µL via the tail vein 2 days prior to 6OHDA surgery in each transfer experiment.

4.5.1 Culture of IL10 producing B lymphocytes

A proportion of C57bl/6 B lymphocytes obtained from the Pan B cell separation above (20 x $10^{7)}$ were resuspended in cell culture medium (RPMI with glutamine (Gibco 21875-034 and 10% foetal calf serum). They were cultured overnight in 2mL of media (5 x 10^6 cells per well) in a 24 well plate with CD40 ligand (murine Peprotech Cat 315-15) (0.01µg per 2 ml), CPG (0.6µM, (Cambridge Bioscience #Hycult HC4039)) and IL2 (100IU/ml, proleukin, Novartis). The cells were scraped off the bottom of the plate after 24 hours and washed once in sterile PBS and then spun down(5 minutes, 1300 RPM) and resuspended in sterile PBS with 1 x 10^7 cells in 300 µL. Nine CD20 depleted mice were injected as above via the tail vein 2 days prior to 6OHDA surgery.

4.5.2 Behavioural testing

Initial experiments used two motor tests (rotarod and balance beam) in order to identify the test that provided the most consistent readout (the rotarod is more reproducible but the balance beam, particularly "errors per step" is more sensitive to subtle differences). Subsequently only the rotarod protocol was run at weekly intervals (and both pre-and post surgery for the experiments using the toxin based models). Transgenic animals were tested at regular intervals depending on the experiments (see results section).

i)Rotarod – protocol 1 (short test)
Training was done on day one at two different speeds (16rpm and 24rpm) for a total of four trials. If a mouse fell off, it was put on again up to a maximum of one minute. Mice were given a break of at least twenty minutes between trials. Latency to falling was recording in seconds as well as the speed of rotations (the mouse holds on to the rod rather than walking on it). During training all mice

were able to stay on the rotating rod for at least a minute on at least one occasion. Training was done over 3 days. Testing was then completed at 30rpm with scores recorded across three trials. The test days were done a week apart for 4 weeks post surgery.

ii)Rotarod – protocol 2 (long test)

The mice were trained over 3 consecutive days using an accelerating protocol. They were kept on the rotarod for 5 minutes for each training session with the starting speed set at 10RPM (revolutions per minutes) on day 1 (ending at 30 RPM), 12 RPM on day 2 (ending on 32 RPM) and 16 RPM on day 3 (ending on 36 RPM). Mice were put back on the rotarod if they fell off within the 5 minute period. If a mouse consistently fell off at faster speeds, it was put on at a slower speed to ensure it had a full 5 minutes of training. The first fall time was recorded. Each training day had 3 separate training sessions with at least a 20 minute break between each session. On testing days the rotarod was started at 24RPM (with a maximum speed of 40 RPM after 5 minutes). The time of the first fall was recorded. The performance was recorded as the mean of 4 separate tests, at least 20 minutes apart. If there was more than 1 month between testing periods, mice were retrained for 2 days prior to re-testing.

ii) Balance beam

The balance beam consists of a metre long rod with a 'safe place' at the end (dark box containing bedding) elevated approximately 30cm from the bench. The bench is covered in a soft mattress in case of falls. During training mice were placed on a 20mm rod approximately 5-10 cm away from the safe box (see Figure 4-3). They were then encouraged into the box and allowed to explore for 5 minutes. They were then placed half way along the rod and encouraged to go towards the safe box. Lastly they were placed at the beginning of the rod until they were able to walk without hesitation to the safe box. A light was focused on

the other end of the rod as an aversive stimulus. On testing days, mice were placed at the end of a 15mm, 10mm, 8mm and 6mm rod. No encouragement was given on these days to enter the safe box. Their traverse was video recorded to facilitate accurate time recording. In the event of a fall, mice were picked up and placed back on the rod where they fell. After a fall, if they started off in the wrong direction, the trial was terminated and re-started.

Mice were timed from the start to the moment that their noses hit the safe box on the video recordings. The number of falls and foot slips were also noted from video recordings.

Y maze testing

Mice were positioned in the middle of a Y shaped maze and their activity was recorded over 8 minutes. Spontaneous alternation through each arm was taken as a fraction of total activity (with the expectation that the mouse should spontaneously explore each arm in turn rather than going back into the arm that has just been visited). At the beginning of each recording session the maze was cleaned thoroughly with water and then 70% alcohol. Each arm was labelled (A, B or C). When scoring the videos, mice were considered to have entered an arm if their snout and both front paws crossed an imaginary line (as shown in Figure 4-2).

Marble burying

Mice were placed in a standard rat cage that had 20cm depth of wood chip bedding in which twenty standard marbles had been buried in a grid. They were left to explore for 30 minutes (with video monitoring). At the end of the testing session, the number of marbles that had been buried were counted. Any marble buried more than two-thirds in the wood chip was counted as being “buried”.

Figure 4-2

Y maze set up

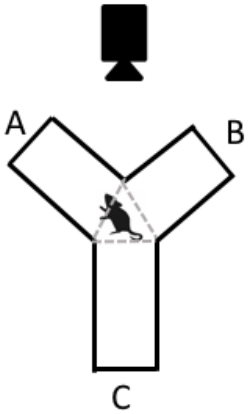

Figure 4-2: The mouse is placed in the centre of the maze and then its activity is recorded by a camera above the maze for eight minutes. In this example, entry into arm "A" would be recorded when the snout and two front paws have crossed the line.

Figure 4-3

Balance beam set up

Figure 4-3: Balance beam showing a mouse walking on an 8mm wide beam towards the safe house (in black)

4.5.3 Animal culling and tissue dissection

Mice were culled using a lethal overdose of intraperitoneal pentobarbitone sodium (Merial, UK, 200mg/mol) followed by intracardiac perfusion with ice cold phosphate buffered saline (PBS). Lymph nodes, spleens, blood and meninges were obtained following saline perfusion if cells were going to be used for flow cytometry. After PBS perfusion, the animals were perfused intracardially with 4% paraformaldehyde (PFA) (made from paraformaldehyde powder Sigma Aldrich 158127). The brains were removed from the skull and placed in 4% paraformaldehyde (PFA) overnight for histology. They were then placed in 30% sucrose for forty eight hours. Meninges were dissected out using the methodology described in (N. Derecki, Louveau, & Kipnis, 2015). For flow cytometry they were placed in cold PBS and for whole mount they were placed in 2% PFA. Meninges used for RNA extraction were placed in RNA later immediately after dissection (Sigma Aldrich R0901). Brains for flow cytometry were placed in ice cold PBS prior to processing. In order to differentiate between intravascular and extravascular cells, animals in some experiments (detailed in the methods) were injected IV with CD45 FITC approximately 5 minutes prior to being culled.

Brain sectioning

The brain was serially sectioned at 30µl with every 6th section stored in the same well in a 24 well plate using a sledge microtome (Leica SM1400). The sections were stored in anti-freeze solution at 4°C for subsequent staining (0.02M Na_2HPO_4, 0.01M $NaH_2PO_{4,,}$ 0.3% ethylene glycol [Sigma E9129], 0.3% glycerol [Sigma G7893]).

4.5.4 Preparation of tissues and blood for flow cytometry

All processing of tissues was done on ice. Lymph nodes and spleens were placed in a cell strainer (70µm) in a small petri dish and minced with scissors. Digestion mix (collagenase D 1mg/ml, DNAse I 0.1mg/ml and 1% foetal calf serum in PBS) was added to the lymph nodes (but not spleen). The meninges were mashed through a cell strainer (70µm) into a 50mL falcon tube with 40-45mL of RPMI culture medium used to wash through the strainer. All tissues were mashed through the cell strainer using a plunger from a 1ml syringe. The cell strainer was washed with additional digest mix or PBS. The solution was left for 15 minutes at room temperature before being mixed with cold PBS and placed on ice. Cells were transferred to FACS tubes. The suspension was spun at 1300 RPM for 5 minutes. Red cell lysis was performed on spleen tissue using red cell lysis buffer for 1 minute (155mM NH_4Cl, 12mM $NaHCO_3$ and 0.1mM EDTA). The cell pellet was then washed twice in PBS. Rat serum was added for blocking (to a concentration of 2%)[Normal rat serum Aviva Systems Biology, OORA01679). Conjugated cell surface antibodies and a live/dead stain were then added to the cell suspension (listed in the specified for each experiment in the results section and listed) and incubated for an hour. The cells were then washed in 5mL of PBS and re-suspended in FACS fix (1% PFA). They were then run on the flow cytometer (BD LSR Fortessa).

4.5.5 Immunohistochemistry

Primary antibodies were used to stain single forebrain sections and titrated at concentrations of 1:100, 1:200, 1:500 and 1:1000 (mouse anti-tyrosine hydroxylase, Millipore, MAB31 and sheep anti-tyrosine hydroxylase, Millipore, 1542). Biotinylated secondary antibodies were tested at concentrations of 1:1000 or 1:500 (biotinylated horse antimouse IgG, BA, 2000 and biotinylated rabbit anti sheep

IgG BA, 6000). The final protocol used the sheep anti tyrosine hydroxylase (Millipore 1542) at a concentration of 1:200 and the biotinylated rabbit anti-sheep IgG (BA, 6000).

Wells containing every 6th section were used for staining. Sections were quenched with 3% hydrogen peroxide/10% methanol for 10 minutes. They were then washed three times before being blocked with 5% rabbit serum in 0.2% triton for 1 hour at room temperature. Sheep anti-mouse tyrosine hydroxylase was added (Millipore 1542) at a concentration of 1:1000 over night. Sections were then washed and biotinylated rabbit anti-sheep antibody was added and incubated at room temperature for an hour. Secondary antibody was washed off and the sections were then incubated with ABC avidin/biotin reagent (Vectastain ABC Kit, Vector Laboratories) for 45 minutes. Sections were then washed again. Diaminobenzidine solution (Sigma D4293) tablets were added until the staining was clear at which point the sections were washed. They were then dehydrated using 50%, 75%, 90% ethanol and xylene before being mounted in DPX mounting medium (Fluka).

4.5.6 Stereological estimation of TH+ neuron density

Sections from each mouse were mounted in anatomical order (caudal-rostral). Each animal had 5-6 sections from the substantia nigra (SN). Estimations of the number of cells in the SN were performed using a standard methodology (Olympus CAST grid system (Guillery & Herrup, 1997)(Stott & Barker, 2014). The substantia nigra was defined anatomically as described in previous work in the Barker lab ((Stott & Barker, 2014). Briefly, a vertical line was drawn through the most medial tip of the cerebral peduncle that then formed the medial border (excluding the ventral tegmental area). The dorsal border included all of the TH+ cells with the ventral border following the cerebral peduncle until it met

the medial vertical line. Between 5 and 6 sections of SN were counted per brain. A 4x objective was used to define the region of interest which was then visualised under a 40x objective. The number of TH+ cells in each counting frame (90 µm x 90 µm) was recorded. Estimated section thickness after processing (dehydration, mounting) was 20 µm. Depth (z section) data was used to create a frequency-distribution curve. A final estimation was performed using the optical fractionator formula to allow for variable antibody penetration (as in (Stott & Barker, 2014)).

4.5.7 Western blots

Protein extraction from flash frozen PBS perfused brains
Whole brains were homogenised with homogenisation solution (20% extraction buffer Abcam ab 193970, 2% extraction buffer enhancer Abcam ab193971 and 2% protease inhibitor Abcam ab65621 made up in ice cold Tris-buffered saline) using a 1mL glass homogeniser which had been pre-cooled on ice. The homogenate was placed on ice in an eppendorf tube once there were no visible solid pieces. The homogeniser was cleaned with de-ionised water between samples. Samples were incubated on ice for at least 20 minutes. They were then centrifuged at 4°C for 20 minutes at 14000RPM. The supernatant was transferred to a pre-cooled Eppendorf and aliquoted into 20µL aliquots. The concentration was confirmed using a BCA assay (Pierce BCA protein assay kit, 23225). Samples were frozen at -80°c for subsequent use.

Samples for loading into the gel for Western blotting were made so that there was 20µg of protein diluted in LDS sample buffer (made from 4 x LDS sample buffer Invitrogen NuPage NP007) and DTT reducing agent (1M Invitrogen NuPAGE NP0009 at a final concentration of 0.1M). Samples were then spun for a

few seconds. They were then boiled on a hot place for 10 minutes at 70°C. They were then centrifuged for 5 minutes on full power (13000 RPM) to remove bubbles. Samples were then loaded to a total volume of 20µl. A Biorad ladder 1610377 was added to one well. Pre-made NuPAGE 10% Bis-Tris gels were used in a cassette which was fitted in a tank. MOPS running buffer was then poured in to cover the lanes (Novex NuPage MOPS SDS Running buffer 20x NP0001).The gel was run for 30 minutes at 100V and then the voltage was increased to 120V and run for approximately 1 hour and 30 minutes. The reaction was stopped when the ladder reached the bottom of the gel. The transfer buffer was prepared fresh for each run (1 x transfer buffer Novex NuPage 20x NP0006-1, 20 % methanol made up in de-ionised water and kept at 4°C. The gel was removed from the cassette and soaked in transfer buffer for 20 minutes. Sponges and a PVDF membrane were also soaked in transfer buffer. The gel was then placed in the apparatus on a PVDF membrane in between filter paper and 3 sponges. The tank was then loaded with chilled transfer buffer and run at 30V for 2-3 hours. The membrane was then blocked in 5% milk (Sigma-Aldrich ERMBD283) and TBS-T (0.1% Tween TBS) for 1 hour at room temperature on a shaker. The primary antibody was then applied to the membrane (Abcam ab1903 mouse anti-human alpha synuclein, 1:2000) overnight at 4°C. The next day the primary antibody was washed off with 3 x 10 minute washes with TBS-Tween (0.1%) on a shaker. An HRP conjugated secondary antibody was added in 5% milk TBS-Tween (0.1%) blocking buffer (Thermo-Fisher 62-6520 goat anti-mouse, 1:5000) and the membrane was incubated for 1 hour at room temperature on a shaker. It was then washed 7 times in TBS-Tween (0.1%) for 10 minutes each on a shaker. A SuperSignal West Femto Kit (Thermoscientific 34094) was used to prepare the membrane which was first incubated in the dark for 5 minutes with a mixture of peroxidase and enhancer in a 1:1 ratio (as per the kit instructions). The signal was developed on the UVI Tech alliance. The membrane was then incubated in stripping buffer for 30 minutes(1.5% glycine Fisher Scientific BP381-500, 0.1% SDS

Sigma L3771, 1%TWEEN Sigma Aldrich 27434-8, pH adjusted to 2.2 with hydrochloric acid). It was then washed x 3 in TBS-Tween (0.1%) and then incubated with HRP conjugated anti-B actin antibody for 1 hour at room temperature for a loading control. The membrane was prepared and imaged as above. The images were analysed using FIJI and normalised to beta actin and analysed using Graphpad Prism (version 7.0).

4.5.8 Meningeal wholemounts

Skull caps were removed prior to extraction of the brain (as described in (N. Derecki et al., 2015). They were placed in 2% PFA overnight and then in PBS. The meninges were then carefully dissected off the skull cap and washed for 5 minutes in PBS. The meninges were then incubated for 1 hour at room temperature in block/perm solution (0.1M PBS, 1% BSA, 2% serum, 0.1% triton X100, 0.05% tween). They were then incubated overnight in antibody dilution solution (0.1M PBS, 1% BSA, 0.5% Triton X100) with the antibody. The next day they were washed in PBS (x3). The meninges were then gently spread on a glass slide using a paintbrush and mounted using mounting media . Antibodies are specified in the results section (and Appendix I).

4.5.9 RNA extraction

RNA was extracted from mouse striatum and meninges. The tissue was placed in RNA lysis buffer (ThermoFisher 4305895) in precellys tubes and then homogenised using a precellys benchtop homogeniser (Precellys 24). The RNA was extracted using the Ambion Purelink RNA minikit (cat 12183025) according to the instructions of the manufacturer (available at https://www.thermofisher.com/document-connect/document-

connect.html?url=https://assets.thermofisher.com/TFS-Assets/LSG/manuals/purelink_rna_mini_kit_man.pdf).

4.5.10 qPCR of extracted RNA (meningeal or striatum)

The RNA yield was measured using a Nanodrop. RNA was converted to cDNA using the ThermoFisher VILO RNA-to-cDNA kit (cat. 11754050). Samples were incubated with reverse transcriptase buffer and enzyme mix as per the manufacturer's instructions and placed in a PCR machine (37°C for 60 minutes, 95°C for 5 minutes and 4°C for hold). The cDNA obtained was then loaded into a PCR plate containing Taqman advanced master mix (ThermoFisher 4444557), RNAase free water and primers to a total volume of 10µl. Samples were loaded in triplicate and the plate was spun down prior to running on the RT-PCR machine (Viia7 system) with 50 PCR cycles. Relative expression (normalised to GAPDH) was calculated using excel (version 16.24).

Primers:
IL10: mo1288387
IL6: mm00446190
GAPDH: mm9999915_j

4.5.11 Additional mouse strains used in experiments

All mice bred in house were genotyped according to standard protocols. C57bl/6 mice were obtained from Jackson laboratories (JAX) or from in house breeding stock. B cell deficient µMT mice were obtained from in house breeding stock. They have a mutation affecting the immunoglobulin heavy chain (µ chain) that means that they are unable to express membrane bound IgM. The result is that

they are unable to produce B cells beyond the pre-B stage. Tissue from MI-2 mice was kindly given to us by Michal Wegrzynowicz and Maria Grazia Spillantini. These mice are a new model of Parkinson's disease created by expressing a truncated version of human alpha synuclein (asyn 1-120) on the tyrosine hydroxylase promotor (TH)(Wegrzynowicz et al., 2018) on the background of a C57bl/6J mouse with a spontaneous deletion in SNCA (C57BL/6J OlaHsd mice (Snca–/–). These mice were bred in house and the SNCA knockout mice and C57bl/6 mice were used as controls. IL10 knock out mice for transfer experiments were obtained from Jackson Laboratories (https://www.jax.org/strain/002251).

4.5.12 Statistical analysis

Behavioural experiments were analysed using two way ANOVAs with motor outcome as the dependent variable and genotype as an independent variable. Between group differences in B lymphocyte proportions or subsets were tested using either unpaired t-tests (for parametric data), Mann Whitney U tests or ANOVA depending on the number of comparisons. Further statistical details are described in the results section.

4.6 Results

4.6.1 Circulating B lymphocytes in PD transgenic models

Given that I had found that circulating B lymphocytes were decreased in PD patients compared to controls, I looked at circulating B lymphocytes in two different transgenic mouse models of PD and wild type control animals, the thy1 SNCA mouse (overexpression of human alpha synuclein on the thy1 promotor) and then the MI-2 mouse (expression of an aggregation prone truncated version of human alpha synuclein, h1-120 on the tyrosine hydroxylase promotor). The MI-2 mice were compared to two different controls: alpha synuclein null mice that carry a spontaneous deletion of a murine alpha synuclein gene (C57BL/6J OlaHsd mice ($^{Snca-/-}$) and C57bl/6 mice. The MI-2 mice are on a C57BL/6J OlaHsd background.

Figure 4-4 and Figure 4-6 show representative gating for these experiments. There was a statistically significant reduction in the proportion of B lymphocytes in both alpha synuclein transgenic models versus controls as shown in Figure 4-5 and in Figure 4-7 (thy1 SNCA versus control Mann Whitney U = 32, p = 0.0064, MI-2 versus c57bl/6 Mann Whitney U = 0, p = 0.008, versus alpha synuclein null Mann Whitney U = 1, p = 0.02). There was also a significant decrease in the absolute numbers of B cells in the MI-2 mice versus C57bl/6 mice (t[8]=2.38, p = 0.04) but not alpha synuclein null mice. There was no significant difference in the absolute counts in the thy1 SNCA mice versus controls (Mann Whitney U = 21, p = 0.10). In the thy1 SNCA experiments (done over 3 separate experiments), I looked at further additional markers including markers of activation (CD69, MHC Class II, CD21/35 and plasma cells CD138 as well as looking at neutrophil and inflammatory monocyte numbers). There were no between-group differences.

Figure 4-4

Flow cytometry plots showing gating for the analysis of peripheral blood (thy1 SNCA study)

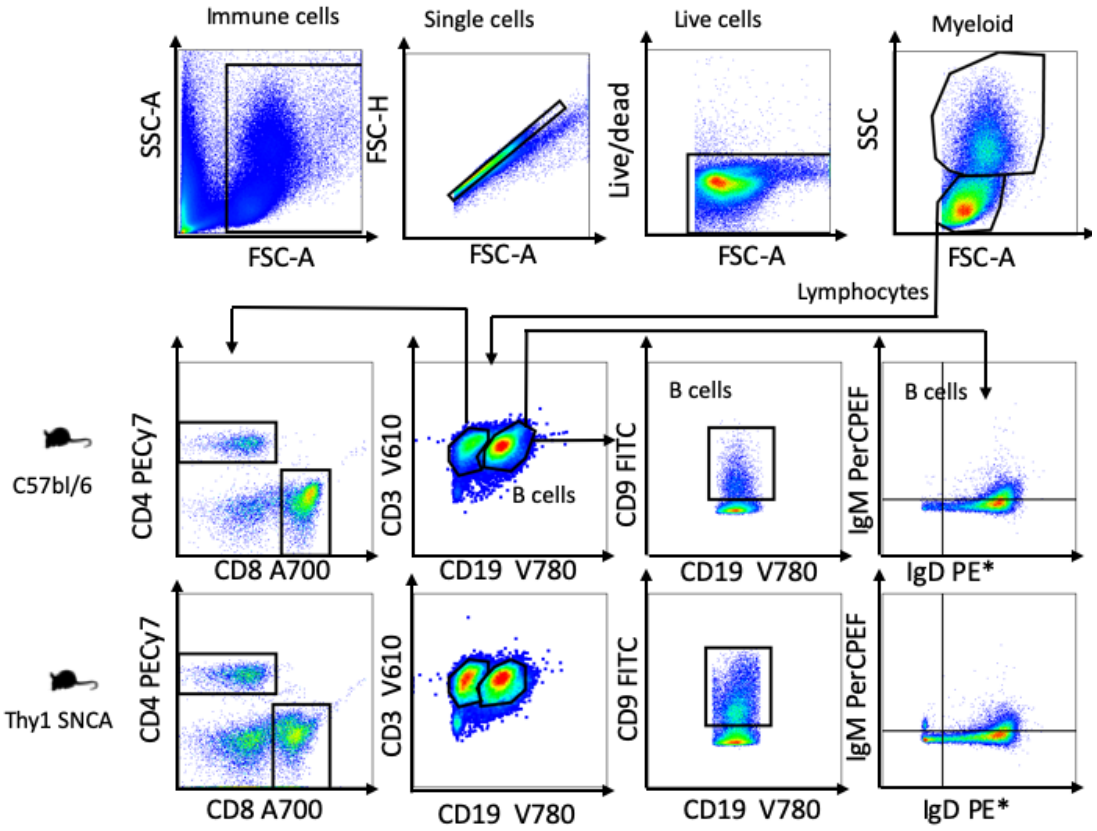

Figure 4-4 shows initial flow cytometry gating (first row) and then a comparisons of representative flow plots showing B cells in the C57bl/6 (middle row) and Thy1 SNCA mice (bottom row) showing T cells (CD3+), B cells (Cd19+), CD9+ B lymphocytes and IgM/IgD staining. The phenotyping was done over 3 separate experiments using mouse flow cytometry panels 1,2 and 3 respectively (details in Appendix 1). PerCpEF = PerCPefluor 710.

Figure 4-5

B lymphocyte counts and proportions in the peripheral blood of Thy1 SNCA mice and littermate controls

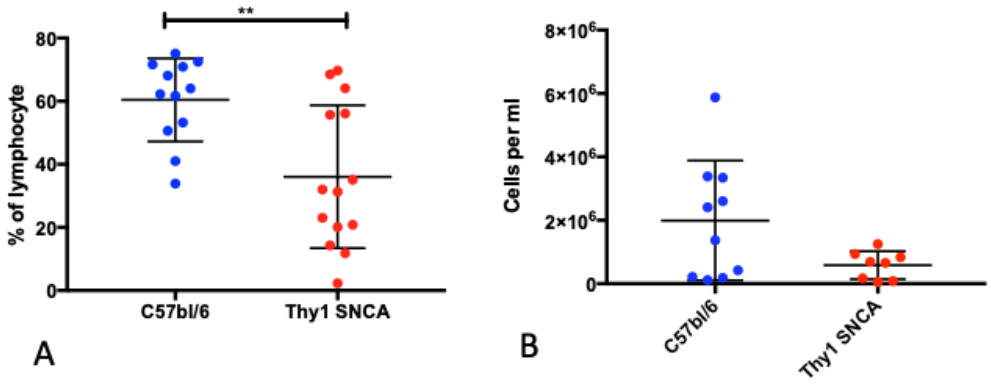

Figure 4-5 A) shows the differences in the proportion of B lymphocytes and B) shows the differences between the absolute counts between th1 SNCA mice and littermate controls. Proportions c57bl/6 mean 36.6% (SD 22.63), thy1 SNCA mean 60.4% (SD 13.15). Absolute counts C57bl/6 mean 1.9 x 10^6 (SD 1.9 x 10^6), thy1 SNCA mean 0.5 x 10^6 (SD 0.43 x 10^6). ** $p < 0.01$. The data was obtained over 3 separate experiments, from 13 C57bl/6 mice (N=13, 6 females; mean age 19.1 months, SD 1.5 months) and 13 Thy1 SNCA mice (N=13, 8 females; mean age 18.7 months, SD 1.72).

Figure 4-6

Flow cytometry plots showing gating for analysis of peripheral blood (MI-2 study)

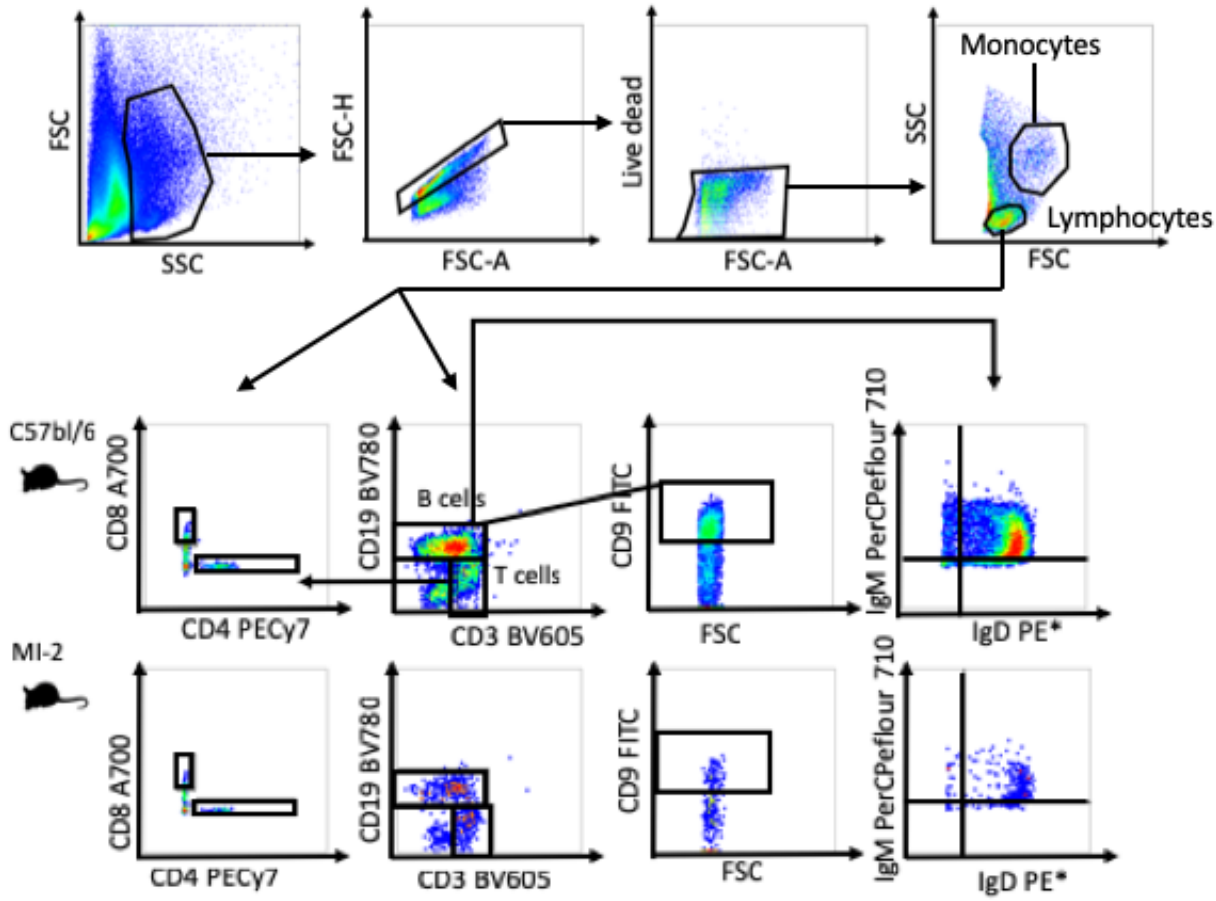

Figure 4-6 shows initial flow cytometry gating (first row) and then a comparisons of representative flow plots showing B cells and T cells in the C57bl/6 (middle row) and MI-2 mice (bottom row). Cells were stained using flow cytometry panel 2 (see Appendix 1).

Figure 4-7

B lymphocyte proportions and absolute counts in peripheral blood of MI-2 mice and controls

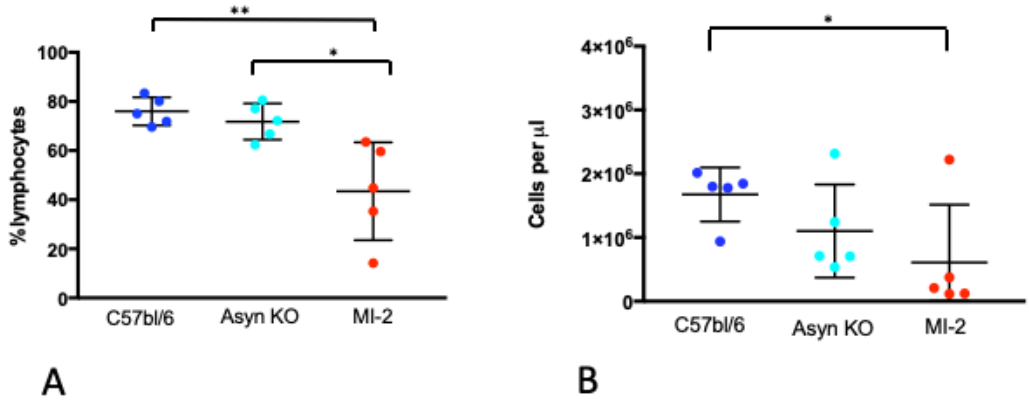

Figure 4-7 A) B lymphocyte proportions (of total lymphocytes) in MI-2 mice and two different control groups (C57bl/6 and C57bl/6J OlaHsd (asyn KO). The MI-2 mice are on a C57bl/6J OlaHsd (asyn KO) background. Mean in C57bl/6 76% (SD 5.7%), mean in Asyn KO 71.8% (SD 7.3%), mean in MI-2 43.4% (SD 19.9%). B) Absolute B lymphocyte counts C57bl/6 mean 1.6 x 10^6 cells/µl (SD 0.42), Asyn KO 1.1 x 10^6 cells/µl (SD 0.72), MI-2 0.6 x 10^6 cells/µl (SD 0.9). There were 5 male mice in each group, all aged between 17 and 18 months. Asyn KO = alpha synuclein null mice. ** $p < 0.01$ * $p<0.05$

There were no significant differences between the proportions of CD9+ (regulatory B cells) or IgM and IgD positive cells in either the MI-2 transgenic mice or the thy1 SNCA mice versus controls (see Figure 4-8). There were also no differences in the proportion of T cells, inflammatory monocytes or neutrophils (data not shown).

There was a significant interaction between genotype and B lymphocyte subset in a repeated measures ANOVA with IgM IgD subgroups as the repeated

measure and genotype as the between subjects variable (interaction term F [1,24] = 5.3, p = 0.03). There was no independent main effect of genotype. Inspection of the plot in Figure 4-8 D shows that there is a decrease in the transgenic animals away from naïve B cells (IgD+IgM+ mainly) with a slight increase in the IgD-IgM- population that is driving this interaction effect.

Figure 4-8

B lymphocyte subsets in transgenic and control mice

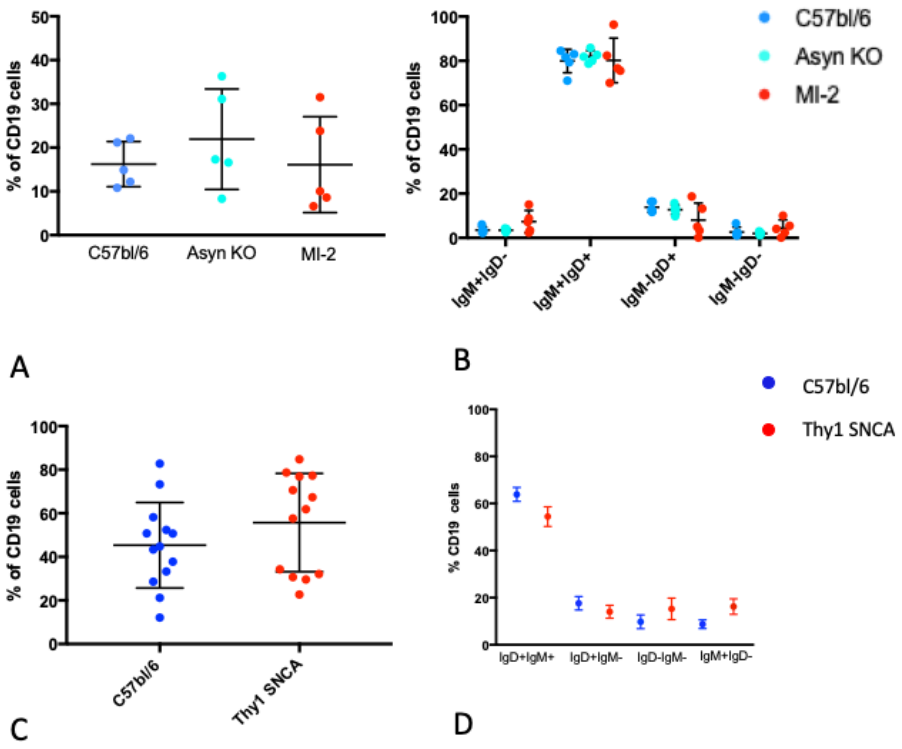

Figure 4-8 A) the proportion of CD9+ B lymphocytes in MI-2 mice versus controls B) IgD and IgM in B lymphocytes in C57bl/6, Asyn KO (alpha synuclein null) and MI-2 mice (N = 5 males in each group, 18 months old). C) the proportion of CD9+ B lymphocytes in thy1 SNCA mice versus controls D) Mean and SEM IgD and IgM in C57bl/6 mice and Thy1 SNCA (N=13 in each group).

4.6.2 μMT 6OHDA experiments

Once I had established that there were decreased B cells in PD patients and their associated models compared to controls, I wanted to find out whether B cell deficiency changed the disease outcome.

After surgical lesioning, μMT mice performed significantly worse on the rotarod forced walking test than their wild type counterparts (see Figure 4-9). A two way ANOVA with genotype and week of testing as independent variables showed that there was a significant main effect of genotype overall ($F [1, 133] = 26.65$, $p < 0.0001$) and of time ($F[4,133] = 10.33$, $p < 0.0001$) with a significant interaction between the two terms ($F[4,133] = 3.02$, $p = 0.02$).

I also carried out balance beam testing in a sub-group of these mice in order to show that the motor phenotype was robust and to select a behavioural test for subsequent experiments. Figure 4-10 shows that the μMT mice also performed worse on this test of motor function with a significant main effect of genotype on the 15mm ($F[1,61] = 15.75$, $P = 0.0002$), 10mm ($F[1,61] = 10.19$, $P=0.002$) and 6mm rods ($F[1,75] = 7.40$, $P=0.002$). There was only a significant overall effect of time point in the 15mm ($F [3,61] = 2.81$, $p = 0.04$) and the 6mm rods ($F[4,75] = 3.06$, $p = 0.02$). The interaction term was not significant for any of the analyses (data not shown). For subsequent experiments I decided to use the rotarod alone as it gave a robust behavioural readout of the surgical lesion that was consistently different between the groups. It was also relatively straightforward to perform in comparison to the balance beam which required several hours of testing across the different beam sizes.

Immunohistochemistry for tyrosine hydroxylase (TH) confirmed that the lesion was larger in the μMT mice than in control animals (the optical density of

staining in the lesioned striatum as a percentage of the non-lesioned side was less in μMT animals (t[11]= 4.07, p = 0.0006) (see Figure 4-12). There was no difference in the nigral TH+ cell counts between the two strains. Microglial activation and immune cell infiltration are well described in this model. I had not quantified this in the initial experiments due to the unexpectedly early birth of my son. Once I had come back from maternity leave it took a while to breed enough mice to repeat the experiment. The histology is currently ongoing.

Figure 4-9

Performance on the rotarod (short protocol)

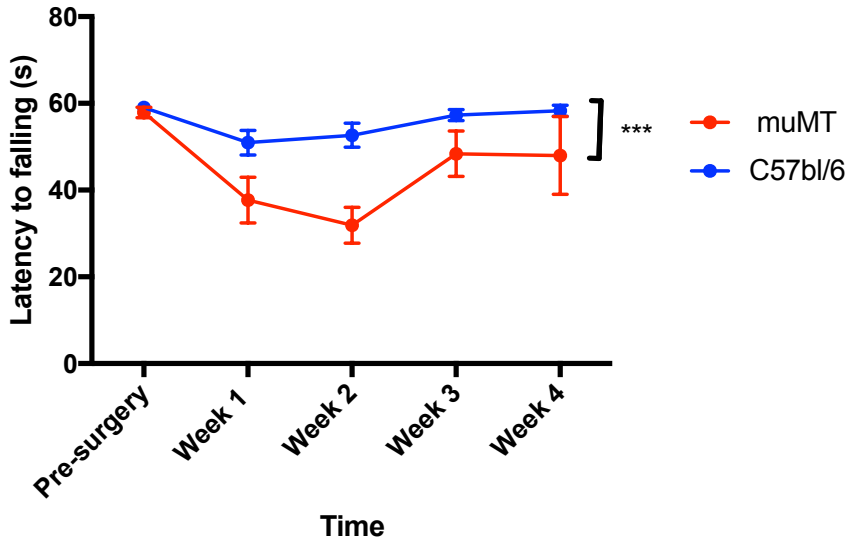

Figure 4-9 Rotarod performance shown for N = 28 muMT mice (15 male) and N = 28 C57bl/6 mice (11 male) collected across two experiments (with equal numbers in each group for both experiments). All mice were aged between 11 and 14 weeks at the time of the experiment. The figure shows mean and standard error of the mean (SEM). Lower latencies in this test suggest poorer performance (mice fall off sooner). This short protocol test has a ceiling effect (a limit of 60s on the bar) meaning that the C57bl/6 did not show a significant change after surgery.

Figure 4-10

Balance beam performance

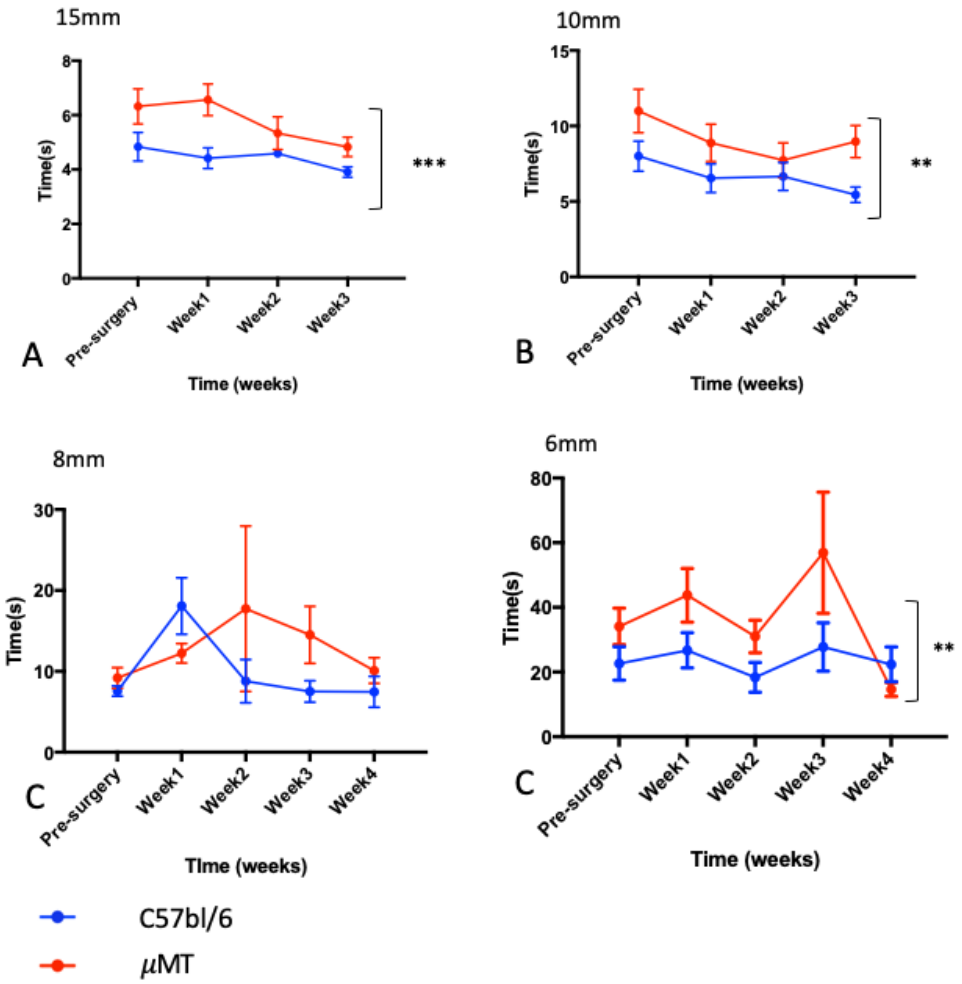

Figure 4-10 Balance beam performance in a subgroup of mice from the first experiment (10 muMT [5 male] and 10 C57bl/6 mice [4 males]) (the same mice were also tested on rotarod). The differences highlighted on the graphs show the main effect of genotype which was significant at either a p <0.0001 (***) or p<0.001 (**) level. Longer times in this test suggest poorer performance (the mouse takes longer to traverse the beam). The performance on the smaller beam sizes was much more variable with many mice falling off so many times that it was difficult to calculate total scores

Figure 4-11

Tyrosine hydroxylase staining showing a worse lesion in µMT mice

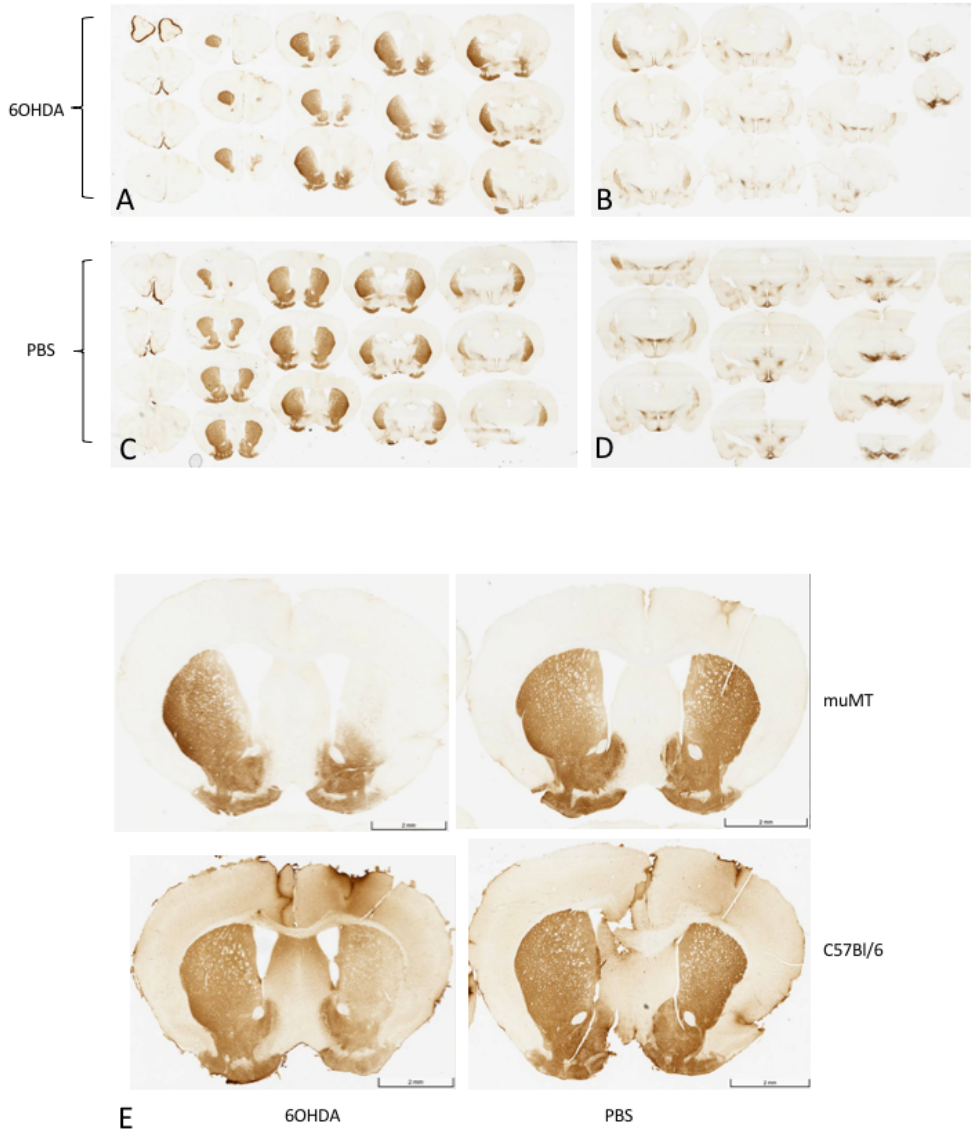

Figure 4-11 A-D shows representative slices through the entire brain of µMT mice (A+B injected with 6OHDA and C+D with PBS as a control). E shows representative images of the lesion in the striatum, showing that this is more extensive in the µMT mouse.

Figure 4-12

Quantification of TH+ staining

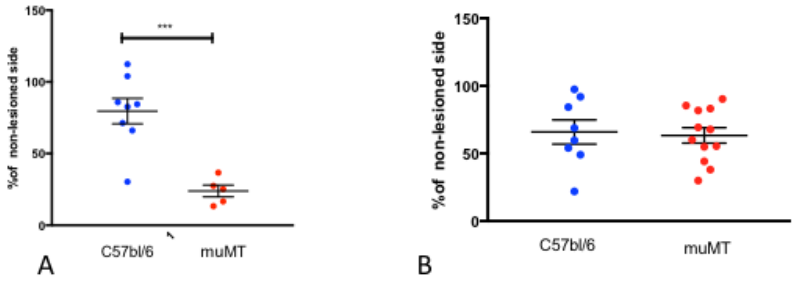

Figure 4-12 A Optical density staining in the striatum showing the staining as a percentage of the non-lesioned side (N = 8 C57bl/6, N = 5 μMT) from mice culled 4 weeks after surgery. B Substantia nigra TH+ cell counts as a percentage of the non-lesioned side (N = 8 C57B/6, N = 12 μMT).

4.6.3 μMT cell transfer experiment

To attempt to rescue the deficits observed in the previous experiments, I transferred either B lymphocytes or normal mouse serum into μMT mice one week prior to surgery (see Figure 4-13) . The B lymphocyte transfers were not successful in the μMT animals (see Figure 4-14) with only one animal having measurable B lymphocytes in the peripheral circulation after culling. There were also no B lymphocytes in the secondary lymphoid tissues of the μMT mice that had had cell transfers. In the rotarod test, there was a significant main effect of condition in a two way ANOVA ($F[3,49]=p = 0.008$) with the μMT mice performing worse overall as in previous experiments. The differences were driven by the μMT versus C57bl/6 difference rather than by treatment group. Neither the cell transfer or serum transfer was able to rescue the behavioural

phenotype. As the cell transfer was not successful, further analysis was not done on this experiment. Subsequent more detailed review of the literature suggested that in the μMT mice, strongly inhibitory T cells block reconstitution of transferred B cells (both B1 and B2)(Baumgarth, Jager, Herman, Herzenberg, & Herzenberg, 2000). Therefore it is not a useful model for this sort of manipulation (or at least would require irradiation prior to reconstitution which was not possible within the limits of our animal license). The results do suggest that the antibodies are not playing a protective role the serum transfer did not rescue the phenotype.

Figure 4-13

The design of the μMT transfer experiment

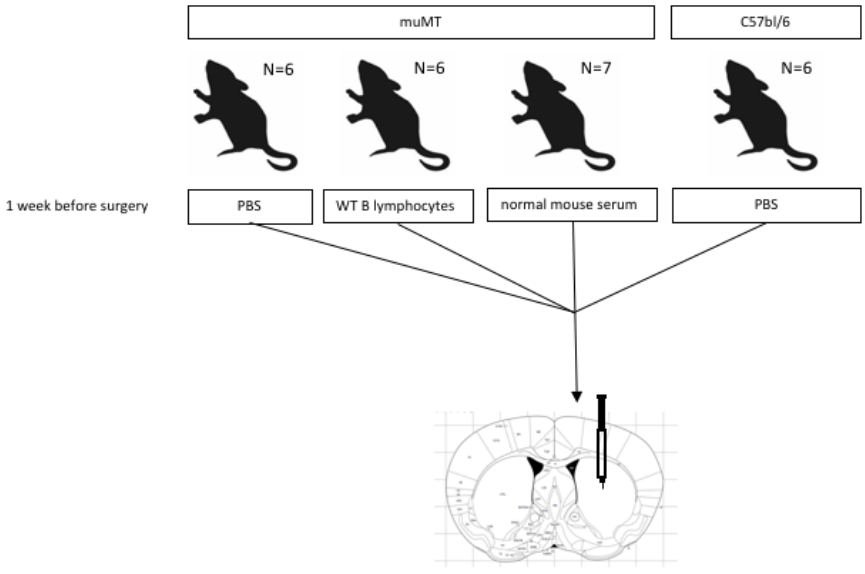

Figure 4-13 In order to work out which part of the B lymphocyte response was responsible for the effect, I attempted to rescue it by transferring B lymphocytes, mouse serum (antibodies) or control (PBS) 1 week prior to surgery.

Figure 4-14

B lymphocyte proportions in μMT and control mice following cell or serum transfer

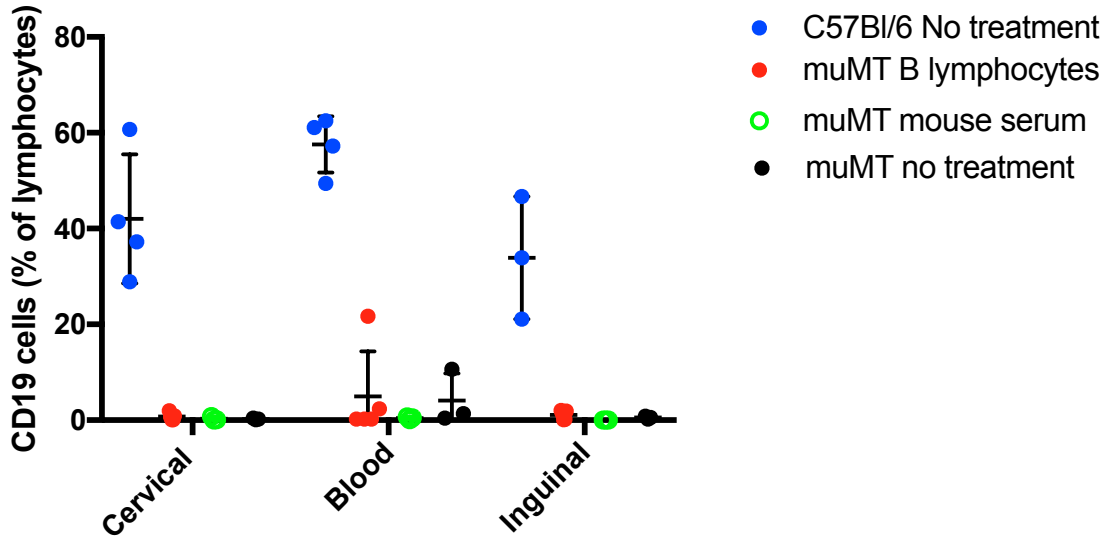

Figure 4 14 6 μMT (2 males) mice received B lymphocytes derived from 4 C57bl/6. 7 μMT (3 males) mice received normal mouse serum. Mice were between 5 and 6 months of age at the start of the experiment. Cervical and inguinal refer to lymph nodes. Cells stained using mouse flow cytometry panel 4 (see Appendix I).

4.6.4 µMT meningeal qPCR

I hypothesised that one of the reasons that the µMT mice perform worse following 6OHDA could be that they lack IL10 producing B cells in their meninges which would be expected to attenuate the T lymphocyte and microglial response to cell death in the striatum, preventing further cell loss.

There was an increase in the expression of meningeal IL10 following UTI infection compared to baseline but this was the case across both the µMT mice and the controls. There were no differences in IL10 or IL6 following 6OHDA surgery (see Figure 4-15) but the data points were variable.

Figure 4-15

Meningeal cytokines in µMT mice

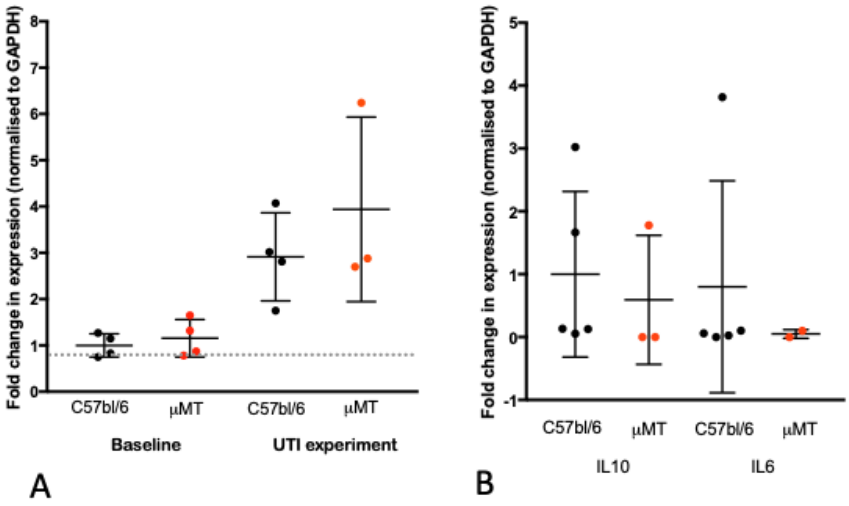

Figure 4-15 A) shows IL10 expression (relative to GAPDH) in µMT mice and controls (N=4 in each group, 12 week old females) at baseline and in the context of a urinary tract infection (UTI) (N = 4 in each group, 12 week old females).B) shows the IL10 and IL6 expression (relative to GAPDH) following 6OHDA surgery (5 C57bl/6 mice and 3 µMT mice, 11-12 weeks old).

4.6.5 CD20 6OHDA experiments

As an alternative to using transgenic B cell depleted animals, I therefore decided to deplete B cells using an anti-CD20 monoclonal antibody (mIgG2a, kind gift from Biogen). B cell depletion was done 2 weeks prior to surgery as shown in Figure 4-16.

Figure 4-16

Experimental design for B cell depletion experiment

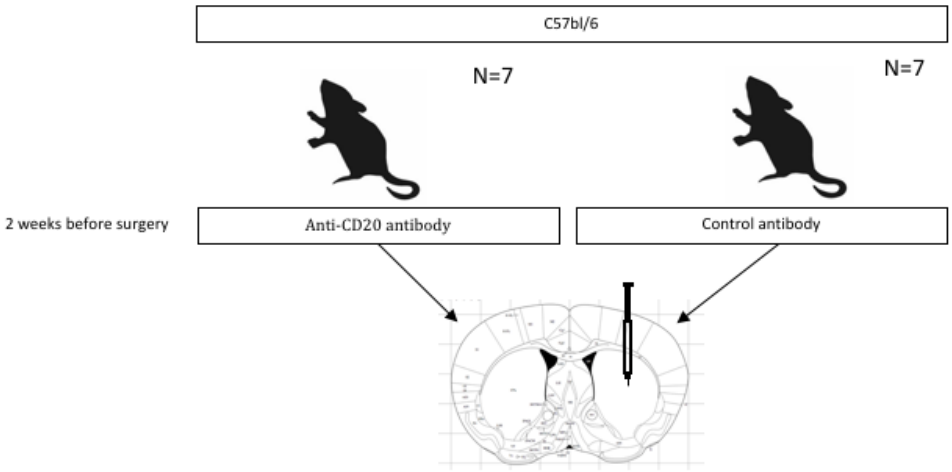

Figure 4-16 12-18 week old female c57bl/6 mice were obtained from in house breeding stock

Some mice were culled early due to weight loss following surgery (N=3 control group, N=1 in the treatment group). The behavioural testing showed a trend towards decreased performance in the B cell depleted animals (one tailed unpaired t-test week 3 showed a significant difference (day 21) $t[2] = 3.97$, $p = 0.03$) but the overall two way ANOVA showed no main effect of treatment ($F[1,8]$

= 1.78, p = 0.23) (likely because the experiment was underpowered) (see Figure 4-17).

Figure 4-17

Performance on the rotarod (long protocol)

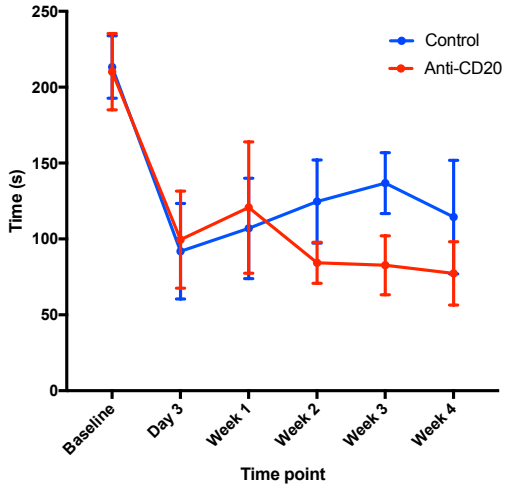

Figure 4-17 12-14 week female mice were used in this experiment. There was a trend towards poorer performance in the anti-CD20 animals. There were only 4 mice in the control group and 6 in the CD20 group that had all time points for the repeated measures ANOVA.

The histological examination of brains from this experiment is ongoing.
The CD20 depletion experiment was repeated with two additional cell transfer groups prior to surgery (B lymphocytes or IL10+ B lymphocytes) (see Figure 4-18.)

In the follow up experiment, B cells (either IL10 producing B cells or just B cells) were transferred into CD20 depleted mice 2 days prior to surgery as shown in

Figure 4-18). The rotarod data is shown below (Figure 4-19). Three mice in the anti-CD20 + B lymphocytes group and 1 in the anti-CD20 and IL10+ B lymphocytes group were culled early due to weight loss, There were no overall statistically significant differences between the three groups (anti-CD20 and IL10+ B cells, anti-CD20 and B cells and the control group) on a two way repeated measures ANOVA($F[1,12]=1.234$, $p=0.28$) (there was a significant decrease in performance following surgery as expected) Histological examination is ongoing.

Figure 4-18

Experimental design for B lymphocyte depletion and transfer

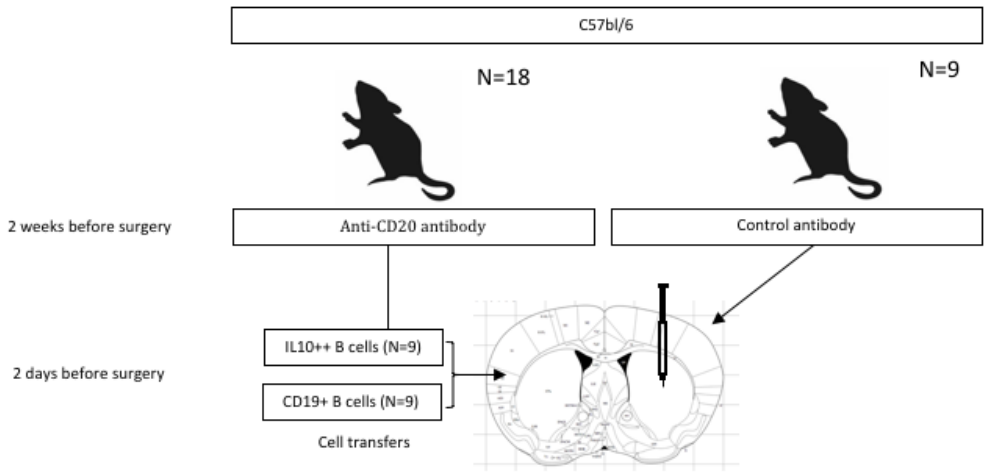

Figure 4-18 12-14 week old female mice were used for this experiment divided into three main groups: CD20 depletion + cell transfer of IL10++ cells, CD20 depletion + cell transfer of normal B cells and a group only given the control antibody.

Figure 4-19

Performance on the rotarod (long protocol)

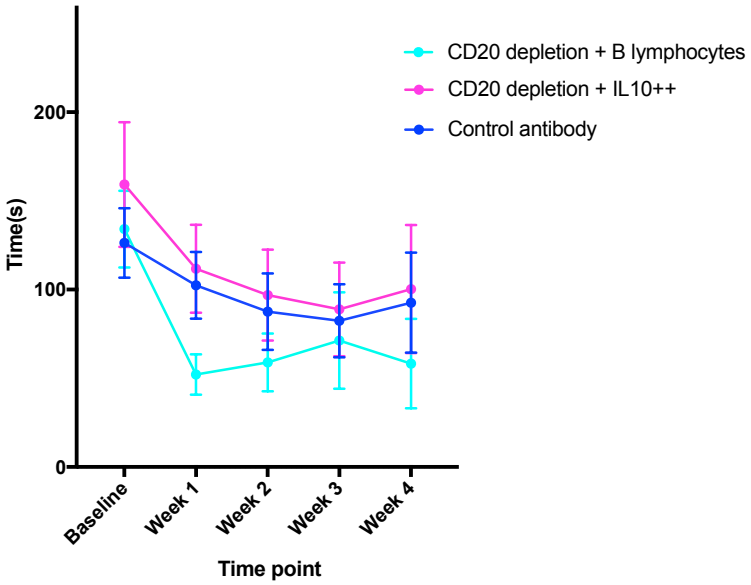

Figure 4-19 12-14 week old female mice were used in this experiment. There were 6 mice in the anti-CD20 + B lymphocytes group, 8 mice in the CD20 depletion + IL10 group and 9 mice in the control group that had data for all time points shown above. Graph shows mean and standard error of the mean.

I then tried a similar experiment using IL10 KO B cells instead of IL10 producing B cells to see whether the outcome was worse (see Figure 4-20). The rotarod data showed that there was no significant difference between the treatment groups at least on the behavioural readout for the experiment (two way ANOVA, $F[2,20] = 0.21$, $p = 0.8$) (see
Figure 4-21). There were a total of 5 mice culled early in this experiment due to weight loss (1 in the B lymphocyte group, 2 in the IL10- group and 2 in the control group). As with previous experiments, histological analysis is ongoing.

Figure 4-20

Experimental design for B lymphocyte depletion and transfer

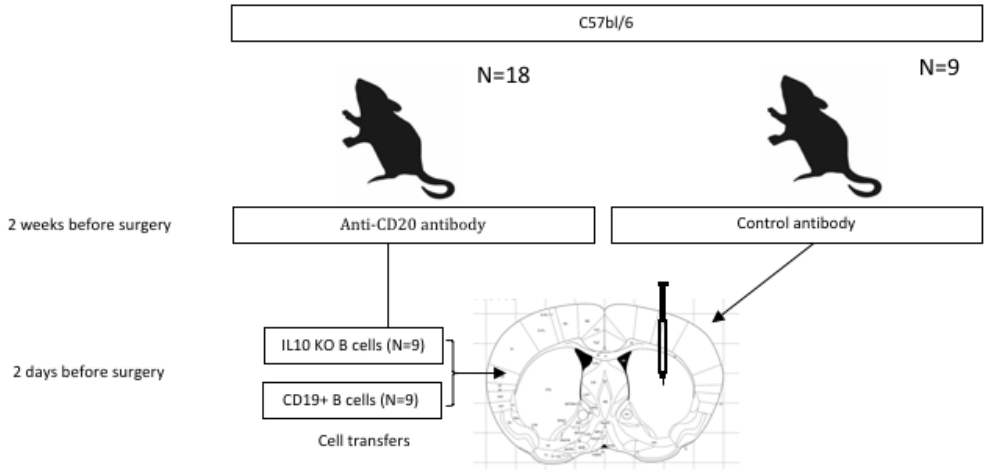

Figure 4-20 12-14 week old female mice were used in this experiment.

Figure 4-21

Performance on the rotarod (long protocol)

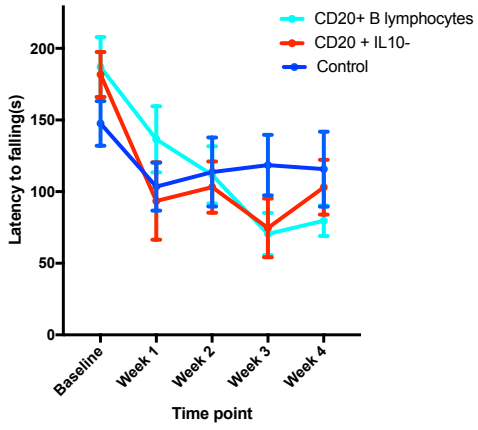

Figure 4-21 12-14 week old mice were used. There were 8 mice in the anti-CD20 and B lymphocytes group, 7 mice in the anti-CD20 and IL10- group and 7 in the control group that provided data for all time points.

To complete the B lymphocyte depletion experiments, I looked at whether the timing of B cell depletion made a difference (see Figure 4-22). Analysis of the rotarod data from this experiment showed that there was no difference between the treatment groups (anti-CD20 or control) (two way repeated measures ANOVA $F[1,24] = 1.05$, $p = 0.31$)(see Figure 4-23).

Figure 4-22

Experimental design showing B cell depletion at a later time point

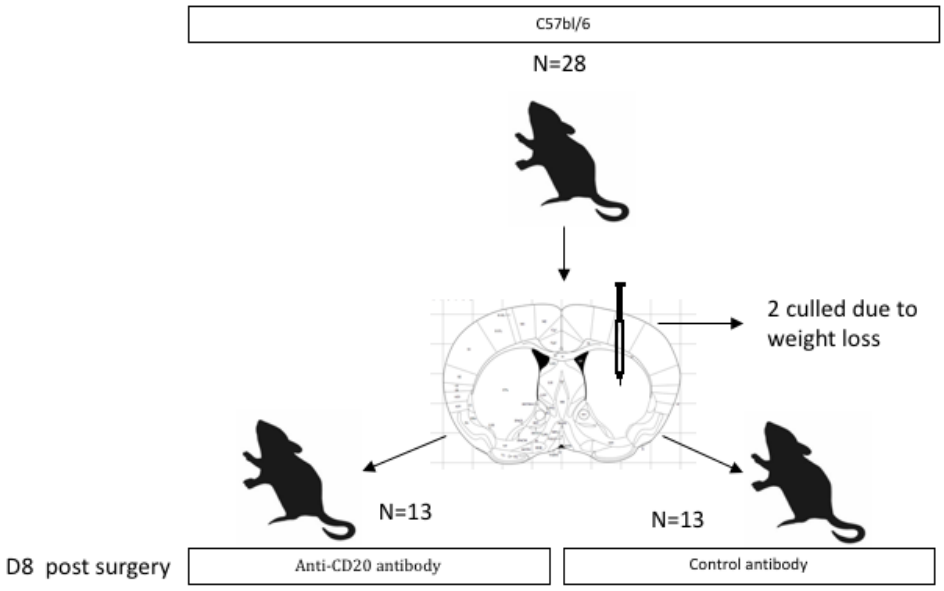

Figure 4-22 showing B cell depletion occurring after surgery (rather than before as in previous experiments).

Figure 4-23

Performance on the rotarod (long protocol) – delayed B cell depletion

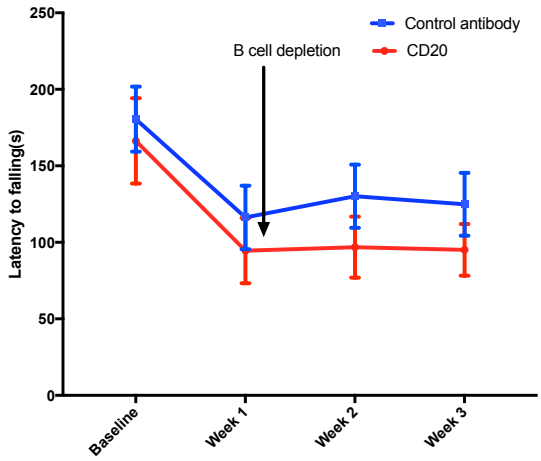

Figure 4-23 12-14 week old mice were used in this experiment. N=13 in each group had data from all time points.

4.6.6 Looking for a model with increased numbers of IL10 producing B cells in the meninges

At the same time as doing the experiments described above, I attempted to find a mouse model with an increased number of IL10 producing B cells in the meninges. Such a model would allow us to interrogate the role of these cells without relying on cell transfers.

I was able to look at B cells in the tissue of a knock in mouse expressing a mutation in the phosphoinositide-3-kinase δ. This mutation causes an immunodeficiency syndrome in humans characterised by recurrent pneumococcal infections ($P110\delta^{E1020K\text{-}GL}$). I was only able to look at the meninges in a knock in mouse in which the mutation was expressed in all cells. The same group had generated a B cell specific knock in which has been shown to have a population of tissue resident IL10 producing B cells in the lung (Stark et al.,

2018).Figure 4-24 shows a non-significant trend towards larger numbers of CD45+ cells in the meningeal compartment. As described in the methods, IV FITC anti-CD45 was injected prior to culling the animals in order to differentiate between cells that were resident in the tissues (extravascular, EV, should not be stained) and those that are in blood vessels (intravascular, IV, should be stained).

Figure 4-24

Extravascular cells in the meninges in the PI3K knock in model

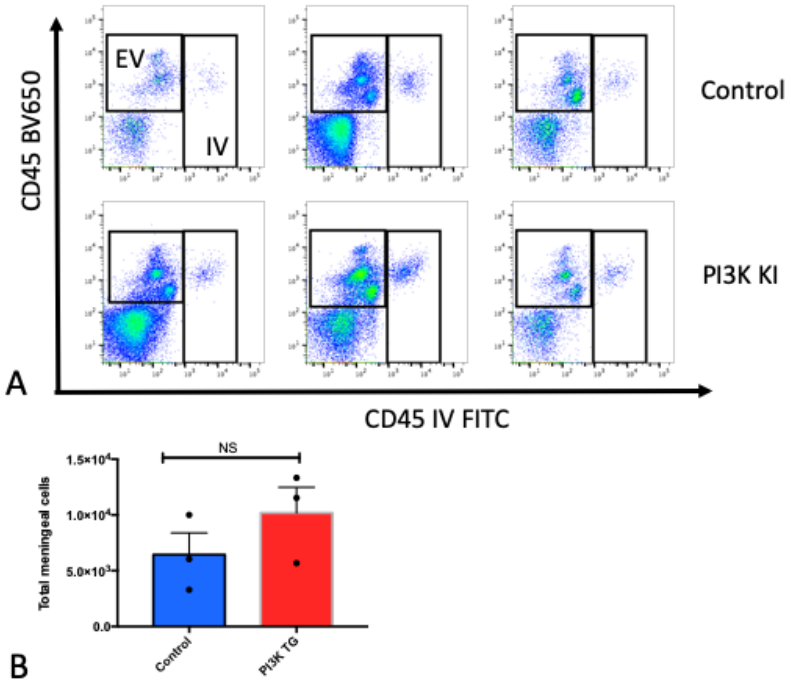

Figure 4-24 A gating of CD45+ extravascular and intravascular cells. EV extravascular IV intravascular. B Estimated absolute cell counts in the meninges. PI3K TG PI3K transgenic. N = 3 in each group. All mice were 8 week old females. Cells were stained using flow cytometry panel 5 (see Appendix I).

There was a shift in B lymphocyte phenotype in the PI3K knock in mice, with the transgenic mice having more IgD-IgM- B lymphocytes than the controls (see Figure 4-25). There was also a trend to a larger number of B1 cells in the transgenic mice (Figure 4-26). Unfortunately, I was unable to get more animals to increase the sample size or to look at the B cell specific knock in. These preliminary results suggest that this would be a useful alternative to using cell transfers to increase the meningeal B cells (but further work would be required to confirm that these B cells are IL10 producing).

Figure 4-25

PI3K transgenic mice have a shift towards IgM-IgD- B lymphocytes in the meninges

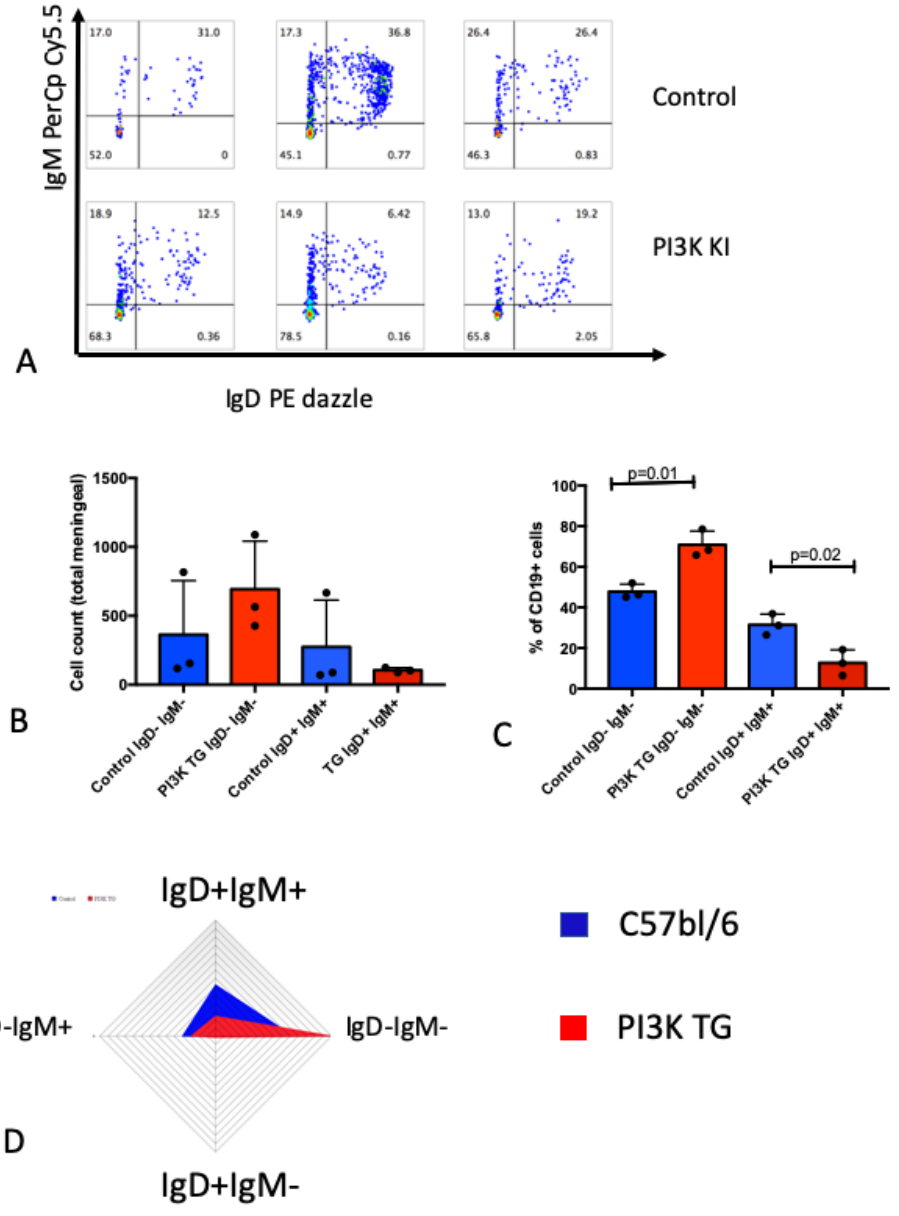

Figure 4-25 A) shows gating of CD19+ extravascular B lymphocytes. B) , C) and D) show a shift to IgM-IgD- B lymphocytes in the transgenic mice versus controls. Statistics shown represent unpaired t-tests. N= 3 in each group. All mice were 8 week old females.

Figure 4-26

B1 B lymphocytes in PI3K transgenics and controls

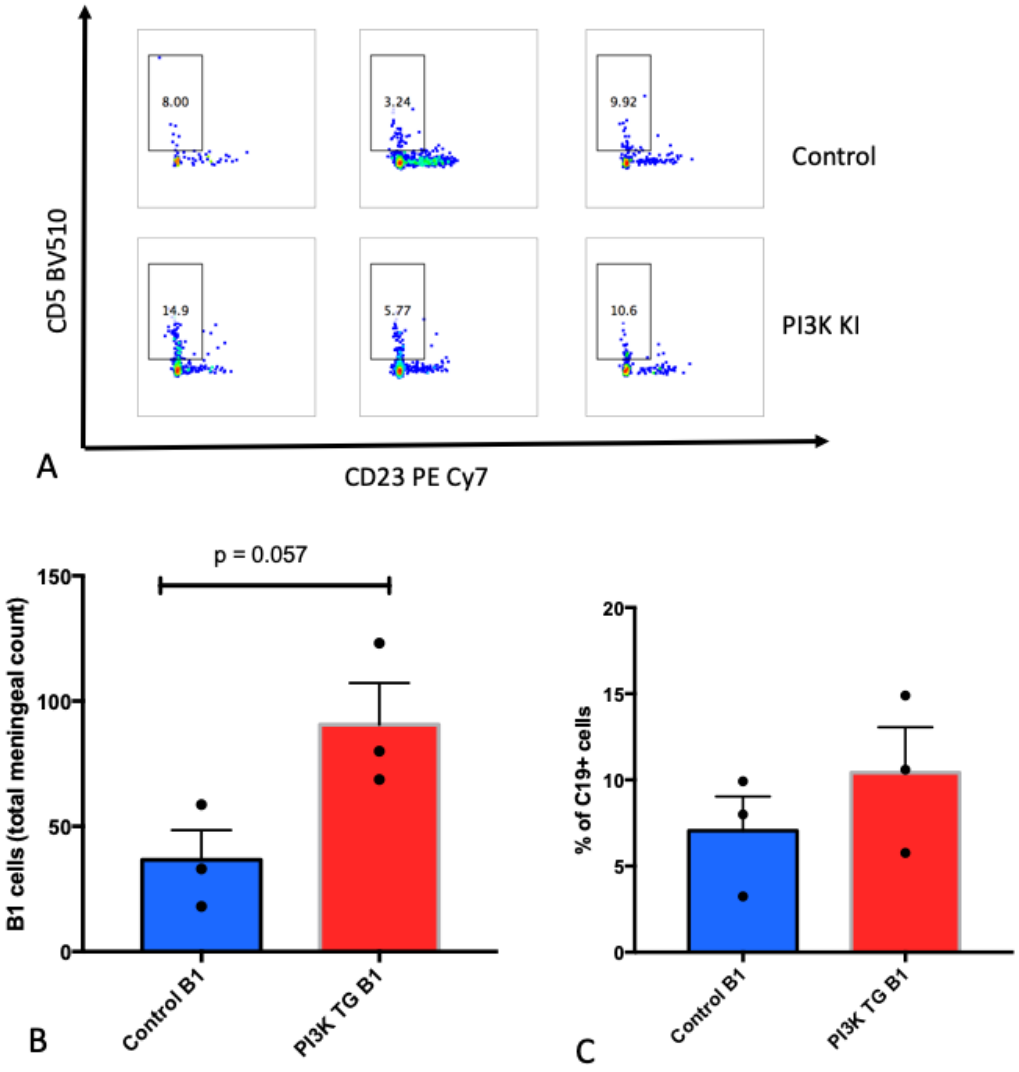

Figure 4-26 shows B1 B cells (as defined by CD5+ Cd23-). N=3 in each group, all mice were 8 week old females.

4.6.7 Thy1 SNCA behavioural experiments

I ran multiple behavioural experiments longitudinally in order to see whether I could identify an appropriate behavioural readout in aged mice to use to assess outcomes after possible manipulation of the B lymphocyte compartment in a non-toxin based model. I was ideally looking for a test that was relatively quick to perform that showed a large difference between transgenic (thy1 SNCA) and wild type animals (C57bl/6) animals. The initial relatively quick behavioural tests showed no significant differences between the transgenic animals and controls (see Figure 4-27). Given that other studies (e.g. (Marie-Francoise Chesselet et al., 2012) had found some subtle motor deficits I looked in detail at possible motor phenotypes using the balance beam (see Figure 4-28). There were no between group differences in performance on this task, including more subtle deficits that may be detected by calculating the number of errors per step. All mice got worse at the balance beam as the beam got thinner but this did not differ according to genotype (statistics not shown).

Figure 4-27

Initial behavioural tests in transgenic Thy1 SNCA mice and littermate controls

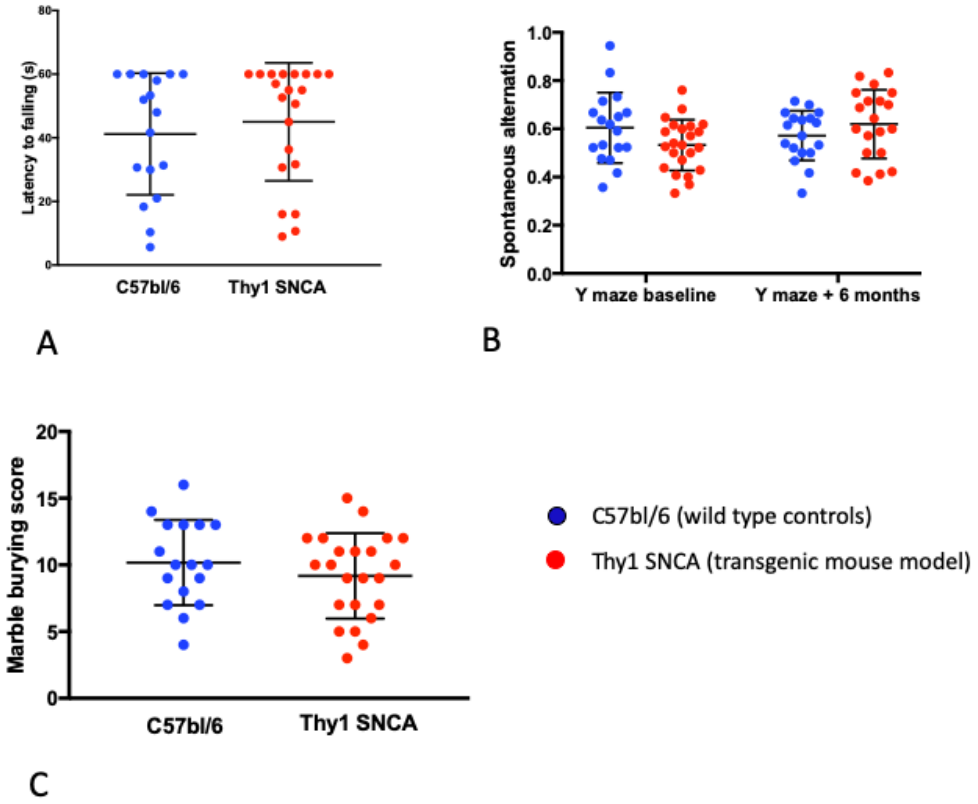

Figure 4-27 A) Shows the rotarod results recorded as a latency to falling (shorter times indicate worse performance). B) shows performance on the Y maze (spontaneous alternation) measured as a fraction of overall alternations across a 6 month period. C) Shows the marble burying scores (total marbles buried over a 30 minute period). There were 21 thy1 SNCA (mean age 10.6 months, SD 1.85, 14 females) and 18 c57bl/6 mice (mean age 10.3 months, SD 1.11, 8 females) for initial behavioural testing.

Figure 4-28

Balance beam results for a cohort of Thy1 SNCA and littermate controls

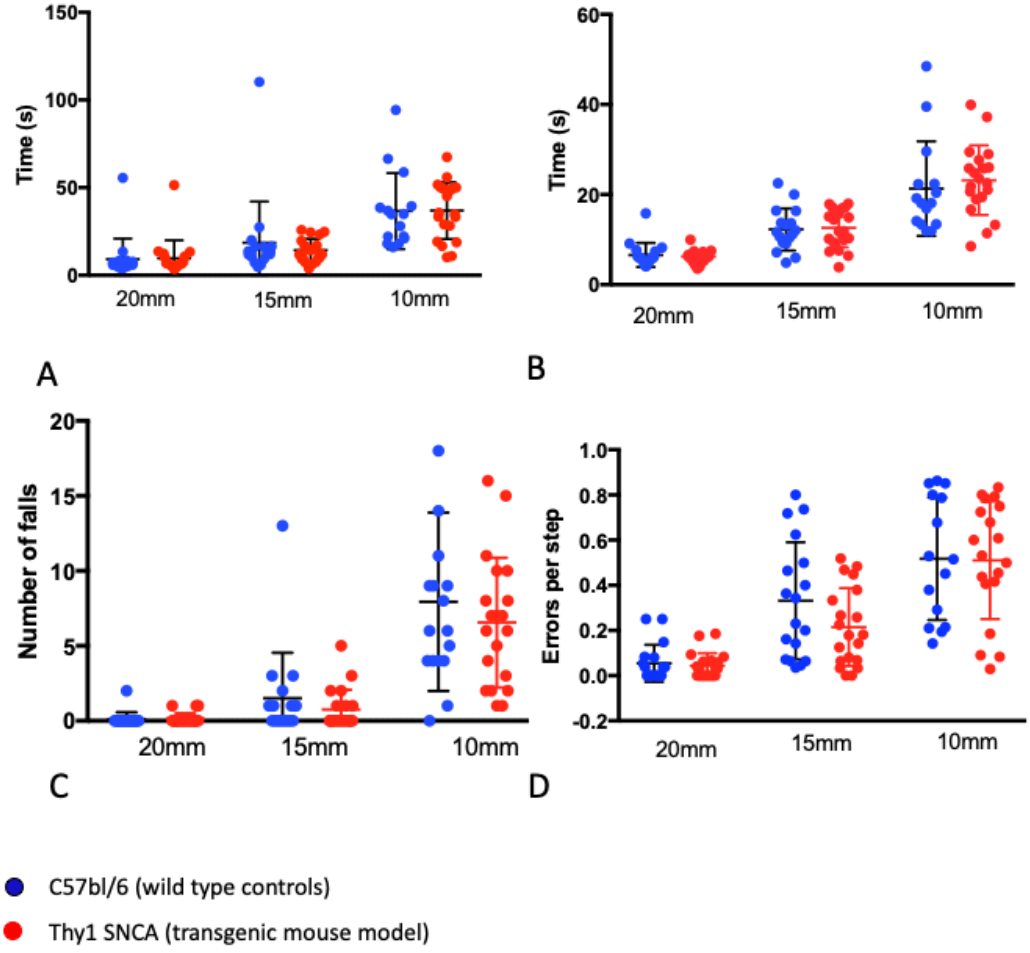

Figure 4-28 A) shows the total time from start to entry of the 'safe house' on the balance beam. B) shows 'test' time, defined as the time spent moving (excluding periods spent grooming/not moving) on the beam. C) Shows the number of falls per test and D) shows the number of errors divided by the total number of steps taken during the test (giving a measure of errors per step). The results are from a total of 36 mice , the same cohort tested previously but several months later (18 thy1 SNCA, 12 female, mean age 12.8 months SD 1.36; 18 c57bl/6 littermate controls, mean age 12.72, SD 1.12, 8 female).

4.6.8 Western blots and genotype checking

I ran western blots on whole homogenised brain tissue from thy1 SNCA animals and C57bl/6 controls to confirm that they did overexpress alpha synuclein in case there had been an error with breeding (see Figure 4-29). All mice were genotyped using ear tags at 5-12 weeks and again after they were culled to ensure that genotypes were appropriately assigned (data not shown).

Figure 4-29

Western blot confirming overexpression of alpha synuclein in thy1 SNCA brains

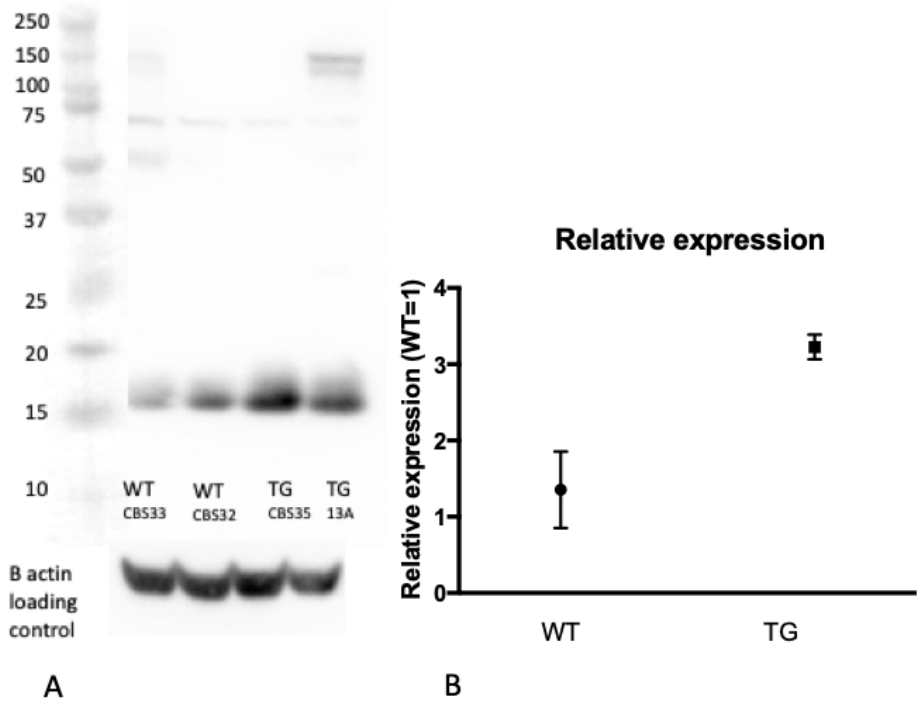

Figure 4-29 shows increased expression of alpha synuclein in the thy1 SNCA mice (TG, 2 males, one 8 week old mouse CBS35 and one 77 week old mouse 13A) versus C57bl/6 controls (WT, both 8 week old males). A) Western blot with beta actin loading control.

4.6.9 Additional 'hits' to thy1 SNCA model

In the experiments described in 4.5.2,Figure 4-42 I had hoped to be able to find simple behavioural readouts to use in experiments where I depleted or otherwise modulated the B lymphocyte compartment. As the behavioural tests over time did not show a significant difference between the controls and the transgenic mice I added further lesions (or 'hits'), initially repeated lipopolysaccharide(LPS) injections (see Figure 4-30 and Figure 4-31).

As expected all animal weights increased significantly over the 42 weeks of the experiment (Figure 4-31 A). I carried out a repeated measures ANOVA with genotype, treatment (LPS versus PBS) and gender as independent variables and weight as the dependent variable. There was a significant main effect of time ($F[7,126] = 32.02$, $p = 2.3 \times 10^{-25}$) and a significant main effect of genotype with the transgenic mice consistently being heavier than their C57bl/6 littermates ($F[1,18] = 36.5$, $p = 0.00001$). There was a trend towards LPS animals having lower weights ($F[1,18]=3.07$, $p = 0.097$) and a borderline interaction between genotype and treatment (LPS versus PBS) ($F[1,18] = 3.74$, $p = 0.069$). When looking at the differences within the thy1 SNCA animals there was a significant effect of LPS treatment over time, with the LPS animals weighing less ($F[1,8] = 0.045$). I had therefore planned to use weight as an outcome measure but the finding was not replicated in a second cohort (which was housed in a different animal house after the closure of the original animal house (N=21 thy1 SNCA, N=18 C57bl/6).

There was no significant effect of either genotype or treatment (LPS versus PBS) on marble burying (Figure 4-31 B), spontaneous alternation (Figure 4-31 C) or the inspection ratio on the novel object recognition test (done at one time point at the end of the experiment) (Figure 4-31 D). At the time I was limited to doing

non-regulated behavioural tests due to the restrictions of the Clatworthy animal license and therefore did not do motor tests in these animals.

Figure 4-30

Experimental design showing additional "hits" provided by LPS injection

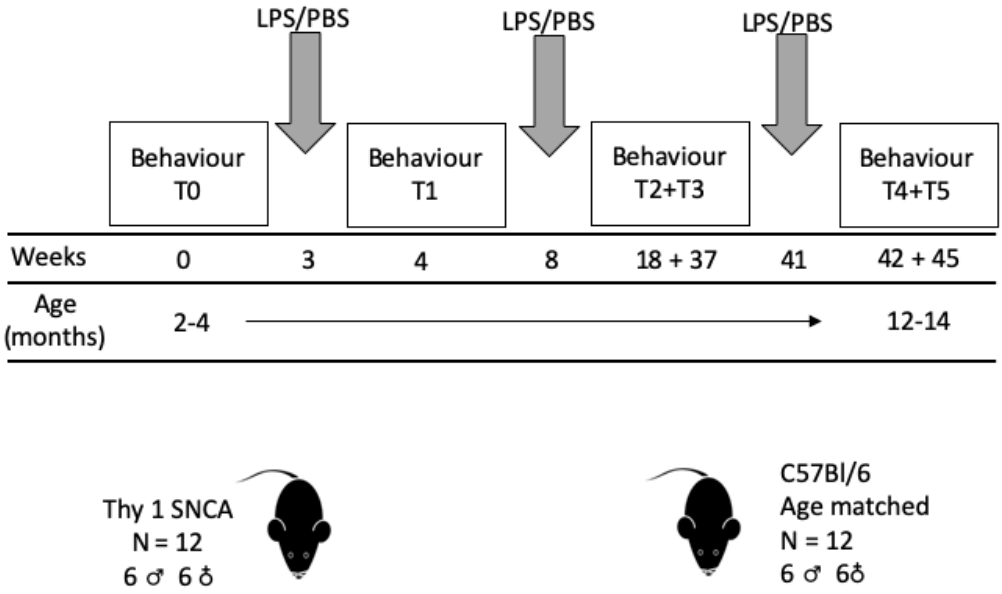

Figure 4-30 LPS lipopolysaccharide, PBS phosphate buffered saline. T refers to time point. 6 mice of each genotype were given LPS.

Figure 4-31

Behavioural tests and weight in mice given multiple LPS injections over time

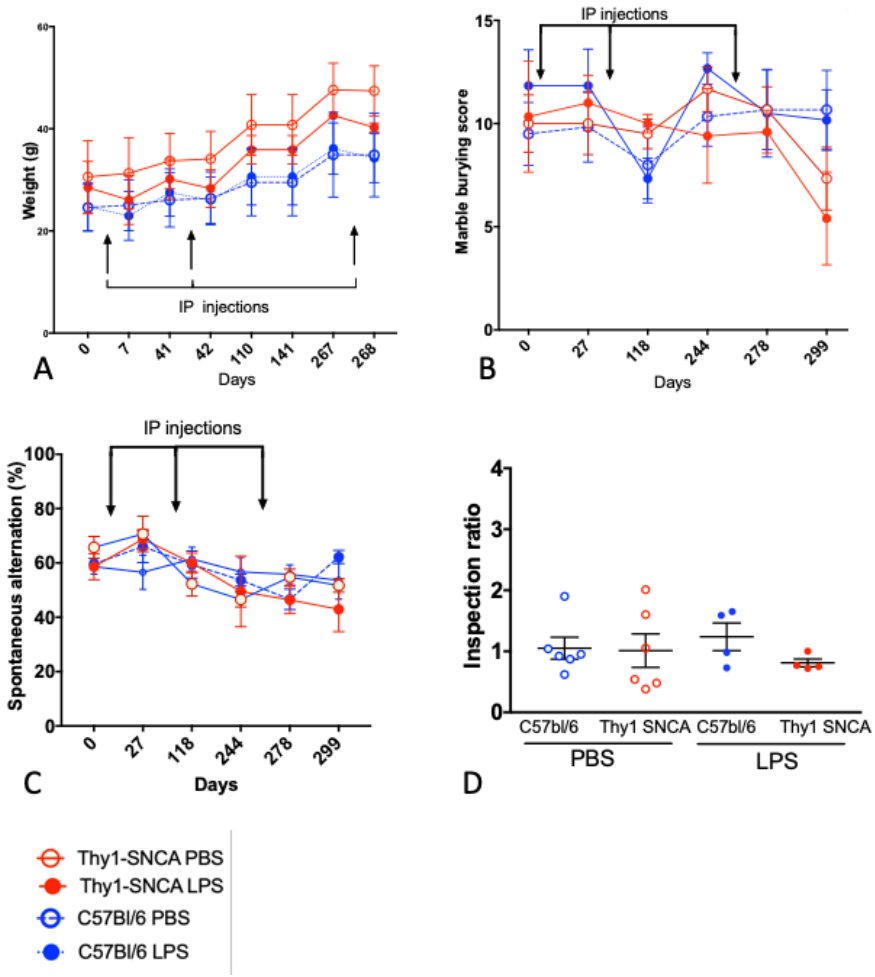

Figure 4-31 shows A) mouse weights over time following IP injections B) Marble burying C) spontaneous alternation and D) Novel objection recognition (at the end of the experiment). Results from 12 C57bl/6 mice (6 female, mean age at the start of the study was 13 weeks, SD 5.06), 12 thy1 SNCA mice (6 female, mean age at the start of the study was 13 weeks, SD 3.9). 6 mice from each group were given LPS injections as shown (with control mice receiving PBS). Females were counterbalanced across groups.

As I had not managed to clearly obtain a behavioural phenotype using additional "hits" with LPS, I then decided to add a further hit (B cell depletion) (see Figure 4-32). There was no significant difference between the B cell depleted group and the control group on the Y maze and rotarod (see Figure 4-33). I collected motor performance using digi-gait and performed olfactory testing (the analysis is ongoing).

Figure 4-32

Experimental design showing addition LPS and B cell depletion to the transgenic model

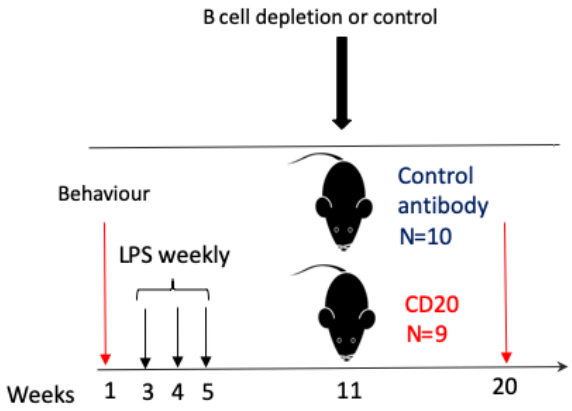

Figure 4-32 Mice had behavioural testing at baseline (week 1) and at the end of the experiment (week 20). All mice were female. Mean age in the depleted group was 30.4 weeks (SD 10.5), mean age in the control group was 29.1 (SD 10.74).

After the last time point for behavioural testing, the mice were culled. Flow cytometry was performed on homogenised single cell suspensions of brain and splenic tissue looking for evidence of microglial activation. Figure 4-34 shows representative gating from the brain cells. There were no differences in the

number or proportion of microglia between CD20 treated animals and controls or in the number or proportion of lymphocytes (CD3/CD4/CD8 or CD19) as shown in Figure 4-35. Histological examination of this experiment is ongoing.

Figure 4-33

Difference from baseline on the Y maze and rotarod

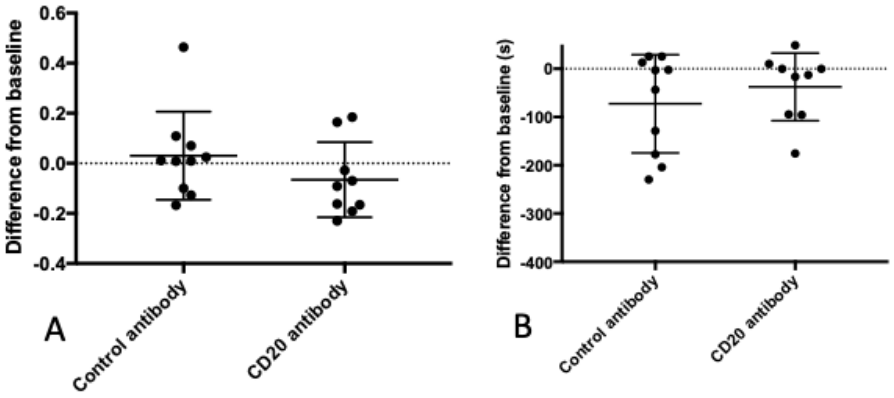

Figure 4-33 A) difference in spontaneous alternation (Y maze) from baseline and B) difference in rotarod performance from baseline on mice from the experiment described in Figure 4-32).

Figure 4-34

Gating of flow cytometry plots for brain tissue (on extravascular live cells)

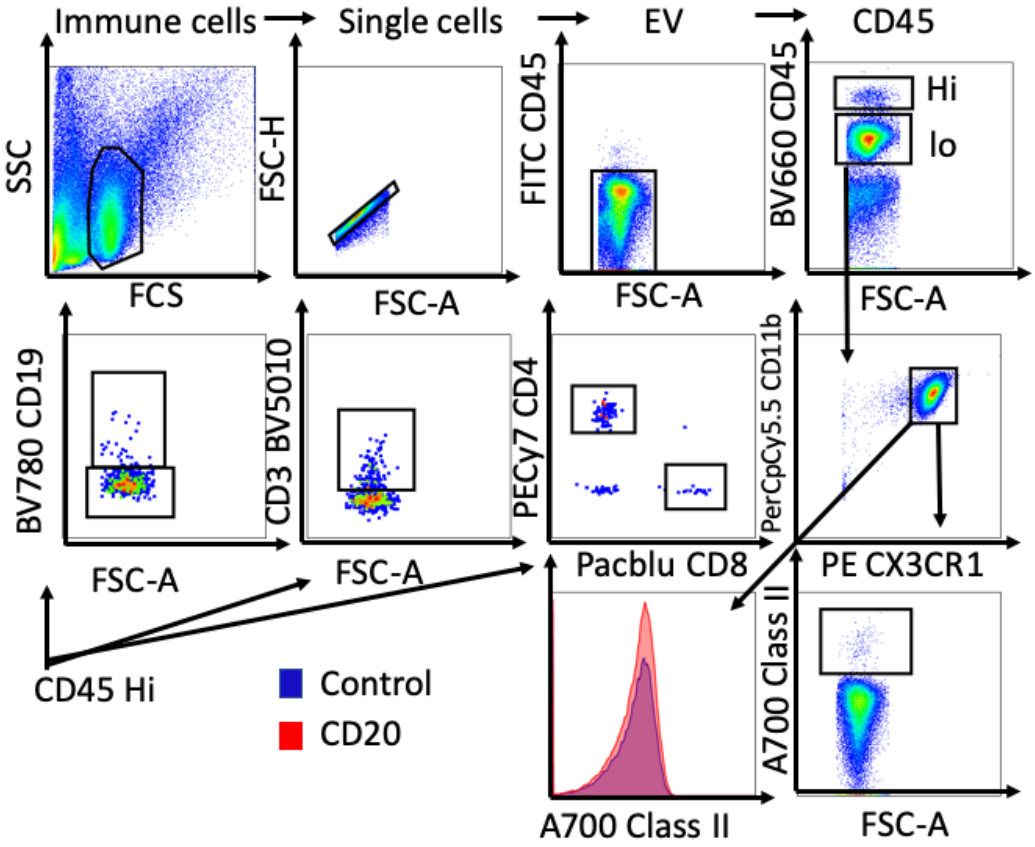

Figure 4-34 shows the gating on brain tissue with the initially gating of infiltrating cells on CD45hi (then on CD19, CD3, CD4 and CD8). The microglia were identified by being CD45lo and CD11b/CX3CR1hi. The histogram shows MHC Class II MFI on the microglia from a representative control sample and CD20 sample (no difference). Cells stained using staining panel 6 (see Appendix I)

Figure 4-35

Cell counts in homogenised brain tissue

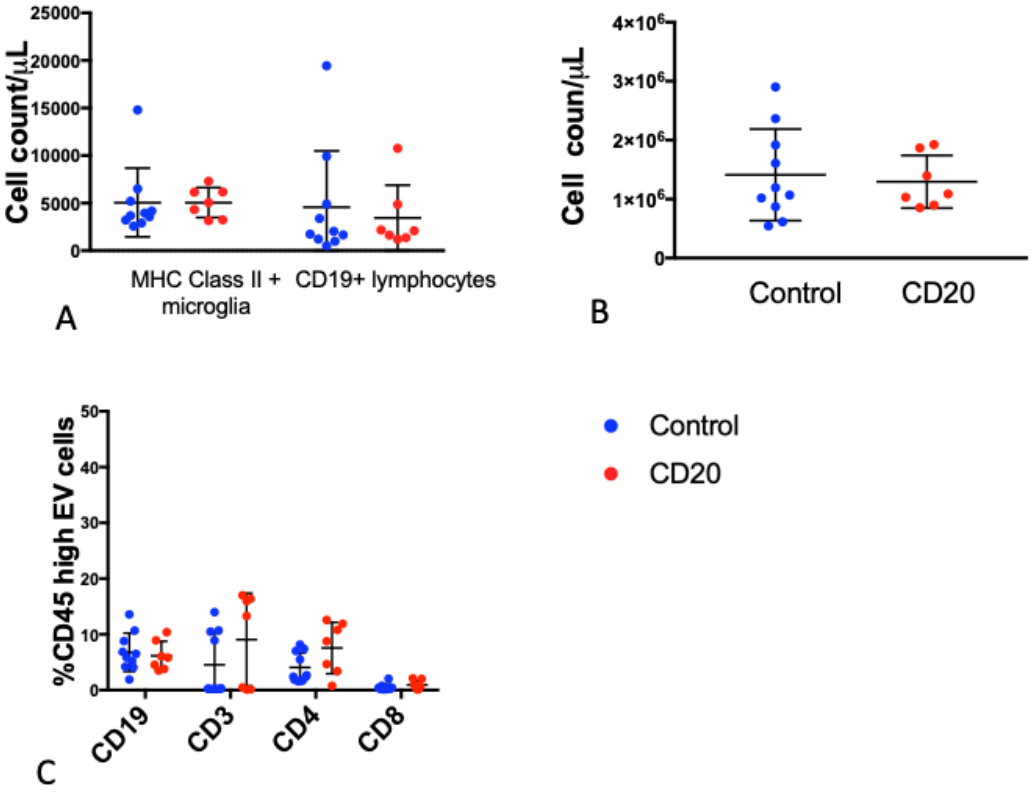

Figure 4-35 A shows cells counts of MHC Class II positive microglia and CD19 lymphocytes. B shows microglial cell counts C shows the proportions of lymphocytes. Data from two separate experiments (the mice were culled in two batches).

4.6.10 B lymphocytes in the meninges, other lymphoid tissue and the CNS

Once I had established that B cells were decreased in PD patients and associated animal models compared to controls and that this was relevant to disease outcomes (at least in a toxin based model of disease). I aimed to see whether there was a change in B lymphocyte proportions in other compartments.

I did some initial experiments attempting to optimise the identification of B lymphocytes in CNS tissue and the meninges by flow cytometry (data not shown). I realised while doing these experiments that it was almost impossible to prove that the cells I was seeing were genuinely in the tissue I had homogenised and stained. It was always possible to argue that the organs were poorly perfused with saline or that the cells were adherent to the vascular endothelium and therefore not truly 'resident' in the tissues. This was important particularly in the case of the meninges as I was surprised by the numbers of cells that I was finding as at that stage no one had described B lymphocytes in the meninges.

I therefore added an additional step for subsequent experiments. I injected an IV CD45 FITC antibody (1:200) into the tail vein 5-10 minutes prior to culling the animals in order to gate out the intravenous (IV) cells. Figure 4-36 shows an example of the initial gating for these experiments, with the extravascular CD45+ cells shown in blue boxes and the intravascular cells shown in red (the cells from blood are almost all in this box as one would expect). This also shows the population of meningeal B lymphocytes.

Given the observation that there were less circulating B lymphocytes in the transgenic models of Parkinson's disease, I looked in the other tissues, with the hypothesis that these B lymphocytes had moved into the CNS compartment in response to disease. Figure 4-39 shows that there was no increase in the number

or proportion of CD19+ lymphocytes in the brain or the meninges in transgenic versus wild type mice (by flow cytometry) with the spleen and cervical lymph nodes also showing no difference. The only statistically significant difference was an increase in CD8+ cells in the brains of transgenic mice compared to controls ($t[3] = 4.4$, $p = 0.02$) which does not remain significant after correcting for multiple testing. I also looked at the meningeal wholemounts using confocal microscopy to see whether there was an increase in the number of B lymphocytes using an alternative method (see Figure 4-40 and Figure 4-41). There was no difference in the number of B lymphocytes in the meningeal compartment between the thy1 SNCA mice and C57bl/6 littermates (aged 38-48 weeks).

Figure 4-36

Representative figures showing initial gating for B lymphocytes from multiple organs

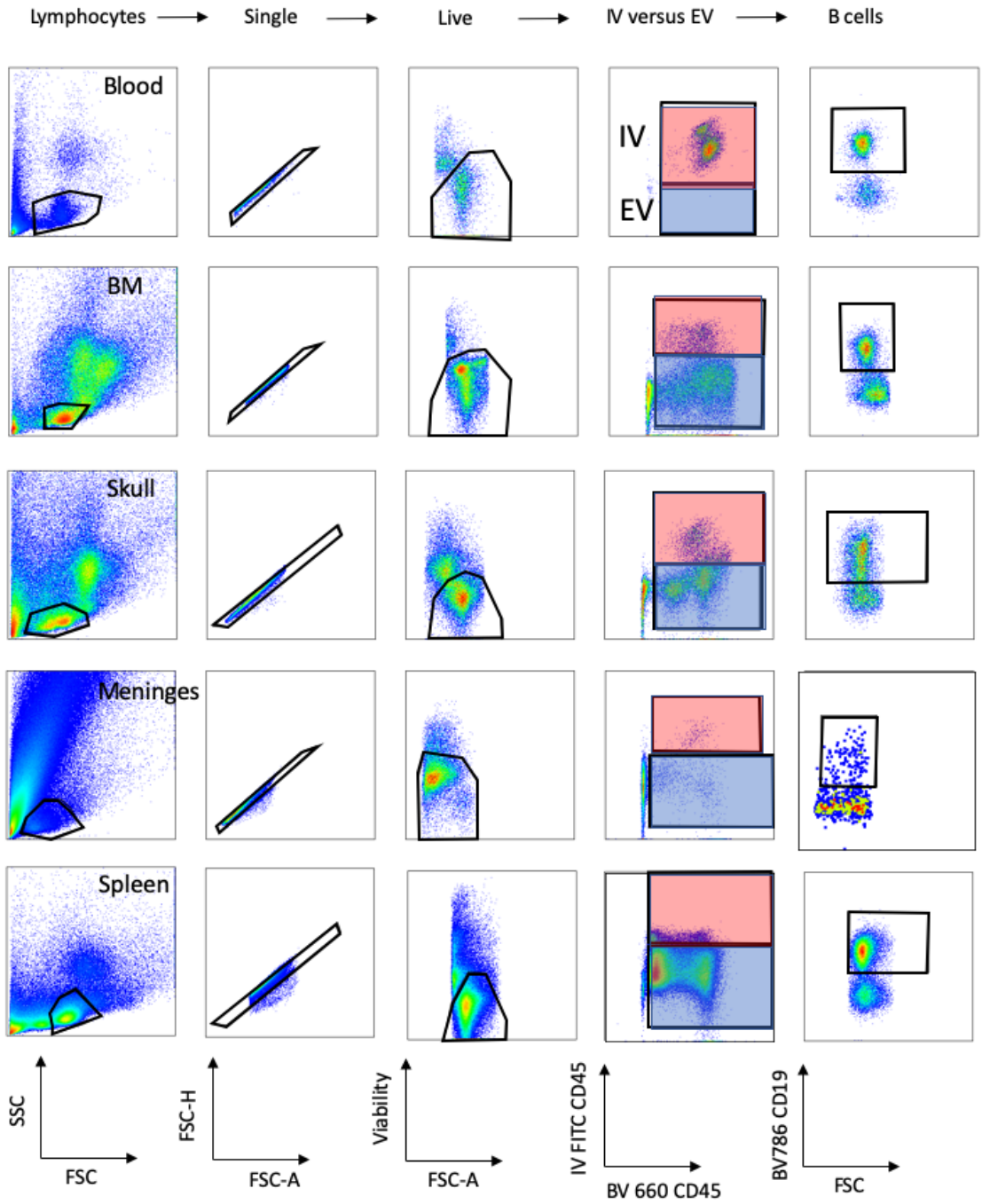

Figure 4-36 Axis labels shown at the bottom. EV extravascular, IV intravascular.

Figure 4-37

Representative gating (on splenocytes) for characterisation of peripheral lymphoid tissue and meninges

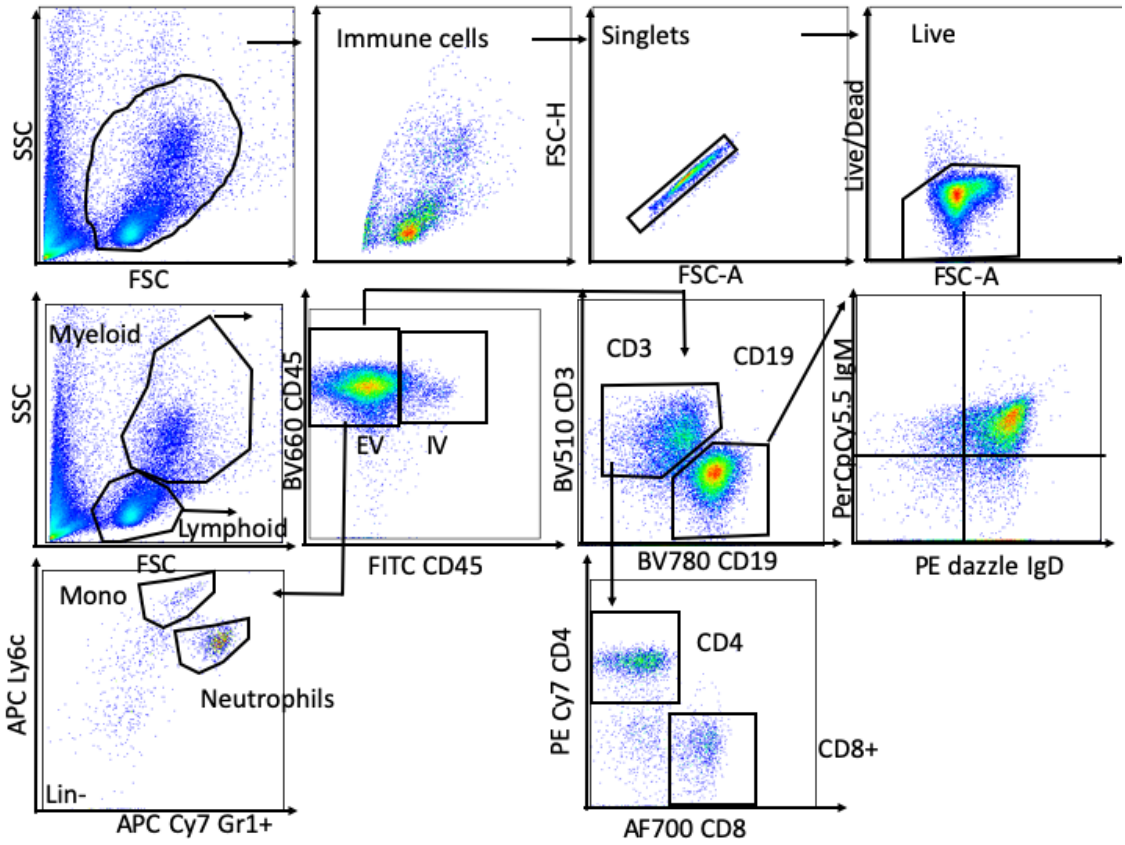

Figure 4-37 Representative FACS plots showing gating of lymphocytes and myeloid cells (example used is splenocytes). Cells stained using flow cytometry staining panel 7 (see Appendix 1)

Figure 4-38

Representative gating showing lymphocytes and myeloid cells in the brain

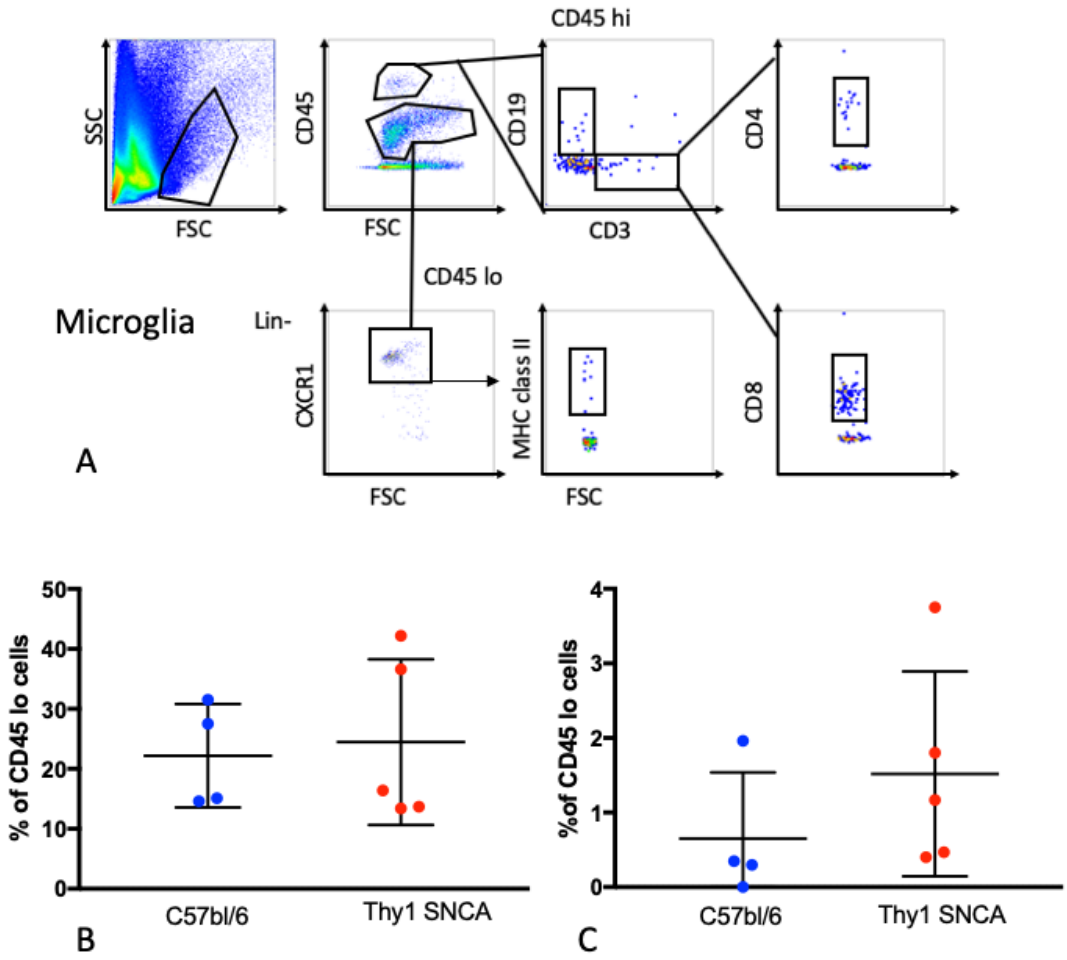

Figure 4-38 A shows initial gating separating the CD45hi (infiltrating cells) and CD45lo populations (microglia/macrophages) with subsequent gating for T cells (CD4, CD3, CD8), B cells (CD19) and CXCR1+ cells (and a subgroup that is CXCR1+ and MHC Class II positive. B) shows the proportion of microglia and C) proportion of MHC Class II microglia. Cells were stained using flow cytometry panel 9 (see Appendix 1).

Figure 4-39

Distribution of lymphocytes in CNS and lymphoid tissue in thy1 SNCA and C57bl/6 mice

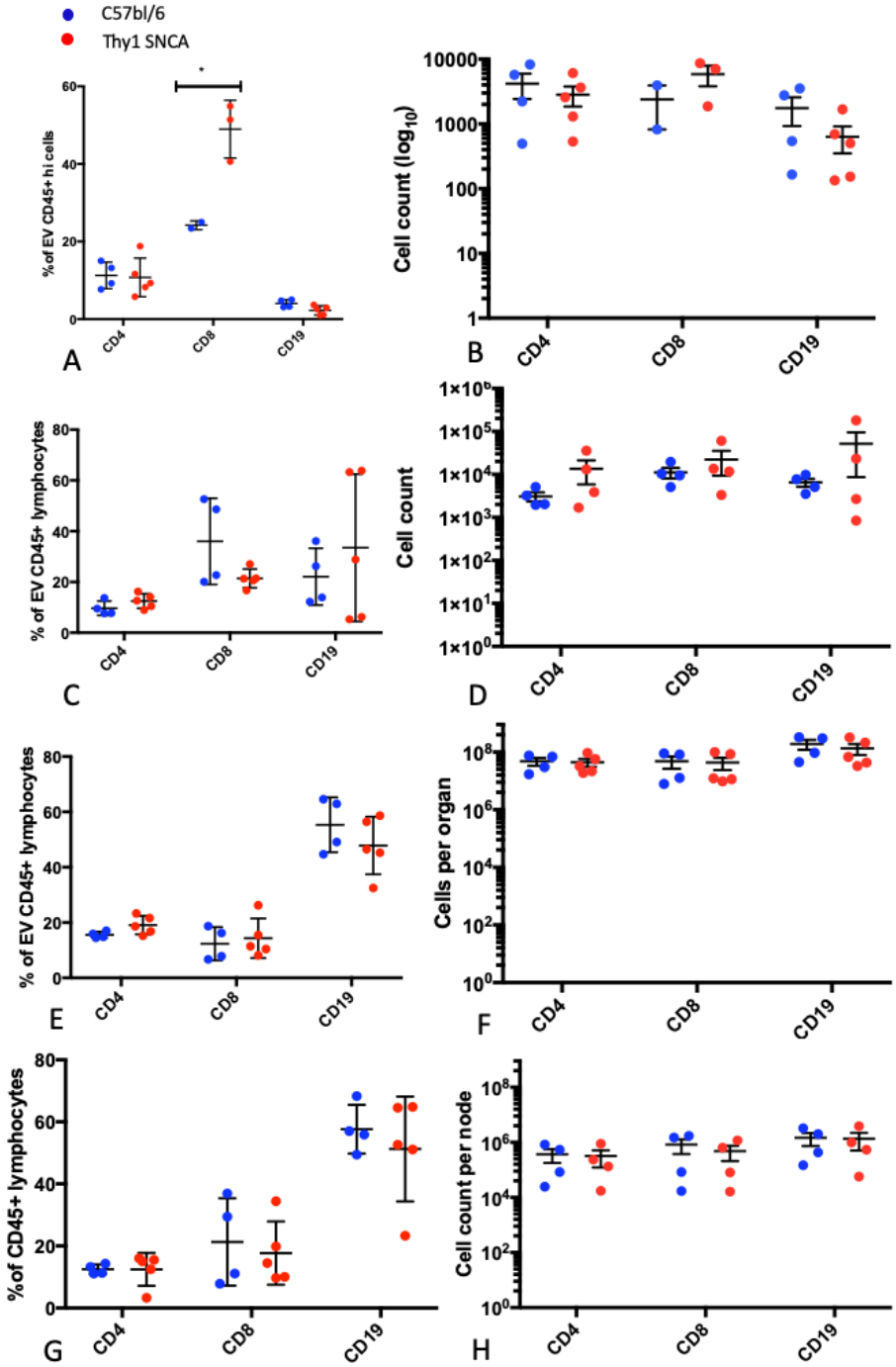

Figure 4-39 shows the distribution of lymphocytes across A + B) brain tissue C + D) meninges E + F) spleen and G + H) cervical lymph nodes. Graphs on the left show the proportions (%) of T cells and B cells (of CD45+ lymphocytes) and graphs on the right show the estimated absolute cell counts. Data from 2 separate experiments using 5 thy1 SNCA mice (mean age 75.6 weeks, SD 25; 3 female) and 4 C57bl/6 littermate controls (mean age 81.75, SD 17.9, 2 females). CD8+ staining on brain did not work for the second experiment and is therefore not shown.

Figure 4-40

B lymphocytes in meningeal lymphatics

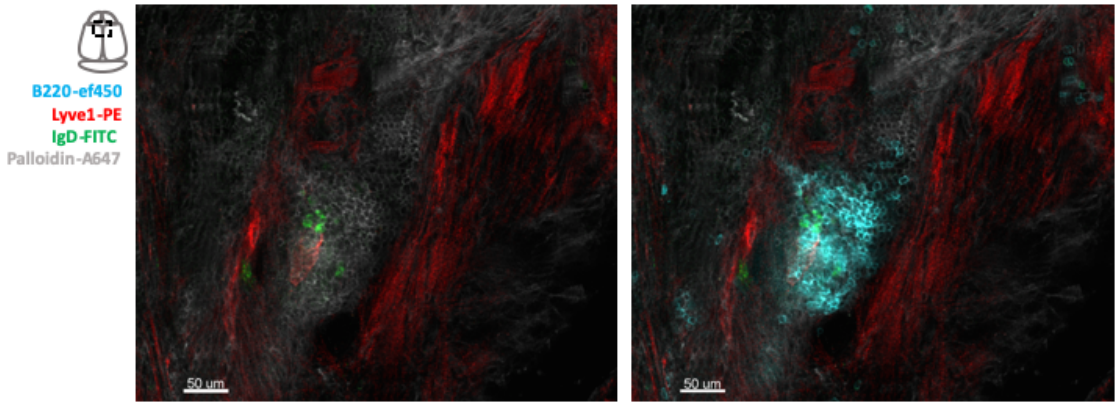

Figure 4-40 shows the dural lymphatics (schematic shows that this is adjacent to bregma) with a cluster of B lymphocytes shown in blue (B220) (B220-ef450 1:200, Lyve-1 PE 1:150, FITC IgD 1:200, Phalloidin-AF647 1:25).

Figure 4-41

Cell counts from meningeal whole mounts (confocal microscopy)

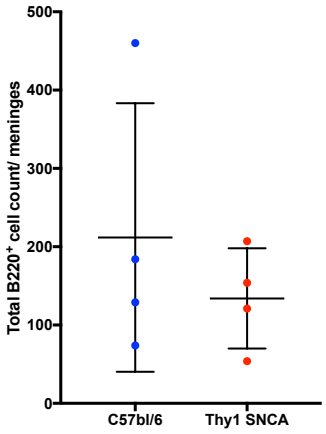

Figure 4-41 shows meningeal B lymphocyte counts from 4 thy1 SNCA mice (female, 38-48 weeks old) and 4 C57bl/6 littermates (female 37-48 weeks old)

It was also difficult to be sure that the meningeal cells that I was finding by flow cytometry were truly from the meninges. Dissecting the meninges off the skull is a delicate procedure and it is possible that these are contaminated by B lymphocytes from the skull bone marrow. Figure 4-42 shows that there are a significant number of cells from the skull (after removal of the dura), including a population of B lymphocytes making it difficult to be sure of the original of the cells in the meningeal homogenate. Figure 4-42 also shows that in a group of thy1 SNCA mice B lymphocytes make up the majority of the lymphoid population in the blood (mean 48%, SD 15.73), spleen (mean 61.85%, SD 16.21), bone marrow (52.29%, SD 11.29) and skull (mean 63.43%, SD 63.43). Cd19+ B lymphocytes make up 22.01% of the meningeal lymphoid population (SD 8.55). There were no differences in this distribution between "old" (11-19 month old mice) and "young" mice (3 months) (data not shown). The overall distribution

across tissues was similar when comparing the absolute cell counts (Figure 4-42 B).

Figure 4-42

B lymphocytes in haemopoietic tissue, secondary lymphoid tissue and meninges

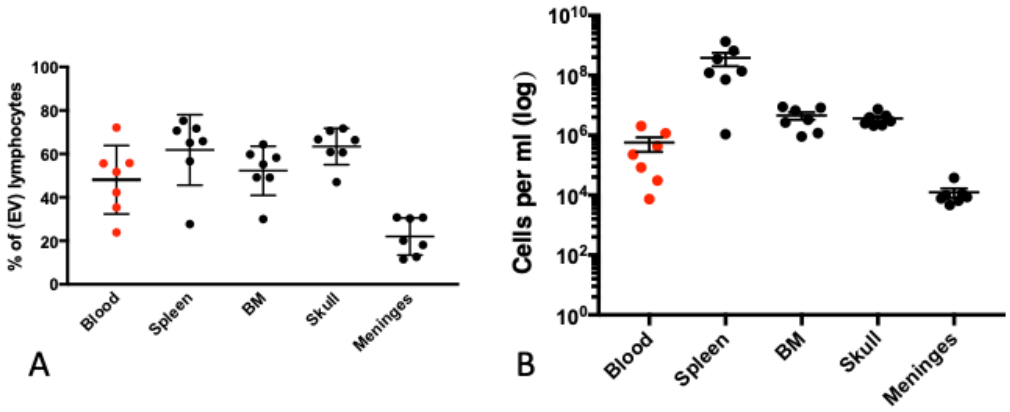

Figure 4-42 shows the proportion (A) and absolute number (B) (log concentration per ml) of B lymphocytes in each organ (that were extravascular) The red dots show blood (intravascular). Data from one experiment with 7 male thy1 SNCA mice (3 "old" mice 11-19 months old, 4 "young" mice 3 months old.

There were significant differences in the distribution of IgD+IgM+ (naïve) and IgD-IgM- (assumed to be antigen experienced) B lymphocytes between the different tissues (see Figure 4-43 and Figure 4-44). While blood, bone marrow and spleen were all dominated by naïve B lymphocytes, the meninges and skull were dominated by IgD-IgM- cells. There was no effect of age on this distribution (data not shown, Repeated measures ANOVA $F[1,29] = 0.94$, $p = 0.34$). There was a significant main effect of organ ($F[14,29] = 5.45$, $p = 0.002$) and a significant interaction between IgMIgD status (naïve versus IgM-IgD-) and

organ ($F[4,29]$)=57.132, $p = 2.4 \times 10^{-13}$). There were more CD5+ and CD23-CD5+ positive cells in older mice (in bone marrow) than in younger mice (see Figure 4-45) ($t[5] = 6.53$, $p=0.00013$ and $t[5] = 6.19$, $p = 0.0016$ respectively).

This distribution was similar in C57bl/6 and Thy1 SNCA mice (see Figure 4-46) (with the meninges having less naïve cells and relatively more IgM-IgD- than the spleen overall). There were no other differences in the distribution of inflammatory monocytes, neutrophils or T cells between C57bl/6 and Thy1 SNCA mice (statistics not shown).

Figure 4-43

Gating of B lymphocyte subsets in extravascular CD19+ B lymphocytes

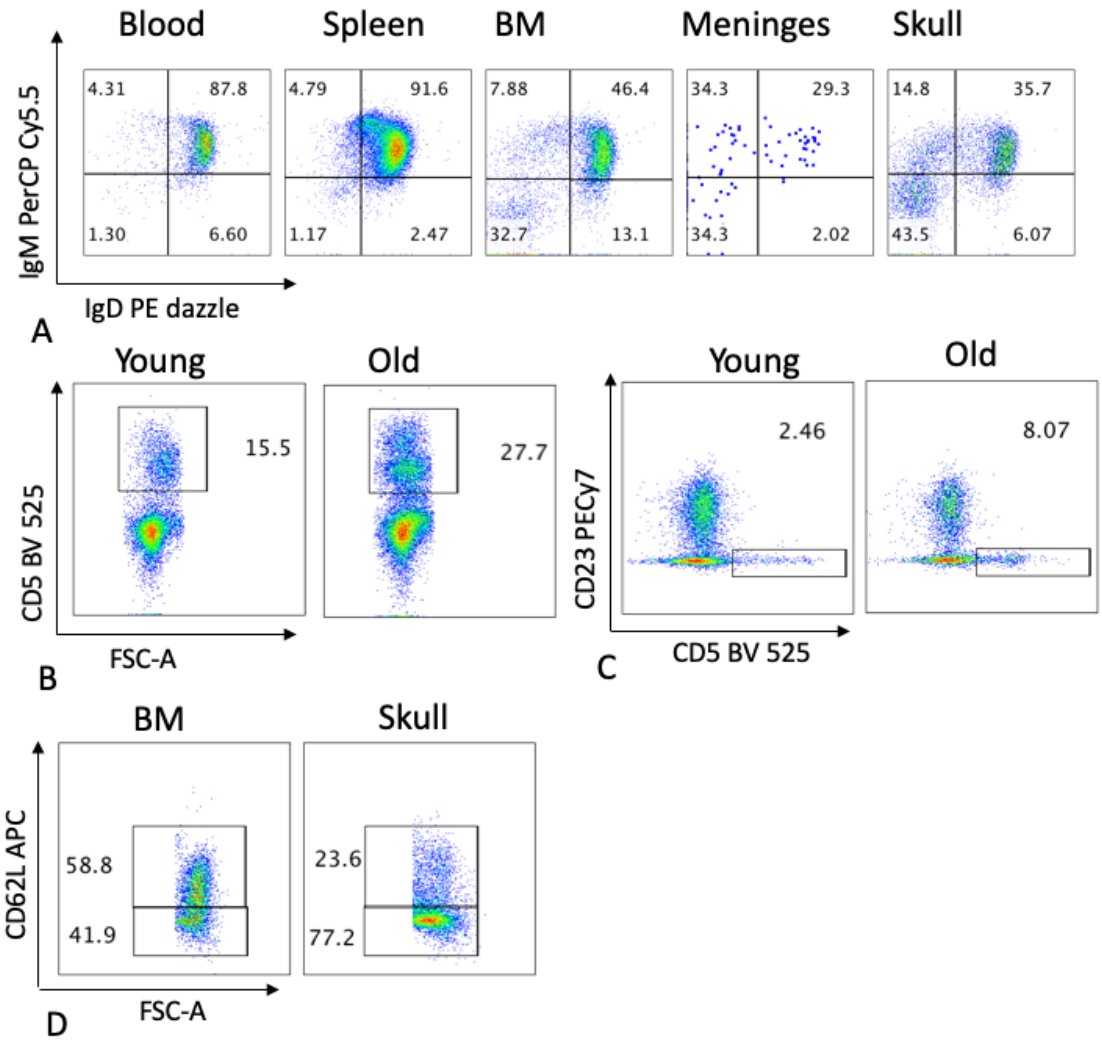

Figure 4-43 A shows representative gating plots illustrating the distribution of naïve B lymphocytes and IgM-IgD- cells across tissues. B shows CD5+ B lymphocytes. C B1b cells (CD23-CD5+) and D CD62 ligand (CD62L) positive and negative cells from bone marrow and skull. Cells stained using flow cytometry staining panel 8 (see Appendix I).

Figure 4-44

B lymphocyte subsets across organs

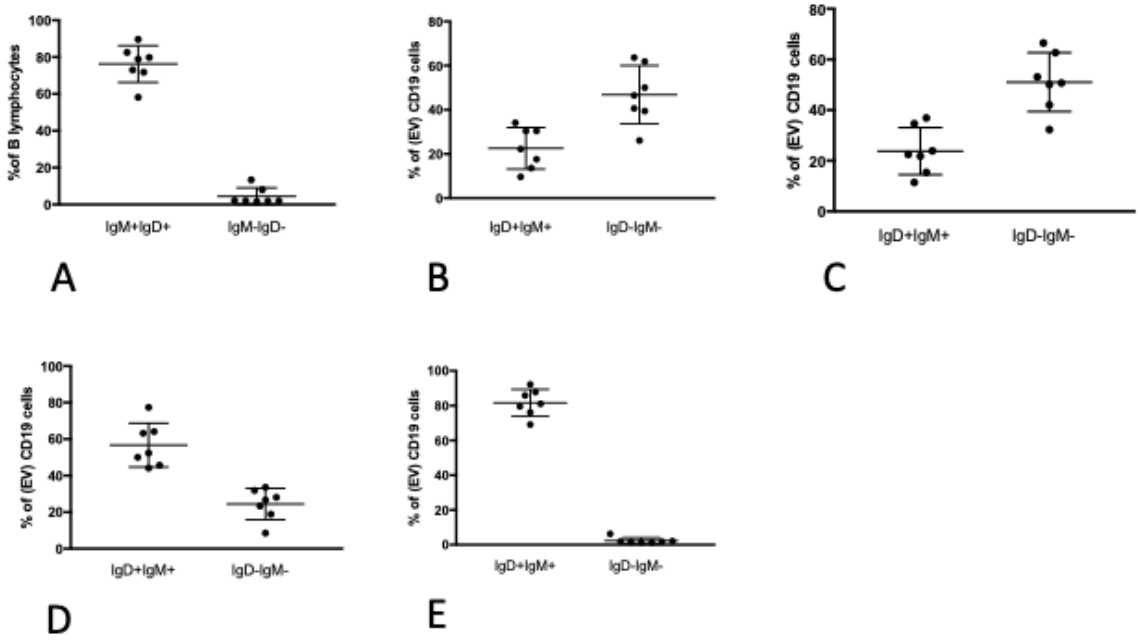

Figure 4-44 shows the distribution of IgM+IgD+ (naïve) B cells and IgM-IgD- cells across A) blood B) meninges C) skull D) bone marrow and E) spleen. Data from one experiment with 7 male thy1 SNCA mice (3 "old" mice 11-19 months old, 4 "young" mice 3 months old).

Figure 4-45

CD5+ lymphocytes and B1b lymphocytes (CD23-CD5+)

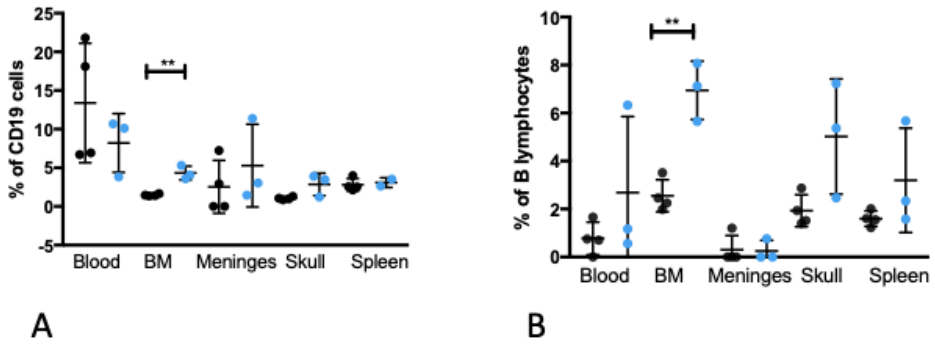

Figure 4-45 shows A CD5+ B lymphocytes and B B1b lymphocytes (Cd23-CD5+). Data from one experiment with 7 male thy1 SNCA mice (3 "old" mice 11-19 months old shown in blue, 4 "young" mice 3 months old shown in black).

Figure 4-46

B lymphocytes in Thy1 SNCA and C57bl/6 mice

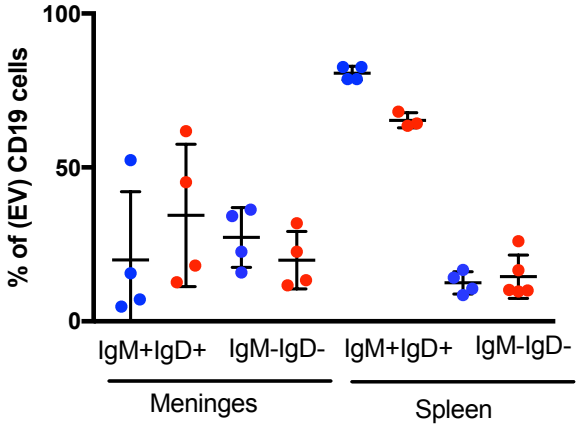

Figure 4-46 Naïve and IgD-IgM- B lymphocytes in 4 thy1 SNCA mice (mean age 75.6 weeks, SD 25; 2 female) and 4 C57bl/6 littermate controls (mean age 81.75, SD 17.9, 2 females). Cells stained using flow cytometry staining panel 7 (see Appendix 1)

4.6.11 Depletion of B lymphocytes from meningeal and lymphoid tissue

I looked at the blood, meninges, cervical lymph nodes and spleens of th1 SNCA and C57bl/6 mice who had been given a single dose of either an anti-CD20 antibody or control antibody (0.33mg/kg). The mice were culled 21 days after B cell depletion. Figure 4-47 shows representative flow cytometry plots confirming that B cells were reduced in all tissues. I noticed that in the meninges in particular, it was mainly a population of CD45 high CD19+ cells that were depleted. There still remained cells that were CD45 low CD19+. Figure 4-48 and Figure 4-48 show that B cells were depleted across tissues. Comparisons of B cell proportions and absolute counts were significant between animals given the control and CD20 antibody (see Figure 4-48). In the meninges in particular, naïve B cells were preferentially depleted over the IgM-IgD- population which was relatively preserved (see Figure 4-49 and Figure 4-50)

Figure 4-47

Representative flow cytometry plots following B cell depletion

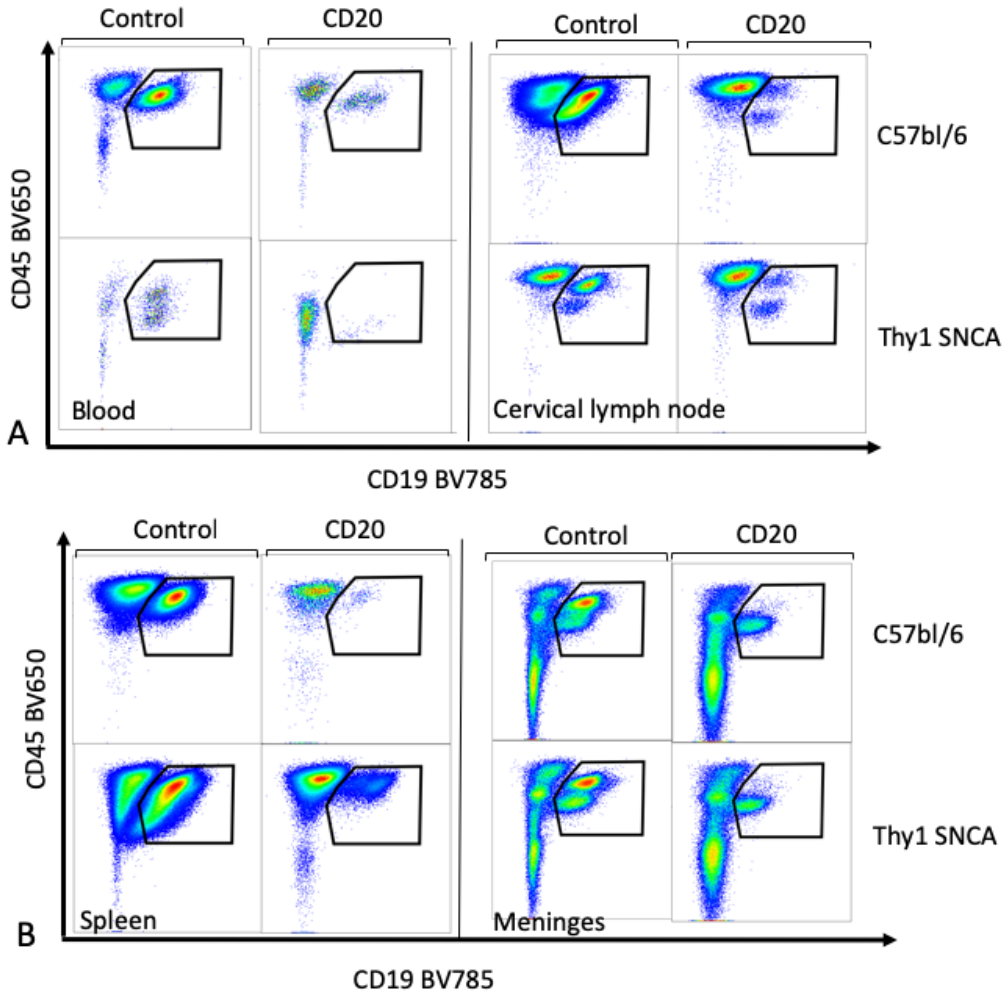

Figure 4-47 B cell depletion in the CD45hi CD19+ population in A) blood and cervical lymph node and B) spleen and meninges. In the meninges there is complete depletion of the CD45hi CD19+ B cell population but not the CD45 lo population in both the Thy1 SNCA mice and C57bl/6 mice. Cells stained using flow cytometry panel 8 (see Appendix 1)

Figure 4-48

B cell depletion across tissues in both thy1 SNCA and C57bl/6

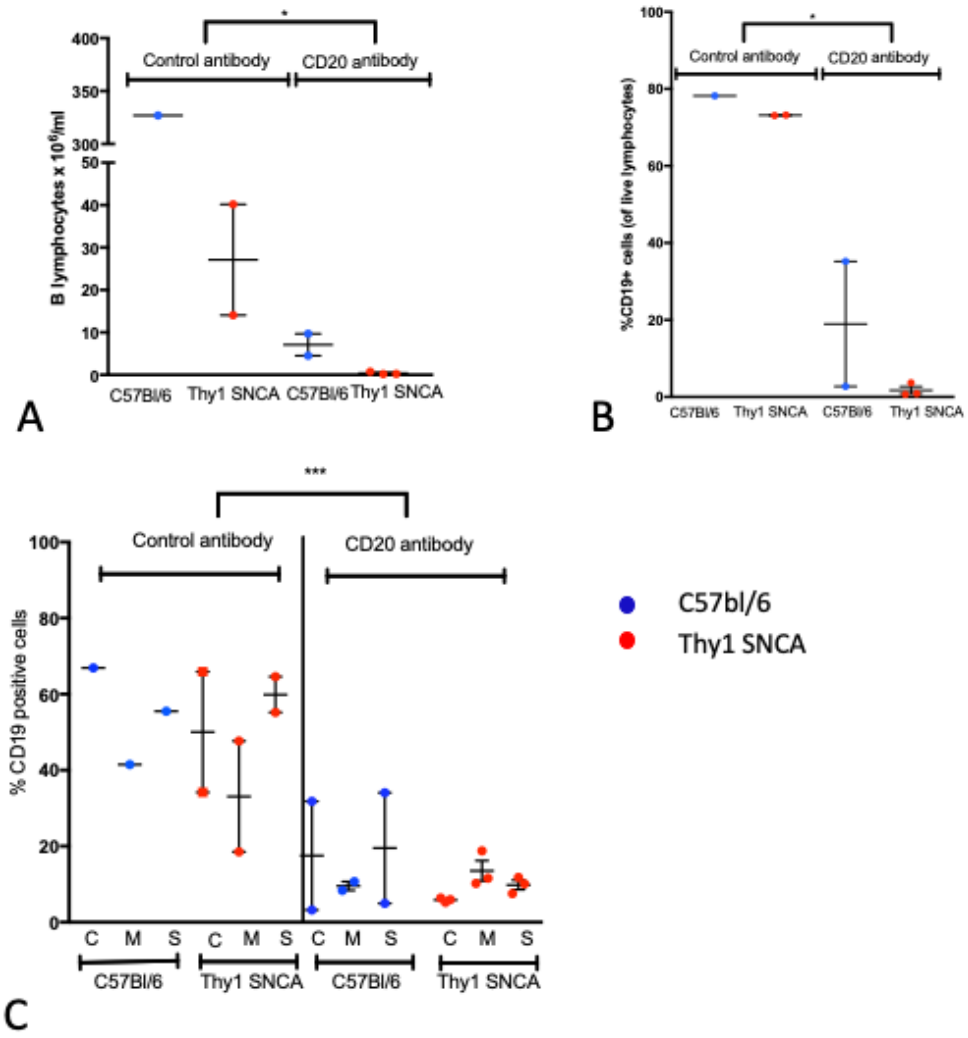

Figure 4-48 B cell depletion in A) blood showing absolute lymphocyte counts B) blood showing percentages and C) in tissues C = cervical lymph nodes M = meninges S = spleen. Mann Whitney U tests * p< 0.5, *** p<0.0001. Experiment performed in 3 C57bl/6 mice (age 16 months, 1 male and 2 female; 2 given CD20 antibody and 1 given control antibody) and 5 thy1 SNCA mice (age 16 months, 3 female, 2 male; 3 given CD20 antibody and 2 given control antibody).

Figure 4-49

Flow cytometry plots showing that naïve B cells are preferentially depleted from the meninges

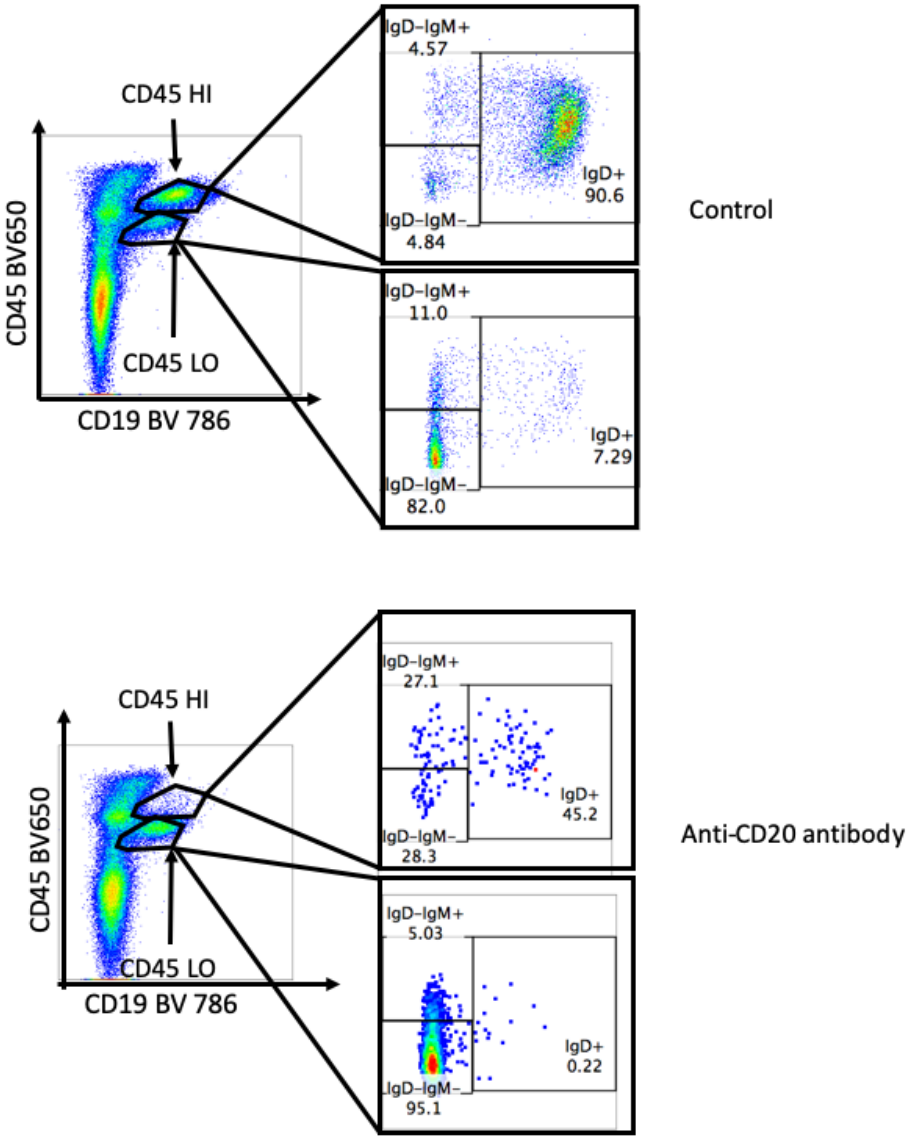

Figure 4-49 B lymphocytes that are left after depletion tend to be CD45 low and IgD-IgM-.

Figure 4-50

Depletion of naïve and IgM-IgD- B cells from organs

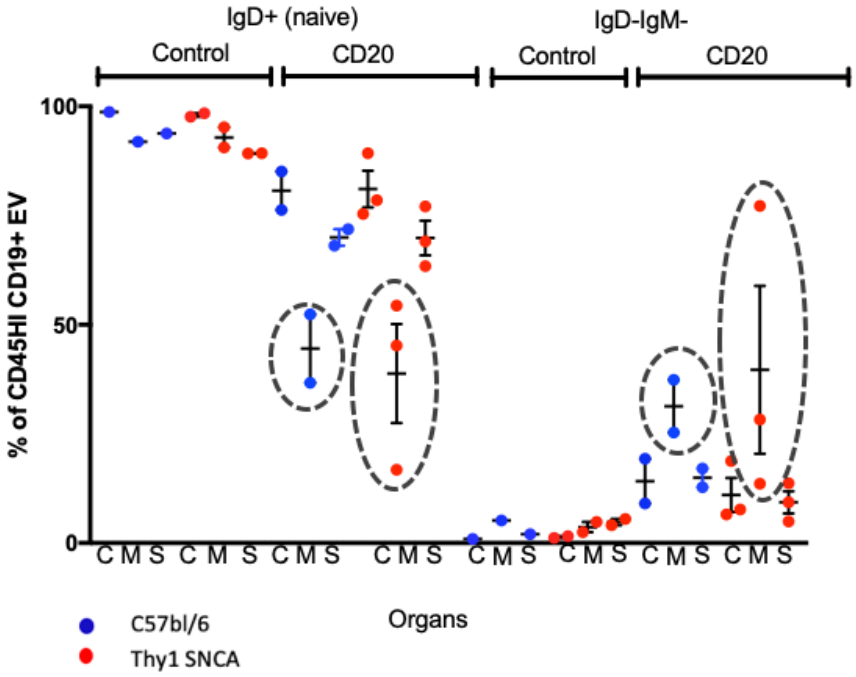

Figure 4-50 The grey circles highlight the meningeal B cells showing depletion of naïve cell with relative sparing of IgM-IgD- cells. C cervical lymph nodes M meninges S spleen. This is from the same experiment shown in Figure 4-48.

4.7 Summary of main findings

The main significant findings from my mouse work were that B cell deficiency results in worse outcomes on motor tests and in a larger neurotoxin (6OHDA) induced histological lesion affecting dopaminergic projections to the striatum in mice with a genetically driven B cell deficiency (μMT mice). A similar trend was observed in mice depleted of B cells using an anti-CD20 monoclonal antibody (but this requires a larger sample size to confirm). I attempted to rescue this phenotype using IL10 producing B lymphocytes, hypothesising that these would be protective in this model based on the clinical data from chapter 2. Although

these mice had better outcomes than mice given back normal B lymphocytes the effect was not statistically significant. I then looked to see whether I could find a mouse model with increased numbers of IL10 producing B cells in the meninges. I explored using the PI3Kδ conditional knock in mouse ($P110\delta^{E1020K\text{-}GL}$, with the E1020K mutation in the Pik3cd gene in all cells). In initial experiments phenotyping this mouse, I did confirm that there are increased numbers of B1 cells in the meninges (of the global knock in mouse) and it would therefore be useful exploring the B cell specific knock in ($P110\delta^{E1020K\text{-}B}$) to use in 6OHDA experiments. If it is the IL10 produced by B cells in the meninges that drives the phenotype then these mice would be expected to have much better outcomes.

My experiments using two different alpha synuclein transgenic mice showed that there was a decrease in circulating B lymphocytes that paralleled the observation in PD patients discussed in Chapter 2, suggesting that this is directly related to alpha synuclein pathology. The exact mechanism behind this remains unclear. I had hypothesised that this decrease in circulating B lymphocytes was due to a shift in B lymphocytes from the periphery to the central nervous system (either directly into the brain to into the meninges). I quantified B lymphocytes in the meninges and the brain using flow cytometry and confocal microscopy (in the meninges) but did not detect the expected difference. I did observe for the first that the phenotype of the B lymphocytes in the meninges and in the skull was different to that of circulating B lymphocytes or those found in secondary lymphoid tissue. These B cells tended to be IgM-IgD- suggesting a shift to a more antigen experienced phenotype which mirrors the shift in human CSF towards CD27+IgD- and away from the predominantly naïve (CD27-IgD+) phenotype in circulating B lymphocytes.

I did several experiments attempting to worsen the phenotype in transgenic models of PD with repeated a repeated inflammatory insult (exposure to LPS)

but these were ultimately unsuccessful (at least in producing a reliable behavioural readout).

4.8 Chapter discussion

Previous studies have looked at the effect of lymphocyte deficiency on motor and histological phenotypes in toxin based models of PD, one using athymic rats (J Wheeler et al., 2014) and another using $RAG^{-/-}$ mice which lack mature T and B lymphocytes (Ip, Beck, & Volkmann, 2015). Both of these studies noted worse outcomes in lymphocyte deficient mice but did not identify the mechanism behind this observation, noting only that the effect was rescued by bone marrow transplantation (Ip et al., 2015). Given my results it is possible that this effect is at least in part mediated by B lymphocytes (particularly in the $RAG^{-/-}$ mice that lack B lymphocytes as well as T lymphocytes). When I attempted to rescue the effect in μMT mice (in order to demonstrate mechanism), the transferred cells did not remain in circulation or in the lymphoid organs. Subsequent more detailed review of the literature in these mice suggested that this had been noted before. Nicole Baumgarth et al. showed two decades ago that reconstitution of μMT mice was blocked by strongly inhibitory CD4+ T cells (Baumgarth et al., 2000). The transferred cells only fully reconstituted when the mice were irradiated. They were able to reconstitute neonatal mice successfully suggesting that tolerance is broken in an early developmental window due to a lack of exposure to B cell antigens in these mice. As a result, I switched to using an anti-CD20 antibody to deplete the mice of B cells. The resulting difference in behavioural testing was not statistically significant although the numbers of animals included in this study was relatively small (N=4 and N=6 in the depleted and non-depleted groups respectively).

Another limitation of this approach is that although the anti-CD20 antibody is able to reliably deplete circulating B lymphocytes but depletion of tissue resident

B cells is less effective, particularly after only one dose. As my hypothesis was that it was likely to be meningeal B lymphocytes that were responsible for the effect observed one would need to ensure complete depletion of 'tissue resident' subpopulations as well as circulating B lymphocytes and those in secondary lymphoid tissue. This requires additional experiments to establish a more effect dosing schedule. The dose that I used (0.33mg/kg) was based on a study in a murine model of systemic lupus erythematosus (Bekar et al., 2010b). In this study they found that one dose was effective at depleting circulating B lymphocytes and those in the lymph nodes and spleen with the peak effect occurring 1-3 weeks after drug treatment. B lymphocytes in the peritoneum (mainly B1 lymphocytes) and the bone marrow were less effectively depleted and it is possible that meningeal B lymphocytes are similarly resistant to depletion as suggested by the flow cytometry plots shown in my experiments where there remains a population of CD19 CD45lo B lymphocytes after anti-CD20 treatment.

It may be that with more robust depletion, for example with repeated or high dosing there would be a larger different between the depleted and non-depleted groups.. It would then be possible to see more clearly the effect of cell transfers on the phenotype. I enriched IL10 producing B lymphocytes after incubation with IL2 overnight (as this had been shown to be an effective method of skewing the phenotype of these cells by another student in the lab, Akimichi Inaba). Other studies have used CD5+CD1d+ cells obtained by FACS sorting. I did initially try this strategy but found that the time and manpower required to sort sufficient numbers of cells to allow the transfer of 1×10^7 cell per mouse was too great.

The concept for these transfer experiments in the CD20 depleted mice was based on a study by Thomas Tedder (Matsushita et al, 2008). In this study in EAE, they showed that B cell depletion resulted in different outcomes depending on the

timing of depletion: depletion prior to the induction of disease resulted in worse EAE scores. They rescued this phenotype by transferring CD20- CD5+ CD1d+ 'regulatory' B lymphocytes. My experiments transferring IL10 producing B cells and IL10-/- B cells did not result in a convincing improvement (or worsening) respectively. One explanation is that the CD20 depletion was insufficient as discussed above. Another explanation is that I did not use CD20 negative B cells (as we did not have these available to use at the time of the experiments). Using CD20- b cells would mean that any residual antibody would not deplete the newly transferred cells. It was also not possible to assess the survival of transferred cells as it was impossible to distinguish them from the host cells. A further modification in addition to using CD20- cells would be to use eGFP+ cells so that host cells could be identified (including trafficking within the tissues such as the meninges).

Given my hypothesis that the protective effect of B lymphocytes was mediated by IL10 producing B cells in the meninges, I also looked for IL10 RNA by RTPCR of meningeal tissue, expecting to find a decrease in μMT mice. I did not find any differences between μMT mice and controls at baseline, in a UTI model or after 6OHDA surgery. The experiment was challenging because of the relatively small concentrations of RNA obtained from the meninges and would benefit from further optimisation before rejecting the hypothesis.

I had hoped to find a simple behavioural readout in the alpha synuclein transgenic mice so that I had an additional (and more chronic) model to use to modulate the B lymphocyte compartment. The published literature suggests that alpha synuclein overexpressing transgenic mice have a stronger behavioural phenotype (Marie-Francoise Chesselet et al., 2012) but the evidence is not consistent. One possible explanation is the additional unmeasured effect of the local microbiome on alpha synuclein pathology. The only clear phenotype that I

did find was a weight difference. When our animal house was shut down and we were required to move our mice, subsequent cohorts did not replicate this pattern. Assuming the effect was true in the initial cohort, there must be an environmental explanation. There is now increasing evidence for the role of the microbiome in PD in both humans and mouse models. Several studies have now shown that the microbiome is altered in PD patients versus controls (Heintz-Buschart et al., 2018; Hill-Burns, Factor, Zabetian, Thomson, & Payami, 2011)(Petrov et al., 2017). It is also possible to induce PD pathology in rodents by transplanting faecal material from PD patients(Sampson et al., 2016). It is possible to speculate that some of the variation in phenotypes across studies may be due to the unmeasured effect of the local microbiome on disease pathology. The further additional of other 'hits' to the transgenic models (including LPS and b cell depletion) was also unsuccessful in providing a behavioural readout. It is possible that there was an effect on microglial activation or alpha synuclein pathology (this histology is ongoing) but this is often harder to quantify and does not lend itself to multiple repeated experiments over time.

I have described a shift in phenotype of the B lymphocytes in the meningeal and skull compartments. I had expected the phenotype of the immune cells in the skull to mirror that in the bone marrow. This was not the case, with the meningeal and skull having a majority of IgM-IgD- B lymphocytes and the blood, spleen and secondary lymphoid organs having a greater proportion of naïve (IgM+IgD+) B lymphocytes. Vascular channels connecting the skull to the brain via the dura have been described in both mice and humans (Herisson et al., 2018). After CNS injury (in this case a murine model of stroke), neutrophils and monocytes are preferentially recruited from the skull niche to the brain through these channels, flowing against the direction of blood flow which was from the brain to the skull (Herisson et al., 2018). Differences in cell populations in the skull bone marrow compared to tibial bone marrow could be due to different

signals from the brain (including inflammatory signals from microglia such as IL1B or damage associated molecular motifs).

4.9 Future directions

(i)Optimise CD20 antibody depletion model. Given that the 6OHDA model gives a clear behavioural and histological phenotype, it makes sense to look at the effects of modulating B lymphocytes in this model going forward, initially beginning by optimising the dose of B cell depletion required and establishing the dose required to completely deplete the meningeal and skull compartments. In addition, using the 6OHDA model in combination with other B lymphocyte transgenics such as the CD19 deficient mouse (that is lacking in CD19 B cells with fewer B1 B cells and CD5+ CD1d+ regulatory B cells in particular) and comparing this to CD19 overexpressing mice which have corresponding decreased proportions of these subsets) could be used to interrogate the mechanism behind the observations made in my PhD (using a similar approach to that described in (K. M. Haas et al. 2005).

(ii)Describe the meningeal B lymphocyte response to injury
Initial subsequent experiments would include characterising B cells in the meninges at an early time point (e.g. 6 hours after surgery) and at later time points. I would also aim to use a data driven approach to look at transcriptome of these cells using single cell RNA sequencing at baseline and in response to injury (using the 6OHDA model and additional models of sterile injury such as murine stroke and sterile meningitis to see whether the response is specific to damage of dopaminergic cells). I would then repeat the experiments attempting to rescue the phenotype in the depleted mice by using $CD20^{-/-}$ eGFP+ cells so

that I could look at trafficking of cells from the circulation to the meninges and the CNS.

(ii)Describe the response of skull B lymphocytes to injury. Given the more recent finding of the relevance of the niche in the skull bone marrow, I would additionally look in more detail at the phenotype of B cells in the skull at baseline and in response to injury, attempting to identify the relevant signals from the brain that result in mobilisation or activation of B lymphocytes in bone marrow and how this relates to trafficking within the meninges. I would also be able to use additional tools such as mouse models with increased numbers tissue resident IL10 producing B lymphocytes. (such as the P110$\delta^{E1020K\text{-}B}$ conditional knock in mouse which has a population of resident IL10 producing B cells that increase susceptibility to streptococcal infection (Stark et al., 2018)). These mice would require further characterisation initially to confirm that the meningeal (and skull) B lymphocytes have a similar phenotype to the cells in the lung.

(iv)Use an additional mouse model (MI2) to confirm the effect. If experiments using 6OHDA confirm that B cells in the meninges producing IL10 are able to rescue the phenotype, I would then aim to test whether this reversed the behavioural and histological phenotype observed in the MI-2 mice (which have only recently become available and do show a clear behavioural phenotype with decreased dopamine production in the substantia nigra).

4.10 Conclusions

The results from the animal studies are consistent with the hypothesis that B lymphocytes play a protective role. I have described the phenotype of meningeal B lymphocytes and observed that they are similar to skull B lymphocytes (but not tibial bone marrow lymphocytes) Further studies are required to clarify the role of meningeal and skull based B lymphocytes in disease.

5 DISCUSSION

5.1 Summary of main findings

Overall, my results show convincingly that changes in B lymphocytes are associated with Parkinson's disease, although exactly how much this contributes to the pathogenesis of this condition in humans remains unresolved.

In clinical cohorts, I have shown for the first time that the decrease in B lymphocytes is particularly driven by a group at high risk of dementia and that cells from these patients produce more cytokine (both IL10 and IL6) after in vitro stimulation than controls. I have also shown that having a greater proportion of 'regulatory' B lymphocytes is associated with better UPDRS scores. This association is also true of the expression of CD1d+ B lymphocytes which are known to present lipid or glycolipid antigens to NK cells and may be involved either in clearance or in the attenuation of Th1 T cell responses. I have shown that there is a trend towards an increase in B lymphocytes in the cerebrospinal fluid (CSF) and described for the first time a shift in phenotype of CSF B lymphocytes from naïve (in the circulation) to memory B cells (antigen experienced). This may be relevant in PD where there are CNS and peripheral antigens associated with pathology (mainly alpha synuclein aggregates). There were no differences between patients and controls (or within groups at low or high risk of dementia) in the numbers or proportions of different B cell subsets in blood or CSF including age associated B cells in the circulation.

I performed a systematic review and meta-analysis of previous studies looking at alpha synuclein antibodies in PD and found that there is evidence that there are increased alpha synuclein antibodies in early disease suggesting that this is part of an early immune response to alpha synuclein pathology that then wanes as the disease progresses. I developed Mesoscale Discovery (MSD) based assays to measure antibodies to alpha synuclein species and epitopes and showed in a small pilot study that there were no differences between patients and controls.

In animal studies, I have shown that there is also a decrease in circulating B lymphocytes in two different alpha synuclein transgenic models (thy1 SNCA that over expresses human alpha synuclein on the thy1 promotor and MI-2 mice that express a truncated version of alpha synuclein prone to aggregation). I did not find any differences in the number of meningeal B lymphocytes between transgenic and control mice. I did show that the phenotype of the meningeal and skull lymphocytes was different to circulating B lymphocytes (and bone marrow B cells from the tibia) which is likely to be relevant to disease. These cells are skewed away from a naïve phenotype towards a more antigen experienced, tissue resident phenotype.

When I looked at the effect of B cell deficiency in a toxin based model of Parkinson's disease (6OHDA) I found that a genetic deficiency of B cells (in μMT mice that lack mature B lymphocytes) was associated with worse behavioural outcomes and a more extensive histological lesion. I replicated the trend in the motor phenotype using an anti-CD20 monoclonal antibody to deplete B cells. The histological analysis of this experiment is pending. Based on experiments done several years ago in experimental autoimmune encephalitis (EAE), I hypothesised that this difference in outcome in depleted mice was due to a loss of the protective effect of regulatory B lymphocytes. I therefore tried to rescue the phenotype by transferring IL10 producing B lymphocytes. The behavioural results suggested a trend towards improved outcomes in the group given IL10+ B lymphocytes but this was not statistically significant and the histological analysis is ongoing.

5.2 Clinical implications

The main implication of this work is that B cell depletion is unlikely to be therapeutically effective in PD as having fewer B lymphocytes appears to be associated with disease and with worse outcomes. On the other hand, the evidence presented in my thesis suggests that increasing the proportion of regulatory B lymphocytes may be a therapeutic strategy. There are a number of existing therapies that increase regulatory B lymphocytes (as well as having effects on regulatory T cells) including low dose IL2 (currently in trials as a disease modifying agent in amyotrophic lateral sclerosis, https://clinicaltrials.gov/ct2/show/NCT03039673) and oral agents used in multiple sclerosis such as fingolimod and glatiramer acetate.

5.3 Discussion of results and future work

The main limitation of my PhD as a whole is that although I have demonstrated several changes in the B lymphocyte compartment in both mice and humans associated with disease and have addressed the original aims of my PhD. This has left many unanswered questions about the mechanistic relevance of my results which will be discussed below.

My clinical studies were limited in that they were cross sectional in design. Longitudinal studies would have been informative to investigate changes in the B lymphocyte populations over time that were associated with disease progression but this was not practical in the time frame of a PhD. I had also considered using a sub-population of patients enriched for B lymphocyte abnormalities: as mentioned in chapter 2, patients who are carriers of a mutation in the glucocerebrocidase (GBA) gene are more likely to get PD and to progress to dementia. These patients are also known to have a number of abnormalities affecting B lymphocytes (including an increased risk of myeloma and B cell

lymphoma)(Mistry et al., 2013). Although their predisposition to PD and to B lymphocyte abnormalities may be coincidence, this would be an interesting group to investigate further. The reason that I did not do this was that we had relatively few patients with the mutation in our research clinic (approximately 5-8 at the time I started my PhD) and it would have meant expanding the project to involve multiple centres which we did not have the resources to do. Looking at how B lymphocytes are involved in clearance, antigen presentation to T cells and antibody production in this group would be interesting.

Another potentially interesting group of patients are those with a leucine-rich repeat kinase 2 (LRRK2) mutation which is the commonest genetic cause of late onset autosomal dominant and sporadic PD (indistinguishable clinically from idiopathic PD)(Klein & Westenberger, 2012). LRRK2 is expressed in immune cells and is a negative regulator of nuclear factor of activated T cells (NFAT) which is involved in regulating the immune response in innate immune cells and T lymphocytes (Liu et al., 2011). Changes in LRRK2 expression have been described across immune cell subsets including B lymphocytes (in PD unselected PD patients versus controls)(Cook et al., 2017) and it carries shared genetic risk with Crohn's disease, an inflammatory disease affecting the bowel (Hui et al., 2018). Disruptions in this gene are linked to a number of possible mechanisms in PD including perturbations of vesicular trafficking, protein synthesis, immune response regulation, inflammation and cytoskeleton homeostasis (Wallings et al., 2015). Further interrogating the role of B lymphocytes in the gut and in the circulation in patient and animal models may also add further insights into relevant pathways involved in driving a peripheral inflammatory response in the gut that is associated with alpha synuclein pathology.

Several epidemiological studies have shown an association between inflammatory bowel disease and Parkinson's disease (Lin et al, 2016; Villumsen et

al, 2019) but this has not been replicated in all studies, including (Camacho-Soto et al, 2018) who found an association in the opposite direction. This may be explained by the confounding effects of immunosuppressive therapies which were different across studies. GI dysfunction is associated with PD and constipation is known to be a prodromal feature(Fasano et al, 2015). There is also data showing a change in the microbiome of PD patients (Heintz-Buschart et al, 2017; Hill-Burns et al., 2017; Sampson et al., 2016; Scheperjans et al., 2014) as well as evidence of increased gut leakiness in PD: there is raised LPS binding protein in the serum of PD patients versus controls as well as increased intestinal mucosa staining for E.coli, nitrotyrosine and alpha synuclein (Forsyth et al., 2011). Given this evidence, factors affecting the host response (and in particular that by B lymphocytes) may be relevant in driving ongoing systemic inflammation related to gut pathology in PD. For example, the Clatworthy lab recently described a marked induction of anti-commensal IgG in the colons of patients with ulcerative colitis (a form of inflammatory bowel disease). This IgG then causes cross-linking of Fcγ receptors on mononuclear phagocytes leading to IL-1β production and the subsequent activation of type 17 immunity (Castro-Dopico et al., 2019). Looking at a group of PD patients with the additional genetic risk of Crohn's disease and attempting to identify a B cell based response to circulating endotoxin or commensals in the gut (from stool samples) would have been a further interesting study. Recruitment of patients with LRKK2 mutations would have been more complicated and time consuming as it requires screening of a large number of patients and a multi-centre approach to get the required number of patients for any study. It may be possible to recruit a sufficient cohort of non-affected carriers of the relevant mutations in LRKK2 using the Cambridge bioresource.

The rationale for looking at alpha synuclein antibodies in PD was to identify whether there was some evidence that the B cell response was antigen specific or

whether it was the non-antibody producing arm of the B lymphocyte compartment that was involved. The alpha synuclein antibody assay that I developed as part of my PhD (and piloted in a small sample of early disease patients and controls) has now been used by an MPhil student under my supervision to show that there is a marked increase in alpha synuclein antibodies (to fibrils and unaltered alpha synuclein but not Y39 or S129D peptides) in a prodromal cohort using serum from collaborators in Oxford (data not included as it forms part of her MPhil thesis). The main limitation of this assay in the data I have presented as part of my PhD is that there was substantial variability between batches. By including a standard control with all plates and being meticulous with laboratory technique across those performing the assay we have now reduced this variability substantially (with mean CVs of 10-15%). This assay provides an initial result but is limited in that it is not exactly clear what post translational modification are present (in the fibrils particularly) and which epitopes are bound by the antibody. It also doesn't answer the question about the provenance of the antibodies – whether they are produced by long lived plasma cells (having had an initial antigen exposure in the past) or if there are ongoing germinal centre reactions driving the response or whether it is primarily a poly-specific B1 type response (which is less likely as I did not measure IgM antibodies). The evidence from the meta-analysis and data from our MPhil student together suggest that there is indeed an early antibody response which subsequently wanes (studies looking at antibodies in later disease show no difference between patients and controls, as summarised in (Scott et al., 2018). Subsequent follow up work could look at specific antibody production by plasma cells or plasmablasts in culture following stimulation as well as using alternative more accurate assays to look at the binding kinetics between serum antibodies and alpha synuclein.

I spent a lot of time during my PhD doing behavioural testing in the alpha synuclein transgenic mice. The original aim had been to identify a clear phenotype that could then be used as a readout following B lymphocyte depletion (as this had been considered the main therapeutic option at the beginning of my PhD). In retrospect, it would have been better to have spent more time interrogating the mechanisms behind the differences observed in the B cell depleted mouse (initially the μMT mice and then CD20 depleted mice) and controls to confirm that the difference in lesion size was associated with an increase in microglial activation and immune cell infiltration (this work is being completed at the moment by an MPhil student who I am supervising). The transgenic alpha synuclein model (thy1 SNCA) is also limited by having a poor histological phenotype (there is known to be minimal neurodegeneration in this model). I did not continue to look for more subtle behavioural deficits, reasoning that this was unlikely to provide a reliable readout. The MI-2 mouse tissue only became available to us at the end of my PhD. These mice do have a clear behavioural deficit on motor testing that has been replicated several times (Wegrzynowicz et al., 2018). One of the reasons for this may be that the mice are on an alpha synuclein null background as previous studies have shown that endogenous mouse alpha synuclein can inhibit the aggregation of human alpha synuclein (Wegrzynowicz et al., 2018). This model would have been a better model to use although the deficit still takes 18 months to develop (which does reflect the time course of PD better despite being inconvenient for experiments). The thy1 SNCA mice have endogenous mouse alpha synuclein in addition to the human alpha synuclein transgene which may have reduced the associated pathology and behavioural phenotype.

The 6OHDA model on the other hand provided a clear behavioural phenotype and the experiments could be done over a 4-5 week period. The major disadvantage (as discussed in Chapter 4) is that the acute neurotoxic nature of

the insult does not reflect PD at all (a complex disease that probably develops over decades) and it is therefore difficult to generalise findings from it to human PD. However, further defining the association between the meningeal B lymphocytes and microglial activation and the relationship with cell death may provide some important insights. In my experiments, I did not find a difference in the numbers of meningeal B lymphocytes between transgenic animals and controls but this was only using small numbers of mice and therefore requires further experiments. I also did not look for differences in function or surface markers in this population of cells which is likely to be relevant.

One possible explanation for the decrease in B lymphocytes in patients and transgenic models is that this is as a result of chronic antigen stimulation of the BCR with associated B cell anergy (decreased responsiveness) (as a result of alpha synuclein in the periphery, repeated infections or apoptosis/cell death). Usually, stimulation via the BCR provides a survival signal in B cells expressing functional membrane bound immunoglobulins ('mature' B cells) (at the immature stage in the bone marrow niche, a high affinity interaction with the BCR and a strong activating signal induces apoptosis as this is usually the result of binding of self antigen in the bone marrow). Some elegant experiments have been done in mice expressing a transgene affecting the immunoglobulin heavy and light chains, resulting in B cells that are highly specific for only one antigen (hen egg lysozyme, HEL)(Cambier, Gauld, Merrell, & Vilen, 2007). If one crosses this mouse with a mouse expressing soluble HEL (ML5 mice), the mice produce transitional B cells in the periphery as expected but the number of mature follicular B cells is very much decreased. These B cells also fail to respond or proliferate in response to antigen(Goodnow et al., 1988). Loss of B cell anergy is associated with auto-immune disease (as the self-reactive B cells are not silenced)(Cambier et al., 2007). However, this does not neatly fit as an explanation because the cells from patients with a high risk of an early dementia

produced the most cytokine (IL6 and IL10) (ie. were less anergic) in vitro while at the same time being decreased in number and proportion in the circulation.

The other possibility that I have not looked at in the patient cohorts is the role of infection in disease progression. It is possible that having lower B lymphocytes is associated with a decreased response to new infections or a slower response to those previously encountered, making these patients more vulnerable to repeated infections. These infections, or systemic inflammatory events, contribute to microglial activation. In Alzheimer's cohorts, having higher levels of TNFα at baseline as well as repeated systemic inflammatory events (SIE) was associated with faster disease progression(Holmes et al., 2009a). Following patients over a longer time period and recording such events may show a similar pattern in PD (with the caveat that it is challenging to define what counts as a significant SIE).

B cells are thought to play a deleterious role in the development of post-stroke dementia where there is delayed infiltration by B cells into the core of the stroke from around 7 weeks after injury (see (Doyle et al., 2015). There is also the eventual formation of intraparenchymal (intralesional) B cell clusters surrounded by T cells and CD11c positive (dendritic cells) producing IgG. Preventing this response with B cell depletion stopped the development of delayed onset dementia in mouse models. The authors did not measure behavioural outcomes or lesion size immediately after the stroke. Based on my work one would hypothesise that they would be worse in the depleted mice initially (in terms of motor testing and lesion size as there is no reason to think that the 6OHDA driven lesion is different to an ischaemic injury in its effect on ensuing inflammation). In fact, this would fit with similar kinetics of the effects of B cell depletion in EAE (Matsushita et al., 2008) where depletion of B cells prior to disease induction results in worse outcomes (in terms of EAE scores,

which is rescued by transferring CD5+CD1d+ B cells) but if done 14-21 days post injury it leads to better outcomes. The effect at the early time point is therefore due to the loss of regulatory B cells and the beneficial effect later in disease is due to the loss of the effector arm of the B cell response (which is mainly inflammatory). Such evidence may raise the question of B lymphocyte depletion in later PD. I have argued that I have not found any evidence in my PhD to support B cell depletion as a therapeutic strategy. Unlike the stroke model, there is not convincing evidence of ongoing B cell effector activity (at least in terms of an antibody response in late disease according to my meta-analysis) and therefore I argue that this should not be considered. However, my data does not definitely address this issue, and it may well be that B cells play a dual role in PD, as in many autoimmune disorders with both a disease ameliorating effect of regulatory B cells and a disease exacerbating effect of inflammatory B cells or antibody.

5.4 Summary of future work

I have listed possible directions for future work at the end of each data chapter. In summary, the main priorities moving forward would be to investigate the role of B lymphocytes (in particular) but also other immune cells within the CSF compartment and meninges (dura) to see how these impact on disease. Single cell RNA-sequencing would allow for these cells to be transcriptionally characterised in detail and compared to circulating B cells. The strength of having well characterised clinical cohorts of PD patients in Cambridge is that we could then ask questions about whether there are particular transcription signatures associated with a poor outcomes. I would also aim to take the antibody work further by looking for B cell receptor specificity for alpha synuclein or its epitopes and seeing whether B cells are capable of presenting these to T cells (looking at cells carrying the HLA alleles associated with PD).

Ultimately, I would also aim to design a trial boosting B regulatory cells in very early disease stage patients (potentially using a prodromal cohort) in order to show that these cells are playing a role in disease progression (and to find a treatment that would delay this progression).

In mouse models I aim to further optimise the dosing of the anti- CD-20 antibody in order to repeat the experiments of transferring IL10++ or IL10-/- cells and using other tools such as CD20- eGFP cells so that I can look at trafficking to and from the meninges at different time points in disease (being sure that the transferred cells aren't depleted by residual circulating antibody). Given that the MI-2 mice have a clearer behavioural phenotype I would also repeat experiments using LPS in these mice and attempt to modulate the B cell compartment at different time points (using both depletion and the transfer to IL10++ B cells) to see whether these have an effect in a more chronic model of PD.

5.5 Conclusion

I have described a large number of changes in B lymphocytes in PD patients and animal models of PD. These changes suggest that pan-B cell depletion is unlikely to be a good therapeutic strategy but that boosting regulatory B lymphocytes and decreasing peripheral immune activation (e.g. B cell production of cytokines) may be a better target for future trials as these are associated with better outcomes. It is important to investigate alterations in this compartment further as there are many existing therapies that target B lymphocytes in different ways.

6 APPENDICES

APPENDIX I: MOUSE FLOW CYTOMETRY ANTIBODIES

Single colour controls were made for each experiment using excess mouse splenocytes.

Staining panel 1 (peripheral blood and lymphoid tissue)

Staining antibody	Concentration
FITC CD8	1:200
PerCPefluor IgM	1:200
APC CD62L	1:200
APCCy7 CD43	1:200
AF700 MHC Class II	1:200
PE CD21/35	1:200
PE dazzle IgD	1:200
PECy7 CD4	1:200
Efluor450 CD9	1:200
BV711 CD138	1:200
BV785 CD19	1:200
Live dead zombie UV	1:500

Staining panel 2 (peripheral blood and lymphoid tissue)

Staining antibody	Concentration
FITC CD9	1:200
PerCPefluor IgM	1:200
APC CD62L	1:200
APCCy7 CD43	1:200
AF700 MHC Class II	1:200
PE CD21/35	1:200
PE dazzle IgD	1:200
PECy7 CD4	1:200
BV421 CD20	1:200
BV711 CD138	1:200
BV785 CD19	1:200
BV605CD69	1:200
BV650CD45	1:200
Live dead zombie UV	1:500

Staining panel 3 (peripheral blood and lymphoid tissue)

Staining antibody	Concentration
FITC CD9	1:200
PerCPefluor IgM	1:200
APC Ly6c	1:200
APCCy7 Gr1	1:200
AF700 CD8	1:200
PE CD21/35	1:200
PE dazzle IgD	1:200
PECy7 CD4	1:200
BV421 CD20	1:200
BV711 CD138	1:200
BV785 CD19	1:200
BV650CD45	1:200
Live dead zombie UV	1:500

Staining panel 4

Staining antibody	Concentration
eFluor450 CD19	1:200
PerCPefluor IgM	1:150
FITC 1gD	1:200
GL7 efluor660	1:150
PE CD21/35	1:150
APCefuor780 CD11b	1:200
AF700 MHC Class II	1:200

Staining panel 5 (meninges and brain)

Staining antibody	Concentration
FITC IV CD45	IV injection (3:100)
PerCPefluor IgM	1:200
APC F4/80	1:200
APCCy7 CD43	1:200
AF700 CD45	1:200
PE CXCR5	1:200
PE dazzle IgD	1:200
PECy7 CD23	1:200
BV450 Gr1	1:200
BV510 CD5	1:200
BV785 CD19	1:200
BV605CD3	1:200
BV650CD11b	1:200
Live dead zombie UV	1:500

Staining panel 6 (Brain)

Staining antibody	Concentration
FITC IV CD45	IV injection (3:100)
PerCPefluor 710 CD11b	1:200
AF700 MHC Class II	1:200
PE CXCR1	1:200
PECy7 CD4	1:200
Pacblu CD8	1:200
BV510 CD3	1:200
BV785 CD19	1:200
BV605CD3	1:200
BV650CD11b	1:200
Live dead zombie UV	1:500

Staining panel 7 (spleen and blood)

Staining antibody	Concentration
FITC IV CD45	IV injection (3:100)
PerCPefluor IgM	1:200
APC Ly6c	1:200
APCCy7 Gr1	1:200
AF700 CD8	1:200
PE dazzle IgD	1:200
PECy7 CD4	1:200
BV450 CD20	1:200
BV510 CD3	1:200
BV785 CD19	1:200
Live dead zombie UV	1:500

Staining panel 8 Peripheral tissues

Staining antibody	Concentration
FITC IV CD45	IV injection (3:100)
PerCPefluor IgM	1:200
APC CD62L	1:200
APCCy7 CD43	1:200
AF700 CD3	1:200
PE CD25	1:200
PE dazzle IgD	1:200
PECy7 CD23	1:200
Efluor450 CD9	1:200
BV510 CD5	1:200
BV785 CD19	1:200
BV605CD69	1:200
BV650CD45	1:200
Live dead zombie UV	1:500

Staining panel 9 (brain)

Staining antibody	Concentration
FITC CD11b	1:200
AF647 Iba1	1:200
AF700 CD8	1:200
PE CXCR1	1:200
PECy7 CD4	1:200
Efluor450 MHC Class II	1:200
BV510 CD3	1:200
BV785 CD19	1:200
BV650CD45	1:200
Live dead zombie UV	1:500

Antibodies used in mouse experiments

Antigen	Fluorophore	Manufacturer	Cat. no
CD8	FITC	Biolegend	100706
IgM	PerCPefluor-710	eBioscience	46-5790-82
CD62L	APC	Biolegend	104412
CD43	APCCy7	Biolegend	121220
MHC Class II	AF700	eBioscience	56-5321-82
CD21/35	PE	Biolegend	123410
IgD	PE dazzle	Biolegend	405742
CD4	PECy7	Biolegend	100528
CD9	eFluor450	eBioscience	48-0091-82
CD138	BV711	Biolegend	142519
CD19	BV785	Biolegend	302240
Live dead zombie UV		Biolegend	423107
CD9	FITC	Invitrogen	11-0091-82
CD20	BV421	Biolegend	150405
CD69	BV605	Biolegend	104529
CD45	BV650	Biolegend	103151
Ly6c	APC	Biolegend	128016
Gr1	APCCy7	Biolegend	108424
CD19	eFluor450	Invitrogen	48-0193-82
GL7	ef660	eBIoscience	50-5902-82
CD3	BV605	Biolegend	100237
IgD	FITC	eBIoscience	11-5993-85
CD11b	APCefluor780	Invitrogen	47-0112-82
CD45	FITC	Biolegend	103108
F4/80	APC	Biolegend	123116
CD45	AF700	BD biosciences	560510
CXCR5	PE dazzle	Biolegend	145504
Gr1	BV405	BD biosciences	560453
CD5	BV510	Biolegend	100627
CD11b	BV650	BD biosciences	563402
CD3	AF700	Biolegend	100216
CD25	PE	Biolegend	102008
CD23	PECy7	Biolegend	101614
B220	efluor450	eBioscience	48-0452-82
Phalloidin	AF647	invitrogen	A22287
Lyve1	PE	R & D	Fab2121p
IgD	FITC	Biolegend	405704

APPENDIX II: HUMAN FLOW CYTOMETRY

Antigen	Fluorophore	Manufacturer	Category number
CD19	BV786	BD bioscience	563325
CD25	BUV395	BD bioscience	564034
CD138	V450	BD bioscience	562098
CD38	APC	BD bioscience	555462
MHC Class II	AF700	BD bioscience	560743
Live dead zombie aqua		Biolegend	423101
CD5	FITC	BD bioscience	555412
CD24	BV605	BD bioscience	562788
CD27	BUV395	BD bioscience	563816
CD38	APC	BD bioscience	555462
IgM	PE	BD bioscience	555783
CD138	V450	BD bioscience	562098
IgD	APCH7	BD bioscience	561305
CD1d	PerCp Cy5.5	Biolegend	350312
CD19	FITC	BD bioscience	555412
CD19	BV605	BD bioscience	562653
CD19	APC	BD bioscience	555415
CD19	PE	BD bioscience	555413
CD19	V450	BD bioscience	560353
CD19	PerCp Cy5.5	Biolegend	363016
CD16	FITC	BD bioscience	555406
CD57	PerCp Cy5.5	Biolegend	359621
TLR4	APC	Biolegend	312816
IgA	PE	Miltenyi Biotec	130-093-128
CD4	PE dazzle	Biolegend	300574
CD3	PECy7	BD bioscience	563423
CD45	BV450	BD bioscience	560397
CD8	BV510	BD bioscience	563919
CD14	BV650	BD bioscience	301836
TLR2	BV711	BD bioscience	742770
CD11c	FITC	BD bioscience	561355
Tbet	PE	BD bioscience	561265
CD86	PerCp Cy5.5	BD bioscience	561129
IL10	PE	BD bioscience	559330
IL6	FITC	BD bioscience	340526
CD25	BUV395	BD bioscience	564034

7 REFERENCES

Aarsland, D., Larsen, J. P., Tandberg, E., & Laake, K. (2000). Predictors of nursing home placement in Parkinson's disease: a population-based, prospective study. *Journal of the American Geriatrics Society*, *48*(8), 938–42.

Abbas, AK, Lichtman, AH, Pillai, S. (2014). *Cellular and Molecular Immunology*. *Elsevier*. https://doi.org/10.1136/pgmj.68.798.305

Akhtar, R. S., Licata, J. P., Luk, K. C., Shaw, L. M., Trojanowski, J. Q., & Lee, V. M.-Y. M.-Y. (2018). Measurements of auto-antibodies to α-synuclein in the serum and cerebral spinal fluids of patients with Parkinson's disease. *Journal of Neurochemistry*. https://doi.org/10.1111/jnc.14330

Alvarez-Castelao, B., Gorostidi, A., Ruíz-Martínez, J., López de Munain, A., & Castaño, J. G. (2014). Epitope Mapping of Antibodies to Alpha-Synuclein in LRRK2 Mutation Carriers, Idiopathic Parkinson Disease Patients, and Healthy Controls. *Frontiers in Aging Neuroscience*, *6*, 169. https://doi.org/10.3389/fnagi.2014.00169

Alves da Costa, C., Dunys, J., Brau, F., Wilk, S., Cappai, R., & Checler, F. (2006). 6-Hydroxydopamine but not 1-methyl-4-phenylpyridinium abolishes alpha-synuclein anti-apoptotic phenotype by inhibiting its proteasomal degradation and by promoting its aggregation. *The Journal of Biological Chemistry*, *281*(14), 9824–31. https://doi.org/10.1074/jbc.M513903200

Anderson, J. P., Walker, D. E., Goldstein, J. M., de Laat, R., Banducci, K., Caccavello, R. J., … Chilcote, T. J. (2006). Phosphorylation of Ser-129 is the dominant pathological modification of alpha-synuclein in familial and sporadic Lewy body disease. *The Journal of Biological Chemistry*, *281*(40), 29739–52. https://doi.org/10.1074/jbc.M600933200

Aravena, O., Ferrier, A., Menon, M., Mauri, C., Aguillón, J. C., Soto, L., & Catalán, D. (2017). TIM-1 defines a human regulatory B cell population that is altered in frequency and function in systemic sclerosis patients. *Arthritis Research & Therapy*, *19*(1), 8. https://doi.org/10.1186/s13075-016-1213-9

Aspelund, A., Antila, S., Proulx, S. T., Karlsen, T. V., Karaman, S., Detmar, M., …

Alitalo, K. (2015). A dural lymphatic vascular system that drains brain interstitial fluid and macromolecules. *Journal of Experimental Medicine*, *212*(7), 991–9. https://doi.org/10.1084/jem.20142290

Aw, D., Silva, A. B., & Palmer, D. B. (2007). Immunosenescence: emerging challenges for an ageing population. *Immunology*, *120*(4), 435–46. https://doi.org/10.1111/j.1365-2567.2007.02555.x

Baba, Y., Kuroiwa, A., Uitti, R. J., Wszolek, Z. K., & Yamada, T. (2005). Alterations of T-lymphocyte populations in Parkinson disease. *Parkinsonism & Related Disorders*, *11*(8), 493–8. https://doi.org/10.1016/j.parkreldis.2005.07.005

Banham, G. D., Flint, S. M., Torpey, N., Lyons, P. A., Shanahan, D. N., Gibson, A., … Clatworthy, M. R. (2018). Belimumab in kidney transplantation: an experimental medicine, randomised, placebo-controlled phase 2 trial. *Lancet (London, England)*, *391*(10140), 2619–2630. https://doi.org/10.1016/S0140-6736(18)30984-X

Barr, T. A., Shen, P., Brown, S., Lampropoulou, V., Roch, T., Lawrie, S., … Gray, D. (2012). B cell depletion therapy ameliorates autoimmune disease through ablation of IL-6–producing B cells. *The Journal of Experimental Medicine*, *209*(5), 1001–1010. https://doi.org/10.1084/jem.20111675

Bas, J., Calopa, M., Mestre, M., Molleví, D. G., Cutillas, B., Ambrosio, S., & Buendia, E. (2001). Lymphocyte populations in Parkinson's disease and in rat models of parkinsonism. *Journal of Neuroimmunology*, *113*(1), 146–52.

Bastarache, J. A., Koyama, T., Wickersham, N. E., & Ware, L. B. (2014). Validation of a multiplex electrochemiluminescent immunoassay platform in human and mouse samples. *Journal of Immunological Methods*, *408*, 13–23. https://doi.org/10.1016/j.jim.2014.04.006

Baumgarth, N., Jager, G. C., Herman, O. C., Herzenberg, L. A., & Herzenberg, L. A. (2000). CD4+ T cells derived from B cell-deficient mice inhibit the establishment of peripheral B cell pools. *Proceedings of the National*

Academy of Sciences of the United States of America, *97*(9), 4766–71. https://doi.org/10.1073/pnas.97.9.4766

Bekar, K. W., Owen, T., Dunn, R., Ichikawa, T., Wang, W., Wang, R., … Anolik, J. H. (2010a). Prolonged effects of short-term anti-CD20 B cell depletion therapy in murine systemic lupus erythematosus. *Arthritis and Rheumatism*, *62*(8), 2443–57. https://doi.org/10.1002/art.27515

Bekar, K. W., Owen, T., Dunn, R., Ichikawa, T., Wang, W., Wang, R., … Anolik, J. H. (2010b). Prolonged effects of short-term anti-CD20 B cell depletion therapy in murine systemic lupus erythematosus. *Arthritis and Rheumatism*, *62*(8), 2443–2457. https://doi.org/10.1002/art.27515

Besong-Agbo, D., Wolf, E., Jessen, F., Oechsner, M., Hametner, E., Poewe, W., … Dodel, R. (2013). Naturally occurring -synuclein autoantibody levels are lower in patients with Parkinson disease. *Neurology*, *80*(2), 169–175. https://doi.org/10.1212/WNL.0b013e31827b90d1

Blair, P. A., Noreña, L. Y., Flores-Borja, F., Rawlings, D. J., Isenberg, D. A., Ehrenstein, M. R., & Mauri, C. (2010). CD19+CD24hiCD38hi B Cells Exhibit Regulatory Capacity in Healthy Individuals but Are Functionally Impaired in Systemic Lupus Erythematosus Patients. *Immunity*, *32*(1), 129–140. https://doi.org/10.1016/j.immuni.2009.11.009

Blesa, J., & Przedborski, S. (2014). Parkinsonâ€™s disease: animal models and dopaminergic cell vulnerability. *Frontiers in Neuroanatomy*, *8*, 155. https://doi.org/10.3389/fnana.2014.00155

Blumenfeld, S., Staun-Ram, E., & Miller, A. (2016). Fingolimod therapy modulates circulating B cell composition, increases B regulatory subsets and production of IL-10 and TGFβ in patients with Multiple Sclerosis. *Journal of Autoimmunity*, *70*, 40–51.

Bonato, J. M., Bassani, T. B., Milani, H., Vital, M. A. B. F., & de Oliveira, R. M. W. (2018). Pioglitazone reduces mortality, prevents depressive-like behavior, and impacts hippocampal neurogenesis in the 6-OHDA model of

Parkinson's disease in rats. *Experimental Neurology*, *300*, 188–200. https://doi.org/10.1016/J.EXPNEUROL.2017.11.009

Borenstein, M., Hedges, L. V., Higgins, J. P. T., & Rothstein, H. R. (2009). *Introduction to Meta-Analysis*. Chichester, UK: John Wiley & Sons, Ltd. https://doi.org/10.1002/9780470743386

Bové, J., Prou, D., Perier, C., & Przedborski, S. (2005). Toxin-induced models of Parkinson's disease. *NeuroRx : The Journal of the American Society for Experimental NeuroTherapeutics*, *2*(3), 484–94. https://doi.org/10.1602/neurorx.2.3.484

Braak, H., Müller, C. M., Rüb, U., Ackermann, H., Bratzke, H., de Vos, R. A. I., & Del Tredici, K. (2006). Pathology associated with sporadic Parkinson's disease--where does it end? *Journal of Neural Transmission. Supplementum*, (70), 89–97.

Brochard, V., Combadière, B., Prigent, A., Laouar, Y., Perrin, A., Beray-Berthat, V., … Hunot, S. (2009). Infiltration of CD4+ lymphocytes into the brain contributes to neurodegeneration in a mouse model of Parkinson disease. *The Journal of Clinical Investigation*, *119*(1), 182–92. https://doi.org/10.1172/JCI36470DS1

Brudek, T., Winge, K., Folke, J., Christensen, S., Fog, K., Pakkenberg, B., & Pedersen, L. Ø. (2017). Autoimmune antibody decline in Parkinson's disease and Multiple System Atrophy; a step towards immunotherapeutic strategies. *Molecular Neurodegeneration*, *12*(1), 44. https://doi.org/10.1186/s13024-017-0187-7

Bryan, T., Luo, X., Forsgren, L., Morozova-Roche, L. A., & Davis, J. J. (2012). The robust electrochemical detection of a Parkinson's disease marker in whole blood sera. *Chemical Science*, *3*(12), 3468–3473. https://doi.org/10.1039/c2sc21221h

Butchart, J., Brook, L., Hopkins, V., Teeling, J., Püntener, U., Culliford, D., … Holmes, C. (2015). Etanercept in Alzheimer disease: A randomized, placebo-

controlled, double-blind, phase 2 trial. *Neurology*, *84*(21), 2161–8. https://doi.org/10.1212/WNL.0000000000001617

Caggiu, E., Paulus, K., Arru, G., Piredda, R., Sechi, G. Pietro, & Sechi, L. A. (2016). Humoral cross reactivity between α-synuclein and herpes simplex-1 epitope in Parkinson's disease, a triggering role in the disease? *Journal of Neuroimmunology*, *291*, 110–114. https://doi.org/10.1016/J.JNEUROIM.2016.01.007

Camacho-Soto, A., Gross, A., Searles Nielsen, S., Dey, N., & Racette, B. A. (2018). Inflammatory bowel disease and risk of Parkinson's disease in Medicare beneficiaries. *Parkinsonism & Related Disorders*, *50*, 23–28. https://doi.org/10.1016/j.parkreldis.2018.02.008

Cambier, J. C., Gauld, S. B., Merrell, K. T., & Vilen, B. J. (2007). B-cell anergy: from transgenic models to naturally occurring anergic B cells? *Nature Reviews Immunology*, *7*(8), 633–643. https://doi.org/10.1038/nri2133

Candore, G., Di Lorenzo, G., Mansueto, P., Melluso, M., Fradà, G., Li Vecchi, M., … Caruso, C. (1997). Prevalence of organ-specific and non organ-specific autoantibodies in healthy centenarians. *Mechanisms of Ageing and Development*, *94*(1–3), 183–90.

Cankaya, S., Cankaya, B., Kilic, U., Kilic, E., & Yulug, B. (2019). The therapeutic role of minocycline in Parkinson's disease. *Drugs in Context*, *8*, 212553. https://doi.org/10.7573/dic.212553

Cao, S., Theodore, S., & Standaert, D. G. (2010). Fcγ receptors are required for NF-κB signaling, microglial activation and dopaminergic neurodegeneration in an AAV-synuclein mouse model of Parkinson's disease. *Molecular Neurodegeneration*, *5*(1), 42. https://doi.org/10.1186/1750-1326-5-42

Castro-Dopico, T., Dennison, T. W., Ferdinand, J. R., Mathews, R. J., Fleming, A., Clift, D., … Clatworthy, M. R. (2019). Anti-commensal IgG Drives Intestinal Inflammation and Type 17 Immunity in Ulcerative Colitis. *Immunity*, *50*(4), 1099–1114.e10. https://doi.org/10.1016/j.immuni.2019.02.006

Chan, O. T. M., Hannum, L. G., Haberman, A. M., Madaio, M. P., & Shlomchik, M. J. (1999). A Novel Mouse with B Cells but Lacking Serum Antibody Reveals an Antibody-independent Role for B Cells in Murine Lupus. *The Journal of Experimental Medicine*, *189*(10), 1639–1648. https://doi.org/10.1084/jem.189.10.1639

Chaplin, D. D. (2010). Overview of the immune response. *The Journal of Allergy and Clinical Immunology*, *125*(2 Suppl 2), S3-23. https://doi.org/10.1016/j.jaci.2009.12.980

Chaudhry, M. S., & Karadimitris, A. (2014). Role and regulation of CD1d in normal and pathological B cells. *Journal of Immunology (Baltimore, Md. : 1950)*, *193*(10), 4761–8. https://doi.org/10.4049/jimmunol.1401805

Chen, S., Le, W. D., Xie, W. J., Alexianu, M. E., Engelhardt, J. I., Siklós, L., & Appel, S. H. (1998). Experimental destruction of substantia nigra initiated by Parkinson disease immunoglobulins. *Archives of Neurology*, *55*(8), 1075–80.

Chen, Z., Chen, S., & Liu, J. (2018). The role of T cells in the pathogenesis of Parkinson's disease. *Progress in Neurobiology*, *169*, 1–23. https://doi.org/10.1016/J.PNEUROBIO.2018.08.002

Cheng, Q., Mumtaz, I. M., Khodadadi, L., Radbruch, A., Hoyer, B. F., & Hiepe, F. (2013). Autoantibodies from long-lived 'memory' plasma cells of NZB/W mice drive immune complex nephritis. *Annals of the Rheumatic Diseases*, *72*(12), 2011–2017. https://doi.org/10.1136/annrheumdis-2013-203455

Chesselet, M.-F., & Richter, F. (2011). Modelling of Parkinson's disease in mice. *The Lancet. Neurology*, *10*(12), 1108–18. https://doi.org/10.1016/S1474-4422(11)70227-7

Chesselet, M.-F., Richter, F., Zhu, C., Magen, I., Watson, M. B., & Subramaniam, S. R. (2012). A progressive mouse model of Parkinson's disease: the Thy1-aSyn ("Line 61") mice. *Neurotherapeutics : The Journal of the American Society for Experimental NeuroTherapeutics*, *9*(2), 297–314. https://doi.org/10.1007/s13311-012-0104-2

Chitnis, T., & Weiner, H. L. (2017). CNS inflammation and neurodegeneration. *Journal of Clinical Investigation*, *127*(10), 3577–3587. https://doi.org/10.1172/JCI90609

Choi, Y. R., Cha, S. H., Kang, S. J., Kim, J. B., Jou, I., & Park, S. M. (2018). Prion-like Propagation of α-Synuclein Is Regulated by the FcγRIIB-SHP-1/2 Signaling Pathway in Neurons. *Cell Reports*, *22*(1), 136–148. https://doi.org/10.1016/j.celrep.2017.12.009

Clatworthy, M. R. (2014). B-cell regulation and its application to transplantation. *Transplant International : Official Journal of the European Society for Organ Transplantation*, *27*(2), 117–28. https://doi.org/10.1111/tri.12160

Cook, D. A., Kannarkat, G. T., Cintron, A. F., Butkovich, L. M., Fraser, K. B., Chang, J., … Tansey, M. G. (2017). LRRK2 levels in immune cells are increased in Parkinson's disease. *NPJ Parkinson's Disease*, *3*, 11. https://doi.org/10.1038/s41531-017-0010-8

Da Mesquita, S., Fu, Z., & Kipnis, J. (2018). The Meningeal Lymphatic System: A New Player in Neurophysiology. *Neuron*, *100*(2), 375–388. https://doi.org/10.1016/j.neuron.2018.09.022

Da Mesquita, S., Louveau, A., Vaccari, A., Smirnov, I., Cornelison, R. C., Kingsmore, K. M., … Kipnis, J. (2018). Functional aspects of meningeal lymphatics in ageing and Alzheimer's disease. *Nature*, *560*(7717), 185–191. https://doi.org/10.1038/s41586-018-0368-8

Delenclos, M., Carrascal, L., Jensen, K., & Romero-Ramos, M. (2014). Immunolocalization of human alpha-synuclein in the Thy1-aSyn ("Line 61") transgenic mouse line. *Neuroscience*, *277*, 647–664. https://doi.org/10.1016/j.neuroscience.2014.07.042

Derecki, N. C., Cardani, A. N., Yang, C. H., Quinnies, K. M., Crihfield, A., Lynch, K. R., & Kipnis, J. (2010). Regulation of learning and memory by meningeal immunity: a key role for IL-4. *The Journal of Experimental Medicine*, *207*(5), 1067–80. https://doi.org/10.1084/jem.20091419

Derecki, N., Louveau, A., & Kipnis, J. (2015). Dissection and immunostaining of mouse whole-mount meninges. *Protocol Exchange*. https://doi.org/10.1038/protex.2015.047

DiLillo, D. J., Matsushita, T., & Tedder, T. F. (2010). B10 cells and regulatory B cells balance immune responses during inflammation, autoimmunity, and cancer. *Annals of the New York Academy of Sciences*, *1183*(1), 38–57. https://doi.org/10.1111/j.1749-6632.2009.05137.x

Dolhun, R. (2016). Alpha-Synuclein: A therapeutic target and potential biomarker in Parkindon's disease. *Practical Neurology*, (December), 1–5.

Doyle, K. P., Quach, L. N., Solé, M., Axtell, R. C., Nguyen, T.-V. V, Soler-Llavina, G. J., … Buckwalter, M. S. (2015). B-Lymphocyte-Mediated Delayed Cognitive Impairment following Stroke. *The Journal of Neuroscience : The Official Journal of the Society for Neuroscience*, *35*(5), 2133–45. https://doi.org/10.1523/JNEUROSCI.4098-14.2015

Engelhardt, B. (2010). T cell migration into the central nervous system during health and disease: Different molecular keys allow access to different central nervous system compartments. *Clinical and Experimental Neuroimmunology*, *1*(2), 79–93. https://doi.org/10.1111/j.1759-1961.2010.009.x

Evans, J. R., Mason, S. L., Williams-Gray, C. H., Foltynie, T., Brayne, C., Robbins, T. W., & Barker, R. A. (2011). The natural history of treated Parkinson's disease in an incident, community based cohort. *Journal of Neurology, Neurosurgery, and Psychiatry*, *82*(10), 1112–8. https://doi.org/10.1136/jnnp.2011.240366

Fan, J., Searles Nielsen, S., Faust, I. M., & Racette, B. A. (2019). Transplant and risk of Parkinson disease. *Parkinsonism & Related Disorders*. https://doi.org/10.1016/j.parkreldis.2019.02.013

Fasano, A., Visanji, N. P., Liu, L. W. C., Lang, A. E., & Pfeiffer, R. F. (2015). Gastrointestinal dysfunction in Parkinson's disease. *The Lancet Neurology*, *14*(6), 625–639. https://doi.org/10.1016/S1474-4422(15)00007-1

Filiou, M. D., Arefin, A. S., Moscato, P., & Graeber, M. B. (2014). "Neuroinflammation" differs categorically from inflammation: transcriptomes of Alzheimer's disease, Parkinson's disease, schizophrenia and inflammatory diseases compared. *Neurogenetics*. https://doi.org/10.1007/s10048-014-0409-x

Forsyth, C. B., Shannon, K. M., Kordower, J. H., Voigt, R. M., Shaikh, M., Jaglin, J. A., … Keshavarzian, A. (2011). Increased Intestinal Permeability Correlates with Sigmoid Mucosa alpha-Synuclein Staining and Endotoxin Exposure Markers in Early Parkinson's Disease. *PLoS ONE*, *6*(12), e28032. https://doi.org/10.1371/journal.pone.0028032

Franceschi, C., Garagnani, P., Parini, P., Giuliani, C., & Santoro, A. (2018). Inflammaging: a new immune–metabolic viewpoint for age-related diseases. *Nature Reviews Endocrinology*, *14*(10), 576–590. https://doi.org/10.1038/s41574-018-0059-4

Frasca, D. (2018). Senescent B cells in aging and age-related diseases: Their role in the regulation of antibody responses. *Experimental Gerontology*, *107*, 55–58. https://doi.org/10.1016/J.EXGER.2017.07.002

Gagne, J. J., & Power, M. C. (2010). Anti-inflammatory drugs and risk of Parkinson disease: a meta-analysis. *Neurology*, *74*(12), 995–1002. https://doi.org/10.1212/WNL.0b013e3181d5a4a3

Gao, H.-M., Zhang, F., Zhou, H., Kam, W., Wilson, B., & Hong, J.-S. (2011). Neuroinflammation and α-synuclein dysfunction potentiate each other, driving chronic progression of neurodegeneration in a mouse model of Parkinson's disease. *Environmental Health Perspectives*, *119*(6), 807–14. https://doi.org/10.1289/ehp.1003013

Gao, X., Schwarzschild, M. A., Chen, H., Schwarzschild, M. A., & Ascherio, A. (2011). Use of ibuprofen and risk of Parkinson disease. *Neurology*, *76*(10), 863–9. https://doi.org/10.1212/WNL.0b013e31820f2d79

Gendelman, H. E., Zhang, Y., Santamaria, P., Olson, K. E., Schutt, C. R., Bhatti,

D., … Mosley, R. L. (2017). Evaluation of the safety and immunomodulatory effects of sargramostim in a randomized, double-blind phase 1 clinical Parkinson's disease trial. *NPJ Parkinson's Disease*, *3*, 10. https://doi.org/10.1038/s41531-017-0013-5

Gerhard, A., Pavese, N., Hotton, G., Turkheimer, F., Es, M., Hammers, A., … Brooks, D. J. (2006). In vivo imaging of microglial activation with [11C](R)-PK11195 PET in idiopathic Parkinson's disease. *Neurobiology of Disease*, *21*(2), 404–412. https://doi.org/10.1016/j.nbd.2005.08.002

Goedert, M. (2015). Alzheimer's and Parkinson's diseases: The prion concept in relation to assembled A , tau, and -synuclein. *Science*, *349*(6248), 1255555–1255555. https://doi.org/10.1126/science.1255555

Goedert, M., Spillantini, M. G., Del Tredici, K., & Braak, H. (2013). 100 years of Lewy pathology. *Nature Reviews. Neurology*, *9*(1), 13–24. https://doi.org/10.1038/nrneurol.2012.242

Goodnow, C. C., Crosbie, J., Adelstein, S., Lavoie, T. B., Smith-Gill, S. J., Brink, R. A., … Basten, A. (1988). Altered immunoglobulin expression and functional silencing of self-reactive B lymphocytes in transgenic mice. *Nature*, *334*(6184), 676–682. https://doi.org/10.1038/334676a0

Greenland, J. C., Williams-Gray, C. H., & Barker, R. A. (2019). The clinical heterogeneity of Parkinson's disease and its therapeutic implications. *European Journal of Neuroscience*, *49*(3), 328–338. https://doi.org/10.1111/ejn.14094

Grozdanov, V., Bliederhaeuser, C., Ruf, W. P., Roth, V., Fundel-Clemens, K., Zondler, L., … Danzer, K. M. (2014). Inflammatory dysregulation of blood monocytes in Parkinson's disease patients. *Acta Neuropathologica*, *128*(5), 651–63. https://doi.org/10.1007/s00401-014-1345-4

Gruden, M. A., Sewell, R. D. E. E., Yanamandra, K., Davidova, T. V., Kucheryanu, V. G., Bocharov, E. V., … Morozova-Roche, L. a. (2011). Immunoprotection against toxic biomarkers is retained during Parkinson's disease progression.

Journal of Neuroimmunology, *233*(1–2), 221–227. https://doi.org/10.1016/j.jneuroim.2010.12.001

Gruden, M. A., Yanamandra, K., Kucheryanu, V. G., Bocharova, O. R., Sherstnev, V. V., Morozova-Roche, L. a., & Sewell, R. D. E. E. (2012). Correlation between Protective Immunity to a-Synuclein Aggregates, Oxidative Stress and Inflammation. *Neuroimmunomodulation*, *19*(6), 334–342. https://doi.org/10.1159/000341400

Grützke, B., Hucke, S., Gross, C. C., Herold, M. V. B. B., Posevitz-Fejfar, A., Wildemann, B. T., … Klotz, L. (2015). Fingolimod treatment promotes regulatory phenotype and function of B cells. *Annals of Clinical and Translational Neurology*, *2*(2), 119–130. https://doi.org/10.1002/acn3.155

Guillery, R. W., & Herrup, K. (1997). Quantification without pontification: choosing a method for counting objects in sectioned tissues. *The Journal of Comparative Neurology*, *386*(1), 2–7.

Gustafsson, G., Eriksson, F., Möller, C., da Fonseca, T. L., Outeiro, T. F., Lannfelt, L., … Ingelsson, M. (2017). Cellular Uptake of α-Synuclein Oligomer-Selective Antibodies is Enhanced by the Extracellular Presence of α-Synuclein and Mediated via Fcγ Receptors. *Cellular and Molecular Neurobiology*, *37*(1), 121–131. https://doi.org/10.1007/s10571-016-0352-5

Haas, J., Korporal, M., Balint, B., Fritzsching, B., Schwarz, A., & Wildemann, B. (2009). Glatiramer acetate improves regulatory T-cell function by expansion of naive CD4+CD25+FOXP3+CD31+ T-cells in patients with multiple sclerosis. *Journal of Neuroimmunology*, *216*(1–2), 113–117. https://doi.org/10.1016/j.jneuroim.2009.06.011

Haas, K. M., Poe, J. C., Steeber, D. A., & Tedder, T. F. (2005). B-1a and B-1b cells exhibit distinct developmental requirements and have unique functional roles in innate and adaptive immunity to S. pneumoniae. *Immunity*, *23*(1), 7–18. https://doi.org/10.1016/j.immuni.2005.04.011

Hampe, C. S. (2012). B Cell in Autoimmune Diseases. *Scientifica*, *2012*.

https://doi.org/10.6064/2012/215308

He, F., & Balling, R. (2013). The role of regulatory T cells in neurodegenerative diseases. *Wiley Interdisciplinary Reviews: Systems Biology and Medicine*, *5*(2), 153–180. https://doi.org/10.1002/wsbm.1187

He, Y., Le, W.-D., & Appel, S. H. (2002). Role of Fcgamma receptors in nigral cell injury induced by Parkinson disease immunoglobulin injection into mouse substantia nigra. *Experimental Neurology*, *176*(2), 322–7.

Heintz-Buschart, A, Pandey, U, Wicke, T, Sixel-Doring, F, Janzen, A, Sittig-Wiegand, E. Trenk-Walder, C, Oertel, WH, Mollenhauer, B, Wilmes, P. (2017). The nasal and gut microbiome in Parkinson's disease and idiopathic REM sleep behaviour disorder. *Movement Disorders*, *In press*.

Heintz-Buschart, A., Pandey, U., Wicke, T., Sixel-Döring, F., Janzen, A., Sittig-Wiegand, E., … Wilmes, P. (2018). The nasal and gut microbiome in Parkinson's disease and idiopathic rapid eye movement sleep behavior disorder. *Movement Disorders : Official Journal of the Movement Disorder Society*, *33*(1), 88–98. https://doi.org/10.1002/mds.27105

Heinzel, S., Gold, M., Deuschle, C., Bernhard, F., Maetzler, W., Berg, D., & Dodel, R. (2014). Naturally Occurring Alpha-Synuclein Autoantibodies in Parkinson's Disease: Sources of (Error) Variance in Biomarker Assays, *9*(12), e114566. https://doi.org/10.1371/journal.pone.0114566

Henry, C. J., Huang, Y., Wynne, A. M., & Godbout, J. P. (2009). Peripheral lipopolysaccharide (LPS) challenge promotes microglial hyperactivity in aged mice that is associated with exaggerated induction of both pro-inflammatory IL-1β and anti-inflammatory IL-10 cytokines. *Brain, Behavior, and Immunity*, *23*(3), 309–317. https://doi.org/10.1016/j.bbi.2008.09.002

Herisson, F., Frodermann, V., Courties, G., Rohde, D., Sun, Y., Vandoorne, K., … Nahrendorf, M. (2018). Direct vascular channels connect skull bone marrow and the brain surface enabling myeloid cell migration. *Nature Neuroscience*, *21*(9), 1209–1217. https://doi.org/10.1038/s41593-018-0213-2

Hill-Burns, E. M., Debelius, J. W., Morton, J. T., Wissemann, W. T., Lewis, M. R., Wallen, Z. D., … Payami, H. (2017). Parkinson's disease and Parkinson's disease medications have distinct signatures of the gut microbiome. *Movement Disorders*, *32*(5), 739–749. https://doi.org/10.1002/mds.26942

Hill-Burns, E. M., Factor, S. A., Zabetian, C. P., Thomson, G., & Payami, H. (2011). Evidence for more than one Parkinson's disease-associated variant within the HLA region. *PloS One*, *6*(11), e27109. https://doi.org/10.1371/journal.pone.0027109

Holmans, P., Moskvina, V., Jones, L., Sharma, M., Vedernikov, A., Buchel, F., … Wood, N. W. (2013). A pathway-based analysis provides additional support for an immune-related genetic susceptibility to Parkinson's disease. *Human Molecular Genetics*, *22*(5), 1039–49. https://doi.org/10.1093/hmg/dds492

Holmes, C., Cunningham, C., Zotova, E., Woolford, J., Dean, C., Kerr, S., … Perry, V. H. (2009a). Systemic inflammation and disease progression in alzheimer disease. *Neurology*, *73*(10), 768–774. https://doi.org/10.1212/WNL.0b013e3181b6bb95

Holmes, C., Cunningham, C., Zotova, E., Woolford, J., Dean, C., Kerr, S., … Perry, V. H. (2009b). Systemic inflammation and disease progression in Alzheimer disease. *Neurology*, *73*(10), 768–774. https://doi.org/10.1212/WNL.0b013e3181b6bb95

Horvath, I., Iashchishyn, I. A., Forsgren, L., & Morozova-Roche, L. A. (2017a). Immunochemical Detection of alpha-Synuclein Autoantibodies in Parkinson's Disease: Correlation between Plasma and Cerebrospinal Fluid Levels. *ACS Chemical Neuroscience*, *8*(6), 1170–1176. https://doi.org/10.1021/acschemneuro.7b00063

Horvath, I., Iashchishyn, I. A., Forsgren, L., & Morozova-Roche, L. A. (2017b). Immunochemical Detection of α-Synuclein Autoantibodies in Parkinson's Disease: Correlation between Plasma and Cerebrospinal Fluid Levels. *ACS Chemical Neuroscience*, *8*(6), acschemneuro.7b00063.

https://doi.org/10.1021/acschemneuro.7b00063

Hui, K. Y., Fernandez-Hernandez, H., Hu, J., Schaffner, A., Pankratz, N., Hsu, N.-Y., … Peter, I. (2018). Functional variants in the LRRK2 gene confer shared effects on risk for Crohn's disease and Parkinson's disease. *Science Translational Medicine*, *10*(423), eaai7795. https://doi.org/10.1126/scitranslmed.aai7795

Ip, C. W., Beck, S. K., & Volkmann, J. (2015). Lymphocytes reduce nigrostriatal deficits in the 6-hydroxydopamine mouse model of Parkinson's disease. *Journal of Neural Transmission*, *122*(12), 1633–1643. https://doi.org/10.1007/s00702-015-1444-y

Irwin, D. J., Lee, V. M.-Y., & Trojanowski, J. Q. (2013). Parkinson's disease dementia: convergence of α-synuclein, tau and amyloid-β pathologies. *Nature Reviews. Neuroscience*, *14*(9), 626–36. https://doi.org/10.1038/nrn3549

Iwata, Y., Matsushita, T., Horikawa, M., DiLillo, D. J., Yanaba, K., Venturi, G. M., … Tedder, T. F. (2011). Characterization of a rare IL-10-competent B-cell subset in humans that parallels mouse regulatory B10 cells. *Blood*, *117*(2), 530–541. https://doi.org/10.1182/blood-2010-07-294249

J Wheeler, C., Seksenyan, A., Koronyo, Y., Rentsendorj, A., Sarayba, D., Wu, H., … Irvin, D. K. (2014). T-Lymphocyte Deficiency Exacerbates Behavioral Deficits in the 6-OHDA Unilateral Lesion Rat Model for Parkinson's Disease. *Journal of Neurology & Neurophysiology*, *05*(03). https://doi.org/10.4172/2155-9562.1000209

Jackson-Lewis, V., Blesa, J., & Przedborski, S. (2012). Animal models of Parkinson's disease. *Parkinsonism & Related Disorders*, *18 Suppl 1*, S183-5. https://doi.org/10.1016/S1353-8020(11)70057-8

Jennewein, M. F., & Alter, G. (2017). The Immunoregulatory Roles of Antibody Glycosylation. *Trends in Immunology*, *38*(5), 358–372. https://doi.org/10.1016/j.it.2017.02.004

Kannarkat, G. T., Boss, J. M., & Tansey, M. G. (2013). The role of innate and adaptive immunity in Parkinson's disease. *Journal of Parkinson's Disease*, *3*(4), 493–514. https://doi.org/10.3233/JPD-130250

Kara, E., Kiely, A. P., Proukakis, C., Giffin, N., Love, S., Hehir, J., … Houlden, H. (2014). A 6.4 Mb duplication of the α-synuclein locus causing frontotemporal dementia and Parkinsonism: phenotype-genotype correlations. *JAMA Neurology*, *71*(9), 1162–71. https://doi.org/10.1001/jamaneurol.2014.994

Karnell, J. L., Kumar, V., Wang, J., Wang, S., Voynova, E., & Ettinger, R. (2017). Role of CD11c + T-bet + B cells in human health and disease. *Cellular Immunology*, *321*, 40–45. https://doi.org/10.1016/j.cellimm.2017.05.008

Karrar, S., & Cunninghame Graham, D. S. (2018). Abnormal B Cell Development in Systemic Lupus Erythematosus: What the Genetics Tell Us. *Arthritis & Rheumatology (Hoboken, N.J.)*, *70*(4), 496–507. https://doi.org/10.1002/art.40396

Kedmi, M., Bar-Shira, A., Gurevich, T., Giladi, N., & Orr-Urtreger, A. (2011). Decreased expression of B cell related genes in leukocytes of women with Parkinson's disease. *Molecular Neurodegeneration*, *6*(1), 66. https://doi.org/10.1186/1750-1326-6-66

Khalid, S. I., Ampie, L., Kelly, R., Ladha, S. S., & Dardis, C. (2017). Immune Modulation in the Treatment of Amyotrophic Lateral Sclerosis: A Review of Clinical Trials. *Frontiers in Neurology*, *8*, 486. https://doi.org/10.3389/fneur.2017.00486

Klein, C., & Westenberger, A. (2012). Genetics of Parkinson's Disease. *Cold Spring Harbor Perspectives in Medicine*, *2*(1), a008888. https://doi.org/10.1101/CSHPERSPECT.A008888

Korin, B., Ben-Shaanan, T. L., Schiller, M., Dubovik, T., Azulay-Debby, H., Boshnak, N. T., … Rolls, A. (2017). High-dimensional, single-cell characterization of the brain's immune compartment. *Nature Neuroscience*,

20(9), 1300–1309. https://doi.org/10.1038/nn.4610

Kronimus, Y., Albus, A., Balzer-Geldsetzer, M., Straub, S., Semler, E., Otto, M., … Mengel, D. (2016). Naturally Occurring Autoantibodies against Tau Protein Are Reduced in Parkinson's Disease Dementia. *Plos One*, *11*(11), e0164953. https://doi.org/10.1371/journal.pone.0164953

Kuo, P. H., Stuehm, C., Squire, S., & Johnson, K. (2018). Meningeal Lymphatic Vessel Flow Runs Countercurrent to Venous Flow in the Superior Sagittal Sinus of the Human Brain. *Tomography*, *4*(3), 99–104. https://doi.org/10.18383/j.tom.2018.00013

Kustrimovic, N., Rasini, E., Legnaro, M., Bombelli, R., Aleksic, I., Blandini, F., … Cosentino, M. (2016). Dopaminergic Receptors on CD4+ T Naive and Memory Lymphocytes Correlate with Motor Impairment in Patients with Parkinson's Disease. *Scientific Reports*, *6*(1), 33738. https://doi.org/10.1038/srep33738

Lampasona, V., & Liberati, D. (2016). Islet Autoantibodies. *Current Diabetes Reports*, *16*(6), 53. https://doi.org/10.1007/s11892-016-0738-2

Langston, J. W., Forno, L. S., Tetrud, J., Reeves, A. G., Kaplan, J. A., & Karluk, D. (1999). Evidence of active nerve cell degeneration in the substantia nigra of humans years after 1-methyl-4-phenyl-1,2,3,6-tetrahydropyridine exposure. *Annals of Neurology*, *46*(4), 598–605.

LeBien, T. W., & Tedder, T. F. (2008). B lymphocytes: how they develop and function. *Blood*, *112*(5), 1570–80. https://doi.org/10.1182/blood-2008-02-078071

Li, Q., & Barres, B. A. (2018). Microglia and macrophages in brain homeostasis and disease. *Nature Reviews Immunology*, *18*(4), 225–242. https://doi.org/10.1038/nri.2017.125

Lin, J.-C., Lin, C.-S., Hsu, C.-W., Lin, C.-L., & Kao, C.-H. (2016). Association Between Parkinson's Disease and Inflammatory Bowel Disease. *Inflammatory Bowel Diseases*, *22*(5), 1049–1055.

https://doi.org/10.1097/MIB.0000000000000735

Lira, A., Kulczycki, J., Slack, R., Anisman, H., & Park, D. S. (2011). Involvement of the Fc gamma receptor in a chronic N-methyl-4-phenyl-1,2,3,6-tetrahydropyridine mouse model of dopaminergic loss. *The Journal of Biological Chemistry*, *286*(33), 28783–93. https://doi.org/10.1074/jbc.M111.244830

Liu, Z., Lee, J., Krummey, S., Lu, W., Cai, H., & Lenardo, M. J. (2011). The kinase LRRK2 is a regulator of the transcription factor NFAT that modulates the severity of inflammatory bowel disease. *Nature Immunology*, *12*(11), 1063–1070. https://doi.org/10.1038/ni.2113

LLC, H. C. (n.d.). Power and Sample Size. Retrieved June 1, 2018, from http://powerandsamplesize.com/

Louveau, A., Herz, J., Alme, M. N., Salvador, A. F., Dong, M. Q., Viar, K. E., … Kipnis, J. (2018). CNS lymphatic drainage and neuroinflammation are regulated by meningeal lymphatic vasculature. *Nature Neuroscience*, *21*(10), 1380–1391. https://doi.org/10.1038/s41593-018-0227-9

Maetzler, W., Apel, A., Langkamp, M., Deuschle, C., Dilger, S. S., Stirnkorb, J. G., … Berg, D. (2014). Comparable Autoantibody Serum Levels against Amyloid- and Inflammation-Associated Proteins in Parkinson's Disease Patients and Controls. *PLoS ONE*, *9*(2), e88604. https://doi.org/10.1371/journal.pone.0088604

Maetzler, W., Pilotto, A., Apel, A., Deuschle, C., Kuebart, G., Heinzel, S., … Berg, D. (2014). In vivo markers of Parkinson's disease and dementia with Lewy bodies: current value of the 5G4 α-synuclein antibody. *Acta Neuropathologica*, *128*(6), 893–895. https://doi.org/10.1007/s00401-014-1364-1

Magen, I., & Chesselet, M.-F. (2010). Genetic mouse models of Parkinson's disease The state of the art. *Progress in Brain Research*, *184*, 53–87. https://doi.org/10.1016/S0079-6123(10)84004-X

Magliozzi, R., Howell, O., Vora, A., Serafini, B., Nicholas, R., Puopolo, M., …

Aloisi, F. (2006). Meningeal B-cell follicles in secondary progressive multiple sclerosis associate with early onset of disease and severe cortical pathology. *Brain*, *130*(4), 1089–1104. https://doi.org/10.1093/brain/awm038

Martinez, B., & Peplow, P. (2018). Neuroprotection by immunomodulatory agents in animal models of Parkinson's disease. *Neural Regeneration Research*, *13*(9), 1493. https://doi.org/10.4103/1673-5374.237108

Masliah, E., Rockenstein, E., Adame, A., Alford, M., Crews, L., Hashimoto, M., … Schenk, D. (2005). Effects of alpha-synuclein immunization in a mouse model of Parkinson's disease. *Neuron*, *46*(6), 857–68. https://doi.org/10.1016/j.neuron.2005.05.010

Matsushita, T., Yanaba, K., Bouaziz, J.-D., Fujimoto, M., & Tedder, T. F. (2008). Regulatory B cells inhibit EAE initiation in mice while other B cells promote disease progression. *The Journal of Clinical Investigation*, *118*(10), 3420–30. https://doi.org/10.1172/JCI36030

Mauri, C., & Bosma, A. (2012). Immune Regulatory Function of B Cells. *Annual Review of Immunology*, *30*(1), 221–241. https://doi.org/10.1146/annurev-immunol-020711-074934

Mauri, C., & Menon, M. (2015). The expanding family of regulatory B cells. *International Immunology*, *27*(10), 479–86. https://doi.org/10.1093/intimm/dxv038

McGeer, P. L., Itagaki, S., Boyes, B. E., & McGeer, E. G. (1988). Reactive microglia are positive for HLA-DR in the substantia nigra of Parkinson's and Alzheimer's disease brains. *Neurology*, *38*(8), 1285–91. https://doi.org/10.1212/wnl.38.8.1285

McGeer, P. L., Rogers, J., & McGeer, E. G. (2016). Inflammation, Antiinflammatory Agents, and Alzheimer's Disease: The Last 22 Years. *Journal of Alzheimer's Disease*, *54*(3), 853–857. https://doi.org/10.3233/JAD-160488

Mistry, P. K., Taddei, T., vom Dahl, S., & Rosenbloom, B. E. (2013). Gaucher

disease and malignancy: a model for cancer pathogenesis in an inborn error of metabolism. *Critical Reviews in Oncogenesis*, *18*(3), 235–46.

Moseman, E. A., Iannacone, M., Bosurgi, L., Tonti, E., Chevrier, N., Tumanov, A., … von Andrian, U. H. (2012). B cell maintenance of subcapsular sinus macrophages protects against a fatal viral infection independent of adaptive immunity. *Immunity*, *36*(3), 415–26. https://doi.org/10.1016/j.immuni.2012.01.013

Mount, M. P., Lira, A., Grimes, D., Smith, P. D., Faucher, S., Slack, R., … Park, D. S. (2007). Involvement of Interferon- in Microglial-Mediated Loss of Dopaminergic Neurons. *Journal of Neuroscience*, *27*(12), 3328–3337. https://doi.org/10.1523/JNEUROSCI.5321-06.2007

Mullard, A. (2019). Anti-amyloid failures stack up as Alzheimer antibody flops. https://doi.org/10.1038/d41573-019-00064-1

Nair, S., Boddupalli, C. S., Verma, R., Liu, J., Yang, R., Pastores, G. M., … Dhodapkar, M. V. (2015). Type II NKT-TFH cells against Gaucher lipids regulate B-cell immunity and inflammation. *Blood*, *125*(8), 1256–71. https://doi.org/10.1182/blood-2014-09-600270

Nalls, M. a, Pankratz, N., Lill, C. M., Do, C. B., Hernandez, D. G., Saad, M., … Singleton, A. B. (2014). Large-scale meta-analysis of genome-wide association data identifies six new risk loci for Parkinson's disease. *Nature Genetics*, *46*(9), 989–93. https://doi.org/10.1038/ng.3043

Nikolich-Žugich, J. (2018). The twilight of immunity: emerging concepts in aging of the immune system. *Nature Immunology*, *19*(1), 10–19. https://doi.org/10.1038/s41590-017-0006-x

NINDS NET-PD Investigators. (2006). A randomized, double-blind, futility clinical trial of creatine and minocycline in early Parkinson disease. *Neurology*, *66*(5), 664–671. https://doi.org/10.1212/01.wnl.0000201252.57661.e1

NINDS NET-PD Investigators. (2008). A Pilot Clinical Trial of Creatine and Minocycline in Early Parkinson Disease. *Clinical Neuropharmacology*, *31*(3),

141–150. https://doi.org/10.1097/WNF.0b013e3181342f32

NINDS NET-PD Investigators. (2015). Pioglitazone in early Parkinson's disease: A phase 2, multicentre, double-blind, randomised trial. *The Lancet Neurology*, *14*(8), 795–803. https://doi.org/https://doi.org/10.1016/S1474-4422(15)00144-1

Niven, D. J., Berthiaume, L. R., Fick, G. H., & Laupland, K. B. (2012). Matched case-control studies: a review of reported statistical methodology. *Clinical Epidemiology*, *4*, 99–110. https://doi.org/10.2147/CLEP.S30816

Noelker, C., Morel, L., Lescot, T., Osterloh, A., Alvarez-Fischer, D., Breloer, M., … Hartmann, A. (2013). Toll like receptor 4 mediates cell death in a mouse MPTP model of Parkinson disease. *Scientific Reports*, *3*(1), 1393. https://doi.org/10.1038/srep01393

Oleinika, K., Rosser, E. C., Matei, D. E., Nistala, K., Bosma, A., Drozdov, I., & Mauri, C. (2018). CD1d-dependent immune suppression mediated by regulatory B cells through modulations of iNKT cells. *Nature Communications*, *9*(1), 684. https://doi.org/10.1038/s41467-018-02911-y

Orr, C. F., Rowe, D. B., Mizuno, Y., Mori, H., & Halliday, G. M. (2005). A possible role for humoral immunity in the pathogenesis of Parkinson's disease. *Brain : A Journal of Neurology*, *128*(Pt 11), 2665–74. https://doi.org/10.1093/brain/awh625

Panda, S., & Ding, J. L. (2015). Natural Antibodies Bridge Innate and Adaptive Immunity. *The Journal of Immunology*, *194*(1), 13–20. https://doi.org/10.4049/jimmunol.1400844

Panza, F., Lozupone, M., Logroscino, G., & Imbimbo, B. P. (2019). A critical appraisal of amyloid-β-targeting therapies for Alzheimer disease. *Nature Reviews Neurology*, *15*(2), 73–88. https://doi.org/10.1038/s41582-018-0116-6

Papachroni, K. K., Ninkina, N., Papapanagiotou, A., & Georgios, M. (2011). Europe PMC Funders Group Autoantibodies to alpha-synuclein in inherited Parkinson ' s disease, *101*(3), 749–756. https://doi.org/10.1111/j.1471-4159.2006.04365.x.Autoantibodies

Papachroni, K. K., Ninkina, N., Papapanagiotou, A., Hadjigeorgiou, G. M., Xiromerisiou, G., Papadimitriou, A., … Buchman, V. L. (2007). Autoantibodies to alpha-synuclein in inherited Parkinson's disease. *Journal of Neurochemistry*, *101*(3), 749–56. https://doi.org/10.1111/j.1471-4159.2006.04365.x

Patel, T. K., Habimana-Griffin, L., Gao, X., Xu, B., Achilefu, S., Alitalo, K., … Holtzman, D. M. (2019). Dural lymphatics regulate clearance of extracellular tau from the CNS. *Molecular Neurodegeneration*, *14*(1), 11. https://doi.org/10.1186/s13024-019-0312-x

Pchelina, S., Emelyanov, A., Baydakova, G., Andoskin, P., Senkevich, K., Nikolaev, M., … Zakharova, E. (2016). Oligomeric α-synuclein and glucocerebrosidase activity levels in GBA-associated Parkinson's disease. *Neuroscience Letters*. https://doi.org/10.1016/j.neulet.2016.10.039

Perry, V. H. (2012). Innate inflammation in Parkinson's disease. *Cold Spring Harbor Perspectives in Medicine*, *2*(9), a009373. https://doi.org/10.1101/cshperspect.a009373

Pescovitz, M. D., Greenbaum, C. J., Krause-Steinrauf, H., Becker, D. J., Gitelman, S. E., Goland, R., … Type 1 Diabetes TrialNet Anti-CD20 Study Group. (2009). Rituximab, B-Lymphocyte Depletion, and Preservation of Beta-Cell Function. *New England Journal of Medicine*, *361*(22), 2143–2152. https://doi.org/10.1056/NEJMoa0904452

Petrov, V. A., Saltykova, I. V., Zhukova, I. A., Alifirova, V. M., Zhukova, N. G., Dorofeeva, Y. B., … Sazonov, A. E. (2017). Analysis of Gut Microbiota in Patients with Parkinson's Disease. *Bulletin of Experimental Biology and Medicine*, *162*(6), 734–737. https://doi.org/10.1007/s10517-017-3700-7

Pieper, K., Grimbacher, B., & Eibel, H. (2013). B-cell biology and development. *The Journal of Allergy and Clinical Immunology*, *131*(4), 959–71. https://doi.org/10.1016/j.jaci.2013.01.046

Poly, T. N., Islam, M. M., Yang, H.-C., & Li, Y.-C. J. (2019). Non-steroidal anti-

inflammatory drugs and risk of Parkinson's disease in the elderly population: a meta-analysis. *European Journal of Clinical Pharmacology*, *75*(1), 99–108. https://doi.org/10.1007/s00228-018-2561-y

Polymeropoulos, M. H., Lavedan, C., Leroy, E., Ide, S. E., Dehejia, A., Dutra, A., … Nussbaum, R. L. (1997). Mutation in the alpha-synuclein gene identified in families with Parkinson's disease. *Science (New York, N.Y.)*, *276*(5321), 2045–7.

Postuma, R. B., Gagnon, J.-F., Bertrand, J.-A., Génier Marchand, D., & Montplaisir, J. Y. (2015). Parkinson risk in idiopathic REM sleep behavior disorder: preparing for neuroprotective trials. *Neurology*, *84*(11), 1104–13. https://doi.org/10.1212/WNL.0000000000001364

Pringsheim, T., Jette, N., Frolkis, A., & Steeves, T. D. L. (2014). The prevalence of Parkinson's disease: A systematic review and meta-analysis. *Movement Disorders : Official Journal of the Movement Disorder Society*. https://doi.org/10.1002/mds.25945

Racette, B. A., Gross, A., Vouri, S. M., Camacho-Soto, A., Willis, A. W., & Searles Nielsen, S. (2018). Immunosuppressants and risk of Parkinson disease. *Annals of Clinical and Translational Neurology*, *5*(7), 870–875. https://doi.org/10.1002/acn3.580

Rauch, P. J., Chudnovskiy, A., Robbins, C. S., Weber, G. F., Etzrodt, M., Hilgendorf, I., … Swirski, F. K. (2012). Innate Response Activator B Cells Protect Against Microbial Sepsis. *Science*, *335*(6068), 597–601. https://doi.org/10.1126/science.1215173

Reale, M., Iarlori, C., Thomas, A., Gambi, D., Perfetti, B., Di Nicola, M., & Onofrj, M. (2009). Peripheral cytokines profile in Parkinson's disease. *Brain, Behavior, and Immunity*, *23*(1), 55–63. https://doi.org/10.1016/j.bbi.2008.07.003

Ricklin, D., Reis, E. S., & Lambris, J. D. (2016). Complement in disease: a defence system turning offensive. *Nature Reviews Nephrology*, *12*(7), 383–401.

https://doi.org/10.1038/nrneph.2016.70

Rocha, N. P., Assis, F., Scalzo, P. L., Vieira, É. L. M., Barbosa, I. G., de Souza, M. S., … Teixeira, A. L. (2018). Reduced Activated T Lymphocytes (CD4+CD25+) and Plasma Levels of Cytokines in Parkinson's Disease. *Molecular Neurobiology*, *55*(2), 1488–1497. https://doi.org/10.1007/s12035-017-0404-y

Rubtsov, A. V, Rubtsova, K., Fischer, A., Meehan, R. T., Gillis, J. Z., Kappler, J. W., & Marrack, P. (2011). Toll-like receptor 7 (TLR7)-driven accumulation of a novel CD11c^{+} B-cell population is important for the development of autoimmunity. *Blood*, *118*(5), 1305–15. https://doi.org/10.1182/blood-2011-01-331462

Rubtsova, K., Rubtsov, A. V, Cancro, M. P., & Marrack, P. (2015). Age-Associated B Cells: A T-bet-Dependent Effector with Roles in Protective and Pathogenic Immunity. *Journal of Immunology (Baltimore, Md. : 1950)*, *195*(5), 1933–7. https://doi.org/10.4049/jimmunol.1501209

Ruddle, N. H., & Akirav, E. M. (2009). Secondary lymphoid organs: responding to genetic and environmental cues in ontogeny and the immune response. *Journal of Immunology (Baltimore, Md. : 1950)*, *183*(4), 2205–12. https://doi.org/10.4049/jimmunol.0804324

Russell, A. C., Šimurina, M., Garcia, M. T., Novokmet, M., Wang, Y., Rudan, I., … Wang, W. (2017). The N-glycosylation of immunoglobulin G as a novel biomarker of Parkinson's disease. *Glycobiology*, 1–10. https://doi.org/10.1093/glycob/cwx022

Sampson, T. R., Debelius, J. W., Thron, T., Janssen, S., Shastri, G. G., Ilhan, Z. E., … Mazmanian, S. K. (2016). Gut Microbiota Regulate Motor Deficits and Neuroinflammation in a Model of Parkinson's Disease. *Cell*, *167*(6), 1469–1480.e12. https://doi.org/10.1016/j.cell.2016.11.018

Saunders, J. a H., Estes, K. a, Kosloski, L. M., Allen, H. E., Dempsey, K. M., Torres-Russotto, D. R., … Gendelman, H. E. (2012). CD4+ Regulatory and Effector/Memory T Cell Subsets Profile Motor Dysfunction in Parkinson's

Disease. *Journal of Neuroimmune Pharmacology : The Official Journal of the Society on NeuroImmune Pharmacology*. https://doi.org/10.1007/s11481-012-9402-z

Schapira, A. H. V., Chaudhuri, K. R., & Jenner, P. (2017). Non-motor features of Parkinson disease. *Nature Reviews Neuroscience*, *18*(7), 435–450. https://doi.org/10.1038/nrn.2017.62

Scheperjans, F., Aho, V., Pereira, P. a B., Koskinen, K., Paulin, L., Pekkonen, E., … Auvinen, P. (2014). Gut microbiota are related to Parkinson's disease and clinical phenotype. *Movement Disorders : Official Journal of the Movement Disorder Society*, *30*(3), 9–12. https://doi.org/10.1002/mds.26069

Scott, K. M., Kouli, A., Yeoh, S. L., Clatworthy, M. R., & Williams-Gray, C. H. (2018). A Systematic Review and Meta-Analysis of Alpha Synuclein Auto-Antibodies in Parkinson's Disease. *Frontiers in Neurology*, *9*, 815. https://doi.org/10.3389/fneur.2018.00815

Shalash, A., Salama, M., Makar, M., Roushdy, T., Elrassas, H. H., Mohamed, W., … Abou Donia, M. (2017). Elevated Serum alpha-Synuclein Autoantibodies in Patients with Parkinson's Disease Relative to Alzheimer's Disease and Controls. *Frontiers in Neurology*, *8*, 720. https://doi.org/10.3389/fneur.2017.00720

Singleton, A. B., Farrer, M., Johnson, J., Singleton, A., Hague, S., Kachergus, J., … Gwinn-Hardy, K. (2003). alpha-Synuclein locus triplication causes Parkinson's disease. *Science (New York, N.Y.)*, *302*(5646), 841. https://doi.org/10.1126/science.1090278

Smith, L. M., Schiess, M. C., Coffey, M. P., Klaver, A. C., & Loeffler, D. A. (2012). α-Synuclein and Anti-α-Synuclein Antibodies in Parkinson's Disease, Atypical Parkinson Syndromes, REM Sleep Behavior Disorder, and Healthy Controls. *PLoS ONE*, *7*(12), e52285. https://doi.org/10.1371/journal.pone.0052285

Sommer, A., Maxreiter, F., Krach, F., Fadler, T., Grosch, J., Maroni, M., …

Winner, B. (2018). Th17 Lymphocytes Induce Neuronal Cell Death in a Human iPSC-Based Model of Parkinson's Disease. *Cell Stem Cell*, *23*(1), 123–131.e6. https://doi.org/10.1016/J.STEM.2018.06.015

Spillantini, M. G., Schmidt, M. L., Lee, V. M., Trojanowski, J. Q., Jakes, R., & Goedert, M. (1997). Alpha-synuclein in Lewy bodies. *Nature*, *388*(6645), 839–40. https://doi.org/10.1038/42166

Stark, A.-K., Chandra, A., Chakraborty, K., Alam, R., Carbonaro, V., Clark, J., … Okkenhaug, K. (2018). PI3Kδ hyper-activation promotes development of B cells that exacerbate Streptococcus pneumoniae infection in an antibody-independent manner. *Nature Communications*, *9*(1), 3174. https://doi.org/10.1038/s41467-018-05674-8

Stevens, C. H., Rowe, D., Morel-Kopp, M.-C., Orr, C., Russell, T., Ranola, M., … Halliday, G. M. (2012). Reduced T helper and B lymphocytes in Parkinson's disease. *Journal of Neuroimmunology*, *252*(1–2), 95–9. https://doi.org/10.1016/j.jneuroim.2012.07.015

Stirling, D. P., Koochesfahani, K. M., Steeves, J. D., & Tetzlaff, W. (2005). Minocycline as a Neuroprotective Agent. *The Neuroscientist*, *11*(4), 308–322. https://doi.org/10.1177/1073858405275175

Stott, S. R. W., & Barker, R. a. (2014). Time course of dopamine neuron loss and glial response in the 6-OHDA striatal mouse model of Parkinson's disease. *The European Journal of Neuroscience*, *39*(6), 1042–56. https://doi.org/10.1111/ejn.12459

Sulzer, D., Alcalay, R. N., Garretti, F., Cote, L., Kanter, E., Agin-Liebes, J., … Sette, A. (2017). T cells from patients with Parkinson's disease recognize α-synuclein peptides. *Nature*, *546*(7660), 656–661. https://doi.org/10.1038/nature22815

Taguchi, Y. V., Liu, J., Ruan, J., Pacheco, J., Zhang, X., Abbasi, J., … Chandra, S. S. (2017). Glucosylsphingosine Promotes α-Synuclein Pathology in Mutant GBA-Associated Parkinson's Disease. *The Journal of Neuroscience*, *37*(40),

9617–9631. https://doi.org/10.1523/JNEUROSCI.1525-17.2017

Takamatsu, Y., Ho, G., Koike, W., Sugama, S., Takenouchi, T., Waragai, M., … Hashimoto, M. (2017). Combined immunotherapy with "anti-insulin resistance" therapy as a novel therapeutic strategy against neurodegenerative diseases. *Npj Parkinson's Disease*, *3*(1), 4. https://doi.org/10.1038/s41531-016-0001-1

Thakur, P., Breger, L. S., Lundblad, M., Wan, O. W., Mattsson, B., Luk, K. C., … Björklund, A. (2017). Modeling Parkinson's disease pathology by combination of fibril seeds and α-synuclein overexpression in the rat brain. *Proceedings of the National Academy of Sciences of the United States of America*, *114*(39), E8284–E8293. https://doi.org/10.1073/pnas.1710442114

Thaunat, O., Morelon, E., & Defrance, T. (2010). Am"B"valent: anti-CD20 antibodies unravel the dual role of B cells in immunopathogenesis. *Blood*, *116*(4), 515–521. https://doi.org/10.1182/BLOOD-2010-01-266668

Uemura, N., Yagi, H., Uemura, M. T., Hatanaka, Y., Yamakado, H., & Takahashi, R. (2018). Inoculation of α-synuclein preformed fibrils into the mouse gastrointestinal tract induces Lewy body-like aggregates in the brainstem via the vagus nerve. *Molecular Neurodegeneration*, *13*(1), 21. https://doi.org/10.1186/s13024-018-0257-5

van de Veen, W., Stanic, B., Yaman, G., Wawrzyniak, M., Söllner, S., Akdis, D. G., … Akdis, M. (2013). IgG4 production is confined to human IL-10-producing regulatory B cells that suppress antigen-specific immune responses. *The Journal of Allergy and Clinical Immunology*, *131*(4), 1204–12. https://doi.org/10.1016/j.jaci.2013.01.014

Van der Perren, A., Van den Haute, C., & Baekelandt, V. (2014). Viral Vector-Based Models of Parkinson's Disease. *Current Topics in Behavioral Neurosciences*. https://doi.org/10.1007/7854_2014_310

Vekrellis, K., Xilouri, M., Emmanouilidou, E., Rideout, H. J., & Stefanis, L. (2011). Pathological roles of α-synuclein in neurological disorders. *The Lancet.*

Neurology, *10*(11), 1015–25. https://doi.org/10.1016/S1474-4422(11)70213-7

Velseboer, D. C., de Bie, R. M. A., Wieske, L., Evans, J. R., Mason, S. L., Foltynie, T., … Williams-Gray, C. H. (2016). Development and external validation of a prognostic model in newly diagnosed Parkinson disease. *Neurology*, *86*(11), 986–93. https://doi.org/10.1212/WNL.0000000000002437

Villumsen, M., Aznar, S., Pakkenberg, B., Jess, T., & Brudek, T. (2019). Inflammatory bowel disease increases the risk of Parkinson's disease: a Danish nationwide cohort study 1977–2014. *Gut*, *68*(1), 18–24. https://doi.org/10.1136/gutjnl-2017-315666

Wagner, M., Poeck, H., Jahrsdoerfer, B., Rothenfusser, S., Prell, D., Bohle, B., … Hartmann, G. (2004). IL-12p70-Dependent Th1 Induction by Human B Cells Requires Combined Activation with CD40 Ligand and CpG DNA. *The Journal of Immunology*, *172*(2), 954–963. https://doi.org/10.4049/jimmunol.172.2.954

Wallings, R., Manzoni, C., & Bandopadhyay, R. (2015). Cellular processes associated with LRRK2 function and dysfunction. *FEBS Journal*, *282*(15), 2806–2826. https://doi.org/10.1111/febs.13305

Wan, X., Wang, W., Liu, J., & Tong, T. (2014). Estimating the sample mean and standard deviation from the sample size, median, range and/or interquartile range. *BMC Medical Research Methodology*, *14*(1), 135. https://doi.org/10.1186/1471-2288-14-135

Watson, M. B., Richter, F., Lee, S. K., Gabby, L., Wu, J., Masliah, E., … Chesselet, M. (2012). Regionally-specific microglial activation in young mice over-expressing human wildtype alpha-synuclein. *Experimental Neurology*, *237*(2), 318–334. https://doi.org/10.1016/j.expneurol.2012.06.025

Wegrzynowicz, M., Bar-On, D., Calò, L., Anichtchik, O., Iovino, M., Xia, J., … Spillantini, M. G. (2018). Depopulation of α-synuclein aggregates is associated with rescue of dopamine neuron dysfunction and death in a new Parkinson disease model. *BioRxiv*, 500629. https://doi.org/10.1101/500629

Wijeyekoon, R. S., Kronenberg-Versteeg, D., Scott, K. M., Hayat, S., Jones, J. L., Clatworthy, M. R., … Williams-Gray, C. H. (2018). Monocyte function in Parkinson's Disease and the impact of autologous serum on phagocytosis. *Frontiers in Neurology*, *9*, 870. https://doi.org/10.3389/FNEUR.2018.00870

Willcocks, L. C., Smith, K. G. C., & Clatworthy, M. R. (2009). Low-affinity Fcγ receptors, autoimmunity and infection. *Expert Reviews in Molecular Medicine*, *11*(August 2009), 1–29. https://doi.org/10.1017/S1462399409001161

Williams-Gray, C. H., Evans, J. R., Goris, A., Foltynie, T., Ban, M., Robbins, T. W., … Barker, R. A. (2009). The distinct cognitive syndromes of Parkinson's disease: 5 year follow-up of the CamPaIGN cohort. *Brain : A Journal of Neurology*, *132*(Pt 11), 2958–69. https://doi.org/10.1093/brain/awp245

Williams-Gray, C. H., Foltynie, T., Brayne, C. E. G., Robbins, T. W., & Barker, R. A. (2007). Evolution of cognitive dysfunction in an incident Parkinson's disease cohort. *Brain : A Journal of Neurology*, *130*(Pt 7), 1787–98. https://doi.org/10.1093/brain/awm111

Williams-Gray, C. H., Mason, S. L., Evans, J. R., Foltynie, T., Brayne, C., Robbins, T. W., & Barker, R. A. (2013). The CamPaIGN study of Parkinson's disease: 10-year outlook in an incident population-based cohort. *Journal of Neurology, Neurosurgery, and Psychiatry*, *84*(11), 1258–64. https://doi.org/10.1136/jnnp-2013-305277

Williams-Gray, C. H., Wijeyekoon, R. S., Scott, K. M., Hayat, S., Barker, R. A., & Jones, J. L. (2018). Abnormalities of age-related T cell senescence in Parkinson's disease. *Journal of Neuroinflammation*, *15*(1), 166. https://doi.org/10.1186/s12974-018-1206-5

Williams-Gray, C. H., Wijeyekoon, R., Yarnall, A. J., Lawson, R. A., Breen, D. P., Evans, J. R., … ICICLE-PD study group. (2016). Serum immune markers and disease progression in an incident Parkinson's disease cohort (ICICLE-PD). *Movement Disorders*, *31*(7), 995–1003. https://doi.org/10.1002/mds.26563

Williams-Gray, C. H., Wijeyekoon, R., Yarnall, A. J., Lawson, R. A., Breen, D. P.,

Evans, J. R., … group, on behalf of the I. study. (2016). Serum immune markers and disease progression in an incident Parkinson's disease cohort (ICICLE-PD). *Movement Disorders*, *31*(7), 995. https://doi.org/10.1002/MDS.26563

Woulfe, J. M., Duke, R., Middeldorp, J. M., Stevens, S., Vervoort, M., Hashimoto, M., … Munoz, D. G. (2002). Absence of elevated anti- -synuclein and anti-EBV latent membrane protein antibodies in PD. *Neurology*, *58*(9), 1435–1435. https://doi.org/10.1212/WNL.58.9.1435

Wykes, M. (2003). Why do B cells produce CD40 ligand? *Immunology and Cell Biology*, *81*(4), 328–31. https://doi.org/10.1046/j.1440-1711.2003.01171.x

Xu, Q., Evetts, S., Hu, M., Talbot, K., Wade-Martins, R., & Davis, J. J. (2014). An impedimetric assay of α-synuclein autoantibodies in early stage Parkinson's disease. *RSC Adv.*, *4*(102), 58773–58777. https://doi.org/10.1039/C4RA10100F

Xu, Y., Yan, J., Zhou, P., Li, J., Gao, H., Xia, Y., & Wang, Q. (2012). Neurotransmitter receptors and cognitive dysfunction in Alzheimer's disease and Parkinson's disease. *Progress in Neurobiology*, *97*(1), 1–13. https://doi.org/10.1016/j.pneurobio.2012.02.002

Yanamandra, K., Gruden, M. A., Casaite, V., Meskys, R., Forsgren, L., & Morozova-Roche, L. A. (2011). α-Synuclein Reactive Antibodies as Diagnostic Biomarkers in Blood Sera of Parkinson's Disease Patients. *PLoS ONE*, *6*(4), e18513. https://doi.org/10.1371/journal.pone.0018513

Ye, C., Brand, D., & Zheng, S. G. (2018). Targeting IL-2: an unexpected effect in treating immunological diseases. *Signal Transduction and Targeted Therapy*, *3*(1), 2. https://doi.org/10.1038/s41392-017-0002-5

Zhao, P., Yang, X., Yang, L., Li, M., Wood, K., Liu, Q., & Zhu, X. (2017). Neuroprotective effects of fingolimod in mouse models of Parkinson's disease. *The FASEB Journal*, *31*(1), 172–179. https://doi.org/10.1096/fj.201600751R

Zou, W., Pu, T., Feng, W., Lu, M., Zheng, Y., Du, R., … Hu, G. (2019). Blocking

meningeal lymphatic drainage aggravates Parkinson's disease-like pathology in mice overexpressing mutated α-synuclein. *Translational Neurodegeneration*, *8*(1), 7. https://doi.org/10.1186/s40035-019-0147-y